ORGANOSILICON BIOTECHNOLOGY: A BIO-INSPIRED APPROACH TO THE HYDROLYSIS OF ALKOXYSILANES and THE LIPASE-CATALYZED SYNTHESIS OF SILOXANE-CONTAINING POLYESTERS AND POLYAMIDES

Mark B. Frampton, B.Sc.

A thesis submitted to the Department of Chemistry and Centre for Biotechnology

in partial fulfillment of the requirements for the degree of

Doctor of Philosophy

January 31, 2013

Brock University

St. Catharines, Ontario

Abstract

The first part of this thesis studied the capacity of amino acids and enzymes to catalyze the hydrolysis and condensation of tetraethoxysilane and phenyltrimethoxysilane. Selected amino acids were shown to accelerate the hydrolysis and condensation of tetraethoxysilane under ambient temperature, pressure and at neutral pH (pH 7±0.02). The nature of the side chain of the amino acid was important in promoting hydrolysis and condensation. Several proteases were shown to have a capacity to hydrolyze tri- and tetra- alkoxysilanes under the same mild reaction conditions.

The second part of this thesis employed an immobilized *Candida antarctica* lipase B (Novozym-435, N435) to produce siloxane-containing polyesters, polyamides, and polyester amides under solvent-free conditions. Enzymatic activity was shown to be temperature dependent, increasing until enzyme denaturation became the dominant process, which typically occurred between 120-130°C. The residual activity of N435 was, on average, greater than 90%, when used in the synthesis of disiloxane-containing polyesters, regardless of the polymerization temperature except at the very highest temperatures, 140-150°C. A study of the thermal tolerance of N435 determined that, over ten reaction cycles, there was a decrease in the initial rate of polymerization with each consecutive use of the catalyst. No change in the degree of monomer conversion after a 24 hour reaction cycle was found.

To my family

Acknowledgements

There are many people that have contributed to the success of this thesis. First and foremost I would like to express my gratitude to my research supervisor Dr. Paul Zelisko for affording me the opportunity to carry out many different interesting research projects. His guidance and patience were always appreciated. We have spent many hours having discussions which were always interesting and fruitful.

I would like to extend thanks to my advisory committee, Dr. Tomáš Hudlický and Dr. Vincenzo DeLuca, whom, from day one, have provided valuable feedback that was always welcome. Dr. Martin Lemaire and Dr. Michael Bidochka are graciously thanked for sitting on my candidacy exam committee, as is Dr. Jeffery Atkinson for acting as chair of my examination committee. I would like to extend thanks to Dr. Heather Gordon and Dr. David Crandles for being a part of my examination committee. I would like to thank my external examiner, Dr. Michael A. Brook, for providing valuable comments on this thesis.

Many thanks must be extended to our collaborators Dr. Travis Dudding for carrying out many theoretical calculations, and to Dr. Thad Harroun and Drew Marquardt for helping with acquiring DSC data. Razvan Simionescu, Tim Jones, and Glenda Hooper are thanked for providing excellent technical service and many useful insights over the years.

I would like to thank all of the past and present members of the Zelisko group. While there haven't been many, they have all contributed to furthering many of the ideas that I had. Special thanks go to Jacqueline Séguin for friendship, patience, and so much more over the last two years

Ellen Robb is thanked for many years of letting me interrupt her lab work, and providing feedback on an early draft of my introductory chapter. Your friendship is irreplaceable.

Finally, I need to thank my mother and father for contributing to my seemingly never ending education. I promise you both it will have been worth it.

"The great tragedy of science - the slaying of a beautiful hypothesis by an ugly fact."

-Thomas Huxley

"We have considered all the known types of organic derivatives of silicon and we see how few are their number in comparison with the purely organic compounds. Since the few which are known are very limited in their reactions, the prospect of any immediate and important advance in this section of chemistry does not seem very hopeful."

-Frederick Stanley Kipping

Table of Contents

List of Figures:

List of Tables:

List of Appendix Figures:

List of Abbreviations

3HP-TMDS	1,3-bis(3-hydroxypropyl)-1,1,3,3-tetramethyldisiloxane
Ac_2O	Acetic anhydride
AcCN	Acetonitrile
AcO	Acetoxy
AcOH	Acetic acid
Asp	Aspartic acid
BBI	Bowman-Birk inhibitor
BSA	Bovine serum albumin
$CaCO_3$	Calcium carbonate
CalA	*Candida antarctica* lipase A
CalB	*Candida antarctica* lipase B
CD	Circular dichroism spectroscopy
$CHCl_3$	Chloroform
COSY	Proton correlation spectroscopy
CPr-TMDS-DME	1,3-bis(3-carboxypropyl)-1,1,3,3-tetramethyldisiloxane
CRL	*Candida rugosa* lipase
de	Diasteromeric excess
DEPT	Distortionless Enhancement by Polarization Transfer
DFT	Density functional theory
DMSO	Dimethylsulfoxide
DP_{avg}	Average degree of polymerization
DSC	Differential scanning calorimetry
ee	Enantiomeric excess
ES	Enyzme-substrate
Et	Ethyl
FTIR	Fourier-transform infrared spectroscopy

GC	Gas chromatography
Glu	Glutamic acid
Gly	Glycine
GPC	Gel permeation chromatography
HA-PDMS	Hydroxyalkyl polydimethylsiloxane
His	Histidine
HLADH	Horse liver alcohol dehydrogenase
HLAP	Horse liver acetonic powder
HMBC	Heteronuclear multiple bond correlation spectroscopy
HSA	Human serum albumin
HSQC	Heteronuclear single quantum correlation spectroscopy
Ile	Isoleucine
K_M	Michaelis-Menton constant
LCPs	Long chain polyamines
Leu	Leucine
Me	Methyl
MHz	Megahertz
M_n	Number average molecular weight
mRNA	messenger RNA
MTMS	Methyltrimethoxysilane
M_w	Weight average molecular weight
NAD^+	Nicotinamide adenine dinucleotide (oxidized)
NADH	Nicotinamide adenine dinucleotide (reduced)
NADPH	Nicotinamide adenine dinucleotide phosphate
NaOEt	Sodium ethoxide
NaOH	Sodium hydroxide
NBS	N-bromosuccinimide
NDO	Naphthalene dioxygenase

NMR	Nuclear magnetic resonance spectroscopy
OMe	Methoxy
PCI	Popcorn inhibitor
PCL	Polycaprolactone
PDI	Polydispersity index
PDMS	Polydimethylsiloxane
PEG	Polyethylene glycol
Ph	Phenyl
Phe	Phenylalanine
PhMe	Toluene
PLE	Pig liver esterase
PLL	Poly-L-lysine
Pro	Proline
PTMS	Phenyltrimethoxysilane
*p*TsOH	*para*-Toluene sulfonic acid
RNA	Ribonucleic Acid
ROP	Ring-opening polymerization
SDV	Silica deposition vesicle
Ser	Serine
SiO_2	Silica
SIRMS	Synchrotron infrared microspectroscopy
^{t}Bu	Tertiary buytl
TDO	Toluene dioxygenase
TEOS	Tetraethoxysilane
TES-PDMS	α,ω-(Triethoxysilylethyl)-polydimethylsiloxane
TGA	Thermogravimetric analysis
THF	Tetrahydrofuran
TMEDA	*N*,*N*,*N*′,*N*′-tetramethylethane-1,2-diamine
TMOS	Tetramethoxysilane

TMS	Trimethylsilyl or tetramethylsilane
TPCK	N-tosylphenylalanine chloromethylketone
TpSIT	*Thalassiosira pseudonana* silica transporter gene
Tris	2-amino-2-(hydroxymethyl)propane-1,3-diol
Trp	Tryptophan
Val	Valine

1 Introduction

Silicon is the second most abundant element in the earth's crust (~27%), second only to oxygen, where it forms crystalline silicate minerals, in conjunction with oxygen and other elements, such as quartz and christobalite, and amorphous silicate minerals such as montmorillonite and muscovite.[1] The chemistry of silicon, from organic, organometallic, polymeric, and inorganic perspectives, has been thoroughly explored over the last hundred years. Less attention, however, has been devoted to the study of organosilicon biotechnology, and in particular the use of enzymes or microorganisms to catalyze transformations of organosilicon compounds. This is perhaps not particularly surprising when one considers that the most common bond in nature is the *Si-O* bond and that, to date, evidence has not been offered in support of the existence of a naturally occurring organosilicon molecule containing an explicit *C-Si* bond. [2,3]

The biological importance of hydrated silica cannot be understated. Diatoms,[4-7] sea sponges, [8-12] marine microalgae, and some terrestrial grasses[13-16] are dependent on this micro-nutrient and have evolved molecular mechanisms to process inorganic silica. Silicic acid, and possibly the dissociated anion and/or sodium silicate, must be transported across an outer cell membrane where it becomes processed intra-compartmentally. After deposition onto a proteinaceous scaffold, the silica is converted into structurally reinforcing aggregates, such as frustules (diatoms), spicules (sea sponges), and other skeletal structures. The biosynthesis of these structures is mediated by proteins (sponges) or short polypeptides in conjunction with long chain polyamines (diatoms). Typically the concentration of available silicic acid in the environments for these organisms is very low, with sea water containing less than 100 μM of silicic acid and fresh water even less.[1,17,18]

Biocatalysis is recognized as a viable alternative to traditional catalytic methods in chemical transformations. The use of microorganisms and isolated enzymes allows for increased stereo- and regio-selectivity without the use of expensive chiral auxiliaries, or the need to perform chemistries at extremes of temperature or pressure.[19] Furthermore, the use of isolated enzymes permits transformations to occur under ambient conditions, sometimes in the absence of solvent, and circumvents the need for potentially toxic or costly catalysts.[19]

Polyesters are industrially and economically important materials and find use as fibres, plastics, resins and coatings.[20] Typical methods of producing polyesters include the direct esterification between an alcohol and a carboxylic acid, transesterification, and the alcoholysis of acid chlorides or anhydrides. Similarly, polyamides (i.e., Nylon) are produced via the condensation of carboxylic acids or acid chlorides and amines. Polyamides are desired for their tensile strength, elasticity and durability.[20] Typical methods of producing polyamides require extremes of heat and pressure, or acid/base catalysts. The physical characteristics of these polymeric materials are derived from the alternating arrangement of the carbonyl- and amine-derived fragments which provide a structural rigidity, in part due to the planarity of the amide linkage and the ability to hydrogen bond with neighbouring polymer chains. The structures of generic polyester (**1**) and polyamide (**2**) polymers are presented in **Figure 1**.

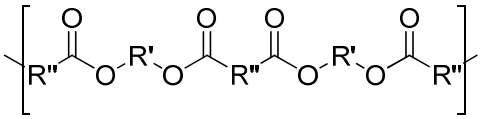

1

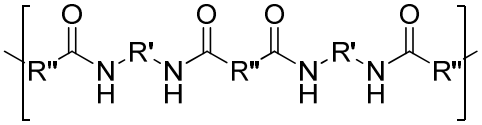

2

Figure 1 The general structures of a typical polyester (top) and polyamide (bottom).

Silicones (or siloxanes) are an important class of synthetic inorganic-organic hybrid (semi-organic) polymers.[21] Silicone-derived materials are desired for their physico-chemical properties, such as resistance to oxidation, low permittivity, hydrophobicity, permeability to oxygen, low glass transition temperatures, and bio-compatibility.[2] The inclusion of silicone monomers into organic polymers imparts altered characteristics when compared to the parent organic polymer. The physical characteristics that make silicone desirable are attributed to the relatively flexible nature of the repeating *Si-O* bonds within the polymer backbone (**Figure 2**).

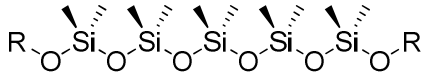

3

Figure 2 The structure of a generic polydimethylsiloxane polymer.

This thesis is composed of two major areas within the general framework of organosilicon biotechnology. First, a discussion will be presented concerning the amino acid

and enzyme-mediated hydrolysis and condensation of alkoxysilanes under mild conditions. The use of enzymes was developed as a solvent-free alternative to the more traditional sol-gel processing of alkoxysilane, which is performed using low molecular weight alcohols as solvent, and carried out under acidic or alkaline conditions. These processing parameters are not necessarily conducive to the long term functioning of proteins, which can often be denatured in aqueous alcohol solvent systems. Three enzymes, representing two major enzyme families, the serine and aspartic acid proteases, were used to produce organically modified silica, in the form of sols, gels and amorphous monoliths. The relative rates of hydrolysis of phenyltrimethoxysilane by trypsin, α-chymotrypsin and pepsin were compared. The mode of catalysis and the environment within the binding pocket of the enzyme contributed to differences in hydrolysis rates.

The second part of this thesis will discuss the use of lipases as catalysts for synthesizing polyesters (**4**) and polyamides (**5**) containing siloxane subunits along the polymer backbone (**Figure 3**). While several proteases and lipases were screened for their capacity to synthesize polyesters, the enzyme that will receive the majority of the focus in this part of the thesis will be lipase B from *C. antarctica*, which is immobilized on a macroporous acrylic resin and is sold by Novozymes under the trade name Novozym-435® (N435).

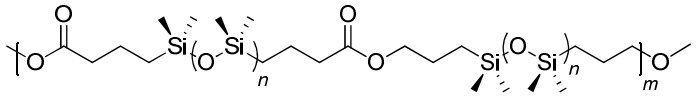

4

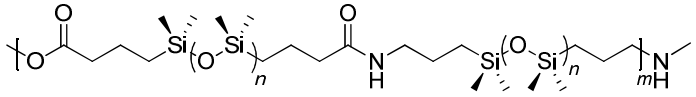

5

Figure 3 A siloxane-containing polyester (**4**) and polyamide (**5**).

This portion of the thesis will include an examination of the kinetics of polymer elongation for both polyester and polyamide synthesis. A discussion will be offered pertaining to: (i) the effect of changing the molecular weight of the acyl acceptor, resulting from an increase in the number of dimethylsiloxy repeat units, on the polymerization kinetics, and (ii) the effect on the polymerization kinetics of interchanging the acyl acceptor from a diol to a diamine for both the disiloxane- and polysiloxane-based systems. These model systems were examined to provide a proof of concept for the use of enzymes as potential catalysts for the synthesis of cross-linked silicone elastomers and branched polymers. The last portion of this section will present our results in this particular area.

Immobilization of enzymes onto solid supports has been thought to increase the thermal stability of the enzyme. The residual activity of N435 was examined after the polyesterification of disiloxane-containing monomers. Residual activity was determined by measuring the production of octyl palmitate from 1-octanol and palmitic acid. The residual activity was consistently found to be 90-100% of the activity of a virgin batch of N435. These results prompted a study of the thermal tolerance of the enzyme catalyst. The thermal tolerance and repeated use of N435 was examined to provide a proof of concept for the industrial use of N435 as a potential catalyst for producing siloxane containing polyesters.

2 Historical

2.1 Silica Biochemistry

Many marine organisms and terrestrial plants have evolved complicated molecular mechanisms that process silicic acid, although some evidence suggests that sodium silicate is a suitable substrate as well. These biomolecules, predominantly peptides and proteins, (in plants carbohydrates may be the important chemical species), act as catalysts, templates and/or scaffolds for the formation of frustules, spicules and other skeletal structures, and in some rare cases crystalline silica (quartz).[14,15] The silicatein proteins from *Tethya aurantia*[8-10] and *Suberites domuncula*,[11,12] the silaffins[5-7] and silacidins[4] from diatoms, and the biopolymer from *Equisetum* species[13-16] have been identified as biocatalysts that process dilute silicic acid into biogenic silica. Structural studies have identified important amino acids that are thought to facilitate the silica deposition process.

2.1.1 Diatoms

Diatoms are the primary model organisms for studying the relationship between biological systems and silica. Diatoms are thought to be the only organisms that have an obligate requirement for soluble silicic acid.[22] The dependence of diatom metabolic processes on silicic acid was studied by Volcani.[22,23] Ribonucleic acid (RNA) expression patterns are affected by changes in silicic acid availability and several silicon responsive messenger RNA transcripts from *Cylindratheca fusiformis* and *Thalassiosira pseudonana* have been identified.[23,24,25]

Diatom frustules are composed largely of inorganic silica and, to a smaller extent, also of an organic component.[26] The frustulins were identified as the major organic com-

ponent of the cell wall of *C. fusiformis*.[27] These Ca^{2+} dependent glycoproteins were originally thought to be the only necessary component for the cell wall deposition of silica, however, a second fraction of protein was recovered from hydrofluoric acid treated cell walls. Displaying a high affinity for silica, these proteins were termed silaffins for '*silica affinity*' proteins.[4,7]

The cell membrane of diatoms is not permeable to free silicic acid, which must therefore be actively transported across the cell membrane. This is accomplished via silicic acid-sodium/potassium symporters and results in the localization of silicic acid in the silica deposition vesicle (SDV) located just beneath the cell membrane.[28-30] Silicic acid transporters have been characterized in rice and corn and are evolutionarily related to the aquaporin family of transmembrane proteins. To date, there are no known homologs of the diatom silicic acid transport proteins in other marine or terrestrial organisms.[17]

Silicic acid transport and storage are highly regulated physiological processes. The intracellular concentration of soluble silica has been estimated to be several orders of magnitude higher than in the surrounding environment; some estimates are in the range of several hundred millimolar depending on the diatom species. At these high concentrations, autopolymerization should occur quickly in the absence of some stabilizing matrix such as a protein or other biomolecule.[1,17,31-33]

In addition to the frustulins, the silaffins constitute a major proportion of the organic material occluded within the diatom frustules. Silaffins have been isolated and characterized from *Cylindrotheca fusiformis* and *Thalassiosira pseudonana*. The amino acid sequences for the major silaffins, silaffin-$1A_1$, silaffin-$1A_2$, silaffin-1B and silaffin-2, have been determined. These peptides are highlighted by post-translational modifica-

tions, such as phosphorylated serine and tyrosine residues, as well as *N*-methyl propylamine and *N*,*N*-dimethyl propylamine modified lysines (**Figure 4**).[5] The unique ε-*N*,*N*,*N*-trimethyl-δ-hydroxylysine was identified for the first time in a protein although this post-translational modification was only found in silaffin-$1A_1$.[7] Lysine residues from *C. fusiformis* silaffins are appended with four to eight propylenimine repeat units; *T. pseudonana* silaffins possess only two propyleneimine units which are typically methylated.[34,35] Cationic moieties have been introduced into the propyleneimine units, through quaternerization of the amines by methylation.[35] Phosphorylation of silaffins is a requirement for silica precipitation.[36] The zwitterionic nature of the silaffins promotes not only silica deposition through electrostatic interactions, between the free amines and quaternary amines of the protein and silicic acid, but also by macromolecular self-assembly.[36]

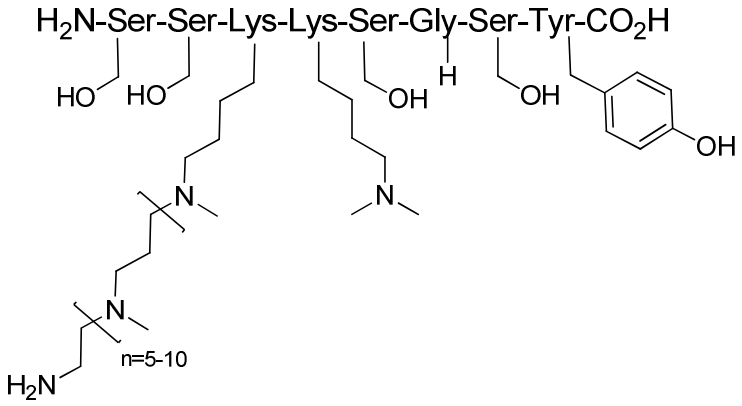

Figure 4 The primary amino acid sequence of a silaffin peptide isolated from the diatom *Cylindratheca fusiformis*. Reproduced from reference 5 (N. Kröger, R. Deutzman and M. Sumper. *Science*, **1999**, *286*, 1129-1133), reprinted with permission of AAAS.

The silica precipitating capacity of silaffin-1A is intimately dependent on the post-translationally modified lysine residues. *In vitro* silica precipitation assays with

silaffin-$1A_1$ and silaffin-$1A_2$ against metastable solutions of silicic acid produced spherical silica particles within seconds; only at pH 5 did silaffin-$1A_1$ precipitate less silica than silaffin-$1A_2$. Silaffins co-precipitate with silica suggesting that the peptides act as a structure-directing template as well as a catalyst. In the absence of any silaffin peptides, silica did not precipitate under the aforementioned conditions.

Three polypeptides were isolated from the cell wall of the diatom *T. pseudonana*.[4] These polypeptides contain a large fraction of serine, glutamic acid and aspartic acid residues and were coined 'silacidins'. Similar to the silaffins, the serine residues of the silacidins were phosphorylated. It has been proposed that the silacidins guide the assembly of long chain polyamines into macromolecular structures.[35] These structures precipitate silica in a concentration dependent manner. Theoretical models for the protein-mediated deposition of silicic acid by diatoms support the idea that serine- and threonine-rich regions of the protein may play an important role in depositing silica at the cell wall.[37,38]

In addition to the silaffins, several long chain polyamines (LCPs) have been isolated from the diatom *C. fusiformis*. These polyamines were originally identified as post-translational modifications of lysine residues and were shown to work synergistically with the silaffins to produce the diatom cell wall.[39] Unbound LCPs have been isolated from *C. fusiformis*, *Nitzschia angularis*, *Chaetoceros debilis*, *Chaetoceros didymium*, *Eucampia zodiacus*, *Stephanopyxis turris*, *Coscinodiscus asteromphalus*, *Coscinodiscus wailesii*, *Coscinodiscus granii* and *Axinyssa aculeate.*[40,41] These LCPs exhibit species-specific patterning and are highly variable in chain length.

Long chain polyamines from *N. angularis* profoundly affect the morphology of precipitated silica. LCPs generally formed spherical silica; however, the presence of

silaffins facilitated the aggregation of the spherical silica into sheet-like structures. Sumper proposed a phase separation model which accounted for the interaction between polyamines and silicic acid in the silica deposition vesicle.[42] This model made the suggestion that LCPs play a role in precipitating silica and pattern formation.

2.1.2 Sea Sponges

Marine sponges express a series of homologous genes that encode for silica precipitating proteins, the silicateins (α, β and γ in a 12:6:1 ratio respectively). These proteins were first isolated from the desmosponges *Tethya aurantia*8 and *Suberites domuncula*8 and, more recently, from the hexactinellid sponge *Monorhaphis chuni*.[43] The silicateins act as both a catalyst and a template for silica deposition.8 Silicatein from *Tethya aurantia* exhibits a structural homology to the cathepsin and papain families of cysteine proteases.[9] Unlike the cysteine proteases, silicatein possesses a catalytic serine residue instead of the characteristic cysteine, making the enzyme catalytically homologous to the serine family of hydrolases.[8-10]

Silicatein filaments from *T. aurantia* hydrolyzed tetraethoxysilane and phenyltriethoxysilane under buffered conditions.[9] Heat denatured silicatein precipitated 90% less silica compared to silicatein with an intact active site. Site directed mutagenesis of the serine and histidine residues (replacing each with alanine) within the active site completely inhibited silica precipitation, suggesting a vital role for these residues in catalysis. The silica esterase capacity of silicatein from *S. domuncula* was examined using the artificial substrate bis(*p*-nitrophenoxy)-dimethylsilane.[43] The Michealis-Menten constant (K_M) was found to be 22.7 μM as compared to a K_M of 1.1 μM for cathepsin L, the closest re-

lated enzyme to silicatein, using benzyloxycarbonyl-Phe-Arg-4-methylcoumarin-7-amide as a substrate.[43]

A mechanism explaining the hydrolysis of tetraethoxysilane by silicatein was proposed by Morse (**Figure 5**).[9,10] The key feature of this proposal was the nucleophilic addition of the catalytic Ser_{26} residue, which is made more nucleophilic by hydrogen bonding to the imidazole moiety of the neighbouring His_{165}, to the silicon atom of tetraethoxysilane with concomitant expulsion of ethanol. It was proposed that a silyl-enzyme intermediate was stabilized as a pentacoordinate silicate by donation of electron density from the sp^2 hybridized nitrogen of the imidazole ring.[10] A model study using a series of imidazole containing alkoxytriphenylsilanes suggested that the imidazole moiety was not coordinated to the silicon centre; however, steric considerations may have been responsible for this observation.[44] The final steps of hydrolysis followed those which are known for peptide hydrolysis, whereby water enters the active site of the enzyme and cleaves the silyl-enzyme intermediate, liberating triethoxysilanol and restoring the active site to a catalytically competent state.

A computational study on the condensation of silicic acid by silicatein from *Suberites domuncula* favoured serine addition to the silicon atom (**Figure 6**).[45] This mechanism also favoured a pentacoordinate silicon atom instead of a direct S_N2 type mechanism. The key difference in this mechanism was the nucleophilic addition of the enzyme bound silicic acid to a second, and then a third molecule of silicic acid to form a linear trimer, which then cyclises to liberate the enzyme from trisilicic acid.

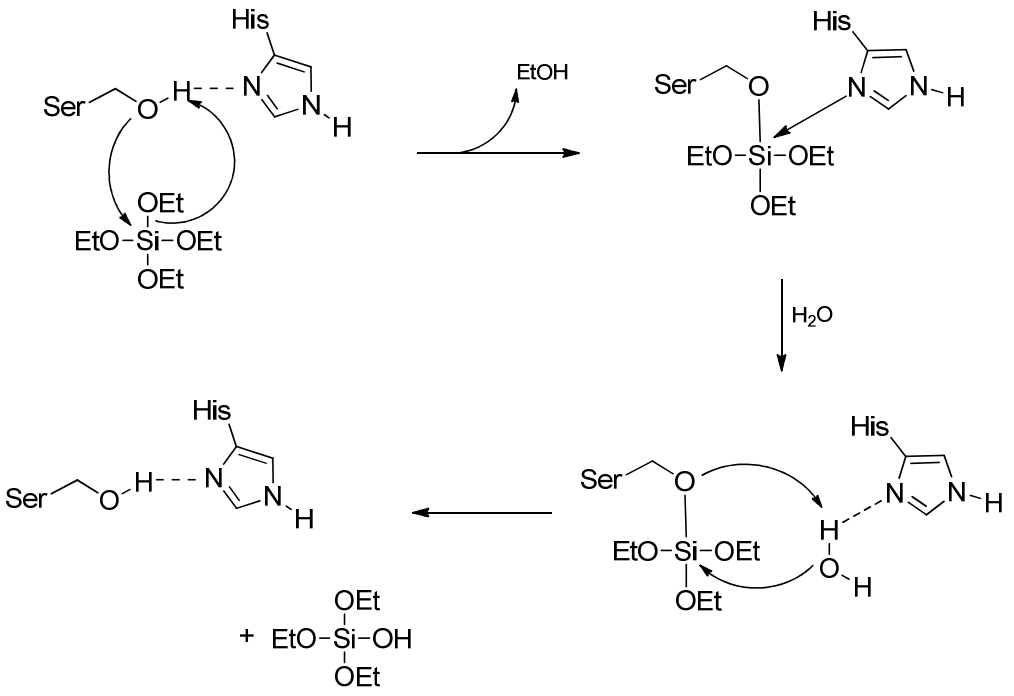

Figure 5 The proposed mechanism of TEOS hydrolysis by silicatein from *Tethya aurantia*. Hydrolysis is dependent upon serine and histidine residues within the active site of the enzyme. Reproduced with permission from reference 9 (J.N. Cha, K. Shimizu, Y. Zhou, S.C. Christensen, B.F. Chmelka, G.D. Stucky and D.E. Morse. *Proc. Natl. Acad. Sci. USA.*, **1999**, *96*, 361-360).

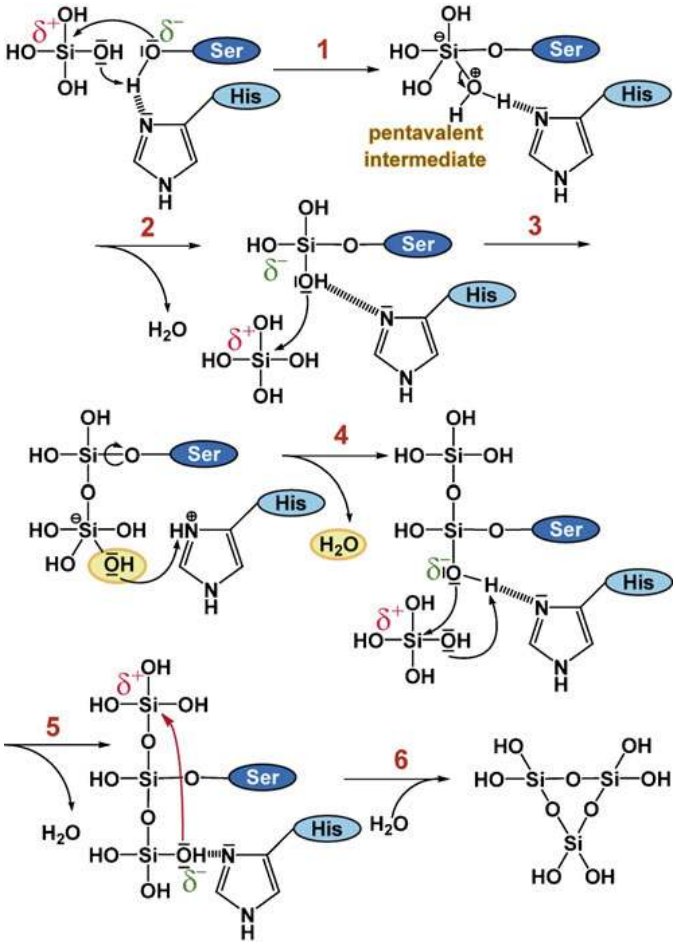

Figure 6 The proposed mechanism for the silicatein-mediated cyclization of silicic acid monomers into trisilicic acid. Reproduced with permission from reference 45 (H.C. Schröder, M. Weins, U. Schloβmacher, D. Brandt, and W.E.G. Müller. *Silicon*, **2012**, *4*, 33-38).

2.1.3 Terrestrial Plants

Terrestrial plants are known to accumulate biogenic silica in the cell wall, the cell lumen, and as extracellular deposits. The cash crops corn (*Zea mays*) and rice (*Oryza sativa*) are frequently studied for their ability to uptake silica from their local environment. Like diatoms, the extracellular silica deposits of some plants can be used as a taxonomic characteristic long after the organic portion of the plant has decomposed, particularly in the Genus *Equisetum*.[46,47]

Of particular interest is the biopolymer from *Equisetum telmateia*, which contains a serine, glutamic acid, and glycine rich peptide and an associated carbohydrate that is rich in xylose and glucose.[13] The combination of the *Equisetum* extract and a silicic acid solution derived from dipotassium-triscatecholatosilicate afforded a 22% increase in the rate of trimer formation.[13] Electron diffraction patterns suggested that some of the silica that was precipitated may have been quartz.[13] Crystalline silica was also extracted from *Equisetum hyemale*.[15]

2.2 Silica Biotechnology

2.2.1 General Comments

The discovery that sea sponges, diatoms and some plants could direct the deposition of silica prompted a number of independent studies focusing on biomimetic approaches for tailoring silica-derived materials. Biomimetic approaches endeavour to design catalysts that have features mimicking those found in living organisms. The following section will provide a brief review of some of the current biomimetic approaches that have been reported for producing tailored silica materials. This section of the thesis will begin with a description of the sol-gel processing of silicate materials and will be fol-

lowed by three sections consisting of brief reviews of silicate materials formed by: (1) amino acids, (2) artificial polymers, and (3) non-silicon processing proteins.

2.2.2 Sol-Gel Processing of Alkoxysilanes

Brinker and Scherer defined the sol-gel process as the preparation of ceramic materials by the preparation of a sol, gelation of the sol, and removal of the solvent.[48] The hydrolysis and condensation of silicic acid precursors during the formation of a silicate gel was originally thought to be analogous to the synthesis of organic polymers. However, Carmen proposed that silica gel formation was a two stage process in which particle size gradually increased, until at a concentration of approximately 1% the particles condensed to yield an open and continuous structure. [49] More specifically, the formation of *Si-O-Si* linkages increased the particles' size, while the formation of intermolecular *Si-O-Si* linkages connected particles together. This idea was elaborated upon by Iler, who described the polymerization of silicic acid as a process in which monomers condense to form discrete particles followed by the aggregation of particles into chains and random networks (i.e. Ostwald ripening).[1]

The sol-gel process can generally be partitioned into three reaction types, namely hydrolysis↔condensation, condensation to produce alcohol↔alcoholysis, and condensation to produce water↔hydrolysis; each of these reaction types exists as an equilibrium.[50] In theory, each of these reactions is reversible, but the equilibrium can be controlled by altering the reaction conditions. The rate of hydrolysis is dependent on the amount of water included, as has been shown by Pouxviel *et al.*[51] The first advantage to increased water is its ability to drive hydrolysis to completion. Furthermore, under low water con-

centrations, alcohol condensations are favoured, whereas in high water situations water condensations dominate; high water concentrations are expected to promote siloxane depolymerisation.[50]

Many studies have sought to probe the mechanism of alkoxysilane hydrolysis and condensation, as well as the kinetics of these processes.[52-55] The techniques that have typically been employed are Raman spectroscopy and small angle x-ray diffraction, but no technique is more valuable than ^{29}Si nuclear magnetic resonance (NMR) spectroscopy. ^{29}Si NMR has proven to be an invaluable technique in describing the reaction kinetics of sol-gel processing and has been used extensively in the last few decades.[52,56] ^{29}Si NMR is ideal not only for its quantitative nature, but also because it allows for the identification of each unique silicon resonance. Typically, as alkoxy groups are hydrolyzed to silanols, the ^{29}Si resonances shift down field with the chemical shifts becoming more positive. This trend appears to be the case for tetra- and tri- alkoxysilanes, but only under certain circumstances for di-substituted alkoxysilanes.[57] The hydrolysis of diethoxydimethylsilane under basic conditions mimicked this trend, but under acidic conditions the observed change in chemical shift was in the opposite direction.[57] Disiloxane bond formation results in an up-field shift to more negative chemical shift values. This trend reversed when small cyclic oligomers formed, which due to the increased ring strain, saw the ^{29}Si resonances shift down field.[58] The magnitude of change in the chemical shift of the ^{29}Si nucleus depends on the degree and the nature of the substitution on silicon. For example, ethoxytrimethylsilane has a ^{29}Si chemical shift of 21 ppm compared to diethoxydimethylsilane and tetraethoxysilane which, due to the electron withdrawing nature of the ethoxy groups, have chemical shifts of -4.3 ppm and -84 ppm respectively.

The utility of ^{29}Si NMR for the analysis of silicate species is impeded by the low abundance, only 4.7%, of the magnetically active isotope. The relative insensitivity of the silicon nucleus, which has a negative magnetic moment and magnetogyric ratio, requires that longer spin-lattice relaxing times be used to allow for all nuclei to return to their equilibrium ground state. Some characteristics of common NMR active nuclei (^{1}H, ^{13}C, and ^{19}F) and ^{29}Si are summarized in **Table 1**.[59]

Table 1 The magnetic properties of some common nuclei.[59]

Isotope	Natural Abundance (%)	Magnetic Moment (μ/μ_n)	Magnetogyric Ratio ($rad*T^{-1}s^{-1}$)	Larmor Frequency (MHz)	Relative Receptivity
^{1}H	99.985	4.8371	26.7510	100	5.68×10^{3}
^{13}C	1.108	1.2126	6.7263	25.145	1.000
^{19}F	100	4.5506	25.1665	94.094	4.73×10^{3}
^{29}Si	4.7	-0.9609	-5.3141	19.867	2.09

2.2.3 Amino Acid-Catalyzed Silica Formation

Scientists have been interested in biomineralization for many years. The interest in biomineralization is not only aroused by the intricate frameworks that organisms produce using inorganic minerals, such as silica and calcium carbonate, but also because it represents a mild method for producing commercially available materials. The mechanism by which diatoms direct the biosynthesis of frustules has been identified as being under genetic control. That is, specific peptides have been identified that interact with soluble silicic acid. For the most part, individual amino acid residues have been implicated in the biosilification process. To that end, the interaction between individual amino

acids and soluble silica had been studied with the dual goals of shedding light on biosilification and producing novel silica-derived materials.

Early work by Coradin and Livages examined the role of four amino acids (serine, lysine, proline and aspartic acid) in the polymerization of aqueous silicic acid under different pH regimes.[60] The addition of amino acids to sodium silicate solutions promoted the formation of polysilicates.[60]

In a more elaborate study into the role played by amino acids (glycine, arginine, aspargine, glutamine, glutamic acid, serine, threonine, tyrosine, proline, alanine, and lysine) in biosilica formation, Belton *et al.* determined the apparent 3rd order rate constant associated with silica condensation.[61] Amino acids affected the kinetics of silica condensation from small oligomer formation to larger aggregates, as well as the overall morphology and surface properties of the silicas. Amino acid hydrophobicity and the isoelectric point of each amino acid were contributing factors. Asparagine, lysine, glutamine, arginine and proline produced larger grains of silica and increased condensation rates. While proline produced larger grains of silica, there was no change in the 3rd order rate constant. Amino acids containing hydroxyl groups in their side chains, or hydrophobic amino acids, favoured the formation of smaller particles.[61]

The aforementioned studies focused on using amino acids to direct the formation of silica from pre-hydrolyzed silicic acid. There are a few studies which report on the hydrolysis of alkoxysilanes, most commonly teteraethoxysilane (TEOS), by individual amino acids or small amino acid oligomers. Sudheendra and Raju used lysine and serine under a neutral pH regime to hydrolyze TEOS.[62] Not surprisingly, the rate of hydrolysis, determined using the silicomolybdate method, which quantifies the amount of dissolved

silicomolybdic acid by determining the absorbance of the solution at 810 nm, was proportional to the amount of lysine or serine that was used.

Hartlen *et al.* prepared monodisperse silica particles using L-arginine from a biphasic system.[63] Their method produced silica spheres of about 25 nm in more than 40 independent trials. The narrow dispersity proved useful, in that the spheres could be used as silica seeds for the Stöber method. Silica nanoparticles have been prepared from sols containing TEOS, water and ethanol using varying amounts of lysine.[64,65] Nanoparticles were consistently found to have a narrow diameter range of 10-20 nm after hydrolysis and hydrothermal ageing. In related work, the emulsification of water and TEOS in the presence of lysine produced silica nanospheres with a diameter of 12 nm.[66]

When consideration is given to the above examples, the characteristic that is common to the amino acids that have been successfully used to hydrolyze TEOS is that they are basic and remain ionized over a large pH range. Lysine and arginine both have a basic side chain consisting of an amino group or a guanidine group, which when protonated can participate in hydrogen bonding with anionic silicate species.

2.2.4 Polymer-Catalyzed Silica Formation

By far most of the work involving amino acids as catalysts for silica formation has focused on the use of variable length homo polypeptides and block copolypeptides. Generally speaking, the architecture of the silica derived from homo-peptides is dependent on the length of the polypeptide chain, the amino acids in the polypeptide and the solution phase conformation of the peptide chain; the structure is dependent upon whether the polypeptide is in an α-helical, β-sheet, or random coil configuration. Polylysine is the

most studied of the homo polypeptides.[60,61,67-75] Other polymers such as poly-L-proline,[60] poly-L-aspartic acid,[60] poly-L-serine,[60] poly-L-histidine,[76,77] poly-L-arginine,[78] poly-L-cysteine,[79] and poly-L-glycine,[61] and the block copolypeptides poly(L-cysteine-*b*-L-lysine)[79] have received somewhat less attention.

Poly-L-lysine (PLL), when combined with a suitable silica precursor such as pre-hydrolyzed tetramethoxysilane or tetraethoxysilane, sodium silicate, or potassium tris(catecholato)silane [$K_2(Si(C_6H_4O_2)^{2-})$] under mild aqueous conditions, promoted the precipitation of silica spheres. It is noteworthy that PLL deposited onto a polycarbonate membrane directed the formation of hollow silica tubes which could be isolated upon $CHCl_3$ dissolution of the polycarbonate membrane.[72]

Tomczak and co-workers reported the synthesis of hexagonal silica platelets from phosphate buffered solutions of PLL.[75] The average degree of polymerization of the PLL affected the morphology of the silica. When poly-L-lysine of 20 repeat units (PLL_{20}) was used, only spherical silica was produced, while PLL_{222} directed the synthesis of hexagonal silica plates. Circular dichroism (CD) spectroscopy suggested that the PLL_{222} transitioned from a random coil to a helical structure when combined with the silica precursor in solution. A model accounting for the synthesis of silica hexagons proposed that PLL interacted with the silica precursors in the solution through hydrogen bonding and electrostatic interactions (**Figure 7**). These interactions brought neighbouring reactive silica species closer together so that condensation was favoured leading to the transition from a random coil to an α-helical PLL structure.[75]

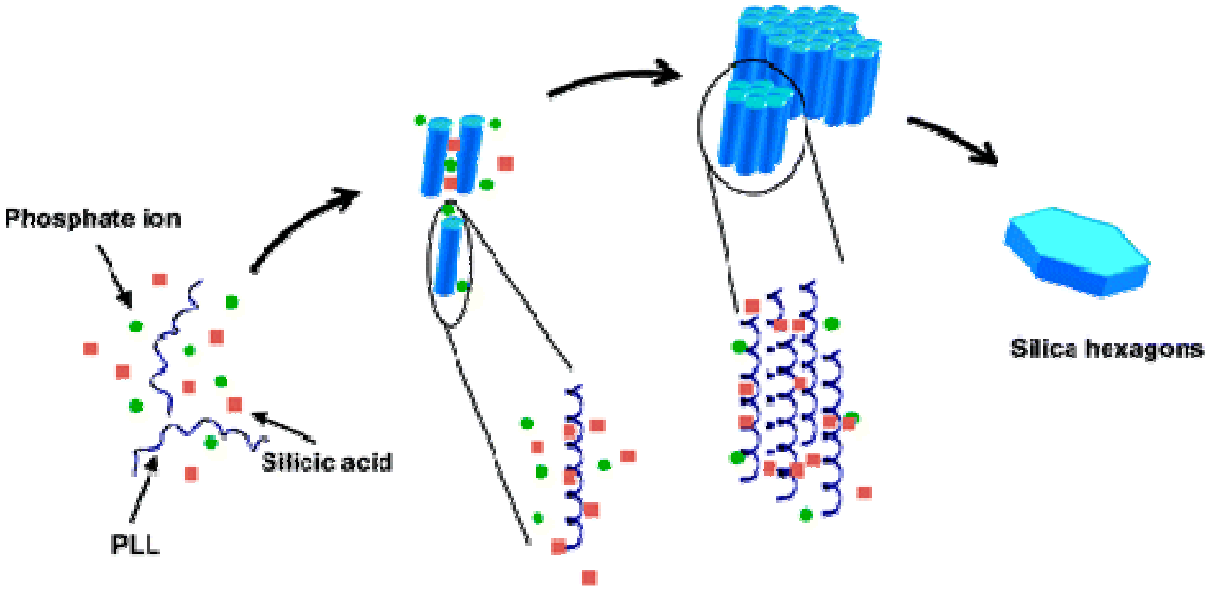

Figure 7 A proposed model for the formation of hexagonal silica from phosphate buffered solution. Reprinted with permission from reference 76 (M.M. Tomczak, D.D. Glawe, L.F. Drummy, C.G. Lawrence, M.O. Stone, C.C. Perry, D.J. Pochan, T.J. Deming, and R.R.Naik. *J. Am. Chem. Soc.*, **2005**, *127*, 12577-12582), © 2005 American Chemical Society.

Patwardhan *et al.* further studied the silica directing capacity of PLL in various spatial conformations.[74] In their study PLL, derived from L-lysine or D-lysine, in α-helical and β-sheet conformations was used to produce hexagonal sheets of silica. The authors unambiguously illustrated that the secondary structural conformation of PLL was a prerequisite for the formation of hexagonally shaped silica. PLL in the α-helical form was converted to a β-sheet conformation by heating and cooling cycles. CD spectroscopy confirmed the helix-sheet structural switch of the PLL. When PLL was combined with buffered pre-hydrolyzed tetramethoxysilane (TMOS) solutions, only spherical silica precipitated.

Cha *et al.* reported the synthesis of ordered silica structures using polypeptides as catalysts to perform the hydrolysis and condensation of TEOS under aqueous buffered conditions.[79] Oligomers of L-lysine, L-histidine, D/L-serine, L-threonine and L-glutamic

acid dissolved in pH 7 buffer did not display any capacity to perform the hydrolysis of TEOS over a 24 hour period. In contrast to these findings, polymers of L-cysteine efficiently catalyzed the hydrolysis and subsequent condensation of TEOS to amorphous silica when handled under an inert atmosphere. Similar reactions performed under air resulted in lower hydrolytic activity towards TEOS due to the oxidation of the sulfhydryl groups of the peptide. Combining hydrophobic poly-L-cysteine blocks with hydrophilic PPL or poly-L-glutamate blocks lead to variable results. The anionic block copolypeptide containing glutamate suppressed all hydrolytic activity that was present in the poly-L-cysteine. The cationic block copolypeptides containing PLL and poly-L-cysteine displayed enhanced hydrolytic activity as a result of the increasing nucleophilicity of the copolymer. These polypeptides produced mesoporous spherical silica. An increase in the length of the cysteine block afforded a slight change in the morphology of the silica from spherical to elongate.

2.2.5 Protein-Mediated Silica Formation

Since the discovery of the silicatein proteins from *Tethya aurantia* and *Suberites domuncula*, many other enzymes have been screened as a part of ongoing research into the application of enzymes for the controlled synthesis of silica. The Morse group demonstrated the hydrolytic capacity of silicatein towards TEOS and phenyltriethoxysilane under ambient conditions.[9] Immobilization of a histidine-tagged silicatein onto a gold surface had little effect on the hydrolysis and condensation of TEOS.[80]

Building on these observations, the Zelisko group found trypsin, a serine protease, to have the capacity to hydrolyze TEOS in the presence of α,ω-bis(2-triethoxysilylethyl)-

polydimethylsiloxane (TES-PDMS, **6**) (**Figure 8**). The biogenic silica cross-linked with the TES-PDMS to form PDMS elastomers (**7**) that were visually and microscopically indistinguishable from those elastomers produced using dibutyltin dilaurate as a catalyst.[81,82]

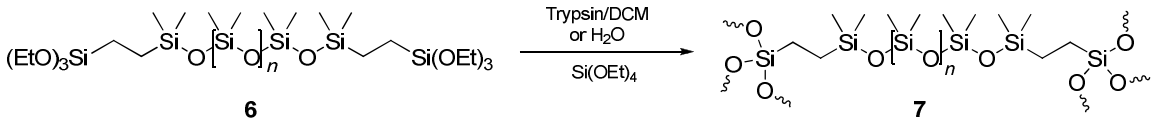

Figure 8 Silicone elastomers produced via the trypsin-mediated hydrolysis and condensation of TEOS and **6**.[81,82]

In related work, Coradin *et al.* compared the silica precipitating capacity of lysozyme and bovine serum albumin (BSA) at pH 4.7 and 7.2 using sodium silicate as a silica source.[83] Neutral solutions of lysozyme precipitated silica-lysozyme composites, whereas BSA solutions favoured gel formation under acidic conditions. The observed BSA-silica interactions suggested that the aggregation of BSA was responsible for controlling the size of the silica particles in a manner reminiscent of the natural biomineralization process. Increasing the amount of lysozyme did not increase the weight content of silica which remained uniform at 50±5%. Increases in the BSA content actually lead to a decrease in the quantity of silica that was precipitated, reducing it from 65±5% down to 45±5%.

2.3 Microorganisms in Organosilicon Chemistry

(Portions of the following sections (2.3, 2.4, and 2.5) have been previously published as part of the following review: M.B. Frampton and P.M. Zelisko, *Silicon*, **2009**, *1*, 147-169.)

Biocatalysis can afford access to chemical species that are not easily obtainable by traditional synthetic methods, or that require a substantial input of energy. Optically active organosilicon compounds are an attractive alternative to traditional pharmocophores and are thought to possess novel bio-physicochemical properties without requiring a drastic alteration to the overall geometry of the parent organic skeleton.

Prior to the 1980s microbial transformation of organosilicon compounds was an unexplored synthetic method. An extensive suite of fungi and bacteria were commonly used to mediate biotransformations of organic substrates, but this technology was slow to penetrate into organosilicon chemistry. The first report of biocatalytic activity involving an organosilicon substrate was published in 1983 by Tacke.[84] This seminal work employed the fungus *Kloeckera corticis* to enantioselectively reduce trimethylsilylalkyl acetoacetate **9** to the corresponding (+)-3-(*S*)-hydroxybutanoate **11**. The larger steric contribution from silicon did not deleteriously affect enzyme function. In fact higher yields were achieved compared to the carbon analog (**8**), with enantioselectivity reaching 80% enantiomeric excess (ee) in some cases.

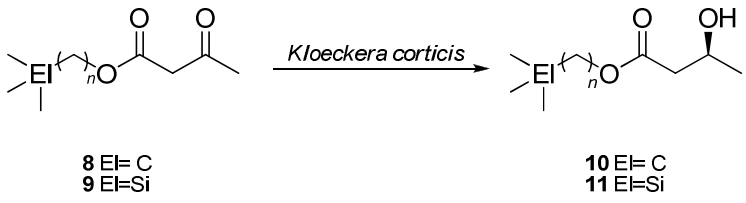

Figure 9 The stereoselective reduction of trimethylsilylalkyl acetoacetates by *K. corticis*.[84]

In a larger survey, more than one hundred fungal, bacterial and algal cultures were screened for the capacity to reduce acetyldimethylphenylsilane (**12**).[85] This work was instrumental in demonstrating that microorganisms from different Kingdoms could transform organosilicon compounds. The majority of the cultures that were assayed successfully carried out the enantioselective reduction of **12.** Actively growing cultures of *Trigonopsis variablis* (DSM 70714) furnished (*R*)-(1-hydroxyethyl)phenyldimethylsilane (**13**) in 54% yield and 62-88% ee while resting cells furnished **13** in 70% yield and 86% ee (**Figure 10**).[85]

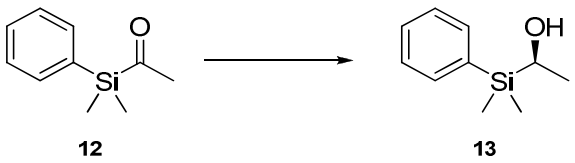

12 **13**

Figure 10 The enzymatic reduction of (acetyl)phenyldimethylsilane.[85]

A series of experiments revealed that the enantiomeric excess of the conversion was entirely dependent upon the concentration of the substrate.[85] At higher concentrations, both substrate and products appeared to inhibit enzymatic activity in resting and growing cultures. Furthermore, an increased proportion of the by-product 1,1,3,3-tetramethyl-1,3-diphenyldisiloxane was observed. While the authors do not speculate how this by-product arises, a silyl migration in the form of a [1,2]-Brook Rearrangement was likely. It was promising to note that the same cell mass could be reused multiple times before losing a significant amount of activity. Interestingly, the germanium analog, acetyldimethylphenylgermane, was also accepted as a substrate by *T. variablis*. In fact,

both the silicon and germanium analogs were reduced to a greater extent than their carbon counterpart, 3-methyl-3-phenyl-2-butanone.[86] Silicon and germanium afford a local reduction in the steric bulk near the carbonyl group due to longer *Si-C* (1.86 Å) and *Ge-C* (1.75 Å) bond lengths, compared to the average *C-C* bond (1.53Å), that are proximal to the acyl group which may be conducive to facilitating the reduction. The authors proposed that a single enzyme was not likely to be responsible for generating the chiral organosilane but that a series of enzymes may have been activated in a manner similar to that seen for the reduction of β-ketoesters by *Sacharomyces cerevisea*.[87,88] The identity of the enzyme system responsible for the reduction was never confirmed.

A 2001 study probing the capacity of the oxidoreductase systems of *S. cerevisea* to act upon several acylsilanes (**14a-j**) determined that this particular strain of baker's yeast was capable of efficiently reducing organosilicon compounds (**Figure 11** and **Table 2**).[89] The steric bulk of the substituent at silicon and the α-carbon were varied and all of the challenge compounds were processed to some extent. When silicon was functionalized with a phenyl ring the reaction yield was poor, except for **14b**, and enantioselectivity was low to moderate (**Table 2**). The enantiomeric purity of the products ranged from 0-95%. It was thought that the low enantiomeric purity was a result of competing oxidoreductase systems with opposite selectivity.

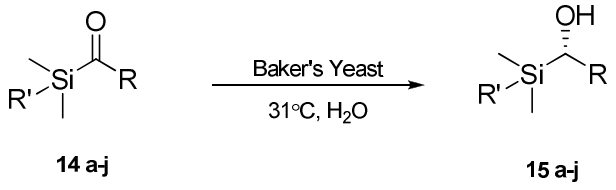

Figure 11 Baker's yeast reduction of acyl silanes.[89]

Table 2 The reduction of organosilicon compounds by Baker's Yeast at 31°C.[89]

Silane	R	R'	Time	Recovered **14**	Yield **15**	%ee **15**
14a	Ph	Me	20 h	5%	**15a** 65%	>95 (*S*)
14b	Ph	Ph	3 days	27%	**15b** 86%	42 (*S*)
14c	*p*-F-C_6H_5	Ph	9 days	90%	**15c** trace	--
14d	cyclohexyl	Me	5 days	75%	**15d** 44%	15 (*S*)
14e	cyclohexyl	Ph	3 days	100%	--	--
14f	n-propyl	Me	18 h	0%	**15f** 70%	60 (*S*)
14g	2-pentyl	Me	2 days	30%	**15g** 54%	35 (n.s.)
14h	(5-glyceropentyl)	Me	18 h	0%	**15h** 65%	43 (n.s)
14i	3-hydroxy-4-phenyl	Me	6 h	0%	**15i** >95%	n.a (4:1 syn:anti)
14j	(2-carboxyethyl) OMe	Ph	20 h	>10%	**15j** 35%	30

While most of the organosilicon compounds that had been reduced by microorganisms were acyclic, later studies focused on the reduction of cyclic organosilanes. Cultures of *K. corticis* were successful in mediating the enantioselective reduction of 1,1-dimethyl-1-sila-cyclohexan-2-one (**16**) to (*R*)-1,1-dimethyl-1-sila-cyclohexan-2-ol (**17**), in a 60% yield and 92% ee.[90] The conversion of **16** to **17** was complete after sixteen hours of incubation at 27°C and similar to a previous report using *T. variablis*,[85] the enantiomeric purity of the product was dependent on substrate concentration. Increasing the substrate concentration from 0.5g/L to 1.0 g/L afforded higher yields, 80% compared to 60%, but enantiopurity was reduced from 92% ee to 82% ee.

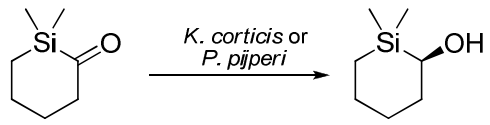

16 **17**

Figure 12 The enantioselective reduction of 1,1-dimethyl-1-*sila*-cyclohexane-2-one.[90]

Similar to **16**, 1-methyl-1-phenyl-1-sila-cyclohexan-2-one (**18**) was accepted by *K. corticis*.[91] From the racemate of **18**, *K. corticis* cells diastereoselectively reduced the α-silyl ketone to a racemic mixture of the (Si*S*, C*R*) and (Si*R*, C*S*) diastereomeric alcohols in 97% yield and 90% diastereomeric excess (de). The diastereomeric products (Si*R*, C*R*) and (Si*S*, C*S*) were detected in only small amounts. Following racemic acylation, *Pichia pijperi* (AT 20127) cells provided nearly optically pure (>96% ee) (*1R*, *2S*)-1-methyl-1-phenyl-1-sila-cyclohexan-2-ol in 60% yield.[91]

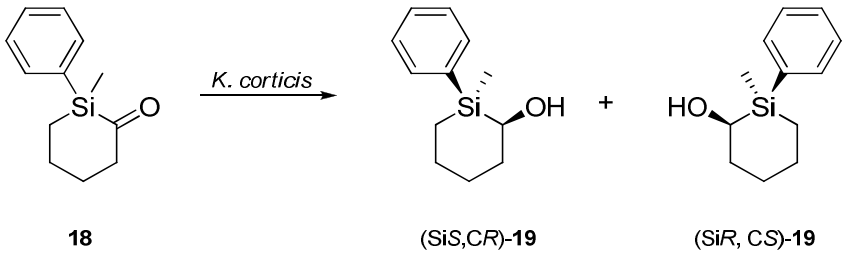

Figure 13 The enantioselective reduction of 1-phenyl-1-methyl-1-*sila*-cyclohexane-2-one.[91]

The chiral syntheses involving silicon containing compounds have focused on introducing chirality at carbon centres. One of the first contributions that focused on the resolution of a chiral silicon centre was published in 1991 by Tacke.[92] The fungus *Trigonopsis variablis* and the bacterium *Corynebacterium dioxydans* afforded the enantioselective reduction of acetyl(*t*-butyl)methylphenylsilane to (Si *R*, C *R*)- and (Si *S*, C *R*)- t-butyl(1-hydroxyethyl)methylphenylsilane from a racemic mixture of diastereomers.[92,93] *T. variablis* outperformed *C. dioxydans* by generating larger yields, 74% and 78% yield compared to 20% and 24% for the (Si *R*,C*R*) and (Si *S*,C*R*) diastereomers. Both microbial cultures reduced the acyl silane with greater than 97% ee.

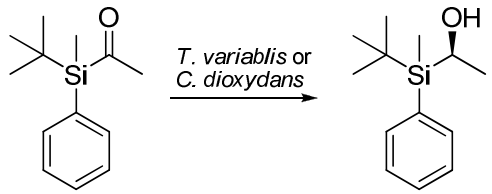

20 **21**

Figure 14 The reduction of acetyl(*t*-butyl)methylphenylsilane to give diastereomeric products.[92,93]

A report from Huber *et al*. involving resting cells from *T. variablis* further illustrated the effectiveness of this organism for carrying out chemical transformations. The reduction of the chiral acylsilane tert-butylmethyl(methoxyphenyl)acetylsilane (**22**) to the corresponding diastereomeric alcohols **(+)-23** and **(+)-24** was demonstrated.[94] Parallel experiments featuring immobilized resting cells and free cells of *T. variablis* produced yields of 70-95% with >96% ee. Immobilized cells repeatedly produced yields of 95% compared to only 70% when free cells were used. Immobilized *T. variablis* cultures were stable for periods of up to two weeks and could be reused in multiple reaction cycles whereas free cells needed to be used immediately. The activity of the free cells dissipated after only one day of storage at 4°C.

The relative rate of reduction by each cell preparation highlighted the differences between the conversion processes.[94] Initially, immobilized cells were less efficient than free cells due to diffusion limitations but by the end of the reaction the immobilized cells outpaced the production from cell suspensions. Increasing the substrate concentration was deleterious to the catalytic efficiency of the microorganism. Michaelis-Menton plots suggested that the optimal concentration of the substrate was 0.1 mg/mL, however, in the opinion of the authors, the reaction remained reasonably quick up to about 1.0 mg/mL

substrate eliciting a specific activity of 0.02 mmol/g/min compared to 0.06 mmol/g/min at 0.1 mg/mL of substrate.[94]

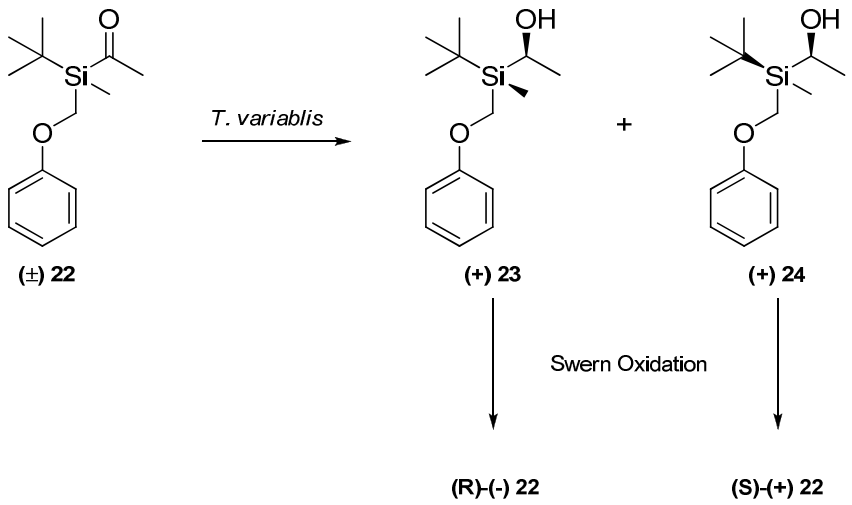

Figure 15 The bioreduction of acyl silane **22** using *T. variablis*.[94]

Microbial dioxygenation of aromatics is well understood thanks to pioneering research by Gibson.[95] The most common approach for dioxygenating aromatic rings uses recombinant *E.coli* expressing toluene dioxygenase (TDO) from *Pseudomonas putida*. A collaborative effort between Dow Corning and Genencor explored the dioxygenation of aryl silanes.[96] The goal was to explore microbial dioxygenation for the production of novel compounds for downstream application in silicon pharmaceuticals, polymer science, and optical materials (**Figure 16**). TDO accepted substrates **25**, **27**, **29**, **31**, **33**, and **35**; but of particular interest was the formation of the *cis*-diol from dimethylphenylvinylsilane (**25**) and dimethylphenylsilane (**27**).

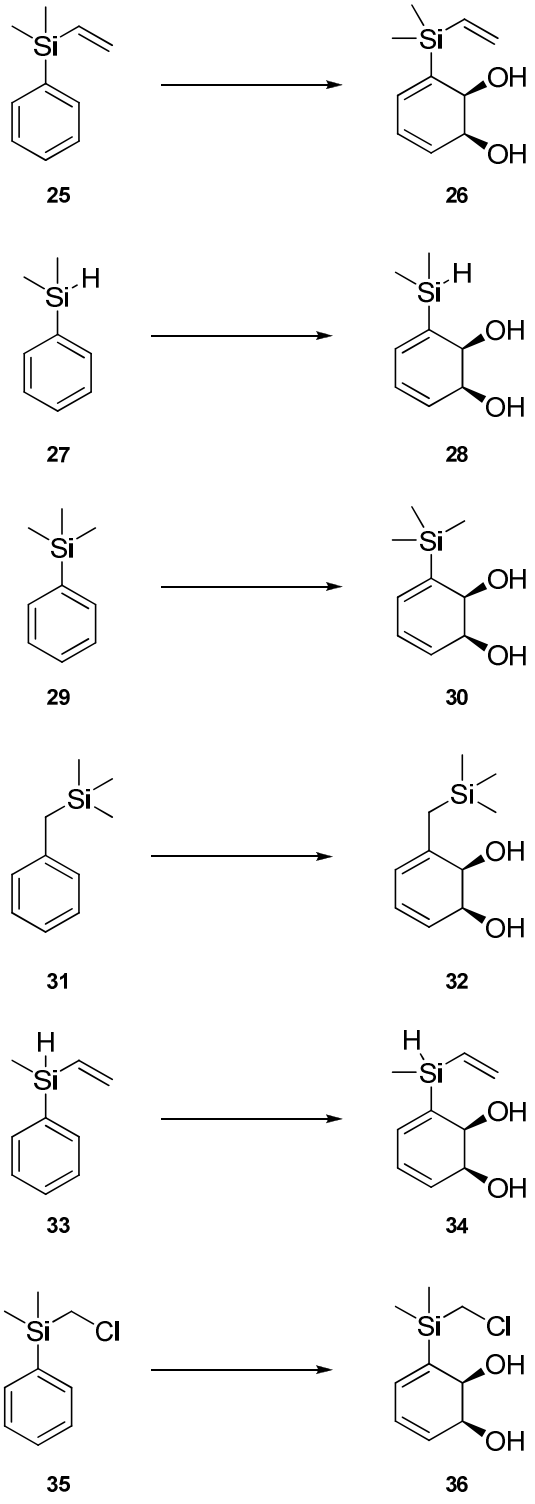

Figure 16 The microbial dioxygenation of aryl silanes.[96]

Most of the compounds could be isolated as the *cis*-diol if strongly acidic conditions were avoided; the exception to this was diol **32** which was found to eliminate water to give cation **37** as a silicon stabilized intermediate which after deprotonation gave *o*-phenol **38** (**Figure 17**).

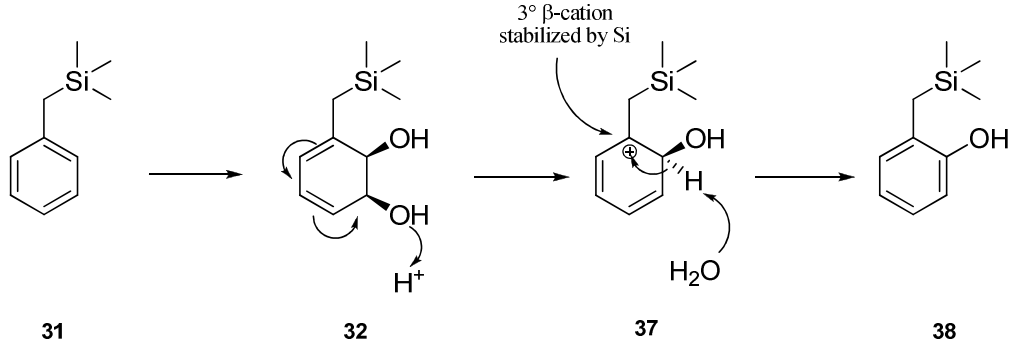

Figure 17 The proposed rearrangement of the *cis*-diol from benzyltrimethylsilane under acidic conditions.[96]

Focusing on silanes **25** and **27** for large scale conversions, the *cis*-diols were produced in 40% and 64% yield respectively; the enantiomeric excess for each diol was reported to be greater than 98% as determined using the ^{1}H NMR method reported by Resnick, Torok and Gibson.[97] Each diol was stable at -20°C for several months while at room temperature each was converted to a mixture of *ortho*- and *meta*- phenols.[96] Parallel experiments using naphthalene dioxygenase (NDO) indicated that the enzyme was less effective than TDO; none of the arylsilanes were converted into their corresponding *cis*-diol.

2.4 Enzymes in Organosilicon Chemistry

The intersection of traditional biochemistry and organosilicon chemistry is experiencing a renaissance due to such researchers as Bassindale, Müller, Morse, and Tacke.

A review by Ryabov in the 1991 illustrated some of the recent advances that resulted from the crossover of biochemistry and organometallic chemistry at that time.[98] The highlights of that review focused mainly on the achievements of Tacke as the primary contributor to the field of organosilicon biotechnology. Since the 1990s, several other groups have made an imprint in this field, particularly in the use of enzymes for mediating transformations of organosilicon compounds. The following section of this chapter will review the contributions and advances that have been made since the Ryabov review.

2.4.1 Enzymatic Resolutions of Organosilicon Compounds

The application of enzymes to facilitate organosilicon chemical transformations has seen a rebirth in the last decade coinciding with the explosion of research dedicated to the mechanism(s) underlying the formation of biogenic silica. Previous reports in organosilicon biotechnology typically used whole cell bioconversions. However, in 1989 Tacke used an enzymatic resolution strategy to resolve the racemate 1,1-dimethyl-1-*sila*-cyclohexan-2-ol (**39**) (**Figure 18**).[99] Initially racemic alcohol **39** was transformed into the racemic acetate ester **40** by treatment with acetic anhydride. Treatment of **40** with a lipase in water afforded the enantioselective hydrolysis of the (*S*)-acetate to regenerate the (*S*)-alcohol (*S*)-**39** with 95% ee. In an alternate approach, the lipase-mediated enantioselective esterification of **39** with triacetin in isooctane yielded acetate (*S*)-**40** with 96% ee.

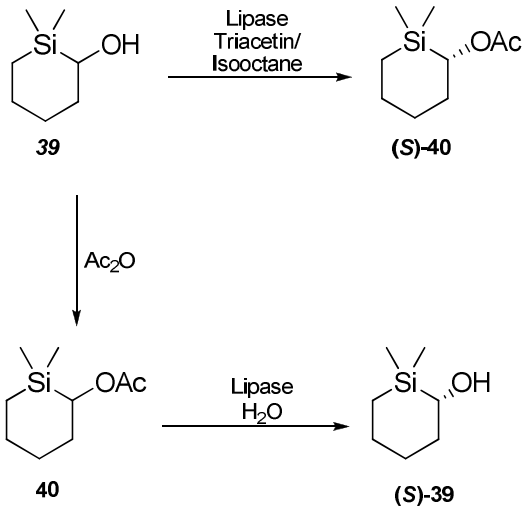

Figure 18 The resolution of 1,1-dimethyl-1-*sila*-cyclohexan-2-ol via two alternative enzymatic routes.[99]

Trimethylsilyl-containing alcohols were shown to be good acyl acceptors for *C. cylindracea* lipase-mediated resolutions of **41** (**Figure 19**).[100] With the exception of **42**, alcohols **43**, **44**, and **45** participated in the resolution of **41** by the enzyme which showed a preference for the *d*-isomer of the acid. Trimethylsilanol (**42**) was not a suitable resolving agent due to the susceptibility of silicon carboxylates to hydrolysis under aqueous conditions.[101]

Trimethylsilylmethanol (**43)** was an excellent substrate for the stereoselective esterification performed by lipase OF 360 from *C. cylindracea*; the rate of hydrolysis of **43** was approximately ten times greater than the rate of esterification using 2,2-dimethylpropanol.[100] Esterification using alcohol **43** was achieved with 96% ee, the highest among the silyl alcohols. A comparison of lipases from different sources showed that regardless of the source of the lipase, ester formation using **43** was preferred. The enzymes were ranked in the following order: lipase OF 360 (100) > lipase Saiken (29) >

lipase Steapsin (8), where the numbers in parentheses represent the relative rates of esterification of **42** and **43**.

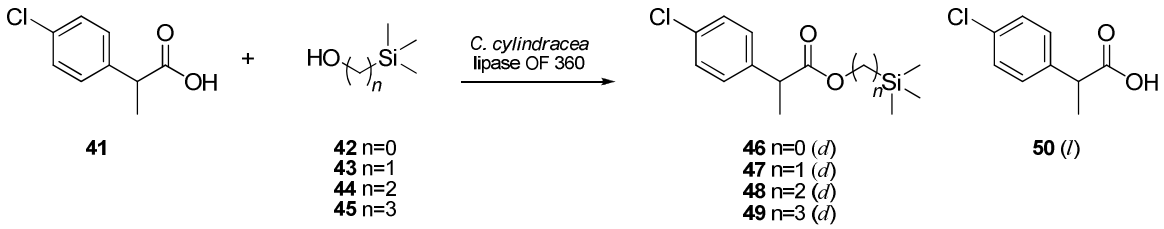

41

42 n=0
43 n=1
44 n=2
45 n=3

46 n=0 (*d*)
47 n=1 (*d*)
48 n=2 (*d*)
49 n=3 (*d*)

50 (*l*)

Figure 19 The resolution of a chiral acid by lipase OF 360 from *C. cylindratheca*, lipase Saiken 100, or lipase Steapsin.[100]

Subsequent to this report, racemic trimethylsilylpropanols **51-53** were used in the stereoselective esterification of 5-phenylpentyl esters by several lipases and esterases (lipase OF 360 from *Candida cylindracea*, lipase Saiken 100 from *Rhizopus japonicus*, lipase from hog pancreas (Steapsin), lipoprotein lipase Type A from *Pseudomonas* sp., and cholesterol esterase Type A from *Pseudomonas* sp.) (**Figure 20**).[111] Generally speaking, the enzymes preferentially esterified silylated alcohols **51b**, **52b**, and **53b**, affording greater yields compared to **51a**, **52a**, and **53a**. The trimethylsilyl moiety affected the stereoselectivity of the outcome as well as the relative esterification rates; α-hydroxyalkylsilane **51b** was processed faster than **51a**, while the rate of esterification of the β-hydroxyalkylsilanes **52b** and **53b** was comparable to **52a** and **53a**. A stereoselective reversal was observed in **56a** to **56b** from (*R*) to (*S*) respectively when lipase OF 360 was used.

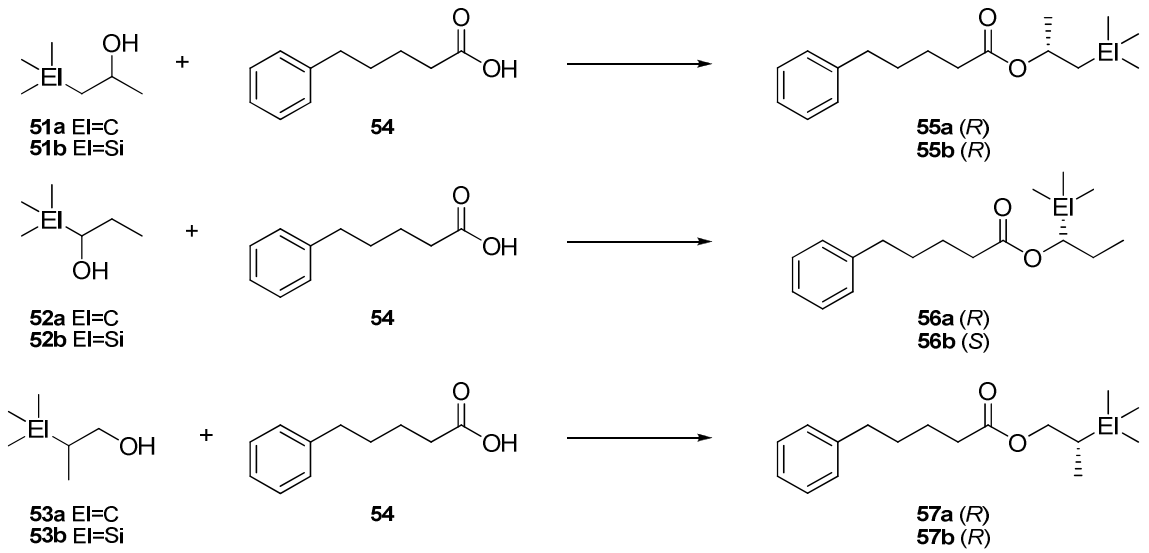

Figure 20 The use of 5-phenylpentanoic acid to resolve trimethylsilylpropanol isomers using five different hydrolases; E= C or Si. *Reaction conditions*: 100 mg lipase adsorbed onto 250 mg Celite 545 suspended in 10 mL of water saturated 2,2,4-trimethylpentane, 30°C with shaking at 120 strokes per min.[111]

De Jeso *et al*., examined the trimethylsilyl-substituted monoesters ethyl (2-trimethylsilyl)propanoate (**58**), ethyl (3-trimethylsilyl)butanoate (**59**), (3-trimethylsilyl)propyl acetate (**60**), and (4-trimethylsilyl)butyl acetate (**61**) as potential substrates for pig liver esterase (PLE), pig liver lipase, horse liver acetonic powder (HLAP) and α-chymotrypsin (**Figure 21**).[102] Esters **58** and **59** were hydrolyzed by PLE to give free carboxylic acids **62** and **63**, while a preparation of HLAP led to the hydrolysis of all the trimethylsilyl esters. α-Chymotrypsin on the other hand, did not display any hydrolytic capacity towards the chosen substrates. Pig liver esterase only hydrolyzed acetate **60**.[102]

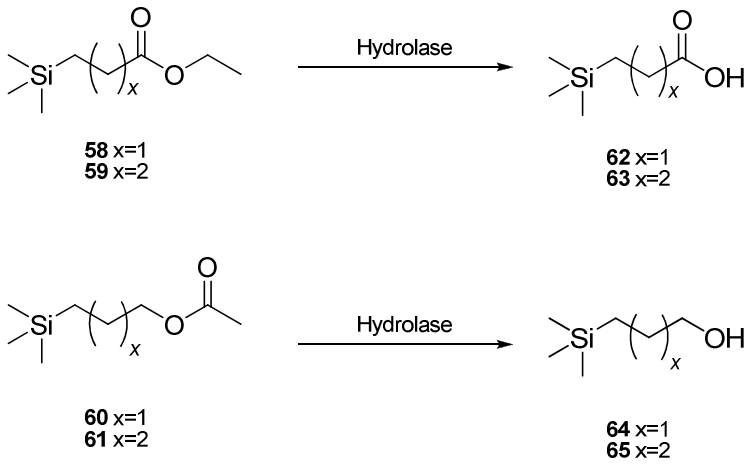

58 x=1
59 x=2

62 x=1
63 x=2

60 x=1
61 x=2

64 x=1
65 x=2

Figure 21 The hydrolysis of trimethylsilyl-substituted monoesters.[102]

Choosing to focus on HLAP and PLE as candidates for hydrolyzing prochiral malonate esters **66-68**, De Jeso *et al.* showed that the substituent alpha to the carbonyl dictated the stereochemical outcome of the reaction (**Figure 22**). While hydrolysis of the malonate esters was typically slow, high enantioselectivity could be realized providing the secondary substituent in the malonate ester was larger than hydrogen. When the malonate ester was substituted with a trimethylsilyl moiety and hydrogen, as in malonate ester **66**, enantioselectivity was low at only 10%.

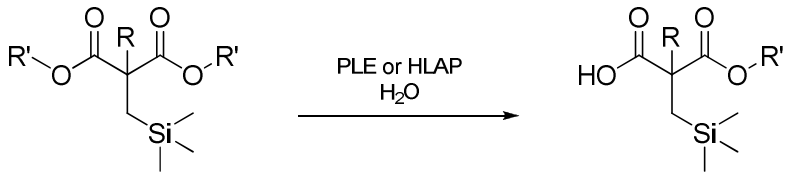

66 R=H, R'=Et
67 R=Me, R'=Et
68 R=R'=Me

69 R=H, R'=Et
70 R=Me, R'=Et
71 R=R'=Me

Figure 22 The stereoselective hydrolysis of substituted malonate esters by PLE and HLAP.[102]

Mixed ester **67** was hydrolyzed by PLE to give **70** in 70% yield with an enantiomeric excess of 80% in 20 hours. HLAP possessed a lower capacity for this transformation hydrolyzing **67** in only 50% yield with an ee of 71% in 144 hours. Dimethyl ester **68** was the better substrate for both enzymes. PLE gave 86% yield of **71** with 88% ee after 7.5 hours while HLAP gave 49% yield with 81% ee.

Santaneillo performed the stereoselective esterification of (*R,S*)-(+)-3-(diphenyl-*t*-butylsiloxy)-2-methylpropan-1-ol (**72**) with vinyl acetate (**73**) using *Pseudomonas fluorescens* lipase (**Figure 23**). The enzymatic reaction gave the corresponding (*S*)-acetate **74** in 39% yield and 98% ee.[103]

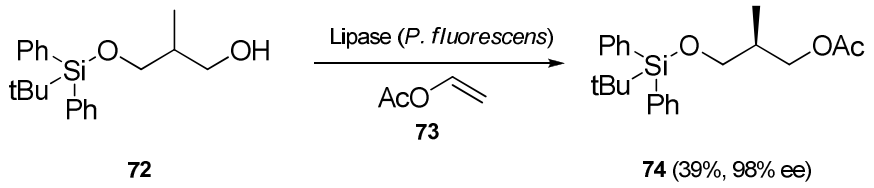

Figure 23 The selective acylation of an alkoxysilane by *Pseudomonas fluorescens* lipase.[103]

Similarly, lipases from *Candida cylindracea* and *Chromobacterium viscosum* selectively acylated 2-methyl-2-phenyl-2-*sila*-1,3-propandiol (**75**) and 2-methyl-2-*n*-octyl-2-*sila*-1,3-propandiol (**76**) using methyl isobutyrate (**81**) as solvent and acylating agent at -20°C (**Figure 24**).[104] Lipase from *C. cylindracea* produced esters **76** and **79** in 63% and 80% yields respectively with 75% and 70% ee; diesters **77** and **80** were produced in lower amounts (2% and 4% respectively). *C. viscosum* lipase furnished monoesters **76** and **79** in 70% and 50% yields with 76% and 70% ee respectively. As with the lipase from *C. cylindracea*, diesters **77** and **80** were produced in 25% and 9% yields respectively. In-

creasing the temperature from -20°C to -10°C, 0°C and 20°C, afforded higher reaction rates but the enantiomeric purity of the mono ester was sacrificed when *C. viscosum* was the biocatalyst; the enantiomeric excess decreased to 67%, 56% and 51% respectively. Poor reaction rates were reported when using **81** as an acylating agent with *C. viscosum* lipase. Acetoxime isobutyrate (**82**) was chosen as an acylating agent in isopropyl ether at 40°C to improve the esterification of **75** to **76**, 50% yield 70% ee, or in THF as solvent at 4°C to improve the esterification of **78** to **79** in 72% yield with 76% ee.

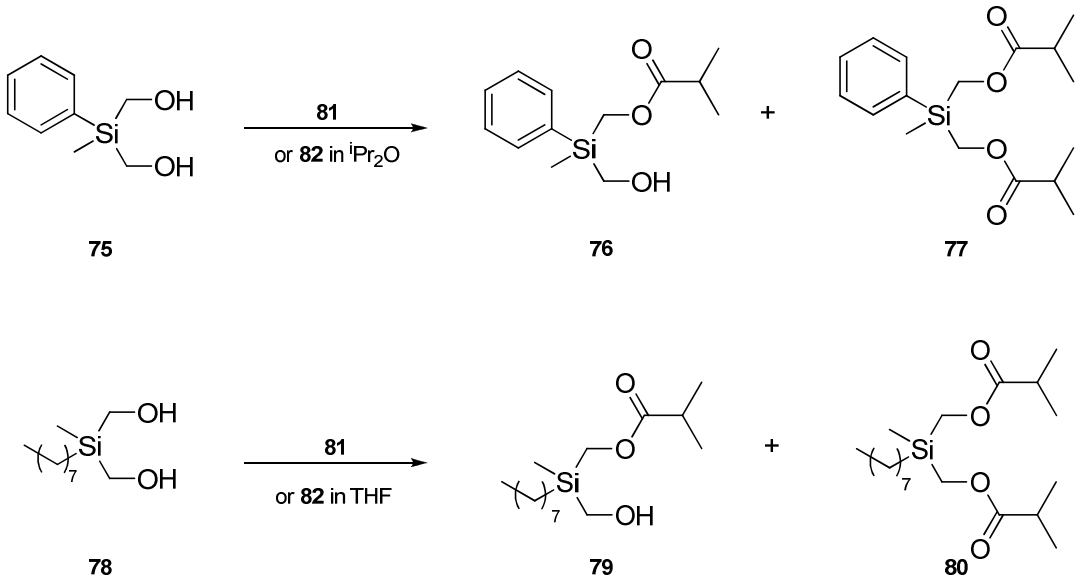

Figure 24 Enzymatic mono- and di-acylation of 2-*sila*-1,3-propanediols.[104]

Penicillin G acylase is an industrially important enzyme that is used in the synthesis of β-lactam antibiotics. Penicillin G acylase catalyzes the hydrolysis of penicillin G into phenylacetic acid and 6-aminopenicillinic acid.[105] The synthesis of phenyldimethyl(1-(phenylacetamido)ethyl)silane (**87**) was initiated by treating (1-chloromethyl)phenyldimethylsilane (**83**) with sec-butyl lithium in the presence of TMEDA in THF and followed by a methyl iodide quench to furnish 1-chloroethylsilane

(**84**) in 66% overall yield. Iodination with NaI in acetone gave acylsilane **85** which, when treated with ammonia, afforded the silylated amine **86** in 94% yield. Treatment of **86** with phenylacetic acid activated by Steglich's reagent to activate the carbonyl, gave **87** as a racemate in 82% yield (42% yield over 5 steps).

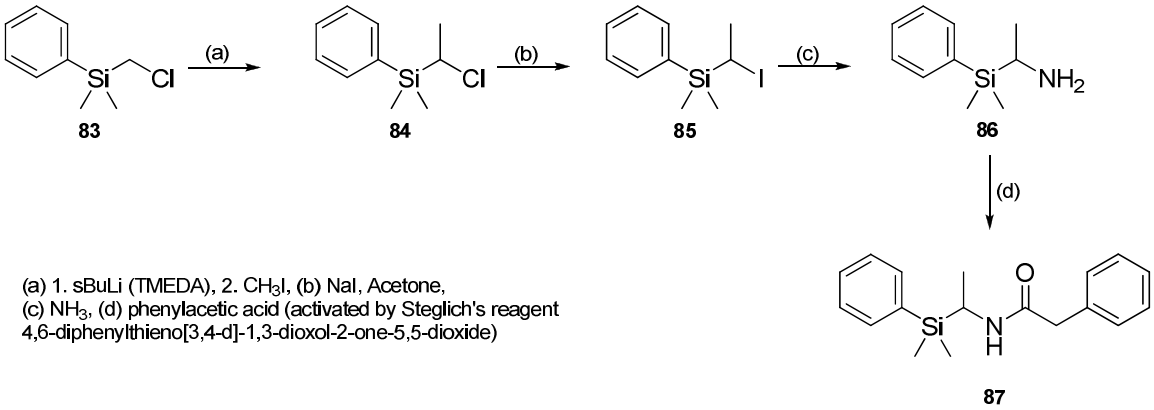

Figure 25 The synthesis of phenyldimethyl(1-(phenylacetamido)ethyl)silane.[106]

The enzymatic resolution of **87** using immobilized penicillin G acylase from *E. coli* afforded the (*R*)-enantiomer of **88** in 40% yield and 92% ee after only 3 hours (**Figure 26**).[106] The unreacted amide (*S*)-**87** was recovered in 50% yield. The optical purity and absolute configuration of **87** was determined by gas-liquid chromatography (GLC) and through ^{1}H NMR on the (*S*)-α-methoxy-α-trifluoromethylphenylacetic acid derivative of **87**.

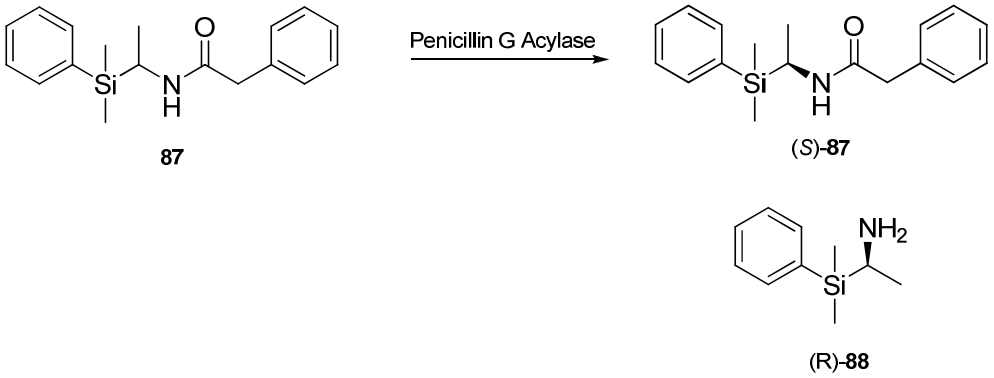

Figure 26 Enzymatic resolution of racemic dimethylphenyl(1-(phenylacetamido)ethyl)silane to *(R)*-(1-aminoethyl)dimethylphenylsilane by penicillin G acylase from *E. coli*.[105]

2.4.2 Enzymatic Oxidation and Reductions of Organosilicon Compounds

The asymmetric reduction of the carbonyl functional group is an important method for introducing chirality into organic molecules. Biologically this is accomplished using dehydrogenases or reductases. These enzymes are found ubiquitously in nature and are most commonly sourced from microorganisms. However, horse liver alcohol dehydrogenase is also commonly used. Horse-liver alcohol dehydrogenase (HLADH) is a dimeric Zn^{2+} assisted enzyme that catalyzes the oxidation of primary and secondary alcohols.[107] Tanaka and coworkers examined HLADH-mediated catalysis for the oxidation of trimethylsilylated alcohols (**Figure 27**).[108] The smallest alcohol, TMS-MeOH (**43**), could not be oxidized to aldehyde **89** by the enzyme. Trimethylsilylethanol (**44**) and trimethylsilylpropanol (**45**) were better candidates for enzymatic oxidation. These alcohols were easily oxidized by the enzyme to give the corresponding aldehydes **90** and **91**.

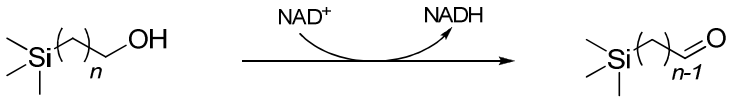

43 n=0
44 n=1
45 n=2

89 n=0
90 n=1
91 n=2

Figure 27 Horse liver alcohol dehydrogenase-catalyzed oxidation of trimethylsilyl-containing alcohols.[108]

Compound **43** could not be oxidized due to the increased electron density at the α-methylene position. This increased electron density made removing a hydride from this carbon unfavourable. Silicon, which is known to stabilize α-anions and β-cations, and to a lesser extent γ-cations, favours the removal of the hydride only from the β- or γ-positions. Binding of NAD^+ with HLADH, opens a hydrophobic tunnel within the enzyme which may promote a favourable interaction between the more hydrophobic TMS moiety of trimethylsilylethanol in a similar manner as was determined for bromobenzyl alcohol.[109]

The kinetic resolution of trimethylsilyl propanol isomers using HLADH was examined by Zong and coworkers and the Tanaka group.[110,112] HLADH, an enzyme that had previously been shown to oxidize primary TMS-alcohols to the corresponding aldehydes, displayed the capacity to stereoselectively dehydrogenate a series of β-hydroxysilanes along with the corresponding carbon analogs (**Figure 28**).[110] Dehydrogenations were carried out using a two phase system to allow for the regeneration of NAD^+ (**Figure 29**). (*R*)-1-Trimethylsilyl-2-propanol ((*R*)-**92**) and (*R*)-4,4-dimethyl-2-pentanol ((*R*)-**93**) were resolved in 50% conversion. Not only did the trimethylsilyl derivatives react quicker than the carbon analog, 51% conversion in 9 hours compared to 50% conversion in 41 hours, they were also produced with excellent stereoselectivity at

99% ee compared to 85% ee for the dehydrogenation of **93**. The dehydrogenation of 2-trimethylsilyl-1-propanol (**94**) and 2,3,3-trimethyl-1-butanol (**95**) proceeded to 68% and 71% yield respectively, but the enantiopurity of the products was lower at 70% ee and 59% ee.[110]

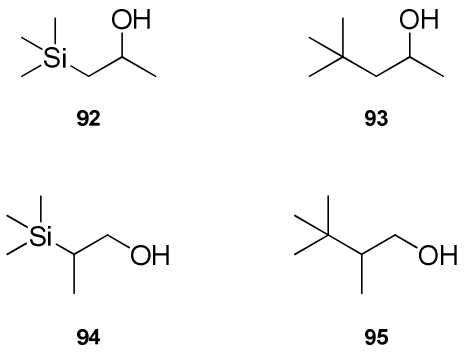

Figure 28 β-hydroxysilanes and corresponding carbon analogs chosen for reduction by HLADH.[110]

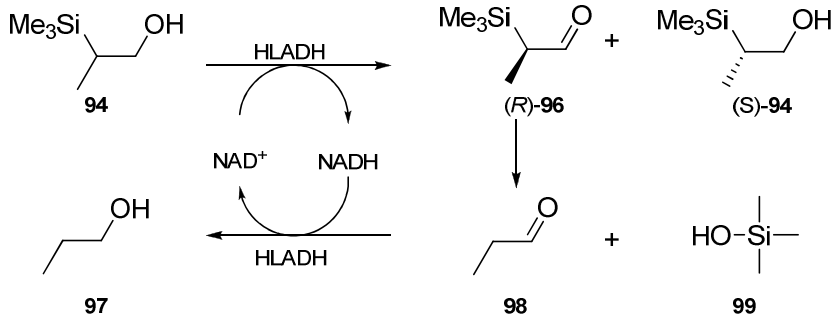

Figure 29 HLADH-mediated enantioselective oxidation of a typical β-hydroxysilanes with the *in situ* regeneration of NAD^+.[110]

One of the concerns when using enzymatic transformations is the requirement of expensive cofactors. A serendipitous discovery by Tsuji *et al.* allowed for catalytic amounts of NAD(P)H to be used in reactions that were mediated by HLADH.[112] When HLADH was charged with **94** and 0.5 μmol of NAD^+, the enzyme enantioselectively de-

hydrogenated only the (+)-isomer although the product 2-trimethylsilyl-1-propanal (**96**) was not recovered (**Figure 29**). The β-carbonyl silane proceeded through a [1,3]-Brook Rearrangement to give trimethylsilanol (**99**) and propanal (**98**), which regenerated NAD^+ with the concomitant production of propanol (**97**). When the secondary silicon-containing alcohol **92** was dehydrogenated, the proposed rearrangement was also realized but acetone did not regenerate the cofactor.

The general success of HLADH in accepting the trimethylsilylated alcohols as substrates was attributed to favourable interactions between the substrate and the two binding pockets of the active site of the enzyme. The larger trimethylsilyl group did not bind into the smaller alkyl binding pocket resulting in enantioselective dehydrogenations. For the primary alcohols, the chiral centre could be positioned within the larger alkyl binding pocket, and as a result decreased selectivity by the enzyme was observed.[112]

2.4.3 Enzymatic Synthesis of Silicon-Containing Amino Acids

Silicon-containing amino acids are useful substrates for natural products synthesis, as well as agricultural and food additives and are expected to have unique properties relative to the corresponding naturally occurring amino acids.[113] The Tanaka group resolved *N*-acetyl-3-trimethylsilylalanine (**104**) using porcine acylase I or *Aspergillus melleus* acylase I. Trimethylsilylalanine was synthesized by treating ethyl acetamidocyanoacetate (**100**) with sodium ethoxide in DMSO and slowly adding (1-bromomethyl)trimethylsilane (**101**) to give the silylated ester (**102**) (**Figure 30**). Complete hydrolysis of the ester and nitrile moieties in sodium hydroxide gave racemic β-trimethylsilylalanine (**103**), which was acylated in acetic anhydride to yield the *N*-

acylated amino acid (**104**). Porcine kidney acylase I was more proficient than the acylase from *A. melleus* in the *N*-deacylation accomplishing 50% conversion in 4.5 hours as compared 24 hours when a ten-fold increase in the amount of the enzyme was used (**Figure 31**). The L- enantiomer was recovered in 72% yield with 99% ee.

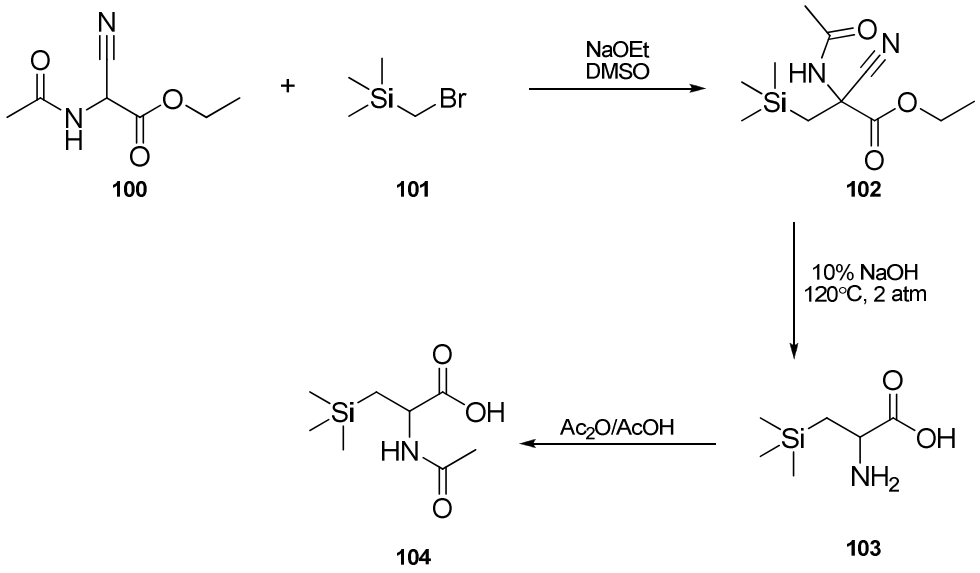

Figure 30 The synthesis of *N*-acetyl-β-trimethylsilylalanine.[113]

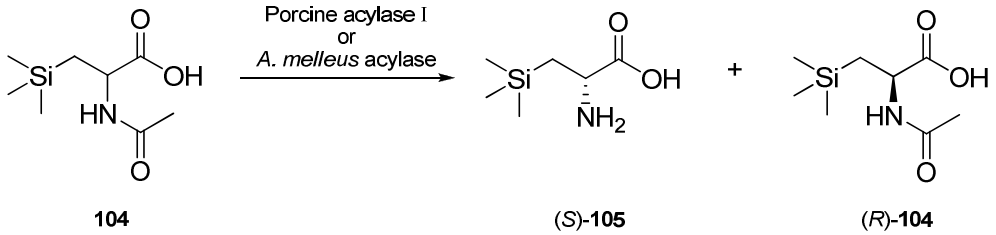

Figure 31 *N*-Deacylation of *N*-acetyl-β-trimethylsilylalanine using porcine kidney acylase I or *A. melleus* acylase.[113]

β-(Trimethylsilyl)phenylalanine was synthesized from β-trimethylsilyl-phenylalanine hydantoin, using a two enzyme approach consisting of a hydantoinase and

an aminohydrolase.[114] The precursor, (trimethylsilyl)phenylhydantoin (**112**), was synthesized as outlined in **Figure 32**. The racemic hydantoin was hydrolyzed with a D-specific hydantoinase to give **113**, and treatment with *N*-carbamoyl-D-amino acid aminohydrolase led to the isolation of (*R*)-**114**.

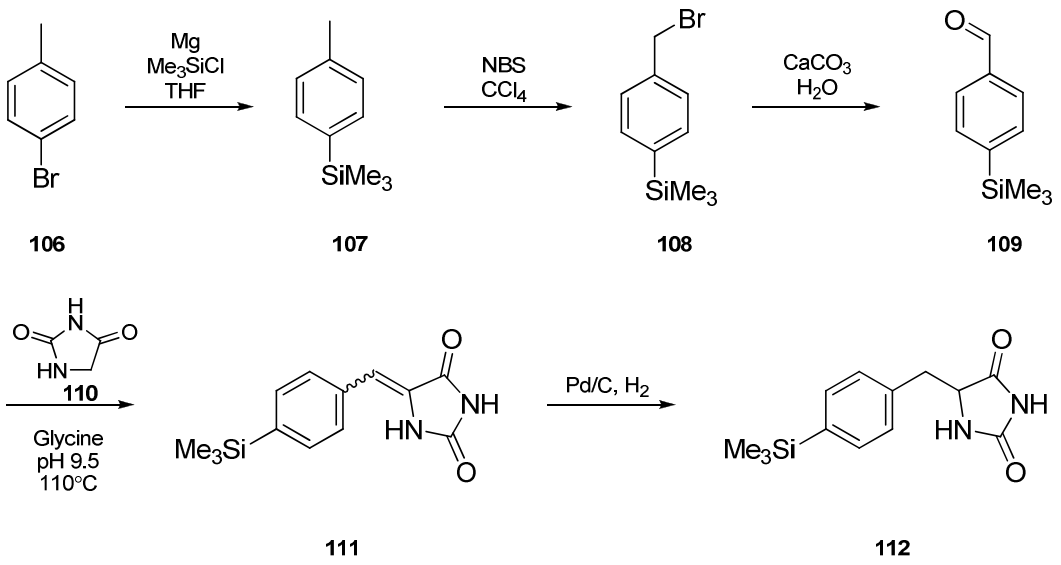

Figure 32 The synthesis of (4-trimethylsilyl)phenylalanine hydantoin.[114]

In a companion report the same year, a cell-free extract from *Blastobacter sp.* A17p-4 containing *N*-carbamoyl-D-amino acid amidohydrolase was used to synthesize optically active trimethylsilylphenylalanine ((*S*)-**114**) (**Figure 33**).[115] Initial results gave only 33.7% conversion and 69% ee due to the presence of competing amino acid amidohydrolases. Yields and enantiomeric purity were improved by inactivating the L-amino acid amidohydrolase. The heat-treated cell free-extract produced optically active D-trimethylsilylphenylalanine in 80% yield and 99% ee. The residual unreacted substrate

could be converted to the L-enantiomer in 89% yield and 99% ee by treatment with a non-heat treated cell free extract.

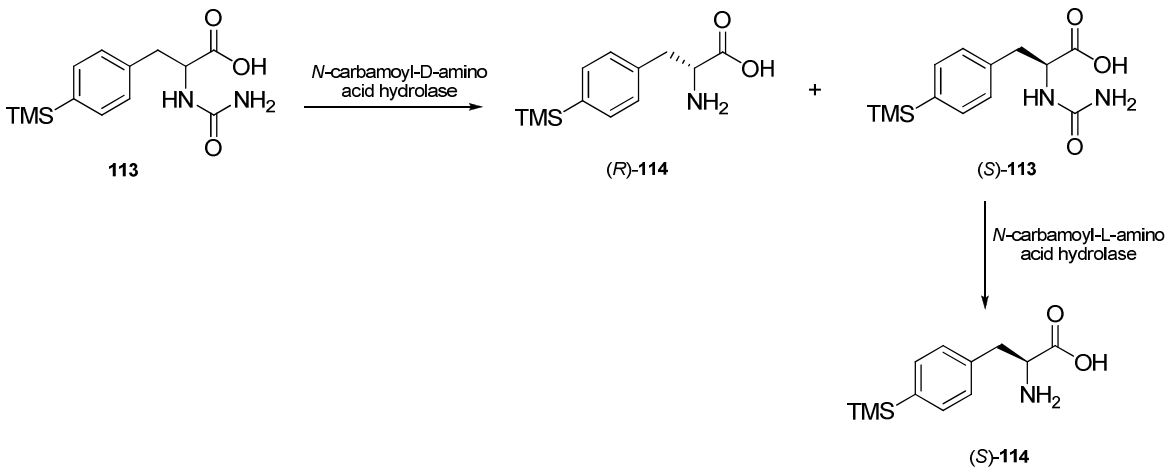

Figure 33 The synthesis of optically active TMS-phenylalanine.[115]

In complementary reports, Pietzsche *et al*.[116] and Smith *et al*.[117] described the synthesis of enriched silylated-alanines through an enzymatic enantioselective hydrolysis of DL-5-silylmethylated hydantoins (**Figure 34**). Pietzsche *et al*.[116] coined the term '*hydantoinase process'* due to the use of enantiospecific hydantoinases and *N*-carbamoylases. In the initial report,[116] *Agrobacterium sp*. IP I 671 and the isolated enzymes, hydantoinase from *Bacillus thermoglucosidasius*, *Thermus sp*., *Arthrobacter aurescens* DSM 3745, and L-*N*-carbamoylase from *Arthrobacter aurescens* DSM 3747, were combined to afford better yields over those reported by Yamanaka's group.[113,115] Whole cell-mediated biotransformations progressed with 88% yield and 95% ee of the D-amino acid.[116] The decreased enantioselectivity was hypothesized to result from the action of an amino acid racemase or an L-*N*-carbamoylase.[116]

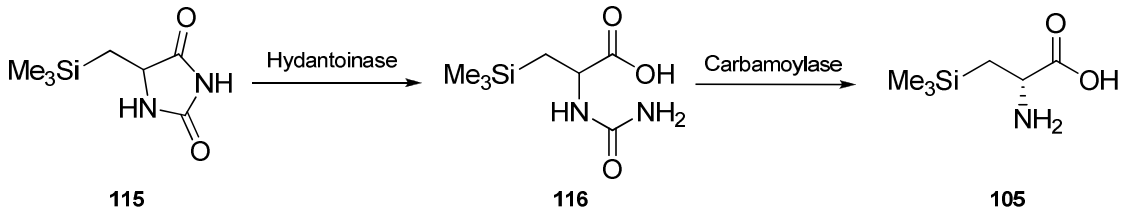

115 116 105

Figure 34 The '*hydantoinase method*' for preparing trimethylsilylalanine.[116]

Treatment of racemic trimethylsilylmethyl hydantoin (**115**) by hydantoinases revealed the general acceptance of the substrate by hydantoinases from *Bacillus thermoglucosidasius*, *Thermus sp*., and *Arthrobacter aurescens* DSM 3745, yielding the D-enantiomer (**116**). Interestingly, the hydantoinase from *A. aurescens* 3745, which is known to change its selectivity depending on the amino acid it is processing,[118] produced the D-enantiomer with 100% selectivity, a first for this enzyme.[116] Treatment of **116** with D-*N*-carbamoylase or L-*N*-carbamoylase afforded the desired enantiomers of **105** after 50% conversion.

To show the generality of the hydantoinase process when using silylated derivatives, dimethylphenylsilylalanine hydantoin (**117**) and (1-methyl-1-*sila*-cyclopentyl)alanine hydanotin (**119**) were used as alternatives to **115** (**Figure 35**). Hydantoin **117** was processed more efficiently than hydantoin **119** (50% conversion in 2 hours compared to 20% in 2 hours). *Bacillus thermoglucosidasius* hydantoinase hydrolyzed the hydantoins to give enantiomeric excesses exceeding 98% for silylated amino acids **118** and **120**. The hydantoinase from *A. aurescens* was marginally more selective in its activity, delivering the D-enantiomer of **118** with 98% ee and the same enantiomer of **120** with an enantiomeric excess of 84% ee. Treatment of the racemic *N*-carbamoyl

amino acids with the L-*N*-carbamoylase mirrored the observed trend with the hydantoinases, that is to say the dimethylphenylsilyl derivatized carbamoyl amino acid was processed more expediently.[117] Additionally, and corresponding to the 3-(trimethylsilyl) derivative reported in earlier work,[116] after 50% conversion of the racemic *N*-carbamoyl amino acids, the L-enantiomers were produced exclusively, the remaining unreacted *N*-carbamoyl amino acids were recovered in a virtually enantiomerically pure form.[117]

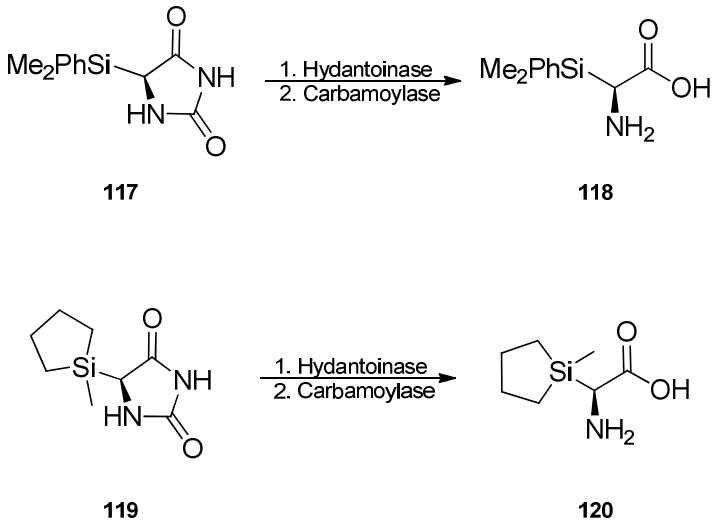

Figure 35 Silyl derivatives of alanine synthesized through the hydantoinase process incorporating increasing steric bulk at silicon.[117]

Non-proteinogenic amino acids are interesting compounds due to the enhanced properties that they potentially offer, such as stability against enzymatic degradation, improved pharmacokinetics, increased lipophilicity, prevention of hydrophobic pocket collapse, and improved inhibitory interactions with enzymes.[117] Thermolysin from *Bacillus proteolyticus* has been a key enzyme in the synthesis of trimethylsilylalanine-containing dipeptides.[119] Dipeptides containing 3-trimethylsilylalanine and a variety of amino acids

with **105** was in the *N*-terminal position could be obtained in a 90% yield. When **105** was in the *C*-terminal position dipeptides could not be synthesized using thermolysin. The architecture of the active site was such that the binding pocket at the *S1'* position was too small to accommodate the larger trimethylsilyl moiety (**Figure 36**).

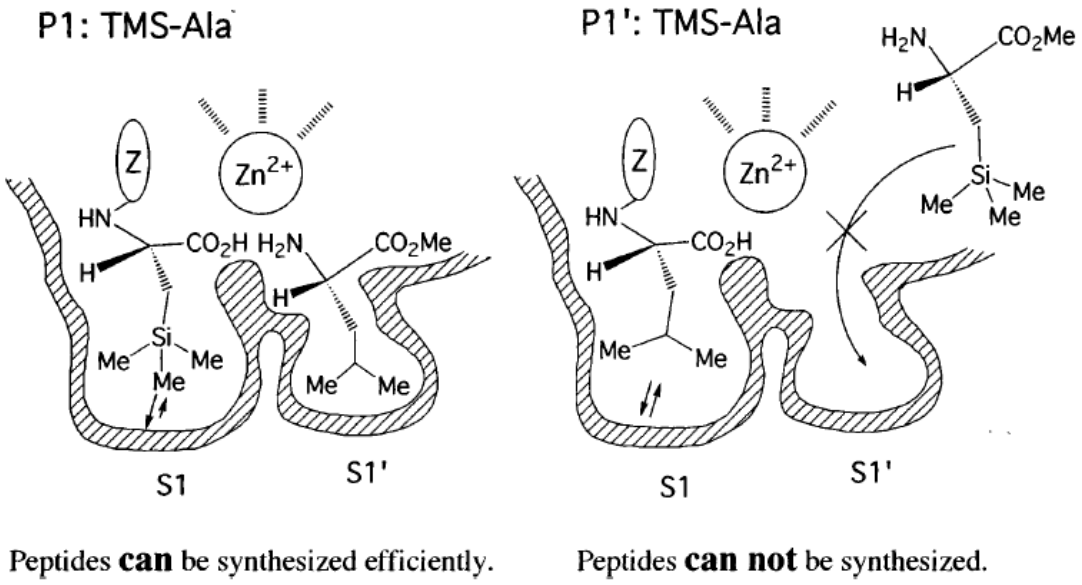

Figure 36 Tanaka's synthesis of trimethylsilyl-containing dipeptides. The geometry of the active site promotes synthesis due to favourable interactions within the binding pockets. Reproduced with permission from reference 120 (H. Ishikawa, H. Yamanaka, T. Kawamoto, and A. Tanaka. *Appl. Microbiol. Biotechnol.*, **1999**, *51*, 470-473), copyright Springer Publishing 1999.

Tacke continues to be a front runner in the arena of organosilicon biotechnology. Tacke's recent publication reports the synthesis of enantiopure (*R*)- and (*S*)-α-[(trimethylsilyl)methyl]alanine (**125**) (**Figure 37**).[120] Using an enzyme-based resolution strategy, a racemic mixture of 2-methyl-2-[(trimethylsilyl)methyl] malonic acid diethyl ester (**123**) was resolved using pig liver esterase to give (*R*)-3-ethoxy-2-methyl-3-oxo-2-[(trimethylsilyl)-methyl]propanoic acid (**124**) in 94% yield and 85% ee. Treatment with

thionyl chloride and sodium azide, followed by hydrolysis, gave (*R*)-**125** in 42% yield. The (*S*)-isomer was obtained by converting (*R*)-**124** into the tertiary-butyl ethyl malonate ester (**126**). This afforded an enantiomeric switch from (*R*) to (*S*). Alkaline hydrolysis selectively hydrolyzed the ethyl ester giving (*S*)-tertiary butyl malonate (**127**). Thionyl chloride directed chlorination of the free acid, followed by treatment with sodium azide, gives the acyl azide which undergoes a thermally induced Curtius rearrangement to give the (*S*)-isocyante. Hydrolysis of the isocyanate affords (S)-**125** in 25% overall yield. The absolute stereochemistry was confirmed by x-ray crystallography.

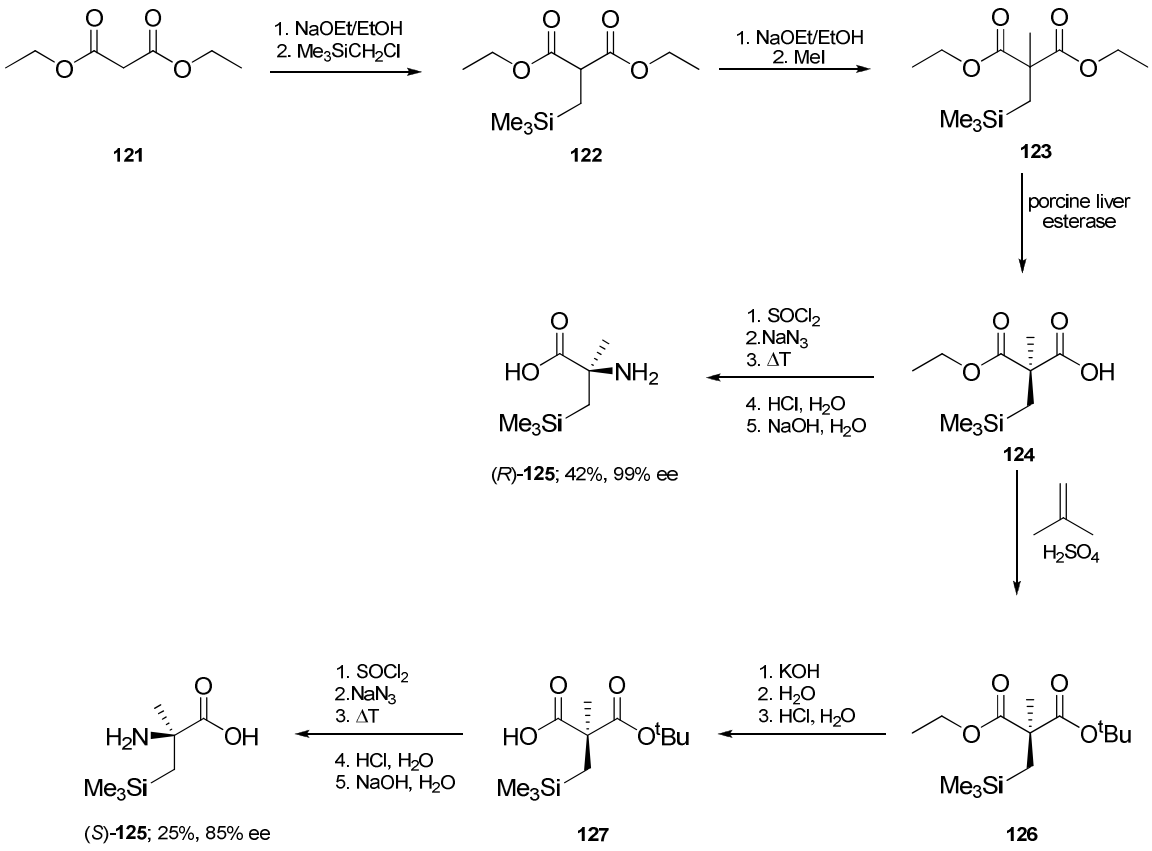

Figure 37 Tacke's synthesis of (*R*)- and (*S*)- α-[(Trimethylsilyl)methyl]alanine was achieved through an enzymatic resolution of a (2-trimethylsilylmethyl)malonate diester.[120]

2.4.4 Other Enzymatic Transformations of Organosilicon Compounds

Enzymatic enantioselective transcyanations have been performed on acetyltrimethylsilanes **128-130** with acetone cyanohydrin using (*R*)-oxynitrilase from crude preparations of apple, almond, and loquat seeds (**Figure 38**).[121-123] (*R*)-Oxynitrilase from apple seed meal converted substrate with 99% yield and enantiomeric excess; other crude preparations generated yields in excess of 95% with comparable enantioselectivity. The acylsilanes were shown to be better substrates than the carbon analogs, affording higher conversions and enantiomeric excesses. The success of the reaction was dependent on pH, hydrophobicity of the organic phase, temperature, and substrate structure. Decreasing the acidity of the buffer afforded higher yields at the expense of enantiomeric purity. Higher reaction temperatures were also deleterious to the enantiomeric purity of the product due to an irreversible inactivation of the enzyme. Lower reaction temperatures required longer incubation periods to achieve comparable results.

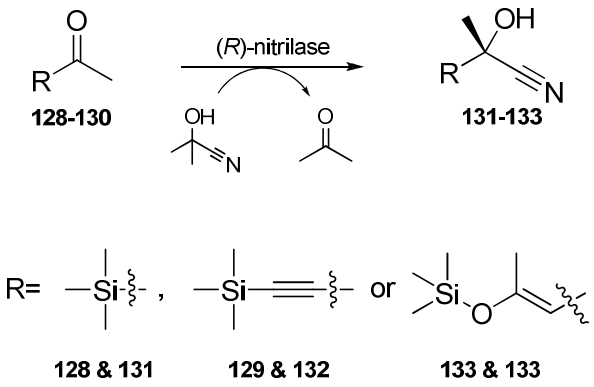

Figure 38 The synthesis of silicon-containing cyanohydrins using and (*R*)-specific nitrilase.[121-123]

2.5 The Use of Plant Cultures in Organosilicon Chemistry

The pioneering work of the Tacke group in the 1980s was expanded to include plant cell suspension cultures to perform enantioselective reductions on organosilicon compounds.[124] Suspensions of *Symphytum officinale* and *Ruta graveolens* cultures were used to enantioselectively reduce acetyldimethylphenylsilane (**12**) to (*R*)-(1-hydroxyethyl)dimethylphenylsilane (**13**) **(Figure 39**). A complete conversion of the starting substrate was achieved in 4 hours as measured by gas-liquid chromatography. Each of the plant culture-mediated bioconversions produced large quantities of the by-products dimethylphenylsilanol and 1,3-diphenyl-1,1,3,3-tetramethyldisiloxane. The recovery of the secondary alcohols was low at 15% and 9% for *S. officinale* and *R. graveolens* respectively. The enantiopurity of the reaction was much greater for *S. officinale*, 81% ee compared to 60% ee for *R. graveolens*; these values were comparable to several earlier reports using microbial bioconversions.[85] The products were derivatized using (R)-α-methoxy-α-(trifluoromethyl)phenylacetyl chloride to assign the absolute configuration.

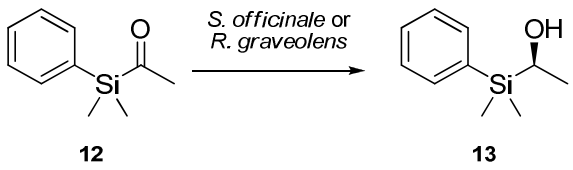

Figure 39 The reduction of acetyldimethylphenylsilane by *S. officinale* and *R. graveolens.*[124]

2.6 Enzyme-Mediated Polymer Synthesis

2.6.1 *In vitro* Polymer Synthesis

The term '*polymerische*' was originally used and coined by Berzelius in 1833; [125] it is a wonderful coincidence that he was also credited with the discovery of silicon as an element in 1824. Berzelius' definition of a *polymersiche*, or polymer, is somewhat outdated and has been replaced by more modern definitions. Despite this, polymers have had a long and prosperous history and hold an unmistakable and not easily replaceable presence in modern times.

The first polymers that mankind used were cotton, starches, and proteins (silk and wool).[126] However, by the early twentieth century the use of synthetic polymers became widespread with the development of phenol-formaldehyde resins by Baekeland[127] (Bakelite, 1907) and synthetic nylon by Carothers in 1935.[128] More recently there has been a push to develop biodegradable polymers, and polymers in which the components are derived from renewable feed stocks. This has led to the exploration of such polymers as polyhydroxyalkanoates, produced by bacterial fermentation, and polylactates.

Nature has overcome the issue of controlling stereochemistry and regiochemistry by tailoring the active site of enzymes. Many of the molecules that an organism requires are not simple, but rather complex polymeric structures, such as polysaccharides, proteins, and nucleic acids. The synthesis of these structures *in vivo* requires exquisite control over the chain-growth polymerization of monomers. However, the use of whole organisms as polymerization catalysts is not always practical. Microorganisms are restricted to a very narrow range of physiological conditions which are often not compatible

with polymer synthesis, and in some cases the products that are produced are toxic to the organism.[19]

Isolated enzymes, on the other hand, have proven to be ideal for carrying out condensation polymerizations. Enzymes offer advantages over more traditional chemical catalytic methods. Firstly, enzymes offer substrate conversion efficiency due to their inherent enantio- and regio- selectivity; although this has been shown to not always be the case for the acrylic resin immobilized lipase from *Candida antarctica*.[129] Some enzymes can be used effectively in the absence of solvents and under relatively mild reaction conditions. Enzyme-mediated catalysis in polymer chemistry is an ever expanding research field, and reviews have been written on the subject.[19,130]

While substrate-specificity is a defining feature of enzyme-catalyzed processes, many enzymes show some degree of promiscuity and allow a range of substrates to be accepted; this has facilitated the increasing use of enzymes for the biocatalysis of polymers.[131] Of particular interest in the field of polymer chemistry are peroxidases, laccases, glycosyltransferases, glycosidases, proteases, and lipases.[131]

Immobilization of enzymes onto solid supports such as acrylic resins, graphene oxide, silica, etc., can increase the thermal stability of many enzymes. Immobilization facilitates removal of the enzyme from the reaction medium and allows for multiple reaction cycles to be carried out with a single batch of enzyme providing that the enzyme has not suffered catastrophic denaturation. Furthermore, the long term thermal tolerance of immobilized enzymes can be examined.

2.6.2 Silicone Polymers

Silicones of the form $(-RR'SiO-)_n$, where R and R' may or may not be identical, have been known for nearly a century. This is due in part to the early work of Frederick Stanley Kipping and co-workers.[132] Their work laid the foundation for nearly 100 years of research in the field of silicone chemistry.

Silicone-derived materials, and in particular dimethylsilicones (polydimethylsiloxane, PDMS), are desired for the many physical characteristics which they possess. PDMS is highly thermal stable, highly hydrophobic and possesses low surface activity (surface tension), has a low glass transition temperature, is resistant to oxidation, highly permeable to gases, and is extremely biocompatible.[2,133,134]

The hydrophobicity and surface activity of silicones is due to the nature of the dimethylsiloxy group. The geminal methyl groups on silicon provide a hydrophobic character to the siloxane chain which is highly mobile and allows the polymer chain to rearrange itself into a more stable orientation when it comes into contact with incompatible surfaces.[2,133] Silicones possess a remarkable surface activity which can be attributed to four characteristics: (1) low intermolecular forces between the methyl groups that are attached to silicon; (2) the unique flexibility of the siloxane framework; (3) the high energy of the *Si-O-Si* bond network; and (4) the ionic nature of the *Si-O* bond.[133]

The thermal properties of silicones have been studied using thermal gravimetric analysis (TGA) and differential scanning calorimetry (DSC). Due to the amorphous nature of the siloxane backbone PDMS has an unusually low glass transition temperature (T_g) of about -125°C.[2,135] PDMS is an extremely thermal stable polymer that does not begin to decompose until temperatures in excess of 350°C are reached.[2] The thermal sta-

bility of silicones can be tuned by altering the organic side chain attached to silicon; the thermal stability of silicones has been seen to increase when the side chains are of the following sizes: ethyl>methyl>phenyl.[136] Thermal degradation is thought to proceed via an "unzipping depolymerisation" mechanism or bond exchange reactions.[136]

Many of the physical characteristics of silicones are derived from the strength and flexibility of the *Si-O-Si* framework, which has a typical bond angle of 145° but has been postulated to extend to 180°, the ionic character of the *Si-O* bond that is approximately 51% ionic,[137] and the weak interactive forces of the geminal dimethyl groups. The bond *Si-O* bond length is 1.64Å compared to the average *C-O* bond length of 1.41Å, which permits a localized reduction in the steric bulk that in turn allows for a higher degree of rotational freedom.[133] A typical siloxane linkage has a bond energy of 452 kJ/mol (108 kcal/mol) (homolytic cleavage), and the ionic bond strength has been reported as 1013 kJ/mol (242 kcal/mol).[137]

Typical routes to synthesizing functionalized linear, branched or cross linked silicones include hydrosilylation using one of several commercially available Pt^0 or Rh^I catalysts, titanium isopropoxide, and dibutyltin dilaurate. Additionally, peroxide induced free radical polymerization of acetoxy- or alkoxy- silanes,[138] photo initiated polymerization,[139] anionic polymerization,[140] and tris(pentafluoroborane)[141,142,143] catalysis has been used to prepare silicones with varying molecular morphologies. If the end use of the silicone materials lies in the biomedical or agrichemical fields, the use of potentially toxic catalysts should be avoided. One increasingly common route to generating the biocompatible materials has been the incorporation of enzymatic catalysis.

2.6.3 Biocatalysis of Siloxanes

The following section will review the literature concerning the biocatalysis of siloxanes and modified siloxane materials.

The enzymatic synthesis of polydimethylsiloxane oligomers was carried out by Okahata and co-workers.[144] Using lipase D from *Rhizopus delemar*, which has been coated in a glycolipid to enhance its solubility in organic solvents, the oligomerization of diethoxydimethylsilane (**134**) was performed in isooctane containing 2wt% water (**Figure 40**). The combination of the lipase and **134** afforded low average molecular weight polymers (**135**), M_w=1500 g/mol, with a low dispersity of molecular weight, PDI=1.06. In a similar manner, Müller *et al.* produced low molecular weight PDMS from dimethoxydimethylsilane (**136**) using silicatein from *Suberites domuncula*.[145,146] The authors were able to show that the enzyme enhanced siloxane condensation, by forming 11-mers with a molecular weight of 925 g/mol (as demonstrated by Matrix-Assisted Laser Desorption/Ionization Time of Flight Mass Spectrometry; MALDI-TOF MS) after one hour of incubation.

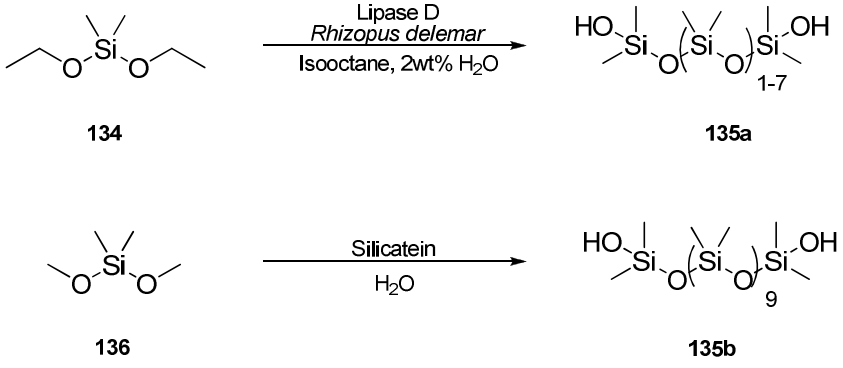

Figure 40 The *in vitro* hydrolysis and condensation of bis-alkoxysilanes using enzymes under mild reaction conditions.[144-146]

In a related vein, Bassindale and co-workers focused on the bio-synthesis of a single siloxane bond. Citing the uncontrollable nature of tetraalkoxysilane hydrolysis, ethoxytrimethylsilane (**137**) was chosen as a model silane.[147-150] A large scale screen of several serine and cysteine hydrolases revealed that trypsin and α-chymotrypsin were particularly adept at mediating the hydrolysis and condensation of **137**. Trypsin, treated with *N*-tosyl-L-phenylalanine chloromethylketone to eliminate any contribution from contaminating α-chymotrypsin, displayed the highest capacity for synthesizing hexamethyldisiloxane (**138**) from trimethylsilanol (**99**) (**Figure 41**). The use of the enzyme led to complete hydrolysis of **137** and near complete (84%) condensation of **99** to **138** in 3 hours. Blocking the active site of trypsin with a Bowman-Birk inhibitor or a popcorn inhibitor did not appreciably alter the capacity for hydrolysis, but nearly eliminated the condensation to hexamethyldisiloxane. It was postulated that non-specific surface interactions between the protein and **137** were primarily responsible for the hydrolysis of the alkoxysilane and that the active site was only necessary for the condensation reaction.

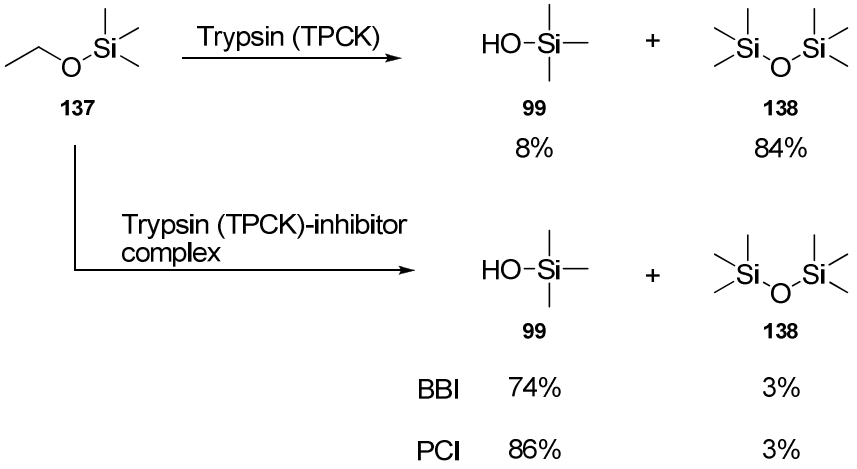

Figure 41 The trypsin-catalyzed hydrolysis and condensation of ethoxytrimethylsilane. Trypsin was treated with TPCK to inhibit α-chymotrypsin activity. BBI=Bowman-Birk inhibitor, PCI=Popcorn inhibitor.[147]

A more extensive analysis comprising more than 80 enzymes, covering seven classes of enzymes, identified the phytases from *Aspergillus ficuum* and *A. niger*, chicken egg white lysozyme, porcine pepsin, and *Rhizopus oryzea* lipase as candidates for mediating the synthesis of siloxane bonds in aqueous media.[149] *Escherichia coli* phytase was a suitable enzyme for use in organic media (95:5 AcCN:water).[148] The common attribute among the enzymes that were deemed to be successful was the presence of one or more serine, histidine, and aspartic acid residues within the active site of each enzyme, although not necessarily composing a 'catalytic triad' as in the serine hydrolases.

Based on the observed results, a mechanism for the condensation of **99** to **138** was proposed, which involved a catalytic triad similar to that found in the serine hydrolases (**Figure 42**).[149] Polarization of the serine hydroxyl by the aspartic acid and histidine residues increased the nucleophilicity of the serine to promote addition to trimethylsilanol forming a silyl-enzyme intermediate. At this point, a second equivalent of trimethylsi-

lanol can attack the silyl-enzyme intermediate, forming hexamethyldisiloxane and restoring the catalytic triad for further catalysis.

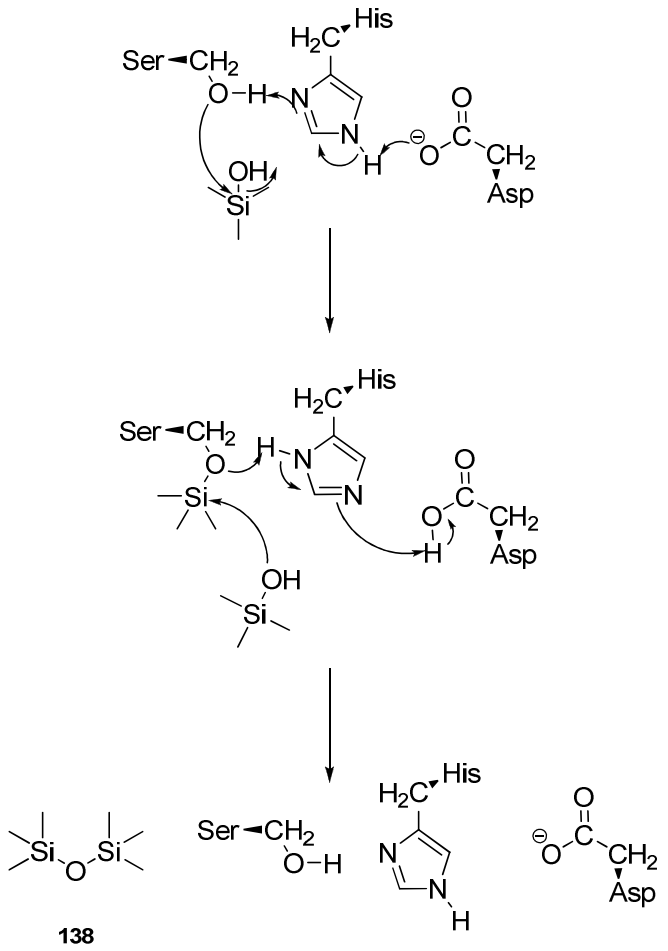

Figure 42 The proposed reaction mechanism implicating a serine catalytic triad in the condensation of trimethylsilanol to hexamethyldisiloxane.[149]

The results concerning the trypsin-catalyzed hydrolysis of ethoxytrimethylsilane from the Bassindale group appeared to be challenged due to an apparent lack of reproducibility.[151] Maraite *et al*. concluded there was not a significant difference between the uncatalyzed- and trypsin-catalyzed rates of hydrolysis of the silane precursor. However, it

was unclear if in their attempts to reproduce the Bassindale results if the procedure was followed precisely.

The hydrophobicity of silicones can make them incompatible with hydrophilic compounds. However, molecules that possess both hydrophobic and hydrophilic domains are commonly used as surfactants. The incompatibility between these two classes of molecules can make the synthesis of surfactants a difficult process. Biocatalysis is well suited to overcome this obstacle. The modification of siloxane polymers through enzymatic methods has become a convenient tool for producing carbohydrate modified silicones. The grafting of amylase onto PDMS has been shown using potato phosphorylase (EC 2.4.1.1) to produce poly(dimethylsiloxane-*graft*-(α1→4)-glucopyranose) (**139**) (**Figure 43**).[152] The carbohydrate-silicone hybrid had only a marginal effect on the functioning of the enzyme; enzyme activity was measured at approximately 70% of a control reaction. While reactions were stopped prior to reaching equilibrium, approximately 300 glucose units could be grafted onto the PDMS-initiator backbone.

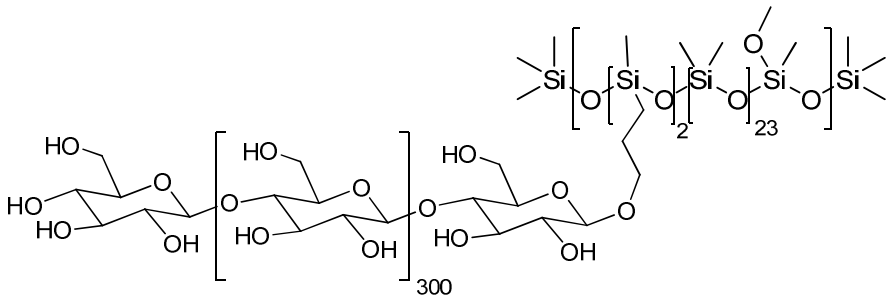

139

Figure 43 A carbohydrate-modified polysiloxane produced by the enzymatic grafting of amylose to polydimethylsiloxane using potato phosphorylase.[152]

Another series of silicone-carbohydrates was synthesized from α/β-ethyl glucoside (**141**) and carboxylic acid terminated PDMS (**140a-c**) by using lipase B from *Can-*

dida antarctica (**Figure 44**).[153] The lipase-mediated esterification progressed with high regioselectivity, 98% as determined by ^{13}C Distortionless Enhancement by Polarization Transfer (DEPT) NMR, preferentially forming the ester from the primary alcohol. When enzymatic reactions were carried out with 1,3-bis(3-carboxypropyl)-1,1,3,3-tetramethyldisiloxane (**140a**), mono- and di- esterified products (**142a** & **143a**) were recovered in a 1:2 ratio. For larger PDMS polymers (**140b** & **140c**), the overall yields were reported as 79% and 83% suggesting that the increased hydrophobicity associated with longer silicone chains was beneficial to the activity of the enzyme.

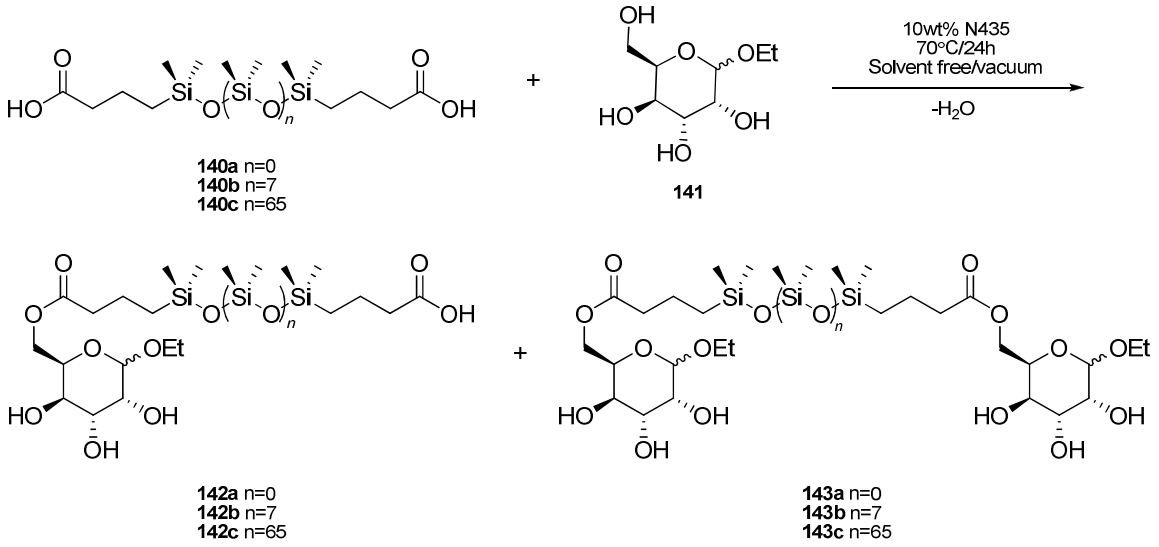

Figure 44 The N435-catalyzed esterification of α/β-ethylglucoside with acid terminated polydimethylsiloxane to give mono- and di- glucosylated PDMS. Figure reproduced from reference 153; Copyright of the American Chemical Society, 2005.

Organosiloxane co-polyimides were produced by combining N435 with phthalic anhydride ether (**144**) and an aminopropyl-terminated PDMS (**145**) (**Figure 45**).[154] Under enzyme-free conditions, the amine opened the anhydride to produce polymer **146**. Only in the presence of 10 wt% of the immobilized lipase was the anhydride ring closed

to produce the imide linkage in **147**. The structure of the co-polymer was confirmed via ^{1}H and ^{13}C NMR and the average molecular mass was determined to be ~75,000 g/mol by GPC.

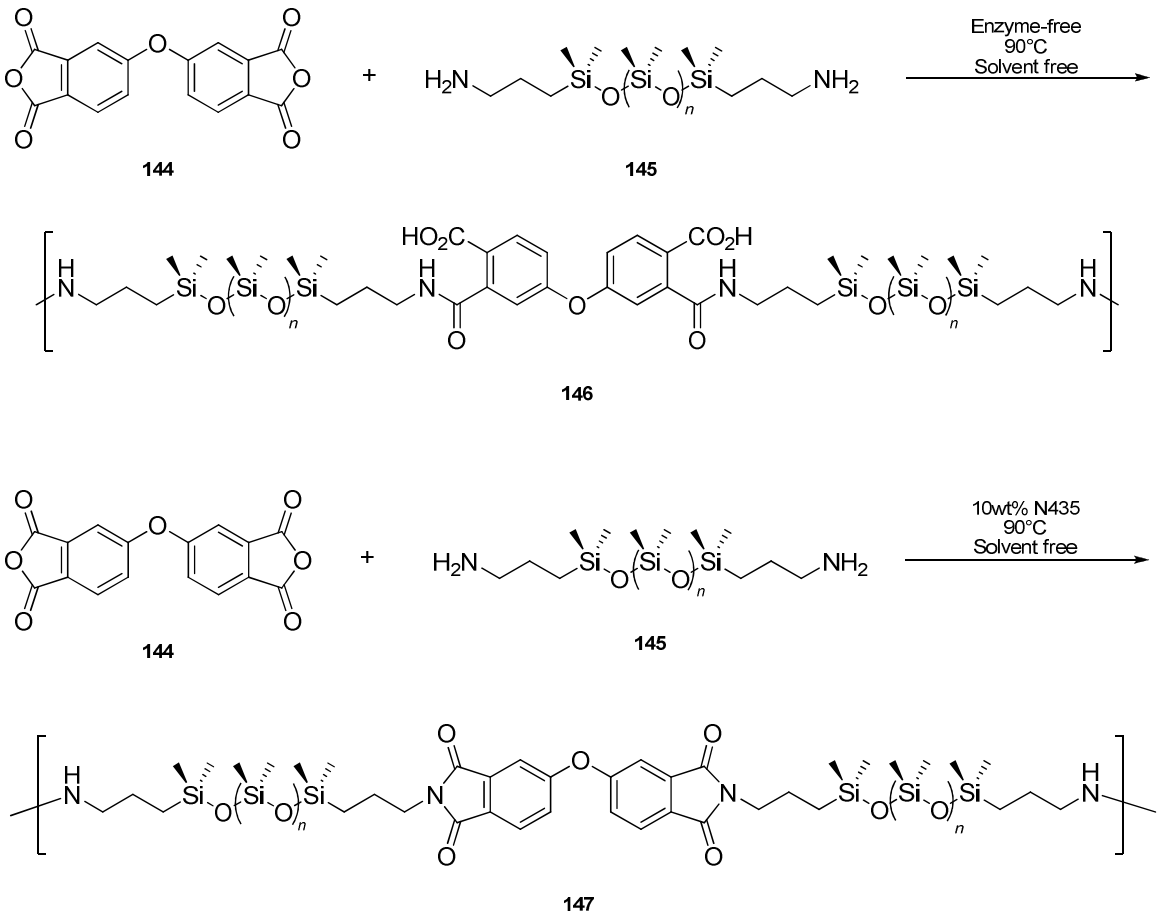

Figure 45 The synthesis of silicone co-polyimides using N435 as the catalyst. The top panel shows the synthesis of silicone co-polymers containing free acid groups. Only with the addition of an enzyme catalyst was the closure of the two phthalimide rings favoured.[154]

Silicone polyamides and polyesteramides derived from varying feedstock ratios of diethyl adipate and aminopropyl-terminated PDMS were produced under enzymatic catalysis (**Figure 46**).[155] Polyesteramides produced from a 1:1 ratio of diamine **145** and

1,8-octanediol (**149**) and diethyl adipate (**148**) gave the highest molecular weight polymer (**150**), M_n=14,000 g/mol, and the majority of the other copolymer systems had M_n ranges of 6,000-11,000 g/mol and low dispersity molecular weight with a polydispersity index (PDI) of 1.5-2.2. A closer examination of the polymerization reactions showed that when polyesters and polyamides were synthesized, polyamides were produced more slowly than polyesters, reaching only 54% compared to 89% yield in 0.25 hours. That being said, monomer conversion was nearly identical for the two systems, reaching 96.1% (polyester) and 96.3% (polyamide) after the application of vacuum at 40 hours and continuing the reaction for an additional 28 hours. When the consumption of functional groups was followed during the terpolymerization of monomers, in the presence or absence of applied vacuum, it appeared that the consumption of amine units progressed more rapidly than the consumption of hydroxyl units.[155]

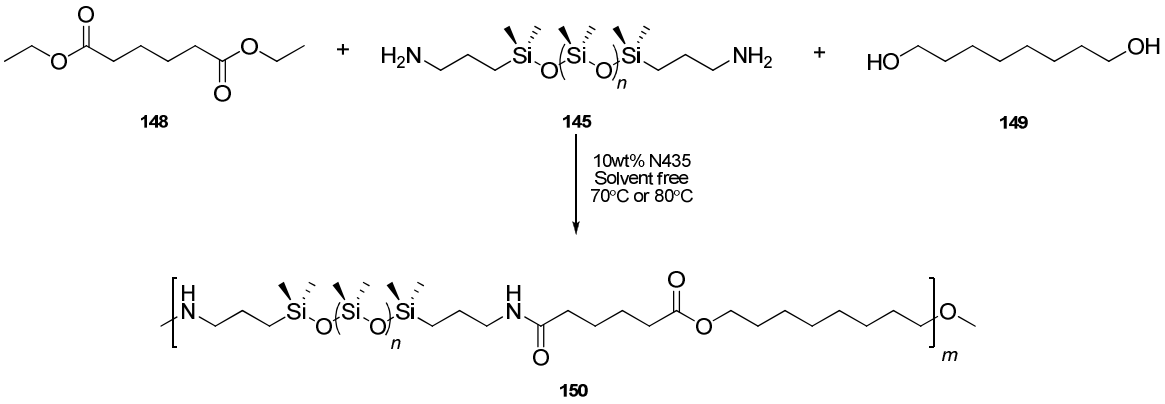

Figure 46 The enzymatic synthesis of polyesteramides containing a PDMS block derived from α,ω-bis(3-aminoporpyl)-PDMS.[155]

A systematic examination of the processing parameters on the N435-mediated polymerization of **140a** with various alkane diols was carried out by Poojari *et al.*

(**Figure 47**).[156] The enzymatic polymerizations were monitored over temperatures ranging from 50°C-90°C and, in general, the weight average molecular weight of the polymers increased with each increase in the reaction temperature. The application of vacuum gave results that did not follow a predictable trend. During the early stages of polymerization between disiloxane **140a** and 1,4-butanediol (**151**) at 50 mm Hg, higher molecular weight oligomers were formed compared to the same reaction at atmospheric pressure. Esterification with diol **149,** however, required 300 mm Hg to produce higher molecular weight oligomers. The application of vacuum did not have any apparent effect on the molecular weight distribution when 1,6-hexanediol (**152**) was used. However, during later stages of the reaction when the viscosity was increasing, the applied vacuum appeared to permit a greater degree of condensation.

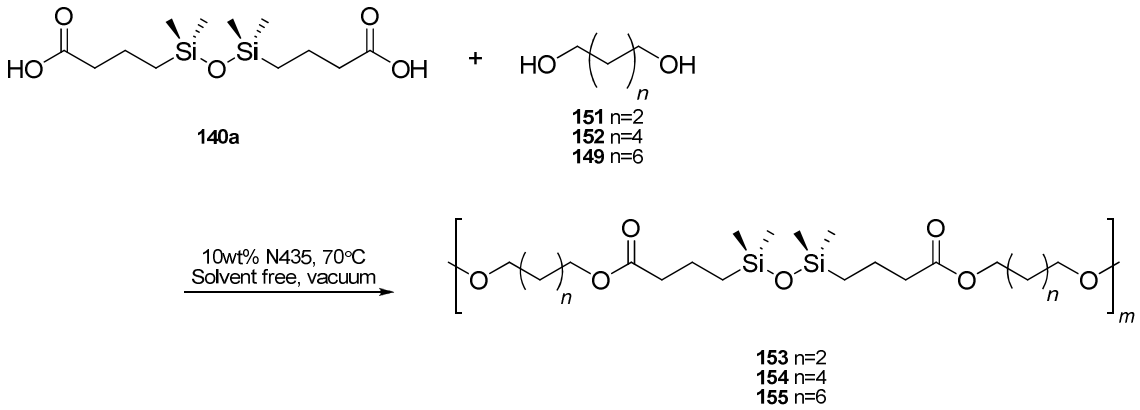

Figure 47 The enzymatic polyesterification of a disiloxane dicarboxylic acid with three alkane diols.[156]

The reported specific activity of the lipase affected the average degree of polymerization. Two lipases, differing only by 10% in their specific activity (as stated by the manufacturer), produced very different results. The enzyme with the higher activity

gave nearly a 9-fold increase (6,070 g/mol vs. 670 g/mol) in the M_n of the co-polymer when diol **151** was used, and nearly twice the M_n (11,170 g/mol vs. 5,700 g/mol) when diol **149** was included as the second monomer. There was only a marginal difference, ~1.2 fold, for the esterification of diol **152** with the acid **140a**.

Subsequent to this report the Clarson group published a series of papers where the focus was on using N435 as the enzyme catalyst to produce silicone-containing block co-polymers in which the second block was either ε-caprolactone,[157] or ethylene glycol.[158] Additionally, reports appeared showing the synthesis of aromatic silicone polyesters and polyamides.[159,160]

Poojari and Clarson demonstrated the synthesis of triblock co-polymers from ε-caprolactone (**156**, PCL) and bis-hydroxyalkyl polydimethylsiloxane (**157**) in toluene at 70°C using N435 as the catalyst (**Figure 48**).[158] The composition of the polycaprolactone-*co*-polydimethylsiloxane-*co*-polycaprolactone (PCL-PDMS-PCL) block copolymer (**158**) was determined for different feed ratios of the monomers. When PCL:PDMS was 20:80, the M_n was 4,400 g/mol but could be increased to nearly 14,000 g/mol by altering the feed ratio to 80:20 PCL:PDMS. The thermal tolerance of the enzyme catalyst was determined over two successive 4.5 hour reaction cycles at 70°C and, in all cases, the M_n of the copolymer was higher when the enzyme was used a second time.

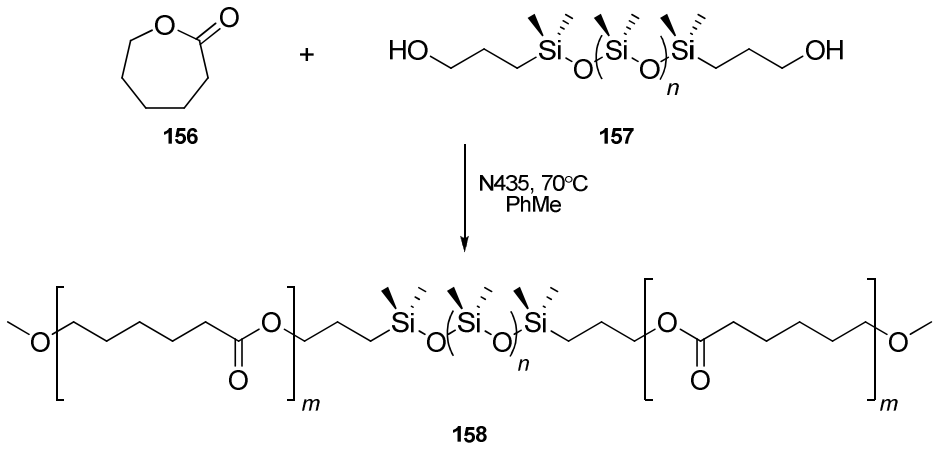

Figure 48 The lipase-catalyzed synthesis of triblock co-polymers from ε-caprolactone and α,ω-bis(3-hydroxyalkyl)-polydimethylsiloxane in toluene at 70°C.[158]

In another report, the synthesis of polydimethylsiloxane-*co*-ethylene glycol was examined from two perspectives (**Figure 49** and **Figure 50**).[157] First, diacid **140a** and ethylene glycol (**159a-c**) of different number average molecular weight (**a**=400 g/mol, **b**=1,000 g/mol, and **c**=3,400 g/mol) were combined under solvent free conditions at 80°C in the presence of 10 wt% of N435 (**Figure 49**). In the second system, diacid functionalized polyethylene glycol (**161**) (M_w=600 g/mol) was reacted with **162** (**Figure 50**). The average degree of polymerization for each of the experimental conditions was analyzed. In the first system, increasing the M_n of the polyethylene glycol (PEG) block lead to a sharp decrease in the average degree of polymerization from 17 (PEG M_w=400 g/mol) to 5 (PEG M_w=1,000 g/mol) and 3 (PEG M_w=3,400 g/mol); when the PEG-diacid was combined with the PDMS diol the average degree of polymerization was found to be only 5.[157] The decrease in the degree of polymerization was attributed to phase separation between PEG and PDMS.[157]

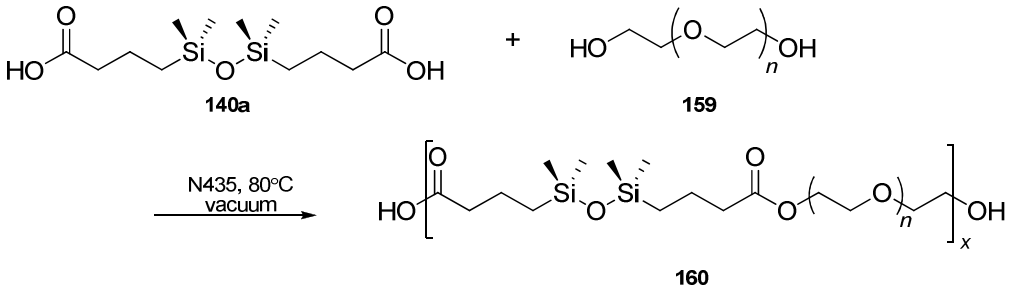

Figure 49 The lipase-catalyzed synthesis of disiloxane-containing copolymers produced from a diacid-terminated disiloxane and polyethylene glycol oligomers.[157]

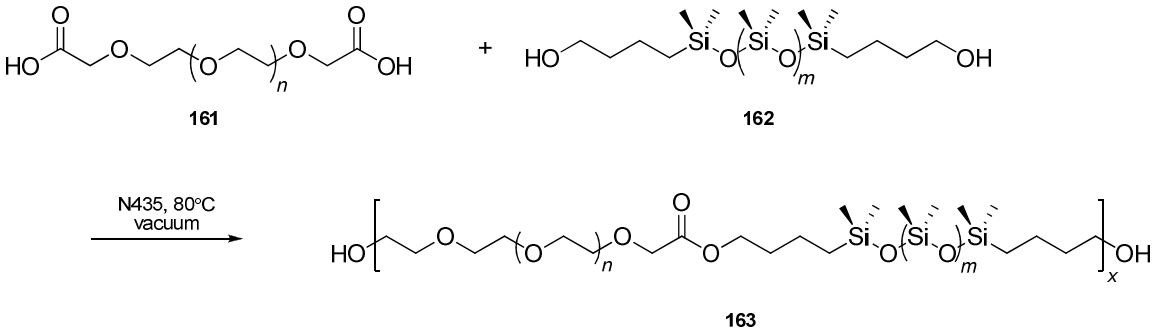

Figure 50 The lipase-catalyzed synthesis of polysiloxane-containing copolymers produced from a diacid-terminated polyethylene glycol and α,ω-bis(hydroxyalkyl)-polydimethylsiloxane.[157]

Polyesters and polyamides containing silicone and aromatic blocks have been produced using N435 as the catalyst from dimethyl terephthalate (**164**) and hydroxyalkyl PDMS (**138a**) (2,500 g/mol) or diamine **145** (1,000 g/mol or 4,700 g/mol) in toluene at 80°C-90°C (**Figure 51** and **Figure 52**).[159,160] The molecular weight build-up of aromatic silicone polyesters (**166**) was shown to increase over a 96 hour period, increasing from M_w=17,300 g/mol (M_n=10,300 g/mol) after 24 hours to M_w=47,000 g/mol (M_n=31,000 g/mol) at 48 hours to M_w=52,000 g/mol (M_n=38,000 g/mol) after 96 hours.[159] Over the same time period the dispersity of the molecular weights (PDI) decreased from PDI=1.68 to 1.52 to 1.37.[159] The change in the molecular weight distribution of aromatic silicone

polyamides (**167**) was much less dramatic, showing smaller increases under similar reaction conditions; however, because the molecular weights of the diol and diamine blocks were dissimilar, a direct comparison reveals nothing. We must consider the PDI of the polyamide-derived systems to glean useful information. When diamine **145a** (1,000 g/mol) was used, the PDI marginally increased from 1.60 (48 hours) to 1.68 (96 hours) and, when **145b** (4,700 g/mol) was the diamine, the PDI decreased from 1.98 (48 hours) to 1.5 (96 hours).[160] This result established that increasing the chain length had a positive effect on the outcome of the enzymatic polyamidation process.

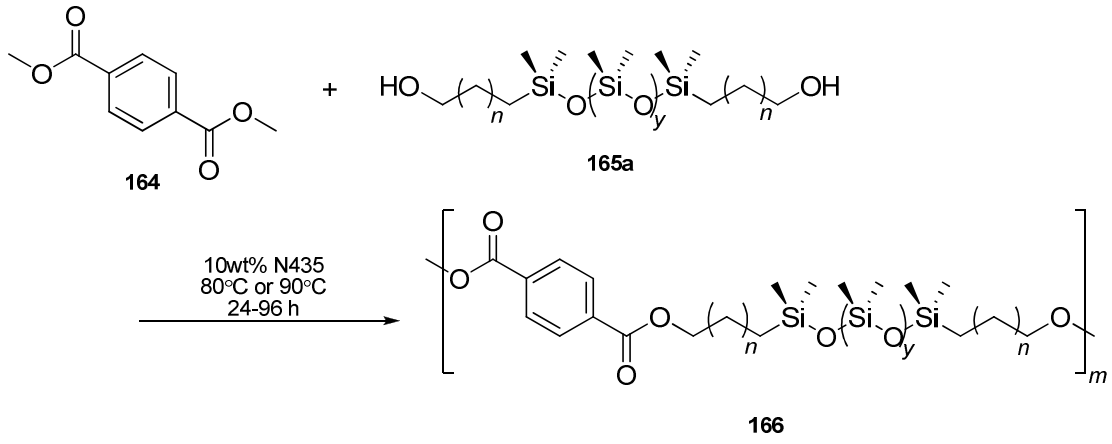

Figure 51 The enzymatic synthesis of aromatic silicone polyesters from dimethyl terephthalate and an aminopropyl terminated polydimethylsiloxane**.**[159,160]

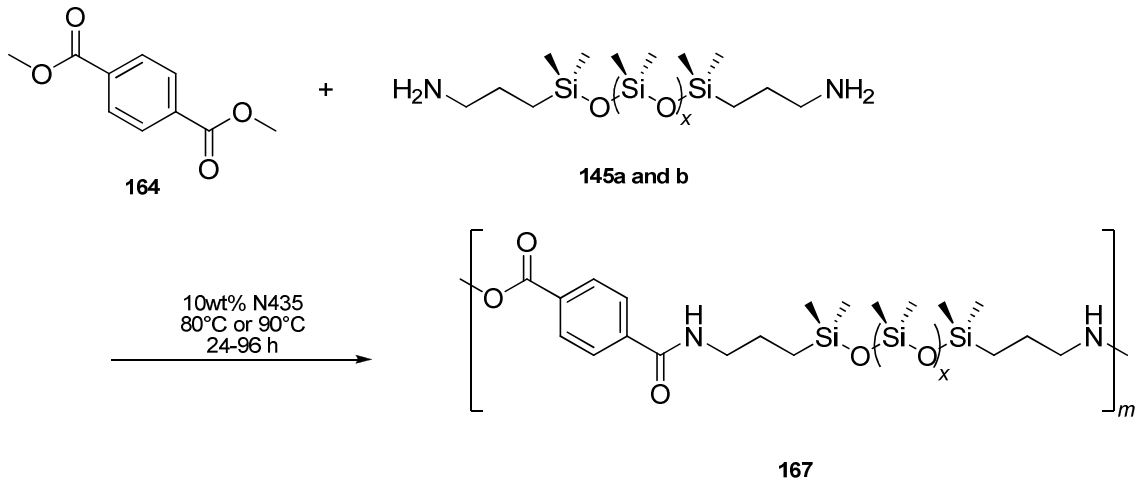

Figure 52 The enzymatic synthesis of aromatic silicone polyamides from dimethyl terephthalate and a bis-hydroxyalkyl terminated polydimethylsiloxane at 80-90°C over 24-96 hours.[159,160]

In 2008, Guo *et al.* synthesized a series of polydimethylsiloxane-containing diols to be used in the biosynthesis of silicone copolyesters (**Figure 53**).[161] Tetramethyl-disiloxane (**168**) and octamethylcyclotetrasiloxane (**169**, D_4) were hydrolyzed over concentrated sulphuric acid to yield two different α,ω-bis(hydrido)-polydimethylsiloxanes (**170a** & **b**). The hydride-PDMS was end-capped by adding allyloxytrimethylsilane (**171**) and chloroplatinic acid to yield the corresponding α,ω-bis(3-allyloxytrimethylsilyl)-PDMS (**172a &b**). Quantitative deprotection to reveal diols **165b** and **165c** was achieved using neat methanol at room temperature for 6 hours.

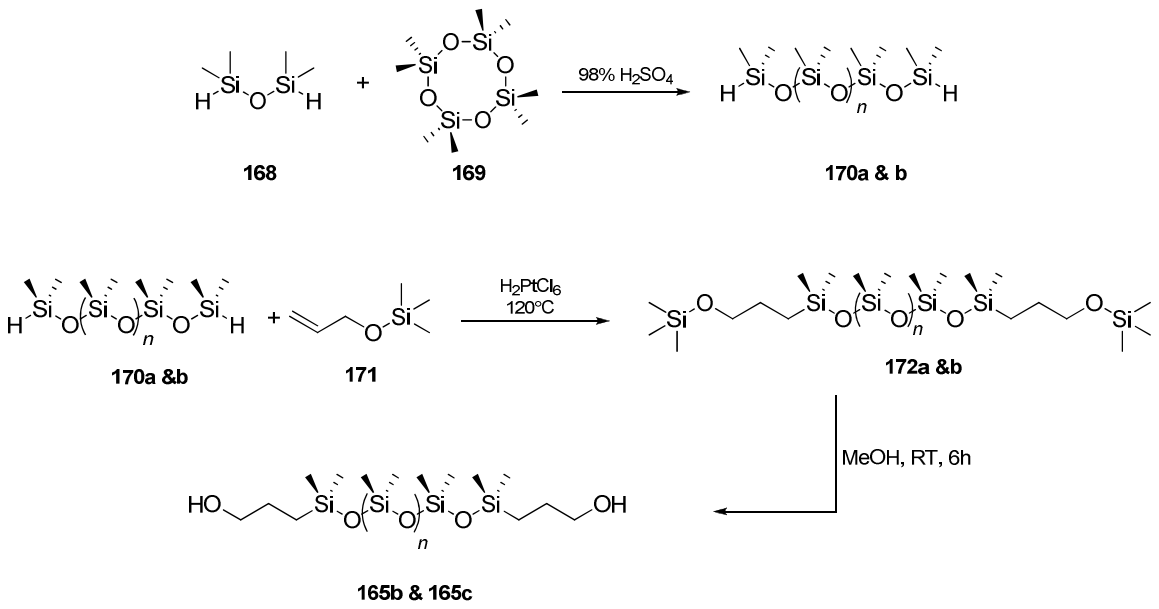

Figure 53 The synthesis of silicone-diols from tetramethyldisiloxane and D_4.[161]

Enzymatic polymerizations involved combining stoichiometric quantities of the silicone diols with one of succinic (**173**), adipic (**174**), or caprylic acid (**175**) as outlined in **Figure 54**. Polycondensation reactions were carried out under solvent-free conditions or in hexanes using a Dean-Stark trap to facilitate the removal of water. Regardless of the reaction conditions employed the dispersity of the molecular weights was in the range of PDI=1.4-2.1. Prolonged reaction times correlated with increased average degree of polymerization at all reaction temperatures, although the difference between each temperature was not particularly large. Despite this observation, the polymer derived from acid **173** was of the highest average degree of polymerization, containing 10 repeat units. The largest number average molecular weight was achieved at 50°C reaching a maximum of ~ 9,000 g/mol compared to 8,000 g/mol at 70°C and 600 g/mol at 90°C; enzyme denaturation was credited as the cause of the poor performance of the enzyme at higher temperatures. Finally, when using 1 wt% of catalyst, compared to the mass of the monomers,

at 90°C, the equilibrium could be forced to the products side by performing the polycondensations in hexanes using a Dean-Stark trap rather than by performing the reactions under solvent-free conditions using only an applied vacuum to remove water from the reaction mixture. While the reactions were slower to start, the number average molecular weight increased to ~7000 g/mol compared to ~6250 g/mol using only vacuum to remove water.

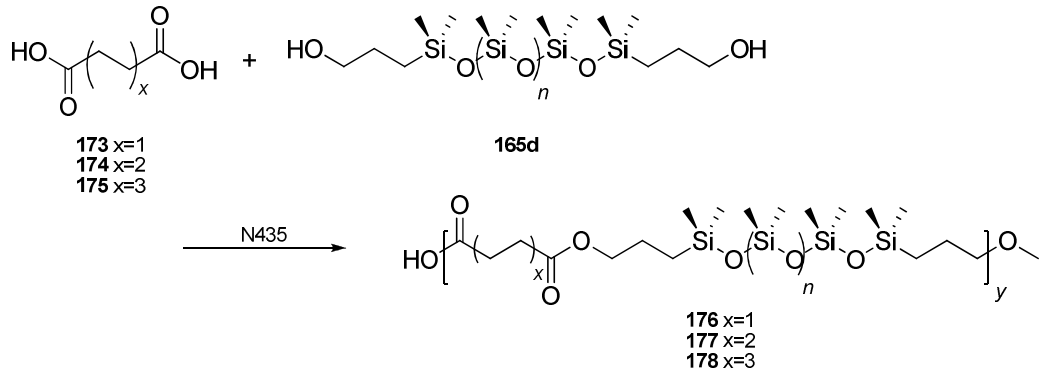

Figure 54 The N435-catalyzed condensation of succinic, adipic, and caprylic acids with silicone diols of two chain lengths.[161]

2.6.4 Lipases

Lipases (EC 3.1.1.3) are in the serine family of hydrolases and hydrolyze triacylglycerides into glycerol and free fatty acids *in vivo*. *In vitro*, lipases have the capacity to hydrolyze other types of esters making the distinction between lipases and esterases somewhat blurred. Lipases, at least to some extent, are known to function optimally at lipid-water interfaces resulting in a phenomenon known as *interfacial activation*.[162]

X-ray crystallographic studies of lipases have been used to determine the structural features of these enzymes. Lipases generally share the serine triad motif in the active site which is common to all serine hydrolase enzymes.[163] Lipases typically contain some part of, or all of, the features of the α/β-hydrolase fold. This fold is characterized by a β-sheet surrounded by several α-helices. The active site of many lipases is occluded from the bulk solvent by a hydrophobic lid which is involved in the interfacial activation of some lipases. When the lid is blocking the active site, the enzyme is said to be in the *closed* conformation. In the case of *Candida rugosa* lipase, Glu_{66} and Pro_{92} are involved in opening the lid; a *trans* to *cis* isomerisation of Pro_{92} opens the lid so that the enzyme is in the *open* conformation and available for catalysis.[164]

The lipase of the most relevance to this thesis is lipase B from *Candida antarctica* (CalB) for which the crystal structure was solved in 1994.[165] CalB is a globular protein composed of 317 amino acids and has a total molecular mass of 33,273 Da. Its key features are the α/β-hydrolase fold with seven strands comprising the β-sheet which is surrounded by ten α-helices, as well as the absence of a hydrophobic lid (**Figure 55**).

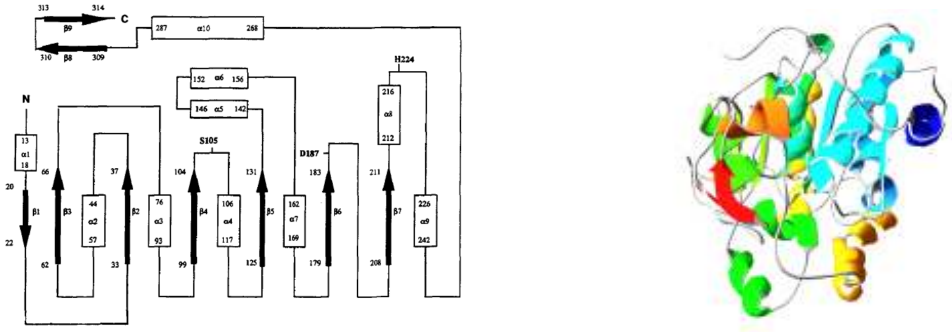

Figure 55 Schematic diagram of CalB[165] (left) and a ribbon structure from PDB 1TCA[165] (right).

The enzyme possesses as large hydrophobic surface region which surrounds the active site and likely plays a role in stabilizing enzyme-substrate interactions. This region surrounds a narrow channel, 10Å x 4Å wide and 12Å deep which is predominantly lined with hydrophobic residues and leads to the active site which contains the catalytic Ser_{105}, His_{224}, and Asp_{187} triad. There is only one histidine residue in the entire protein which strongly suggests a role in catalysis. An X-ray structure of CalB complexed with *n*-hexylchlorophosphonate ethyl ester identified Ser_{105} as the active nucleophile.[163] The active site is solvent exposed, that is to say that there is no hydrophobic lid, although the small helix α5 may have some minor role in interfacial activation, and as such, interfacial activation is not thought to play a role in CalB catalysis.[163,165]

Two channels have been defined near the active site of CalB which can accommodate its substrate. One channel accepts the acyl donor and the other channel accepts the acyl acceptor (**Figure 56**).[163] These channels have been used to denote the two sides of the active site as the "acyl side" and the "alcohol side".[163] The acyl side is the larger of the two channels and the opening is enclosed by Leu_{140}, Leu_{144}, and Ile_{185}. The alcohol side channel lies on the other side of a border that has been arbitrarily defined by Ile_{189} and Ile_{285}, and the opening is lined by Ile_{285} and Leu_{278}. Given the relative proximity of Ile_{189} and Ile_{285}, it has been proposed that the protein must undergo a major rearrangement in order to accommodate a triglyceride.[163]

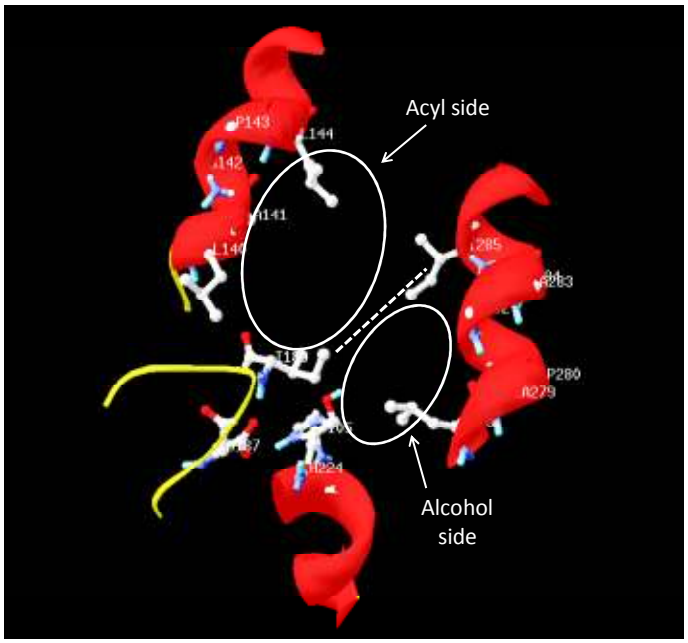

Figure 56 A ribbon diagram created with Deep View/Swiss PDB Viewer[166] showing the top view of the active site of PDB ID 1TCA.[163] The arbitrary definitions of the acyl side and the alcohol side of the channel leading into the active site cavity are indicated. The dashed white line represents the border between the two channels.

Lipases have attracted much attention as catalysts because they exhibit a high degree of control over chemo-, regio-, and enantioselectivity, they can be produced in large quantities using modern microbiological technologies, and they do not generally require cofactors for activation.[167] Lipases have been used extensively in many industries such as food, detergent, pharmaceutical, textile, cosmetic, and paper.[162]

Novozym-435 (N435) is composed of CalB immobilized onto a macroporous acrylic resin (Lewatit VP OC 1600, Lanxess, Germany). This biocatalyst is renowned for its high activity and selectivity and has been used in the synthesis of small molecules and polymer systems alike. It has been suggested that there is approximately 10 wt% of CalB immobilized on the resin.[168-170] The distribution of the enzyme within the acrylic

matrix is not uniform. Synchrotron infrared microspectroscopy (SIRMS) was used to examine the lipase containing beads at 10 μm resolution. The SIRMS spectra showed that CalB was localized only to the external portions of the enzyme beads, penetrating into the bead approximately 80-100 μm, and that within these regions the distribution was not uniform (**Figure 57**).[171] The secondary structure of the immobilized CalB showed the characteristic vibrational modes associated with amide carbonyl groups and was compared to the free enzyme; no obvious differences were detected, suggesting that the immobilization of the enzyme did not alter the three dimensional structure of the enzyme. Scanning electron micrographs showed that the pore sizes within the acrylic resin were approximately 10X larger than a CalB molecule, suggesting that the non-uniformity of the distribution was not attributable to any physical barrier within the acrylic resin. Polystyrene of a comparable molecular weight to CalB was shown to freely diffuse throughout the acrylic matrix.

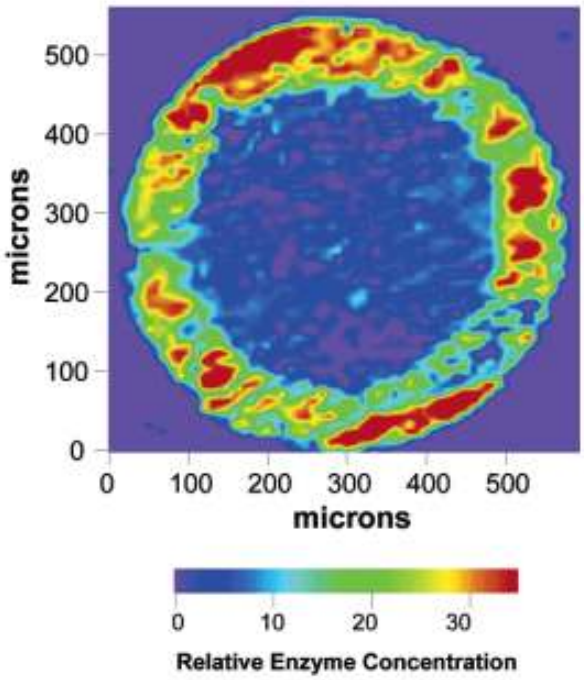

Figure 57 Synchrotron infrared microspectroscopy spectrum showing the distribution of CalB immobilized on an acrylic resin (N435). Reproduced with permission from Reference 163, Copyright 2003, the American Chemical Society.

The preceding chapter has reviewed two main areas under the umbrella heading of organosilicon biotechnology; the interaction between biomolecules and silica, and biotransformations of organosilicon compounds by microorganisms and isolated enzymes. The previous work which has been reviewed spawned several hypotheses that were tested, and which will be presented in the following chapters.

The first set of hypotheses that will be tested will relate to the interaction between amino acids and proteins, and TEOS and phenyltrimethoxysilane. Previous work had been primarily focused on employing amino acids, polyamino acids, and polyamines to precipitate silica from pre-hydrolyzed solutions of a silica precursor such as sodium silicate, TMOS, TEOS, or potassium tricatecholatosilane, in an attempt to understand how

these molecules participate in the biosilicification process. Only work from the Morse group,[79] which showed that some polyamino acids and the silica processing enzyme silicatein were catalysts for performing the hydrolysis and condensation of TEOS and phenyltriethoxysilane, Sundheendra and Raju,[62] using lysine and serine, and Hartlen *et al*.,[63] using arginine showed that amino acids could be used to prepare monodisperse silica from TEOS sols.

There are two major hypotheses that will be tested. Firstly, this thesis will test the hypothesis that amino acids are candidates for performing the hydrolysis and condensation of TEOS at pH 7. It is hypothesized that the nature of the side chain of the amino acid will have some effect on the capacity of each amino acid to direct the hydrolysis and condensation of TEOS. The second hypothesis to be tested, from this section, will be that enzymes, namely serine and cysteine proteases, have the capacity to perform the hydrolysis and condensation of TEOS and PTMS under neutral or near neutral pH regimes. Using trypsin as a model enzyme, the requirement of a catalytically competent active site will be tested by using a Kunitz type inhibitor which is known to block tryptic catalysis.

The second body or work of this thesis will focus on the capacity of free and immobilized lipases to carry out the synthesis of siloxane containing polymers. There are but two groups currently working in this field. The Gross group has shown that the immobilized lipase B from *Candida antarctica* can a catalyst for producing copolymers containing a polysiloxane diamine block.[155] The Clarson group has shown that the same lipase can produce polyesters that contain either a disiloxane-containing acyl donor, or a polysiloxane acyl acceptor.[156-160] The primary hypothesis to be tested in this thesis is that lipases can be employed as catalysts in the synthesis of polyesters, polyamides, and poly-

ester-amides in which the acyl donor and the acyl acceptor contain disiloxane or polysiloxane blocks. Several secondary hypotheses will be tested that will complete this area of research. Namely that the length of the siloxane chain, temperature, the geometry of the acyl donor and acceptor, and the proximity of the siloxane chain to the reactive functionality affect the rate of the enzyme-mediated polymerization of siloxane-containing monomers.

3 Disclaimer

Portions of Section 4 have been previously published in parts of the following articles:

1. M. Frampton, A. Vawda, J. Fletcher, and P.M. Zelisko. *Chem. Commun*., **2008**, 5544-5546. The candidate performed the majority (>90%) of the experiments. The remainder of the enzyme-mediate experiments (<10%) were carried out by A. Vawda and J. Fletcher. The writing of the manuscript was initiated by the candidate with subsequent revisions being a joint effort between the candidate and P.M. Zelisko.

2. M. Frampton, R. Simionescu, and P.M. Zelisko. *Silicon*, **2009**, *1*, 47-56. The majority of the experiments (>90%) were carried out by the candidate the remaining NMR experiments were performed by R. Simionescu. The writing of the manuscript was initiated by the candidate with subsequent revisions being a joint effort between the candidate and P.M. Zelisko.

3. M.B. Frampton, R. Simionescu, T. Dudding, and P.M. Zelisko. *J. Mol. Cat. B:Enz*., **2010**, *66*, 105-112. The majority of the ^{29}Si NMR experiments (>90%) were carried out by the candidate the remaining ^{29}Si NMR experiments were performed by R. Simionescu. All theoretical calculations were performed by T. Dudding. The writing of the manuscript was initiated by the candidate with subsequent revisions being a joint effort between the candidate and P.M. Zelisko.

4. M.B. Frampton and P.M. Zelisko. *Silicon*, **2012**, *4*, 51-56. All experiments were carried out by the candidate. The writing of the manuscript was initiated by the

candidate with subsequent revisions being a joint effort between the candidate and P.M. Zelisko.

5. M.B. Frampton, I. Subczynska, and P.M. Zelisko. *Biomacromolecules*, **2010**, *11*, 1818-1825. The majority of the syntheses of starting materials (>95%) and all enzyme-mediated reactions were carried out by the candidate. The remaining syntheses of starting materials were carried out by I. Subczynska. The writing of the manuscript was initiated by the candidate with subsequent revisions being a joint effort between the candidate and P.M. Zelisko.

6. M.B. Frampton, J.P. Séguin, D. Marquardt, T.A. Harroun, and P.M. Zelisko. *J. Mol. Cat. B:Enz*., **2013**, *85-86*, 149-155. The majority of the syntheses of starting materials (>90%), all enzyme-mediated reactions, and analyses were carried out by the candidate. The remaining syntheses of starting materials were carried out by J.P. Ségion. Differential Scanning Calorimetry experiments were performed by D. Marquardt and T.A. Harroun. The writing of the manuscript was initiated by the candidate with subsequent revisions being a joint effort between the candidate and P.M. Zelisko.

4 Results and Discussion

The following chapter of this thesis will be divided into two main research areas that fall under the general heading of organosilicon biotechnology: (1) the use of amino acids and enzymes to catalyze the hydrolysis and condensation of alkoxysilanes; and (2) the use of lipases as catalysts for the synthesis of siloxane-containing polyesters and polyamides. The hydrolysis of tetraethoxysilane and phenyltrimethoxysilane by biologically relevant molecules, such as amino acids and proteins will be presented, with a focus on the how the amino acid side chain impacts the rate of hydrolysis. Where enzymes have been used, the nature of the architecture within the *S1* binding pocket will be shown to be of potential importance. This will be followed up by a discussion of a possible mechanism for the hydrolysis of phenyltrimethoxysilane by three different enzymes. A ^{29}Si nuclear magnetic resonance (NMR) study that analyzed the hydrolysis of phenyltrimethoxysilane by three different enzymes will be presented. The final discussion to be offered will pertain to the lipase-catalyzed synthesis of siloxane-containing polyesters and polyamides. Polymerization kinetics will be examined as will the long-term, thermal tolerance and the retention of residual activity by the lipase. Finally, the synthesis of branched polyesters by N435 will be briefly explored.

4.1 The Hydrolysis of Alkoxysilanes

4.1.1 Hydrolysis of Tetraethoxysilane by Amino Acids

The Zelisko group prepared cross-linked silicone elastomers from triethoxysilyl functionalized PDMS (TES-PDMS) and TEOS using a bio-inspired approach.[81] The *in vitro* hydrolysis and condensation of the alkoxy moieties were mediated using anhydrous trypsin suspensions, or trypsin preparations containing minimal amounts of water, as catalyst systems. The resulting cross-linked elastomers were visually and chemically indistinguishable from those synthesized using dibutyltin dilaurate; however, the exact role of trypsin was unknown. Several possibilities were hypothesized: (1) trypsin preferentially hydrolyzed TEOS; (2) trypsin hydrolyzed triethoxysilyl groups of the functionalized PDMS; or (3) trypsin had an equal capacity to hydrolyze both of the compounds. Furthermore, it was unknown if the active site of the enzyme was an obligate requirement for hydrolysis. Previous work by Morse suggested that trypsin could precipitate silica from TEOS without showing that the catalytic triad was performing any catalysis,[8] and if it was, it was not known whether the enzyme was acting in a manner consistent with (1) traditional organosilicon chemistry whereby catalysis was being initiated by the imidazole moiety of the active site His_{57}, or (2) if a mechanism reminiscent of traditional peptide hydrolysis was occurring whereby the hydroxymethyl of Ser_{195} was assuming the role of the active nucleophile.

To begin the search for evidence in support for these hypotheses, a systematic investigation of the hydrolysis of TEOS was performed using only amino acids as catalysts. The condensation of free silicic acid from pre-hydrolyzed silica precursors was shown to

be dependent on the amino acid side chain. The amino acids that were included in this study are presented in **Figure 58**.

Amino acids were prepared in phosphate buffer (pH 7.03±0.02) and combined with 250 μL (1.12 mmol) of TEOS in plastic 1.8 mL Eppendorf tubes. Plastic tubes were chosen rather than glass vials to negate the potential for hydrolysis that may occur from incidental contact between TEOS and the glass vials.

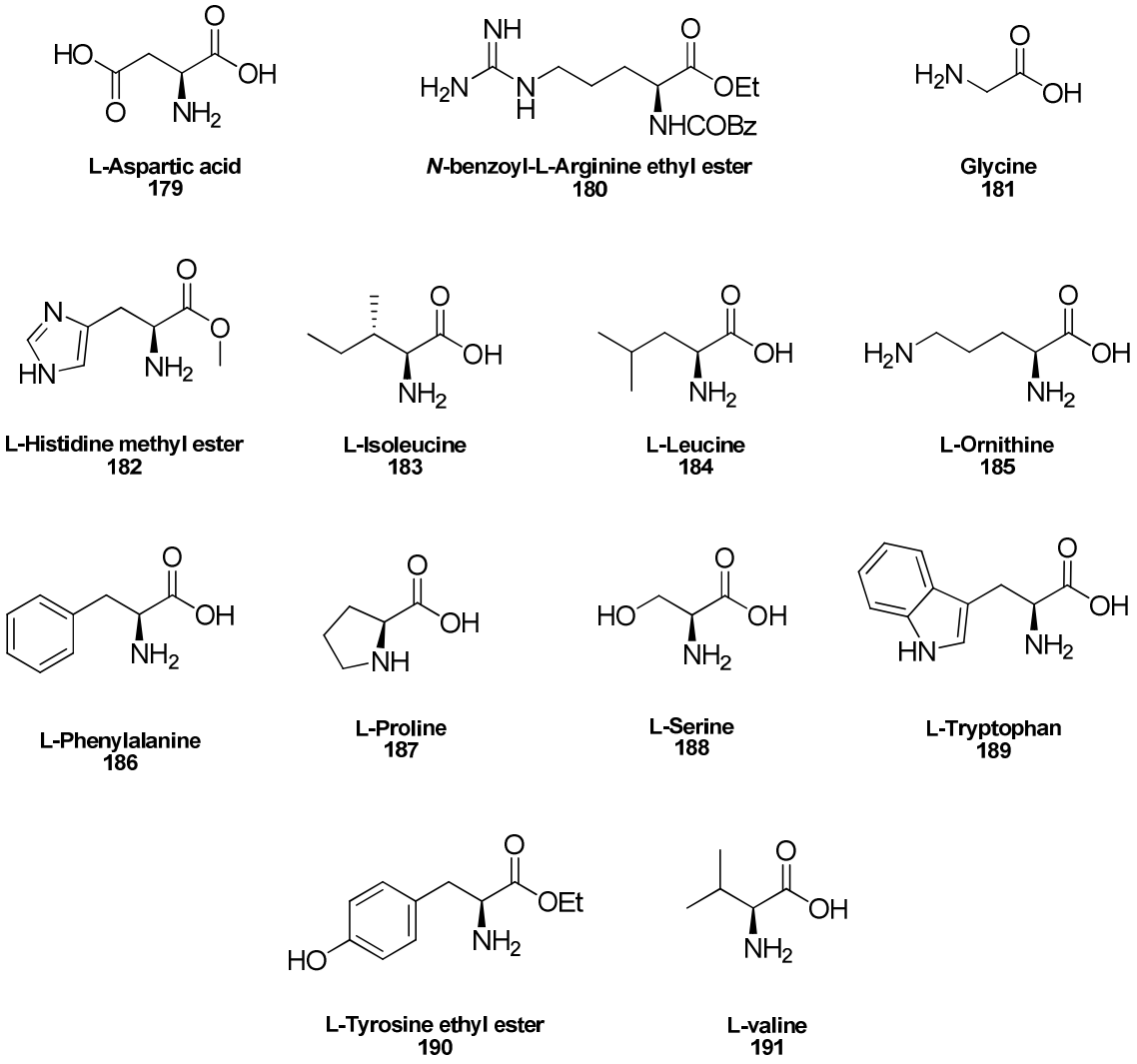

Figure 58 The amino acids examined as potential catalysts for the hydrolysis of TEOS.

The hydrolysis of TEOS (**192**) can proceed through either nucleophilic or electrophilic catalysis.[172] The reverse reaction, silyl ether formation, is more difficult to quantify but can be suppressed if an excess of water is included in the reaction mixture. The hydrolysis of **192** produced four intermediate hydrolysis products in a sequential manner as outlined in **Figure 59**. The condensation of TEOS, as judged by the presence of particulate silica in the reaction medium, was observed after 24 hours when arginine was used as the catalyst. However, a homogeneous mixture such as a sol, sol-gel or gel, was not formed. After centrifugation an opaque silica pellet was isolated for each reaction condition; this silica was isolated, hydrolysed to silicic acid, and quantified using the silicomolybdate method.[1]

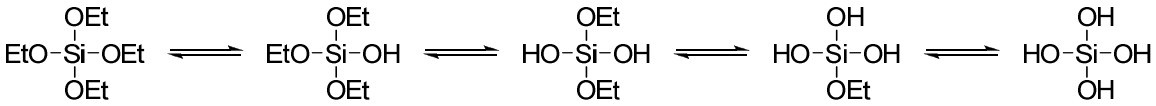

Figure 59 The hydrolysis of tetraethoxysilane proceeds through four sequential hydrolysis products.

The interfacial interaction between TEOS and amino acid preparations gave variable amounts of precipitated silica, approximately 0-7.5 mg, based on the preparation and analysis of sodium silicate standards via the silicomolybdic acid assay. With the exception of tyrosine and arginine, which were used as ethyl esters, and histidine which was used as the methyl ester, all of the amino acids that were used had free carboxylate and amino groups. Therefore, the difference in the amount of silica that was produced can be

attributed to the side chain of each amino acid. In the absence of any amino acid, only small amounts of silica, < 450 μg, could be isolated from the control reactions. The reported quantities of silica have been normalized to reflect this background hydrolysis.

The amino acid side chain was an important factor in facilitating the hydrolysis of TEOS. Arginine, histidine, ornithine, and tyrosine, were the only amino acids that demonstrated any capacity to hydrolyze TEOS over and above the control (**Figure 60**). The other amino acids hydrolyzed only small quantities of TEOS, producing less than 400 μg of silicic acid (**Figure 60**). Sudheendra and Raju suggested that lysine and serine preparations in Tris (2-amino-2-(hydroxymethyl)propane-1,3-diol) buffer hydrolyzed TEOS at pH 6.9,[62] but the same could not be said of arginine. It has since been demonstrated that aqueous solutions of arginine (pH not controlled) produced silica from TEOS/cyclohexane mixtures.[63]

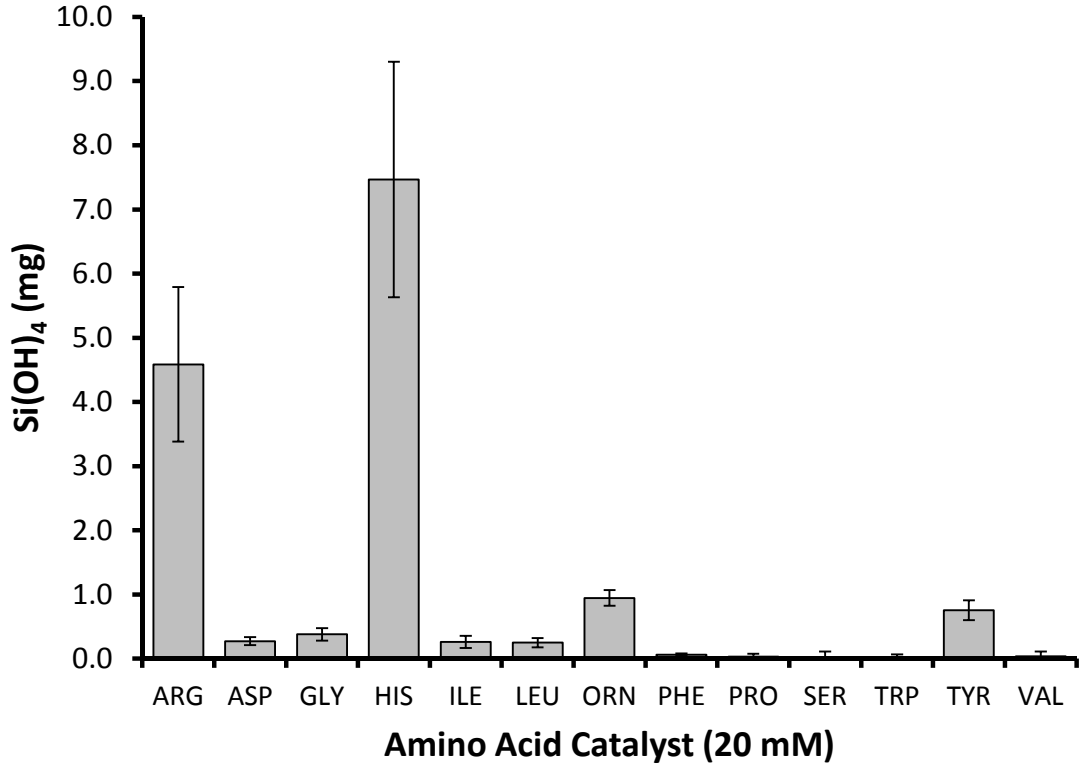

Figure 60 The hydrolysis of TEOS by selected amino acids. Silicic acid was quantified using the silicomolybdate method. Amino acids were dissolved to 20 mM in 0.2 M phosphate buffer at pH 7.03±0.02 and incubated with 1.12 mmol TEOS at room temperature for 24 hours. Each bar represents the average of three trials. Error bars show the standard deviation of three trials.

The amino acids that were the best catalysts for hydrolyzing TEOS share the common feature of an ionizable side chain (**Table 3**). With the exception of proline and serine, the amino acids that were not successful at hydrolyzing TEOS posses side chains that do not contain nucleophilic groups. In fact the non-catalytic amino acids are typically described in biochemistry texts as being non-polar (Gly, Ile, Leu, Val, Phe, Trp), polar neutral (Ser), or neutral (Pro).[184]

Table 3 Characteristics of the amino acids used for silicic acid production from TEOS.

Amino Acid	pK_a Side Chain	Description	$Si(OH)_4$ Produced (mg)
Arginine	12.5	polar, basic	4.586
Histidine	6.04	polar, basic	7.468
Ornithine*	10.8	polar, basic	0.945
Tyrosine	10.1	polar, acidic	0.753
Aspartic acid	3.86	polar, acidic	0.272
Glycine	-	non-polar	0.378
Isoleucine	-	non-polar	0.261
Leucine	-	non-polar	0.250
Valine	-	non-polar	0.034
Phenylalanine	-	non-polar	0.061
Tryptophan	-	non-polar	(0.012)
Proline	-	neutral	0.033
Serine	-	polar, neutral	0.028

* Chemical characteristics for lysine.

The interaction between amino acids and TEOS is not limited to hydrolysis reactions. The condensation of silicic and disilicic acids is affected by the presence of amino acids. Some basic amino acids have been implicated in the deprotonation of silanols making the growing silica chain more nucleophilic.[61] We can therefore postulate that once the hydrolysis of TEOS has commenced, the partially hydrolyzed species interact with the side chain of the amino acid, promoting further hydrolysis of alkoxy moieties and condensation of silanols. In that regard, the results presented here are in agreement with those of Belton *et al*.[61] The Belton study determined that the third order rate constant for silicic acid oligomerization could be increased or decreased by the addition of amino acids. For example, lysine, arginine, and tyrosine each enhanced the rate of oligomer formation, while proline and serine had little effect and both glycine and alanine reduced the rate of oligomer formation. The Belton study further suggested that the basic

amino acids, which posseses an ionized side chain at neutral pH, may be important in the (bio)silification process where they participate in hydrogen bonding with silanols.[61]

4.1.2 Enzymatic Hydrolysis of TEOS

The sol-gel processing of alkoxysilanes is a mild method for producing inorganic-organic hybrid materials. Silica sol-gels have been used as sensors and as scaffolds for entrapping proteins and other delicate biomolecules.[173,174] Sol-gel chemistry is usually performed using an alcohol solvent and is initiated by the addition of an acid or base catalyst. Binary aqueous-alcohol solvent systems are not always compatible with the long term functioning of proteins. Disruption of stabilizing hydrogen bonding networks leads to enzyme denaturation.

In order to alleviate any potential denaturing effects of aqueous alcohol solvent systems, we set out to study the capacity of trypsin and α-chymotrypsin to mediate the hydrolysis of TEOS in a modified approach to the sol-gel process. Silicatein had been shown to possess hydrolytic activity towards TEOS and phenyltriethoxysilane; trypsin was less active during the 15 minute assay.[9] Using the Morse work as a guideline we sought to employ proteases as catalysts for mediating the hydrolysis of TEOS and other alkoxysilanes. Our target enzymes were the serine proteases trypsin and α-chymotrypsin. Trypsin- and α-chymotrypsin-mediated reactions, along with the appropriate enzyme-free and inhibited-enzyme control reactions were prepared by combining enzyme preparations in distilled water with TEOS. The ratio of water-to-silicon was maintained at 4:1 for all reactions. Low water conditions typically have the effect of slowing hydrolysis and condensation while high water conditions favour the hydrolysis process.[51]

TEOS hydrolysis reactions mediated by α-chymotrypsin progressed from a biphasic mixture to a uniform sol that was optically transparent and slightly viscous which, upon continued ageing, resulted in the formation of a silica monolith. The trypsin-mediated hydrolysis of TEOS on the other hand did not progress through the sol stage. What was observed, however, was a silica gel that appeared to correspond to the volume of water that was included in the reaction mixture. Enzyme-free control reactions also did not form sols, sol-gels, or monolithic silica. This agrees well with previous reports where silicatein was used as a catalyst for the hydrolysis and condensation of TEOS.[9]

To ensure that the active site of the enzyme was indeed responsible for hydrolysis and/or condensation, α-chymotrypsin and trypsin were each inhibited using a Kunitz-type soybean inhibitor. A two-fold excess of the trypsin inhibitor and enzyme were combined at room temperature for 2 hours prior to the addition of TEOS. Formation of a silica monolith was never observed following inhibition of the enzyme suggesting that the active site was a prerequisite for the hydrolysis and condensation of TEOS. This is somewhat different from the outcome of Bassindale's experiments in which the active site of trypsin did not appear to be a requirement for the hydrolysis of ethoxytrimethylsilane. An uncompromised active site was, however, required for the condensation of trimethylsilanol to hexamethyldisiloxane.[147]

The macromolecular structure of the enzymatically produced silica monoliths were compared employing solid state ^{29}Si NMR with silica monoliths that were prepared by acid catalysis. Solid state ^{29}Si NMR spectra of enzyme-produced silica gels suggested that catalyst choice had only a marginal effect on the extent of siloxane condensation (**Figure 61**). The ^{29}Si NMR spectra of the three silica monoliths showed resonances aris-

ing at -91.98 ppm, -101.19 ppm, and -110.55 ppm as expected for the Q^2, Q^3 and Q^4 regions of a ^{29}Si NMR spectrum.[48,175] The ratio of the Q^3:Q^4 peaks determined after Gaussian line fitting and deconvolution of the spectra gave a peak ratio of 1.37:1 for the sol-gels derived from α-chymotrypsin, and 1.18:1 for acid-catalyzed sol-gels. The increased relative proportion of the Q_3 peak observed using α-chymotrypsin as a catalyst indicated a lower degree of siloxane condensation. The silica gel produced using trypsin had a decreased proportion of Q^3:Q^4 peak intensities (0.77:1) suggesting that condensation was more complete.

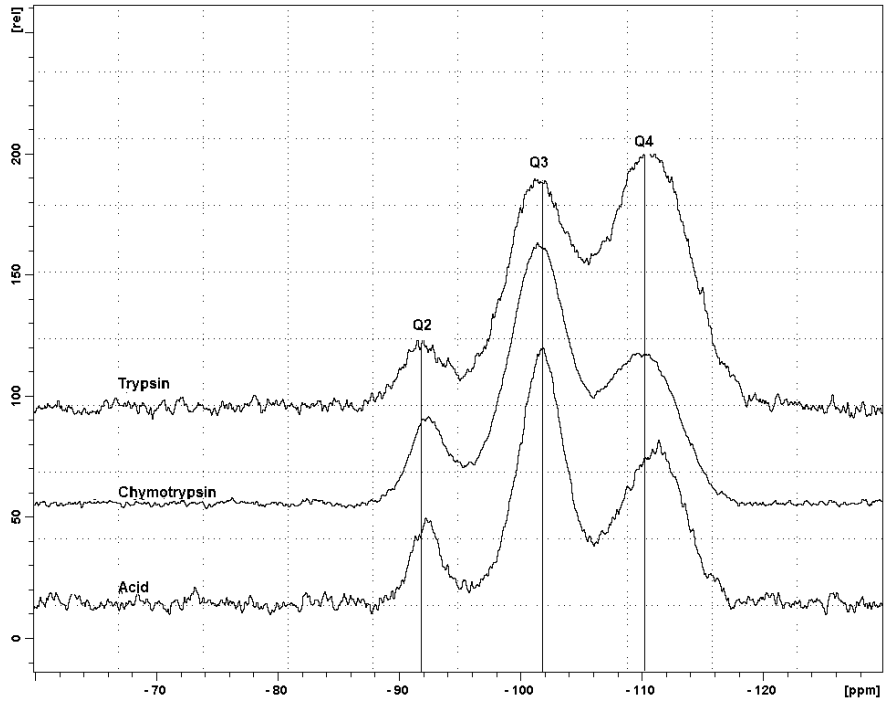

Figure 61 Solid state ^{29}Si NMR spectra of three amorphous silica gels produced using trypsin (top), α-chymotrypsin (middle) and lactic acid (bottom).

The generality of using proteins as catalysts for the hydrolysis of TEOS was extended by including more enzymes. The carboxypeptidase pepsin, the cysteine proteases bromelain and papain, lipase from *Candida rugosa* (which has the same catalytic triad as the serine proteases),[176] and the transport protein human serum albumin (HSA) were in-

cluded as potential catalysts. Similar to trypsin, pepsin and bromelain formed a silica hydrogel from TEOS. Papain, lipase from *Candida rugosa*, and HSA did not produce silica monoliths.

To better understand these observations a study was undertaken to monitor the hydrolysis of TEOS using a fixed amount of enzyme catalyst in an excess of water to ensure that there was a sufficient amount of water to drive hydrolysis, but also to suppress the formation of monolithic silica.

Visual inspection indicated that a small amount of silica was produced after 24 hours. It was noted that for those reactions conducted at pH 7.01, pepsin, papain and bromelain precipitated out of solution. While these preparations produced small quantities of silica, it is not known whether the silica formation was enzymatic, involving the active site of the enzyme, or occurred by non-specific surface interactions between the enzyme and TEOS. These enzymes did not precipitate from solution when the pH of the reaction medium was unbuffered.

The pH of the reaction medium was an important contributing factor to the amount of silica produced (**Figure 62**). At non-optimal pH levels enzymes such as pepsin, are known to irreversibly denature while others, such as trypsin are more robust. When the pH was controlled there was little difference in the amount of silica that was produced ranging from 50-100 μg, however, pepsin, papain and bromelain appeared to denature and precipitate from solution. In the unbuffered reactions, differences in the amount of TEOS that was hydrolyzed became evident. The hydrolysis of TEOS by trypsin was more extensive when the pH of the reaction medium was unbuffered; the amount of silica that was isolated increased from ~100 μg to 200 μg.

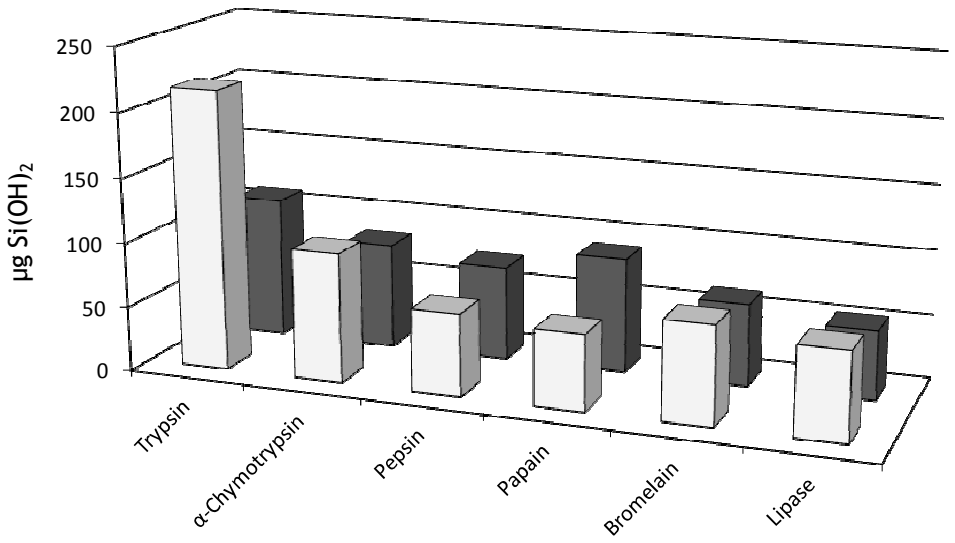

Figure 62 The enzymatic hydrolysis of tetraethoxysilane. Hydrolysis was quantified by measuring the amount of silicic acid using the silicomolybdate method**.** *Legend*: light grey bars=distilled water pH 6.4, dark grey bars=phosphate buffer pH 7.01. *Conditions*: 210 µM enzyme in 1.0 mL water or buffer, 250 µL TEOS.

The hydrolysis of TEOS was greatest using trypsin producing more than 200 µg of $Si(OH)_4$. α-Chymotrypsin which is evolutionarily related to trypsin, but exhibits a preference for hydrophobic amino acids, generated only half the amount of silicic acid. The other enzymes typically produced between 50-100 µg of silicic acid. Why trypsin and α-chymotrypsin should be so different is unclear, but similar observations in other systems have been made.[147,149] The isoelectric point is thought to be a factor in the precipitation of enzyme-silica composites from pre-hydrolyzed silicic acid solutions. For silica precipitation under acidic conditions it has been suggested that the pI of the enzyme must be above 10 (trypsin pI=10.5 and α-chymotrypsin pI=8.67).[177] Surprisingly, *Candida antarctica* lipase (CRL) was among the poorest performers. CRL is known to re-

quire interfacial activation to catalyze the hydrolysis of triacylglycerides, and the interfacial hydrolysis of TEOS would appear to be ideal, however, only about 50 μg SiO_2 was generated. It was believed that CRL would be a suitable candidate enzyme because the inclusion of lipase from *Burkholderia cepacia* increased the condensation of methyltrimethoxysilane (MTMS) and TMOS under similar conditions, but this was not the case.[178]

4.1.3 Trypsin-Mediated Hydrolysis of Terminally-Functionalized Siloxanes

The second hypothesis that came out of the Zelisko group's early work was that trypsin had the capacity to hydrolyze the triethoxysilyl moieties of TES-PDMS. We have since learned that trypsin hydrolyzes TEOS; however, it remained to be seen if trypsin could hydrolyze TES-PDMS.

A series of trialkoxysilyl-functional molecules were synthesized via platinum-catalyzed hydrosilylation chemistry on the *Si-H* and alkene functional groups. This chemistry provided access to a library of functionalized siloxanes and difunctionalized alkane derivatives. This library represented an array of architectures and is presented in **Figure 63**. This suite of substrates covered a broad range of molecules and gave the best chance of evaluating the hypotheses concerning the capacity of trypsin to hydrolyze alkoxysilyl groups. The attempted hydrolysis of trialkoxysilyl groups by trypsin is presented in **Figure 64**.

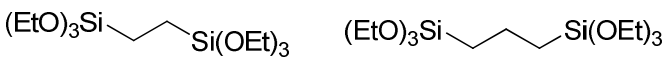

202 **203**

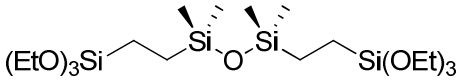

204

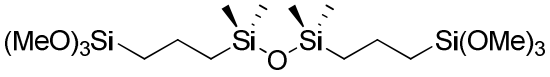

205

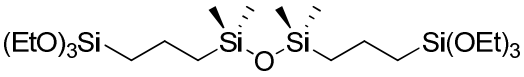

206

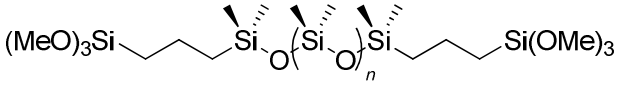

207

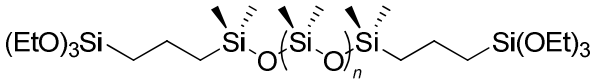

208

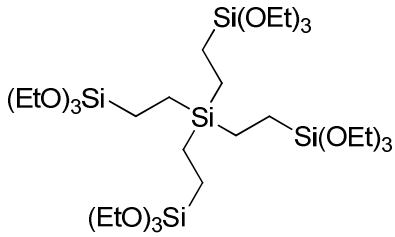

209

Figure 63 The library of bis-trialkoxysilyl substituted compounds prepared for enzymatic hydrolysis experiments.

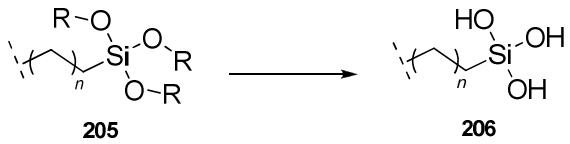

Figure 64 The attempted hydrolysis of trialkoxysilyl functionalized disiloxanes, polysiloxanes, and bis-trialkoxysilylalkanes.

The hydrolysis of the compounds presented in **Figure 63** was attempted using trypsin as a catalyst. Enzyme-free control reactions showed that in the absence of a catalyst hydrolysis was non-existent and not going to interfere with the final analysis. Unfortunately, all reactions using trypsin as the catalyst also failed to result in any detectable hydrolysis by ^{29}Si NMR. A comparison of the ^{29}Si spectra of the enzyme-free and trypsin-catalyzed reactions with the ^{29}Si NMR spectrum for the starting siloxane showed that the spectra were identical.

In some of the reactions that were prepared with an excess of water, a second phase appeared that resembled particulate matter or micelles. Analysis by ^{29}Si NMR spectroscopy confirmed that hydrolysis did not occur. Spurred on by this curious phase segregation, we acquired phase contrast microscopy images of the crude reaction mixture to find that micelles of varying morphologies were present (**Figure 65**). Many of the micelles were spherical, while some were oblong to amorphous in shape with a visible texture present in some of the micelles suggesting that a physical or chemical cross-linking may have occurred. The observed texture was reminiscent of cross-linked silicone elastomers that had previously been prepared using trypsin or dibutyltin dilaurate. However, in the absence of spectroscopic data to confirm this hypothesis, it remains merely as speculation.

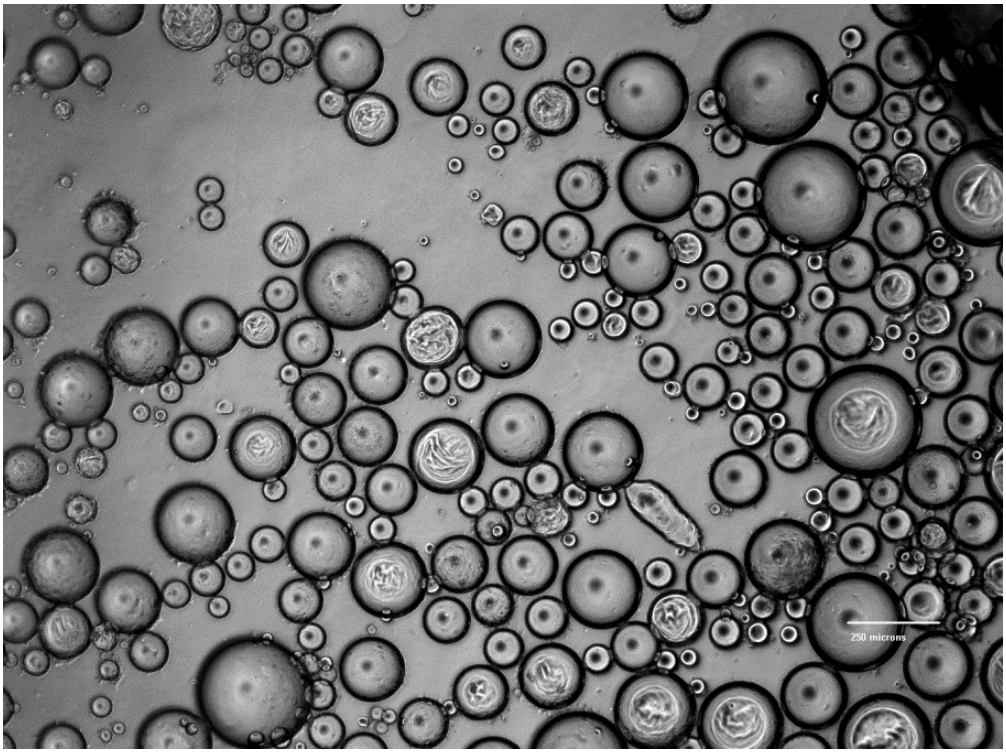

Figure 65 Phase contrast micrograph of the crude reaction mixture containing α,ω-trimethoxysilylpropyl polydimethylsiloxane (TMSPr-PDMS) and 10 mg/mL trypsin. The nature of the cause of the microspheres that have texture is unclear. The scale bar in the image depicts 250 μm.

4.1.4 Hydrolysis of Organically-Modified Trialkoxysilanes

In an effort to probe the selectivity of the active site of the enzymes, we chose to examine the hydrolysis of organically modified alkoxysilanes. Organically modified alkoxysilanes undergo hydrolysis and condensation in a manner consistent with tetraalkoxysilanes to generate silsesquioxanes of varying architectures which include random structures, ladder structures, cage and partial cage structures.[179]

It was believed that by using (3-aminopropyl)triethoxysilane as a substrate that the aminopropyl group would be a good fit for the *S1* binding pocket of trypsin. However, this substrate spontaneously hydrolyzed upon contact with water and thus could not be

used. Knowing that α-chymotrypsin and pepsin could accommodate the side chains of aromatic amino acids, phenyltrimethoxysilane (PTMS) was chosen as a candidate substrate. There is no known colorimetric method of analysis for the hydrolysis of PTMS so ^{29}Si NMR was used as a method to follow the hydrolysis of PTMS. Despite the observation that trypsin does not readily accept amino acids with aromatic in rings in the side chains,[184] we chose to include trypsin because of the previous success that had been observed using this enzyme.

207 **208**

Figure 66 The structures of (3-aminopropyl)triethoxysilane (**207**) and phenyltrimethoxysilane (**208**).

4.1.4.1 Enzymatic Hydrolysis of Phenyltrimethoxysilane

The mere combination of PTMS and water was not sufficient to catalyze the hydrolysis of PTMS (**Figure 67**); after 48 hours, the reaction mixtures remained biphasic and ^{29}Si NMR experiments with PTMS in D_2O confirmed that in the absence of a catalyst hydrolysis of the PTMS was non-existent. The only ^{29}Si NMR resonance that was visible corresponded to PTMS.

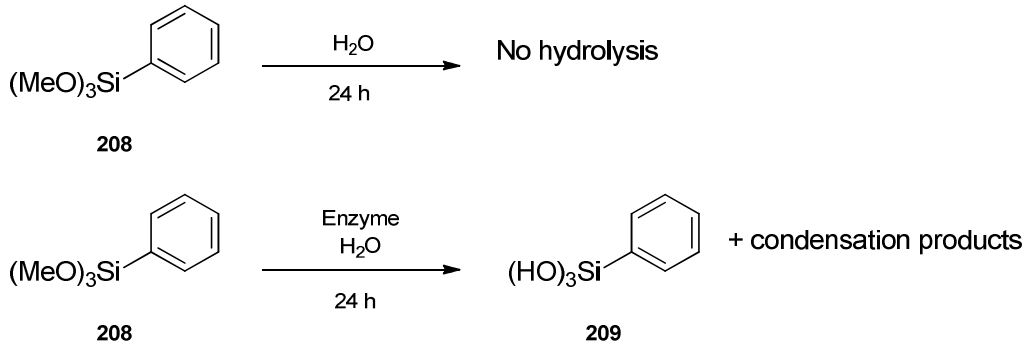

Figure 67 The hydrolysis of phenyltrimethoxysilane under catalyst-free (top) and enzyme catalyzed conditions. In the absence of a catalyst hydrolysis was not detected.

The incorporation of trypsin into reactions led to the hydrolysis, and subsequent condensation of PTMS and its hydrolysis products. After approximately 24 hours the silane and aqueous phases coalesced into a single clear and colourless phase. ^{29}Si NMR experiments confirmed that all of the PTMS had been hydrolyzed after approximately 24 hours. Unfortunately the acquisition parameters for the ^{29}Si NMR experiments did not make it possible to obtain ^{29}Si NMR resonances representing the single and double hydrolysis products (**Figure 68**). The ^{29}Si resonances that were visualized over the course of the reaction are summarized in **Table 4**.

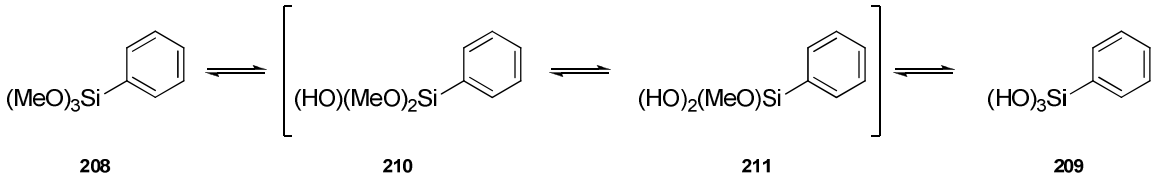

Figure 68 The hydrolysis of phenyltrimethoxysilane showing all of the possible intermediates. The first two hydrolysis products **210** and **211** were not detectable by ^{29}Si NMR**.**

Table 4 Assignment of the ^{29}Si NMR resonances for the hydrolysis and condensation of trimethoxyethylsilane. The chemical shift values in the δ (ppm) column correspond to the underlines and italicized silicon atoms (*Si*) in each chemical formula. Labels are presented according to the nomenclature provided by Brinker and Scherer.[48]

δ (ppm)	Peak Assignment	Structure
-51	T^3_0	Ph*Si*$(OH)_3$
-55	T^0_0	Ph*Si*$(OMe)_3$
-61.1	$T^2_1T^2_1$	Ph$(OH)_2$*Si*-O-*Si*$(OH)_2$Ph
-60.9	$T^2_1T^1_2T^2_1$	Ph$(OH)_2$*Si*-O-SiPh(OH)-O-*Si*$(OH)_2$Ph
-70.5	$T^2_1T^1_2T^2_1$	Ph$(OH)_2$Si-O-*Si*Ph(OH)-O-Si$(OH)_2$Ph

To confirm that the active site of the enzyme was a requisite for catalysis the same Kunitz-type soybean inhibitor that was used to inhibit the active site of trypsin was employed (*vide supra*). The effectiveness of this inhibitor lies in the formation of an extremely low energy intermediate which greatly slows the dissociation of the trypsin-inhibitor complex, for all practical purposes making the complex irreversible.[180] Trypsin was incubated with a two-fold excess of the inhibitor prior to being used in the experiments to ensure that the active site was unavailable for catalysis. The ^{29}Si NMR spectra representing the inhibited trypsin reactions did not display any resonances that would interfere with resonances associated with the hydrolysis and condensation of PTMS. That hydrolysis of PTMS under these conditions did not occur suggests that the active site of trypsin was necessary for carrying out the hydrolysis of PTMS. In addition, the inhibitor itself did not behave as a catalyst for the hydrolysis of PTMS. From these results we can surmise that non-specific surface interactions were not significantly contributing to the hydrolysis of PTMS. However, owing to the low sensitivity of the ^{29}Si nucleus, and the absence of a colorimetric method to quantify minute amounts of silicon, the possibility of some small background rate of hydrolysis that does arise from non-specific surface interactions cannot be ruled out.

4.1.4.2 A Kinetic Analysis of the Enzymatic Hydrolysis of Phenyltrimethoxysilane

A complete description of the kinetics associated with the hydrolysis of phenyltrimethoxysilane is a complicated process. The hydrolysis and condensation of TEOS requires more than 160 rate constants, using a nearest neighbour approach, to fully describe those processes. At nearest neighbour level of analysis iy is not possible to distinguish a silicon atom that is part of a dimer compared to one that is an end group to a larger polymer. These silicon environments can only be distinguished using the knowledge gained through a next-to-nearest neighbour approach. In this context there are 1365 chemically distinct silicon environments which require over 199,000 rate constants to fully describe the hydrolysis and condensation processes.[53,181] The focus here is on describing only the first hydrolysis of phenyltrimethoxysilane under enzyme-catalyzed conditions. The enzymes that are being examined (pepsin, trypsin, and α-chymotrypsin) possess similarities and differences as described below.

The following is a discussion of the hydrolysis of PTMS by pepsin, trypsin and α-chymotrypsin under aqueous conditions at near neutral pH. While this condition may not be optimal for any of these enzymes, it was important to minimize the background rate of hydrolysis which is at a minimum at near neutral pH.[1] It had previously been determined that under buffered conditions, pepsin rapidly precipitated from solution, so for this analysis, unbuffered reaction media were used. Each of the three enzymes possesses one or more binding pockets which can accommodate various amino acid side chains. The working hypothesis for this work was that the secondary interactions between the resi-

dues of the active site and the *S1* binding pocket affect the proficiency with which these enzymes would hydrolyze PTMS.

The reaction under investigation is outlined in the bottom panel of **Figure 67**, (**208→209**). In traditional systems the hydrolysis of alkoxysilanes is catalyzed by the addition of strong acid/base in an alcohol solvent; typically the alcohol is paired with the alkoxide being hydrolyzed to minimize the extent of transesterification with other alcohols, although this has not always been the case.[182] The inherent incompatibility between traditional hydrocarbon-based solvents and free enzymes meant that using ^{29}Si NMR spectroscopy as an analytical tool would require conducting biphasic experiments.

In the absence of any type of catalyst the hydrolysis of PTMS is very nearly non-existent, and over the time scale employed here (10 h), catalyst-free hydrolysis of PTMS was not observed. The enzymatic hydrolysis of PTMS was detected within the first 1-2 hours of the ^{29}Si NMR scale reaction. Hydrolysis was followed by monitoring the change in the intensity of the ^{29}Si resonance for PTMS located at -55.5 ppm. **Figure 69** was constructed from ^{29}Si NMR integration values and graphically depicts the hydrolysis and condensation of PTMS as a function of time. The consumption of PTMS was nearly complete after 10 hours. Fully hydrolyzed species were detectable within the first hour and dimerization products began to appear, although only to a small extent. Tryptic hydrolysis was slower and while phenylsilanetriol could be detected within the first hour, dimers and oligomers were not usually detected until after 10 hours.

The hydrolysis rate constant (k_{hyd}) can be derived from the slope of the initial decay portion of the curve representing the hydrolysis of PTMS. A plot of ln[Si] versus

time gives a straight line from which the hydrolysis rate constant can be acquired. The rate constant associated with each reaction condition is summarized in **Table 5**.

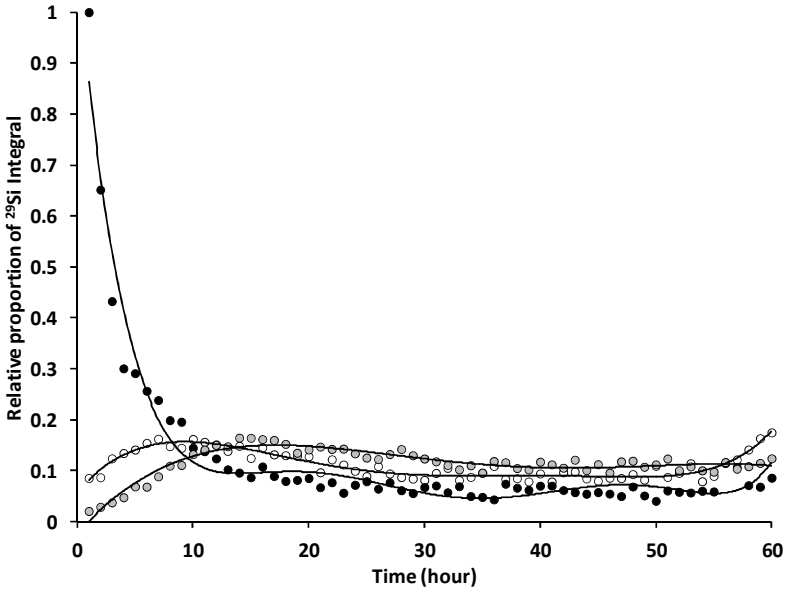

Figure 69 A representative time course profile for the hydrolysis and condensation of PTMS. The enzyme catalyst was pepsin and the evolution and/or disappearance of PTMS (black circles), phenylsilanetriol (white circles) and disiloxanes (grey circles) are shown. The circles represent the actual data points and the lines are provided to guide the eye.

Table 5 The hydrolysis rate constants for the hydrolysis of PTMS ($x10^{-2}$ hr^{-1}). Hydrolysis rate constants include the standard deviation determined from line fitting.

Enzyme	**Pseudo first order rate constant (hr^{-1})**					
	5.0 mg/mL	7.5 mg/mL	10 mg/mL	12 mg/mL	15 mg/mL	20 mg/mL
Trypsin	-	0.02±0.00	0.04±0.13	0.14±0.08	0.22±0.00	-
α-Chymotrypsin	0.11±0.01	0.44±0.11	0.54±0.26	0.83±0.33	1.10±0.22	-
Pepsin	0.54±0.22	-	0.67±0.12	-	0.86±0.00	0.99±0.10

The change in the observed hydrolysis rates was dependent upon the amount of enzyme included in the reaction (**Table 5**). The change in the rate constants was examined by varying the concentration of each enzyme. Trypsin was the least proficient en-

zyme of the three enzymes that were tested. Increasing the amount of trypsin did not correlate with a large increase in hydrolysis (**Figure 70**). Pepsin, on the other hand, displayed the highest rate of hydrolysis, but like trypsin did not exhibit a dramatic change in rate as the amount of enzyme was increased. α-Chymotrypsin possessed an intermediate rate of hydrolysis of PTMS at lower enzyme concentrations, but as the amount of α-chymotrypsin included in the reaction was increased, the rate of hydrolysis increased much more dramatically.

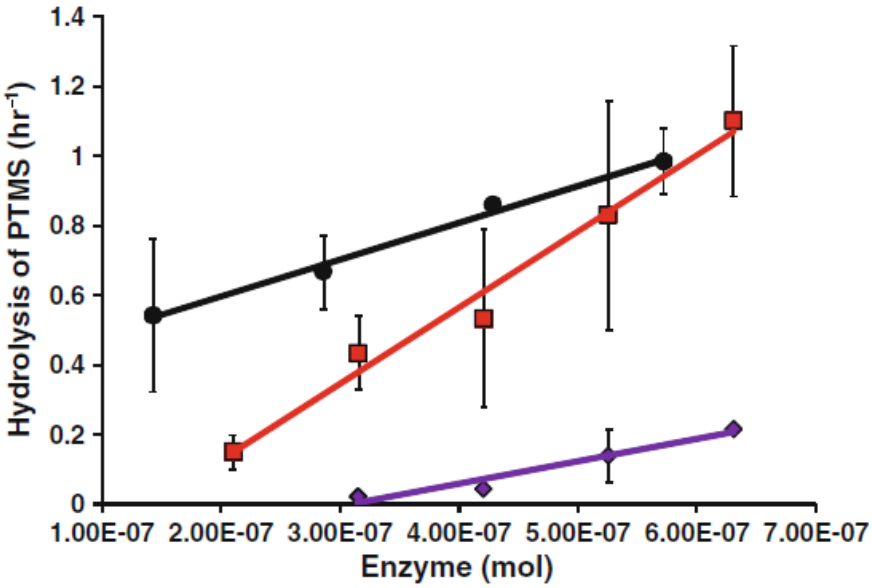

Figure 70 The hydrolysis of PTMS. The pseudo first order rate constant increased with enzyme concentration. *Legend*: Pepsin- black circles, chymotrypsin- red squares, trypsin- purple diamonds. Error bars indicate the standard deviation of three trials.

Enzymes have evolved to accept substrates with particular arrangement of atoms and functional groups. Part of this specificity can be attributed to the local environments within the secondary binding pockets that are located proximal to the active site. This is

particularly exemplified by trypsin and α-chymotrypsin which are evolutionarily related, but accept different substrates. There are many conserved residues between trypsin and α-chymotrypsin, but it is their differences that permit the binding of different substrates. The *S1* binding pockets of all serine proteases are formed by residues 189–195, 214–220, and 225–228[183] of which four of these residues are not conserved between trypsin and α-chymotrypsin; residues 189, 192, 217 and 219. Additionally Ser_{190} is differently oriented within each enzyme. Ser_{190} is found pointing into the *S1* binding pocket of trypsin but in α-chymotrypsin it is pointed away from the *S1* binding pocket where it is hydrogen bonded to Thr_{138}.[183] The bottom of the *S1* binding pocket in trypsin and α-chymotrypsin exhibits an additional dissimilarity; trypsin contains an Asp_{189} which is anionic at neutral pH and stabilizes the positively charged side chains of lysine and arginine residues.[184] The *S1* binding pocket of α-chymotrypsin, on the other hand, does not contain this anionic group which allows it to accept the hydrophobic amino acid side chains of phenylalanine, tryptophan, and tyrosine.[185]

Pepsin is a carboxypeptidase that contains two binding pockets, each of which is large enough to accommodate aromatic ring systems that are located proximally to the catalytic aspartic acid residues, Asp_{215} and Asp_{32}. During catalysis these residues polarize a single molecule of water making it more nucleophilic towards the scissile peptide bond.[186]

The enhanced hydrolysis by pepsin when compared to α-chymotrypsin and trypsin, can be rationalized by considering the nature of the catalytic mode of pepsin and the hydrophobic environment of the binding pockets that are present near the active site. Pepsin contains two aspartic acid residues, one that exists as the protonated acid and the

other as the carboxylate. Working together these moieties serve to polarize a water molecule which acts as the reactive nucleophile. During peptide hydrolysis pepsin does not form an acyl enzyme intermediate in the same manner as the serine proteases. This push-pull mechanism, and potential lack of a covalently bound silyl-enzyme intermediate between the active site residues with the silane, may serve to expedite hydrolysis.

α-Chymotrypsin can favourably accommodate the aromatic side chains of phenylalanine, tryptophan, and tyrosine within its *S1* binding pocket. The difference in the observed rate constants between α-chymotrypsin and pepsin can potentially be explained by the formation of an acyl-silane intermediate by α-chymotrypsin but not pepsin. However, if pepsin were to form a hypothetical silyl-enzyme intermediate, it would be an acetoxysilane type intermediate which under aqueous conditions would be easily hydrolyzed.[2,101] The observed differences between α-chymotrypsin and trypsin may lie in favourable interactions between the phenyl ring of PTMS and the *S1* pocket of α-chymotrypsin. Binding of the phenyl ring to the *S1* pocket of trypsin is not favoured as a result of the anionic Asp_{189} residue.

4.1.4.3 Proposed Mechanism of Alkoxysilane Hydrolysis

The mode of action of silicatein in the hydrolysis of TEOS has been the subject of study.[9,10] A mechanism was proposed to account for the hydrolysis of TEOS by silicatein. The mechanism was predicated on the catalytic Ser_{26} residue adding to silicon with concomitant expulsion of ethanol. It was proposed that the imidazole ring of the His_{165} coordinated to silicon allowing silicon to expand its valence shell to stabilize the silyl-enzyme intermediate. The remainder of the mechanism was thought to proceed in a

manner analogous to peptide hydrolysis in which the silyl-enzyme intermediate was hydrolyzed by water to liberate a free silanol-containing species. Site-directed mutagenesis studies whereby Ser_{26} and His_{165} moieties were separately replaced by alanine abolished nearly all of the catalytic activity of silicatein suggesting that both residues were required to mediate catalysis. A computational study employing Density Functional Theory (DFT) calculations provided a mechanism for the condensation of silicic acid by silicatein. This work provided computational evidence that cyclic siloxanes could be generated within the active site of the enzyme.[187]

Using silicic acid as a model compound, and applying Houk's[188,189] concept of a theozyme as a proxy for trypsin, DFT calculations using the gradient corrected hybrid functional of Becke-Yee-Lang and Parr[190-192] with a double zeta potential 6-31G(d) basis set[193-195] were carried out by Dr. Travis Dudding (Brock University, Department of Chemistry) to determine which residue of the catalytic triad would most favourably bind to silicon.[196]

Upon entering the active site, two options for addition to silicon become apparent. The Ser_{105} residue could instigate nucleophilic attack on silicon. The other option, based on considerations of the known chemistry of silicon, would see His_{57} as the active nucleophile. DFT calculations suggested that Ser_{105} addition to silicon was 15.56 kJ/mol (3.72 kcal/mol) lower in energy than His_{57} addition. These observations were consistent with *Si-O* (477-536 kJ/mol, 114-128 kcal/mol) and *Si-N* (401-434 kJ/mol, 96-104 kcal/mol) bond energies.2 Furthermore, modeling suggested that the transition state for Ser_{105} addition to silicon reached a five co-ordinate, trigonal bipyramidal geometry. Three hydroxyl groups of silicic acid align in the equatorial position to form angles of 114°, 119° and 120°,

while the Ser_{105} hydroxyl and the remaining hydroxyl of silicic acid are in the apical positions and are angled at 178°. This observed geometry is highly reminiscent of an S_N2-type transition state (**Error! Reference source not found.**). On the contrary, His_{57} addition appears to favour an S_N1-type pathway (**Error! Reference source not found.**). This would formally suggest the formation of a silyl cation; the existence of which has been vigorously debated in the literature and generally believed to not be a possible intermediate under biologically permitting conditions.[197]

When the previous example is considered, a complete mechanism can be proposed for the hydrolysis of PTMS (**Figure 71**). The nucleophilic Ser_{105} adds to silicon in the first step leads to a trigonal bipyramidal geometry of PTMS. Once the formation of the silyl-enzyme intermediate has occurred, its transient nature allows for rapid decomposition where a methoxy group is expelled from the coordination sphere of silicon. The methoxy group concommitantly deprotonates the imidazole ring of His_{57}, and in a manner consistent with the secondary steps of peptide hydrolysis, the flow of electrons reverses to restore the aspartate to its anionic state. A molecule of water then enters the active site of the enzyme, becoming polarized by hydrogen bonding to the imidazole ring of histidine, and attacks the silicon atom instigating the formation of the trigonal bipyramidal geometry a second time. Collapse of the trigonal bipyramidal structure is followed by expulsion of the Ser_{105} residue freeing the silane from the bound enzyme.

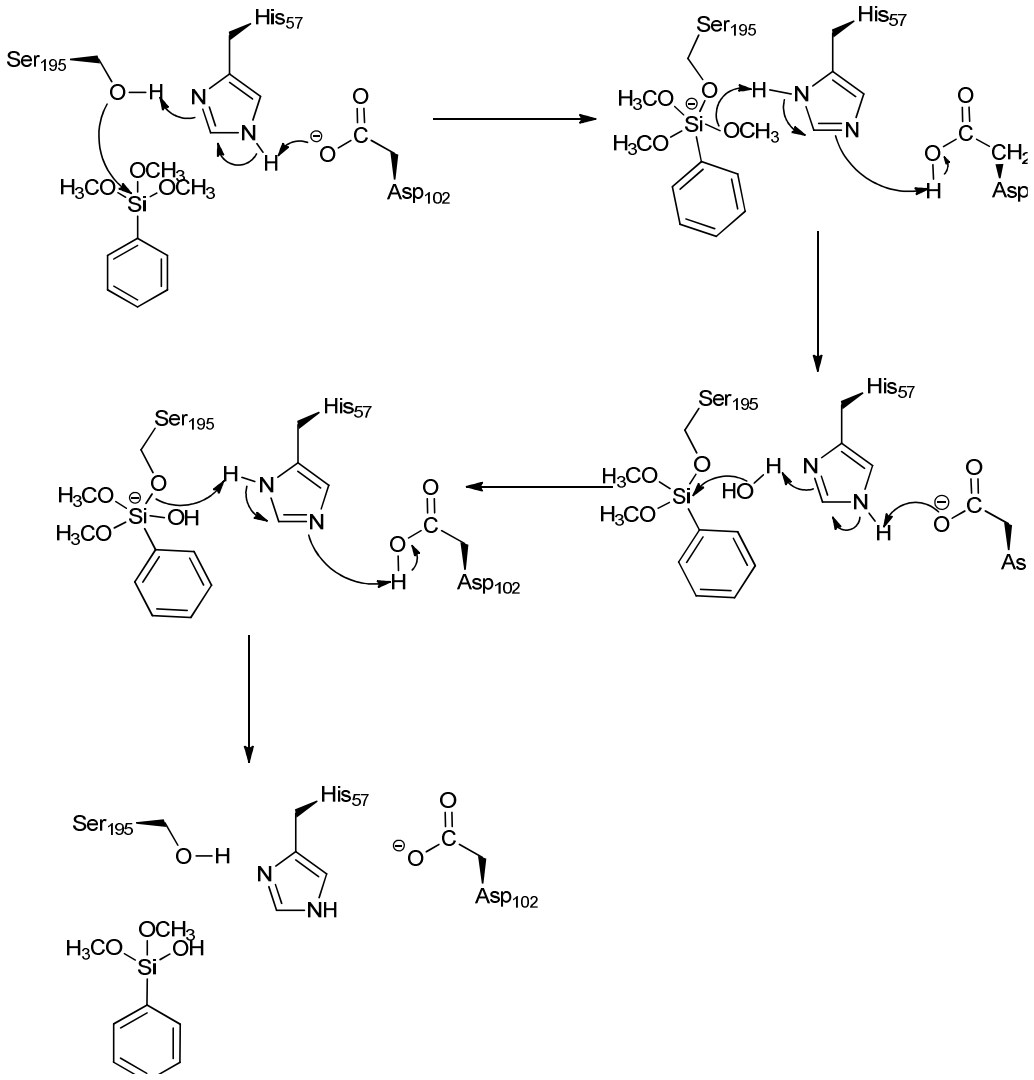

Figure 71 A proposed mechanism for the trypsin-mediated hydrolysis of PTMS. The initial step is predicated upon Ser_{105} addition to silicon leading to the expansion of its valence shell to assume a trigonal planar geometry which is reminiscent of an S_N2-type mechanism.

4.2 Synthesis of Siloxane-Containing Polyesters, Polyamides, and Polyester-Amides

4.2.1 Introduction

The lipase-mediated synthesis of polyesters has been shown to be a viable process in the laboratory. Examples have been reviewed which show that the molecular weight build-up of polyesters was dependent of reaction temperature, applied vacuum, catalyst

loading, and the chain length of the acyl donor and acyl acceptor. The next section will review efforts towards employing biocatalysis for the synthesis of siloxane-containing polyesters and polyamides in which both the acyl donor and acyl acceptor contain siloxane subunits. The schemes for these lipase-mediated reactions are outlined in **Figure 72** and **Figure 73**.

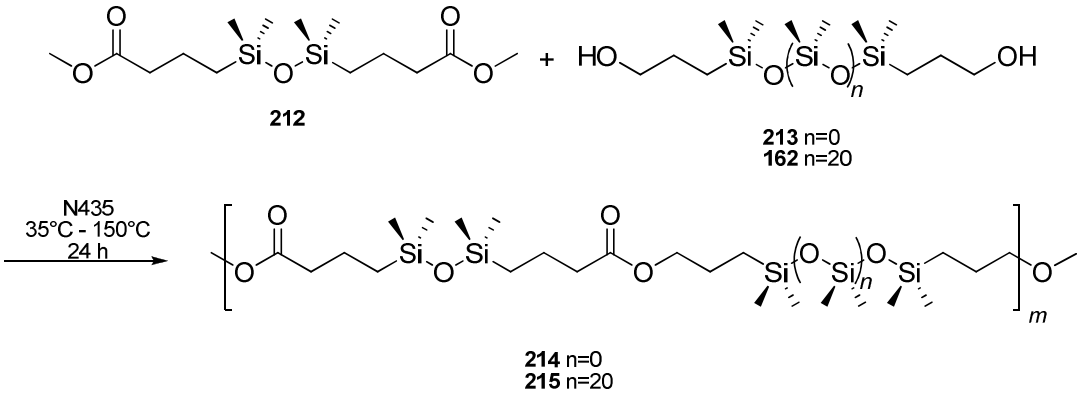

Figure 72 The lipase-catalyzed synthesis of siloxane-containing polyesters.

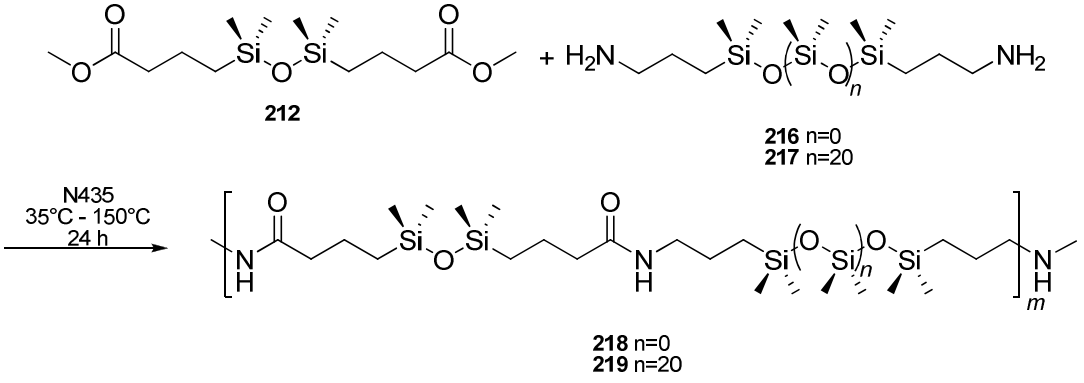

Figure 73 The lipase-catalyzed synthesis of siloxane-containing polyamides.

4.2.2 Siloxane-Polyesters

When diacid **140a** and diol **213** were combined under enzyme-free conditions low background rates of polyesterification were observed. While the reaction rates were low, in the range of 25-40%, these results suggested that AB dimers and ABA (BAB) could be formed. Diacid **140a** has been used in similar systems with alkane diols but it was unclear if a similar phenomenon was observed.[156]

To alleviate the background rate of esterification, dimethyl ester **212** was synthesized by refluxing diacid **140a** in methanol in the presence of pTsOH; the diester was routinely isolated in >95% yields (**Figure 74**). Enzyme-free controls using **212** as the acyl donor did not result in any detectable polytransesterification as determined by ^{1}H NMR over 24 hours regardless of the reaction temperature. Based on these results **212** was selected as the acyl donor for the remainder of the project.

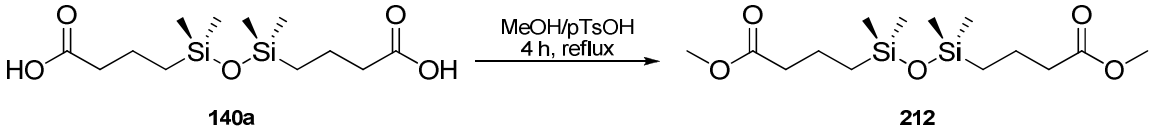

140a **212**

Figure 74 The synthesis of 1,3-bis(3-carboxypropyl)-1,1,3,3-tetramethyldisiloxane dimethyl ester (**212**).

Enzyme-free control reactions were performed using a longer polysiloxane diol (**162**) as the acyl acceptor to ensure that it also would not participate in uncatalyzed esterification. In those experiments no background rate of polytransesterification could be detected by ^{1}H NMR. From those results it was understood that any polyesterification that occurred was due solely to the presence of the enzyme catalyst.

4.2.3 Lipase-Catalyzed Synthesis of Disiloxane and Polysiloxane Polyesters

Stoichiometric amounts of diol **213** and diester **212** were combined with 12.5 wt% N435 relative to the mass of diester **212**. Diol **162** is nearly an order of magnitude more massive than diol **213** and so the stoichiometry between the diester and enzyme catalyst was controlled so that a direct comparison of the reaction rates could be made. This approach has not been typically been followed in lipase-mediated polymerizations in which aliphatic substrates were polymerized. For those cases, increasing the number of methylene groups by one only adds 12 Da to the total mass. However, the mass of the dimethylsiloxy unit is 74 Da, and therefore this larger mass must be taken into consideration. The initial rate of polymer elongation and total monomer conversion were monitored by removing 10 μL of the reaction mixture at predetermined time intervals for analysis by ^{1}H NMR. At the end of the reaction cycle, the reaction was stopped by the addition of 5 mL of diethyl ether or chloroform. The enzyme beads were removed via filtration and the final polymer was characterized by NMR (^{1}H, ^{13}C, ^{29}Si), Fourier-transform infrared spectroscopy (FT-IR), and differential scanning calorimetry (DSC). MALDI-ToF mass spectrometry was used to gain an understanding of the weight average molecular weight (M_w) distribution of the polymers, however, most attempts were less than fruitful.

The N435-catalyzed polyesterification was marked by a noticeable increase in the viscosity of the reaction mixture. On occasion, usually at higher temperatures, the original mixture exhibited a slight opacity and a colour shift from colourless to light straw-coloured over the course of the reaction cycle. The siloxane-polyesters that were produced from diester **212** and diol **213** were somewhat less viscous than those produced from the same diester and diol **162**.

The rate constant associated with polymer elongation was determined from a plot of the average degree of polymerization (DP_{avg}) versus time (in hours), where $DP_{avg}=1/(1-p)$ in which p is the extent of monomer conversion measured in fractional values.[198] Total monomer conversion was determined after each 24 hour polymerization cycle using the integration values from the ^{1}H NMR spectra that correspond to the *O*-methylene protons of the diol before and after esterification. A representative ^{1}H NMR spectrum is presented in **Figure 75** depicting the resonances that were used to determine the reaction rate and monomer conversion. The resonances that are of interested are highlighted by the ellipses.

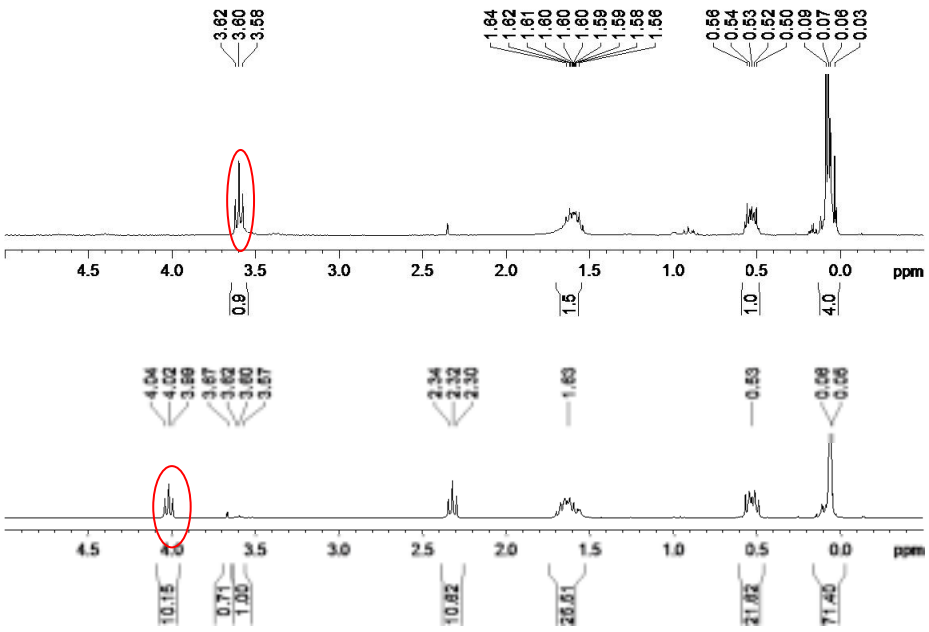

Figure 75 ^{1}H NMR spectra depicting the resonances that were used to determine the reaction rates and total monomer conversion. *Top panel*: Diol **213**; *Bottom panel*: Siloxane-containing polyester **214**.

It was determined that the lipase-mediated polyesterifications were temperature de-pendent. A low-temperature polymerization was carried out in the interest of determining

if the enzyme would polymerize siloxanes. Monomers **212** and **213** were combined with the immobilized lipase and incubated at 4°C in a refrigerator with occasional swirling for 24 hours; unfortunately, polyesterification could not be detected.

The lipase-mediated polymerization of **212** and **213** at moderate temperatures (35-70°C) coincided with low polyester elongation rates (**Figure 76**). At 35°C, the rate constant for elongation was a mere 8.2 $x10^{-2}$ h^{-1}. Increasing the temperature to 50°C, 60°C and 70°C gave minor increases in the rate constant from 0.24 h^{-1} to 0.70 h^{-1} and 0.38 h^{-1}. At these temperatures the passive evaporation of the methanol by-product was not particularly efficient and was often identified in the ^{1}H NMR spectra. Any methanol that remained in the reaction mixture could participate in a transesterification reaction of its own, effectively slowing forward progress of the polyesterification.

Further increases in the temperature, from 80°C to 100°C, led to higher rate constants reaching 1.94 h^{-1} at 100°C. This was partially attributed to the increasing proficiency of the enzyme coupled with the increased removal of methanol. It was thought that temperatures above 100°C would be deleterious to the functioning of the enzyme. Previous reports suggested that the optimal temperature for carrying out N435-mediated polymerizations was in the range of 70-90°C. Even a subtle change from 90°C to 95°C effected N435 to the extent that lower molecular mass polymers were produced compared to the same reactions conducted at 90°C. The authors of that work understood that observation to mean that the enzyme was no longer working at maximum proficiency and that working at lower temperatures would be beneficial for the long term functioning of the lipase. In our hands increases in the reaction temperature did not lead to slower reaction rates. In fact the apparent rate constant continued to increase, until finally at 130°C,

where the rate was 3.11 h^{-1}, the enzyme finally reached its maximum catalytic proficiency. At temperatures above 130°C the rate constant began to steadily decrease. Polymerization cycles were conducted as high as 160°C and even at this temperature the enzyme remained active for at least a few hours as can be seem from **Figure 76**. These observations suggested that N435 is quite tolerant to high temperatures, and that the optimal polymerization temperature, when concerned with maximizing the reaction rate and total monomer conversion, was approximately 130°C, much higher than the temperature reported for the polymerization of poly(caprolactone) and poly(pentadecalactone).[199]

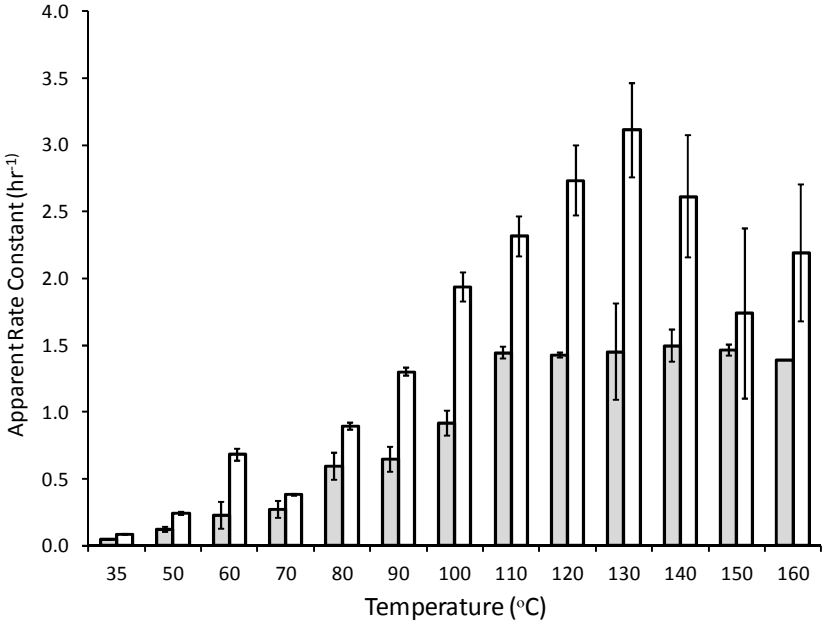

Figure 76 The apparent rate of polymer elongation (hr^{-1}) increases with increasing temperature up to 130°C. White bars: disiloxane diol, grey bars: polysiloxane diol. Each bar is the average of three independent trials; error bars indicate the standard deviation.

The total monomer conversion after 24 hours was monitored to gain an understanding of the proficiency of the enzyme catalyst, and to quantify the molecular weight of the siloxane-containing polyesters. As the temperature was increased from 35°C to

90°C a steady increase in monomer conversion from 40% at 35°C to 80% at 90°C was observed indicating an increase in the M_n of the siloxane polyesters from 5,500 g/mol to 42,000 g/mol. Polymerizations conducted above 90°C did not show the same increase in monomer conversion, but rather seemed to plateau between 85-90% with the average M_n of the polyesters being about 44,000 g/mol.

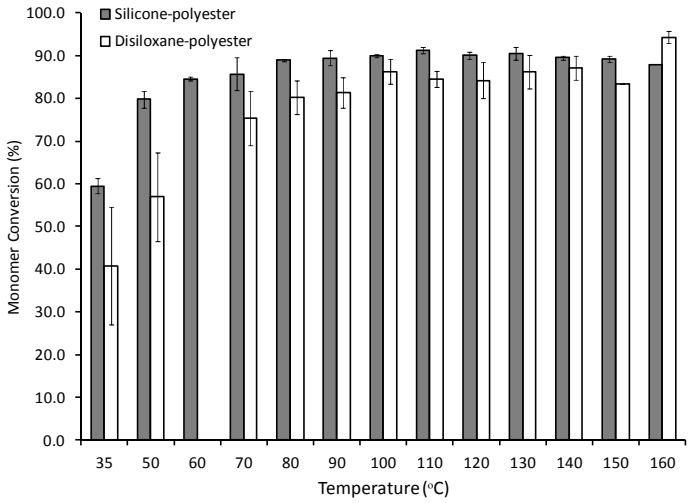

Figure 77 Monomer conversion increases as the temperature is increased. White bars: disiloxane diol, grey bars: polysiloxane diol. Each bar is the average of three independent trials; error bars indicate the standard deviation.

The mass of the polysiloxane-containing diol **162** is nearly an order of magnitude larger than the mass of disiloxane diol **213** (2,000 g/mol compared to 250 g/mol). To ensure that a meaningful comparison could be made between the two systems, the stoichiometry between N435 and **212** was maintained at 12.5 wt% as previously described. As seen with the esterification between **212** and **213**, temperatures of 35-70°C were not sufficient to allow the enzyme to function proficiently and as a result rate constants were generally low at 4.2 x 10^{-2} h^{-1} at 35°C and reaching only 2.71 x 10^{-1} h^{-1} at 70°C. These rate constants were clearly slower than those observed when diol **213** was the acyl acceptor

(**Figure 76**). The reaction rates continued to increase with temperature reaching 1.44 h^{-1} at 110°C. Beyond 110°C the rate constants did not appear to increase. Because the stoichiometry between diester **212** and N435 was held constant, the decrease in the rate constant was attributed directly to the increase in the chain length of diol **162**. The observed decrease was a result of the dilution of the monomers due to the increased chain number of siloxane units; the longer diol acts as the solvent for the reaction. This reduced the frequency of successful binding events between the enzyme and diester **212** slowing the formation of the enzyme-substrate [ES] complex, and slowing the release of the [ES] complex by the incoming nucleophile. This analysis is further complicated by a lack of understanding of the interaction between polysiloxanes and the acrylic resin to which the enzyme is immobilized.

The lipase-catalyzed polyesterification with the polysiloxane diol was similar to the polyesterification with diol **213** in that the degree of monomer conversion increased with each successive increase in temperature. At lower temperatures monomer conversion was limited by the slow rate of the reaction reaching only 60% at 35°C to give a polyester of 5,500 g/mol. Monomer conversion reached nearly 80% (11,000 g/mol) after 24 hours at 50°C and at temperatures higher than 60°C monomer conversion consistently reached 85-95% to give polymers of approximately 20,000-25,000 g/mol. Despite the slower reaction rates when using diol **162**, monomer conversion was typically more extensive suggesting that the increased hydrophobicity of the longer siloxane chain had a positive effect on catalysis. The beneficial effect of increased hydrophobicity of the monomers had been observed previously in the N435-catalyzed polymerization of acid **149a** and three aliphatic diols.[156]

4.2.4 Comparison to Organic Polyesters

The increase in the molecular mass of polyesters has typically been followed by gel permeation chromatography (GPC). This method allows for the number average molecular weight (M_n), weight average molecular weight (M_w), and the polydispersity index (PDI) to be determined. Alternatively NMR-based methods can be employed to gauge the M_n of polymers. Because there are obvious differences between the methodologies that have been presented in the literature and those which have been pursued in this thesis, a direct comparison was not practical or meaningful. To put the current results into context the dimethyl esters **220→225** were synthesized, and series of polyesterifications using a common diol, 1,8-octanediol (**149**), were carried out at 100°C.

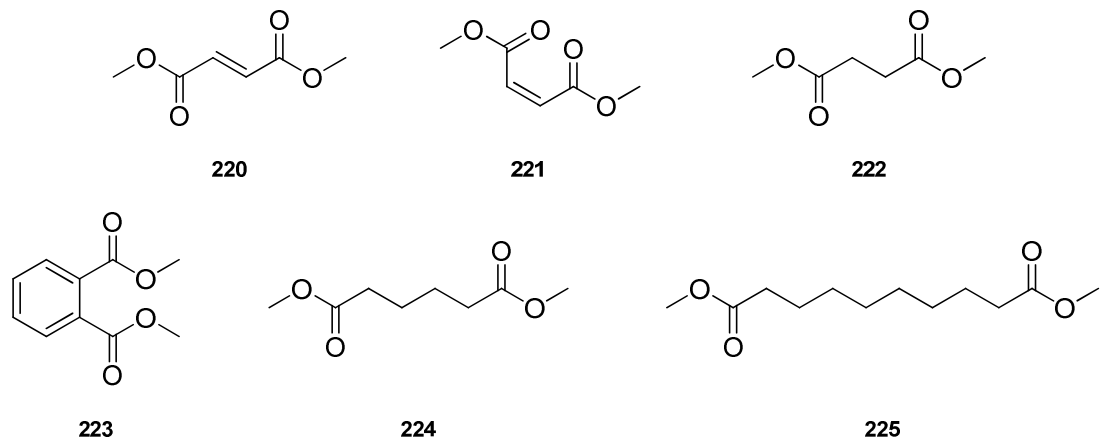

Figure 78 The organic diesters used to probe the selectivity of N435.

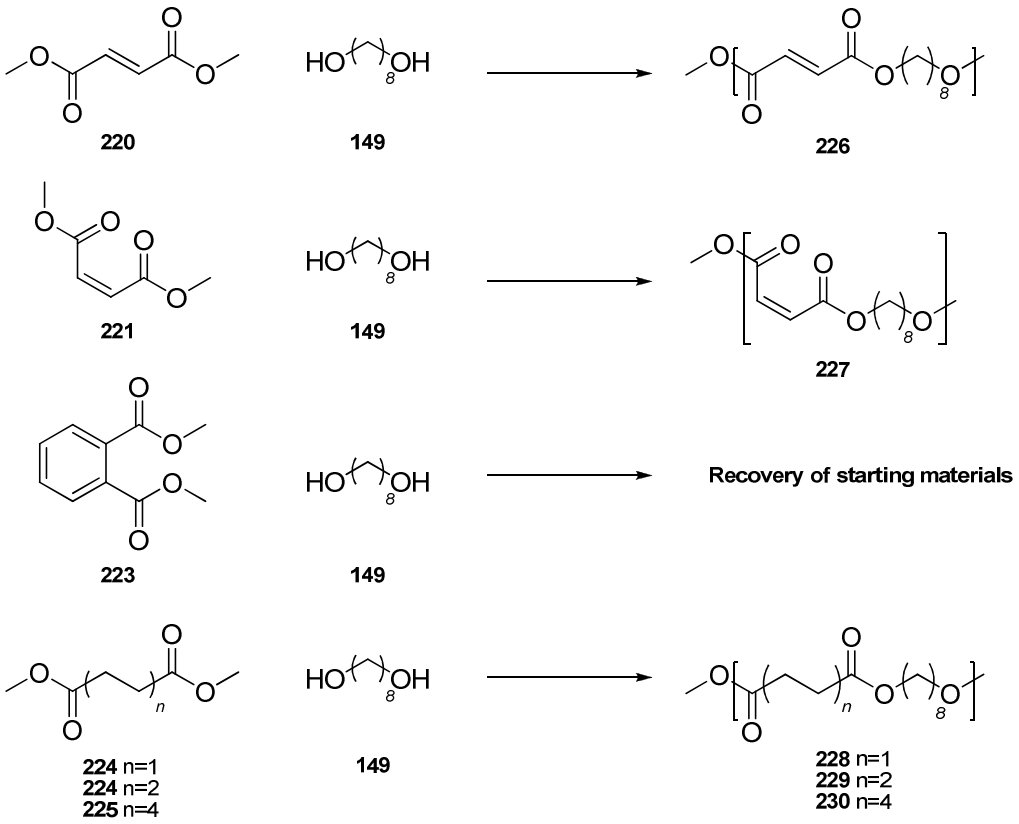

Figure 79 The N435-mediated polymerization of aliphatic, olefinic, and aryl diesters with 1,8-octanediol under solvent-free conditions. Polymerizations were carried out at 100°C for 24 hours.

N435 did not distinguish between the C4 (**222**), C6 (**224**), or C10 (**225**) diesters in the polymerization of polyoctylene esters (**Figure 80**). The olefinic diesters, dimethyl fumarate and dimethyl maleate were less suitable substrates for N435 and produced a significant drop in the rate constant. The rate of polymerization was reduced by approximately 65% when dimethyl fumarate was the acyl donor; with the *cis* isomer, dimethyl maleate, only 5% of the available functional groups were consumed after 24 hours. As a side note, isomerisation of the carbon-carbon double bond was not observed. Furthermore, dimethyl phthalate was also not a suitable acyl donor even though dimethyl terephthalate could be polymerized using N435 as a catalyst.[159,160] These results are tentatively attributed to the geometric arrangement of the reactive groups around the sp^2 hybridized

carbons which prevent the acyl donor from binding to the active serine residue in the active site.

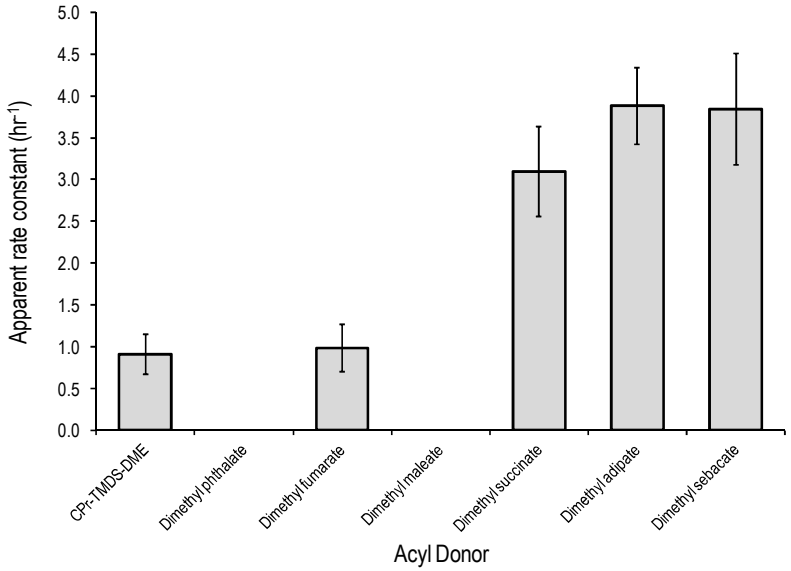

Figure 80 The apparent rate of polymerization for the N435-catalyzed polymerizations of several dimethyl esters with 1,8-octanediol at 100°C. Each bar represents the average of three individual trial ± the standard deviation. ANOVA: $F_{6,13}$=55.46, p=1.63x10^{-8}.

Diester **212** is comparable in length to a C11 ester. Furthermore, siloxanes are some of the most hydrophobic materials that are known which should prove to be a beneficial characteristic for reactions by N435. Despite this hypothesis, N435 demonstrated a lower capacity for producing polyoctylene esters containing a siloxane block. When this information was taken in conjunction with the poorer performance of the enzyme-catalyst with the smaller, and more geometrically constrained acyl donors, it can be concluded that the geometry of the acyl donor may affect the proficiency with which it can be processed by N435. While diester **212** is not constrained by a π-system of electrons in the same manner as the fumarate, maleate, or phthalate methyl esters, the carbon-carbon single bond between the α and β carbons with respect to the dimethylsiloxy group, is rota-

tionally constrained as evident by the complex splitting pattern that is observed in its ^{1}H NMR spectrum (**Figure 81**). This rotational restriction may have been the limiting factor in catalysis which prevented the substrate from rearranging itself within the active site of the enzyme to promote catalysis. Unfavourable steric interactions may also be at play. Even though the CalB molecule has a large acyl binding cleft which can accept aromatic rings and some branched aliphatic esters, the larger size of the *Me_2SiO*- group may be prohibitive. The effect of steric bulk on the hydrolysis of fatty acid esters by CalB has been examined.[200] Ethyl-2-methylbutyrate was hydrolyzed with good conversion, ~90% as determined by GC; increasing the steric bulk on the acid side of the fatty acid ester, to ethyl benzoate and ethyl-2-phenylpropionate, elicited a decrease in conversion to between 35-45%.[200] Our own experiments with vinyl pivalate suggest that too much steric bulk in the acyl donor abolishes catalysis.

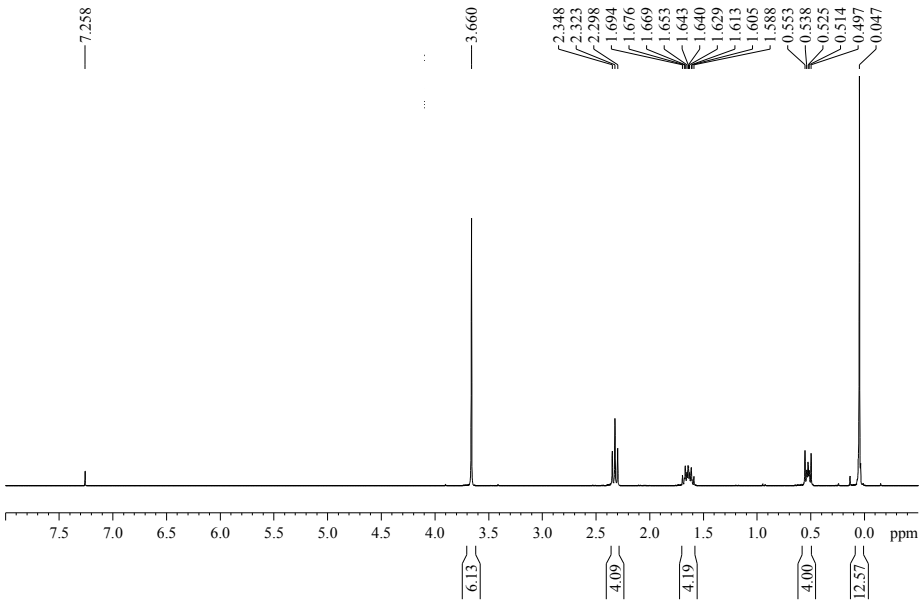

Figure 81 The ^{1}H NMR spectrum of diester **212** showing the second order AA′XX′ splitting pattern of a rotationally contratined carbon-carbon bond.

4.2.5 Disiloxanediol vs. 1,8-Octanediol

To further explore the selectivity of N435 with regards to siloxane-containing substrates, a comparison between the rate constants associated with polyester elongation when diol **213** or 1,8-octanediol were used as the acyl acceptor. If steric considerations were primarily responsible for the poor performance of the enzyme when the diester **212** was the acyl donor, it could be expected that when the disiloxane diol was the acyl acceptor, that the rate would be further reduced compared to the rate of polymer elongation using 1,8-octanediol. From **Figure 83** it can be seen than the enzyme was more receptive to diol **213** than 1,8-octanediol.

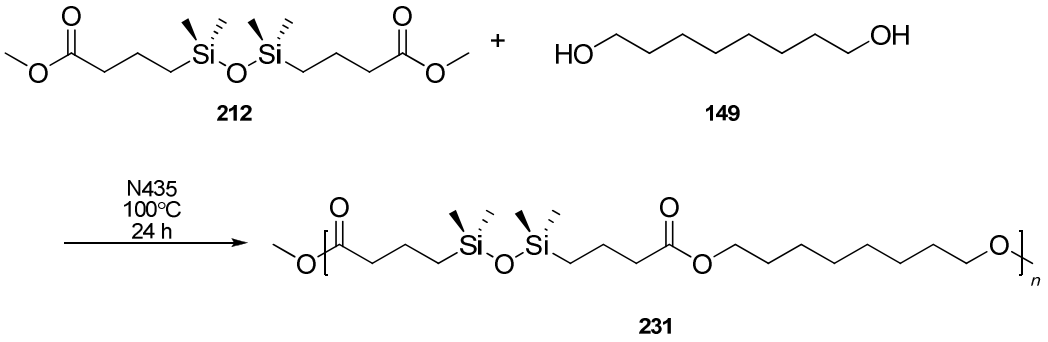

Figure 82 The N435-mediated synthesis of poly(octylene-*co*-(1,1,3,3-tetramethyldisiloxy-1,3-bis(*n*-butanoate)).

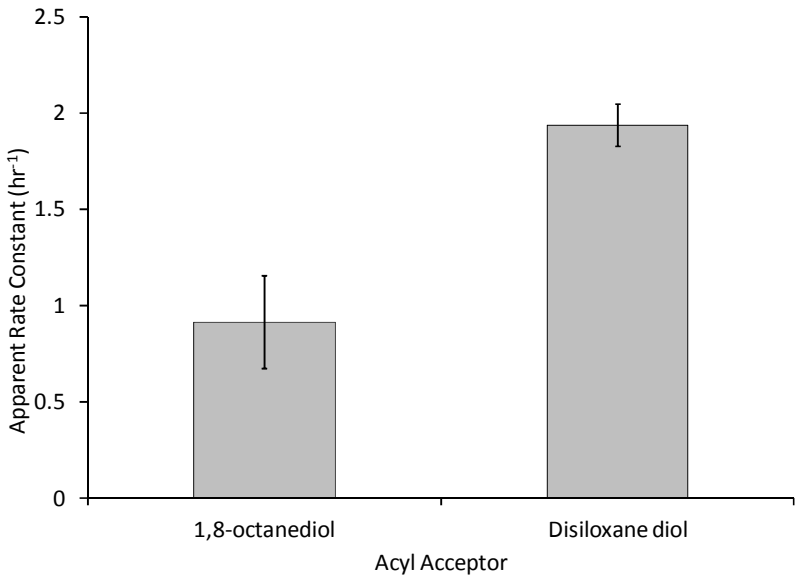

Figure 83 A comparison of the apparent rate of polyester elongation when two different diols are used as the acyl acceptor. Each bar represents the average of triplicate trials, standard error bars are shown. Student's t-test: t=-3.27, df=4, p=0.031.

4.2.6 Mechanical Shear

Many of the forces with which an enzyme may come into contact, fluid shear and mechanical stress, can have deleterious effects on enzymatic activity.[201-205] Most of the enzyme molecules that are immobilized in N435 are found within only 80-100 μm of the surface.[171] A large proportion of the enzyme was bound to the outer surface of the bead which directly contacts the reaction flask and the magnetic stirring bar. Prolonged grinding against the stir bar was postulated to have a detrimental effect on the overall rate of polyester elongation by having a deleterious interaction with the enzyme.

The effect of mechanical stirring on the immobilized enzyme was examined by crushing some enzyme beads in a mortar and pestle, into a fine white powder. This was done in an attempt to simulate the effect of prolonged stirring. The crushed beads were used to catalyze the polyesterification between diol **162** and diester **212**. It was expected

that the brute force approach of physically damaging the enzyme beads would lead to a loss in enzymatic activity. Contrary to this hypothesis the enzyme remained active and carried out the esterification of diol **162** and diester **179** more proficiently than undamaged beads. The crushed beads afforded a rate enhancement of 1.3 over the 'uncrushed' controls. This finding is explained by the creating of a larger surface area exposing more enzyme molecules to the reaction milieu promoting a faster rate of catalysis.

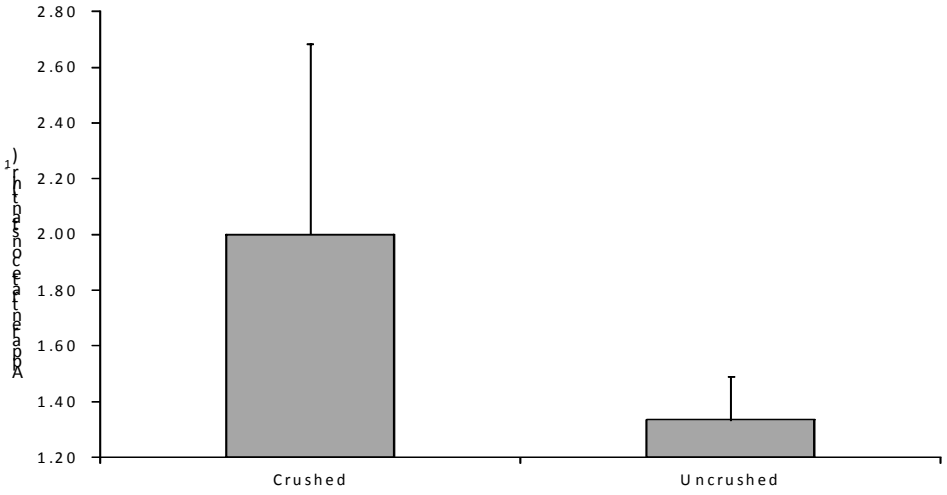

Figure 84 A comparison of the polyester elongation rate when a N435 is used as the catalyst. N435 beads were ground in a mortar and pestle (crushed) or used as purchased (uncrushed). The bars represent the average of triplicate trials; standard deviation bars are included. Student's t-test: t=1.64, df=4, p=0.18.

4.2.7 Comparison of N435 to Some Common Lewis Acid Catalysts

Polymer chemists often justify the use of enzymes over traditional Lewis acid catalysts for polymer synthesis by claiming that enzymes are a milder alternative and offer better regio- and stereo- selectivity than most Lewis acid catalyst complexes.[160,206,207]

There are surprisingly few reports in the literature that compare a given enzyme catalyst with common Lewis acids. One report that attempts just this comes from the Gross group. The selectivity of N435 was compared to dibutyltin oxide for the polymerization of oleic diacid and glycerol.[207]

A direct comparison between some common Lewis acids and N435 as polymerization catalysts was attempted. However, because the actual enzyme loading that is used, in mole terms, is very small it was difficult to measure out an appropriate amount of the Lewis acids. The one change that we were forced to make was to use an excess of the Lewis acid. We chose five common Lewis acids, some of which have been previously used to produce polyesters; dibutyltin dilaurate,[208] tetraisopropoxy titanate,[209] zinc chloride,[210] magnesium acetate, and kaolinite.

The polyesterification of diester **212** and diol **213** was carried out over 24 hours at 100°C using 2.17×10^{-5} mol of Lewis acid compared to the mass of the total monomers. Typically the mass of enzyme for these polymerizations would be 5 wt % N435 to the mass of **212** and **213** which corresponds to a mere 9.32×10^{-8} mol of lipase. Tetraisopropoxy titanate was the best of the Lewis acids esterifying on average 66% of the monomers, next was dibutyltin dilaurate at 60%, $ZnCl_2$ at 9.0%, and finally kaolinite at 5.5%. Magnesium acetate failed to catalyze the synthesis of polyesters. All of these values are less than what N435 esterified, 86%, over the same time period despite the much lower loading of the enzyme catalyst.

4.2.8 Structural Characterization

The structural environments of the siloxane-derived polyesters were probed primarily through NMR and FT-IR spectroscopies. Typical ^{1}H NMR spectra for the disiloxane and polysiloxane polyesters are presented in **Figure 85**. There is a triplet positioned at 4.04 ppm in the disiloxane polyester and 4.05 ppm in the polysiloxane polyester which represents the *O*-methylene protons in the newly formed ester linkage; in the monomer this resonance is located at 3.60 ppm. There is a smaller singlet located at 3.67 ppm which can be assigned as unreacted methyl ester end groups. The methylene protons alpha to the carbonyl in ester **212** experienced a small shift up-field after polymerization and is located at 2.34 ppm while the remaining multiplets, 0.54 ppm and 1.64 ppm, represent the methylene protons that are in the α- and β- positions with respect to silicon in the monomers and final polymer; the geminal methyl groups on silicon are resonating at 0.06 ppm and remained largely unchanged throughout the polymerization process. In the polysiloxane polyester there is an additional resonance at 1.45 ppm representing the internal methylene groups of the alkyl spacer between silicon and the hydroxyl group.

The ^{13}C NMR spectrum corroborated the synthesis of the siloxane polyesters. The resonance for the carbonyl carbon exhibits a downfield shift and sits at 173.62 ppm while the *O*-methylene carbon can be found at 66.64 ppm; the carbon adjacent to the ester linkage was positioned at 37.75 ppm. The remaining resonances were at 13.99 ppm and 17.96 ppm have been identified as $CH_2\mathit{CH_2}Si$ (in monomer and polymer), and 19.06 ppm and 22.57 ppm has been identified as the $\mathit{CH_2}CH_2Si$ environment. The ^{29}Si spectrum possessed two distinct resonances at 7.30 ppm and 7.72 ppm. These signals were in the ex-

pected range for disiloxane linkages and do not represent a possible silanol or alkoxysilane.

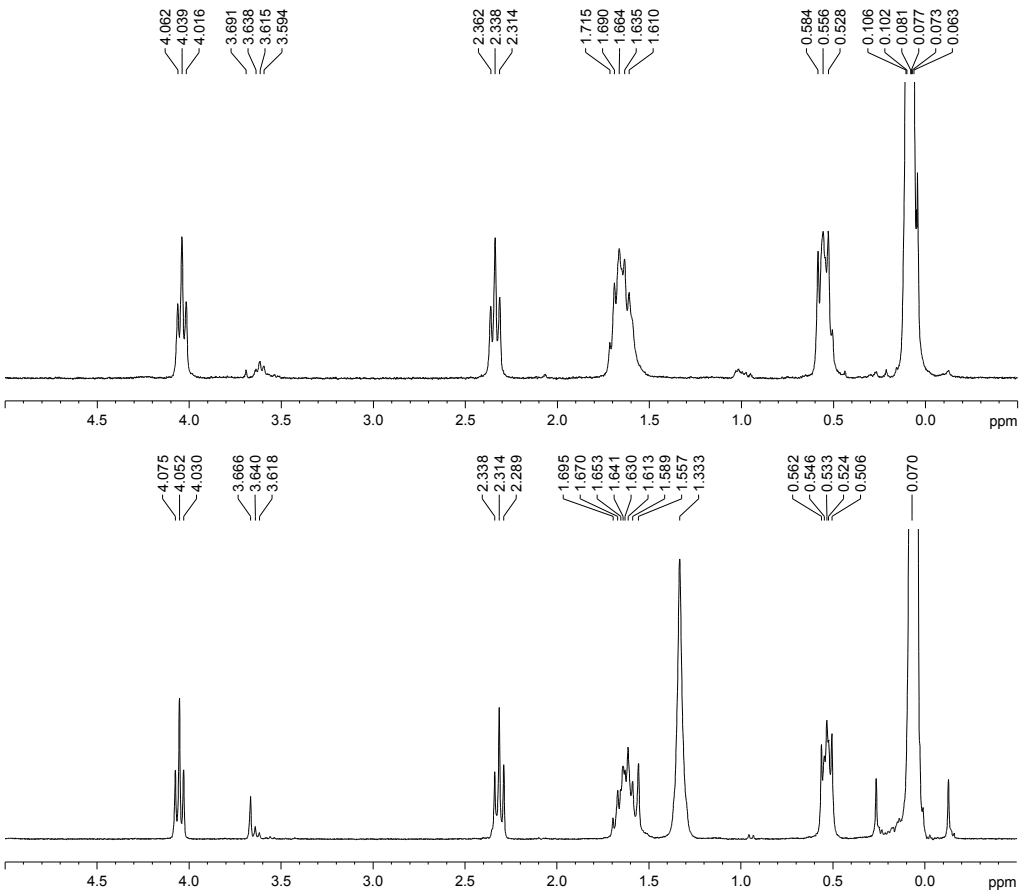

Figure 85 Representative ^{1}H NMR spectra of siloxane-containing polyesters derived from diester **212** and diol **213** (top) or diol **162** (bottom).

FT-IR group assignments were based on assignments previously reported in the literature.[211] There was a strong stretching vibration at 1737 cm^{-1} indicative of the *C=O* bond. The vibrational mode associated with the *Si-O-Si*$_{sym}$ linkage was evident at 1050 cm^{-1}. In the polysiloxane the *Si-O-Si*$_{asym}$ stretch was evident at 1100 cm^{-1}. The absence of

peaks at 3350 cm^{-1} and 750 cm^{-1} where *Si-OH* groups resonate suggest that there was no enzymatic hydrolysis of siloxane linkages.

4.2.9 Thermal Properties of Siloxane-Containing Polyesters

Differential scanning calorimetry (DSC) was used to examine the thermal properties of the siloxane polyesters. Siloxane-polyester samples were cooled to -150°C at a rate of 10°C/min. Each sample was heated at 10°C/min to 200°C and subsequently cooled at 10°C/min to -150°C. The reported thermal transitions were taken from a second heating scan that was done at 10°C/min to 200°C.

Figure 86 presents the DSC thermograms for disiloxane and polysiloxane monomers as well as for representative siloxane-containing polyesters. The glass transition temperature (T_g) for polydimethylsiloxane (PDMS) is -125°C.[212] By comparison, the observed values for the diol **162** and diester **212** were higher, -99°C and -109°C respectively, while the T_g for diol **213** was more comparable at -118°C. The T_g for the polyester synthesized from only disiloxanes was found to be -104°C. While the polyester synthesized from diester **212** and diol **162** had a T_g of -115°C, only slightly higher than diol **213** itself. As a result of the flexibility of the disiloxane linkage and the amorphous nature of siloxanes, the thermal transition associated with melting and crystallization was not detectable.

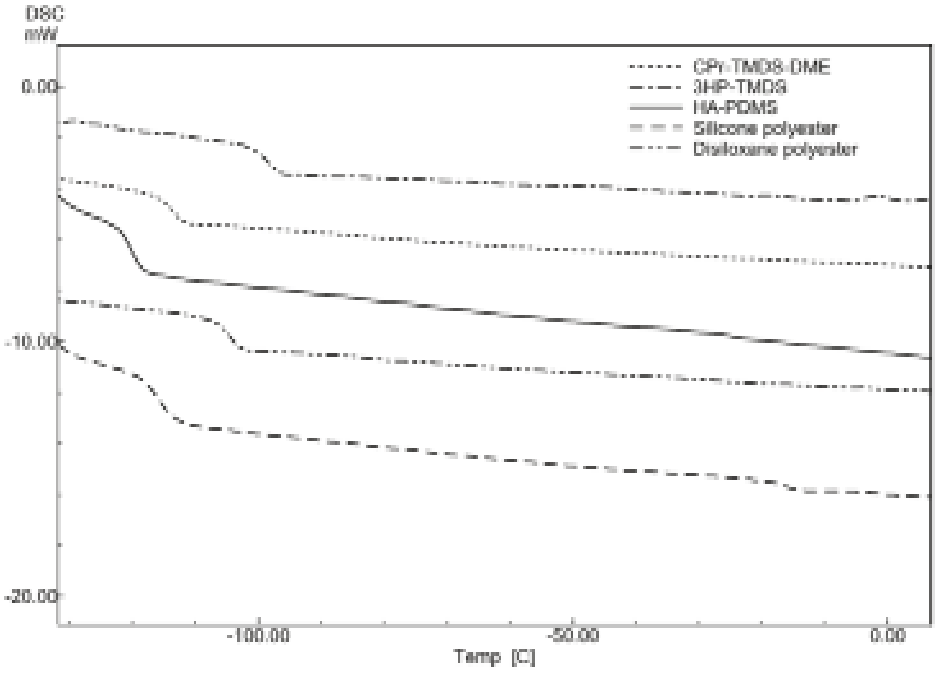

Figure 86 DSC thermograms of siloxane-containing polyesters and their corresponding monomers. The thermograms presented were taken from the second heating scan.

4.2.10 Enzyme-Catalyzed Synthesis of Hybrid Siloxane-Polyesters

Seeking to expand the list of available enzymes that would be able to carry out the polymerization of terminally functionalized siloxanes, we began to survey other lipases and proteases that were relevant in biotechnology, although not necessarily used for mediating polyesterification reactions. Initial experiments were conducted using *Candida rugosa* lipase (LCR) with the polymerization of our model system of diester **212** and diol **213**.

Initial experiments combined LCR with the monomers in the absence of solvent. However, the available ^{1}H NMR data suggested that esterification did not occur. Suspending the enzyme in a small amount of isooctane (2,2,4-trimethylpentane) prior to combining it with the reactants was also not a fruitful idea. Previously O'Hagan had used CRL to produce polyesters of approximately 1,000 g/mol from 10-hydroxyundecanoic acid[213] and Seppälä showed the esterification of (2,2,2-trifluoroethyl)sebacate and 1,4-butanediol in hexanes using CRL to give polyesters with a M_w of 12,800 g/mol.[214] It was postulated that a longer acyl donor resembling a more natural substrate would allow CRL to successfully polymerize the siloxane-derived monomers. Following the lead of those reports, we chose an acyl donor that contained ten methylene units between the carboxyl and dimethylsiloxy groups instead of the three methylene units of diester **212**, and chose α,ω-bis(10-carboxydecyl)-polydimethylsiloxane (**232**, M_w=1,000 g/mol) and carried out the polyesterification in isooctane.

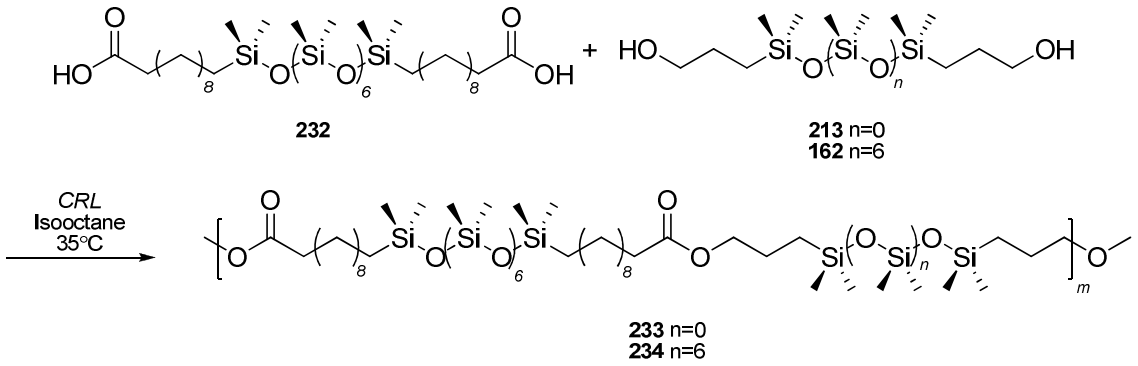

Figure 87 The *Candida rugosa* lipase-mediated polymerization of siloxane-containing polyesters.

CRL had a much higher capacity for polymerizing diacid **232** than diester **212**. This was attributed to the longer alkyl chain between the carboxylic acid and dime-

thylsiloxy moieties. Over the course of a 24 hour reaction cycle CRL attained 56% conversion of the monomers. The siloxane-polyester was isolated as a clear and viscous liquid with a DP_{avg}=2.27 and M_n=2,750 g/mol (^{1}H NMR). This could be marginally improved upon to 64% (DP_{avg}=2.78 and M_n=3,375 g/mol) after 72 hours. Reducing the enzyme loading by 50% elicited a small drop in monomer conversion from 64% to 50% to give DP_{avg}=2.00 and M_n=2,400 g/mol over 72 hours. Furthermore, when diol **213** was replaced with diol **162** monomer conversion also decreased to 50% (DP_{avg}=2.00 and M_n=3,325 g/mol) in a 72 hour reaction cycle. To put this into perspective, the same polymerization catalyzed by N435 resulted in 93% monomer conversion in 72 hours to give DP_{avg}=14.3 and M_n=17,400 g/mol. So while the CRL results appeared to be promising, the enzyme could not compare to N435 in terms of catalytic proficiency. CRL is known to require interfacial activation in the hydrolysis of triacylglycerides, however, water was excluded from the reaction medium in order to drive the equilibrium to polymer formation.

To confirm the hypothesis that the steric bulk imposed by the relative proximity of the dimethylsiloxy group to the ester was prohibitive to the success of CRL as a catalyst a suspension of CRL was combined with two equivalents of palmitic acid and one equivalent of diol **213** in isooctane (**Figure 88**). The reaction was stopped after 6 hours and by ^{1}H NMR 74% of the monomers had undergone esterification suggesting that mono- and di- esterified compounds were present. Similarly, a second CRL suspension was combined with diester **212** and two equivalents of 1-octanol. After 6 hours there was no detectable esterification. The dimethylsiloxy group was sufficiently close to the carbonyl group, in this case in the δ position, and prohibited CRL from forming a silyl-

enzyme intermediate. Furthermore, this steric restriction did not appear to apply to the acyclic acyl acceptor. These results agree well with previous characterizations of the CRL binding pocket. CRL is known to have a narrow acyl-binding cleft that is about 22 Å in length, but only about 4 Å wide, and a much larger alcohol binding cleft that does not share the same steric restriction.

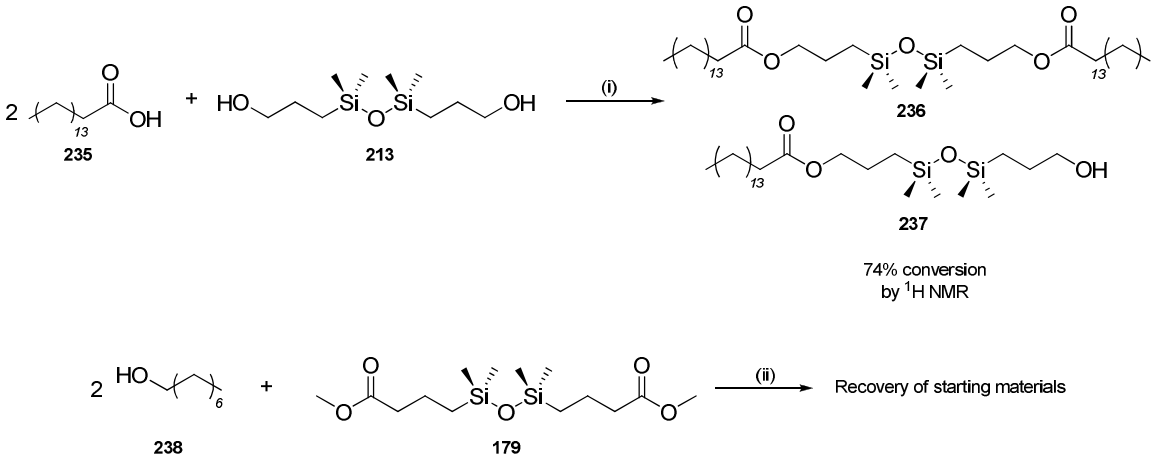

Figure 88 The esterification of palmitic acid and diol **213** (top) and diester **212** and 1-octanol (**238**). *Conditions*: (i) 9.65 mg/mL CRL in isooctane, 2 eq. **235**, 1 eq. **213**, 35°C, 6h; (ii) 9.65 mg/mL CRL in isooctane, 2 eq. **238**, 1 eq. **212**, 35°C, 6h.

Once it was shown that CRL would be a moderately useful biocatalyst for polymerizing siloxane-derived monomers, we set out to produce a series of hybrid organic-siloxane polyesters in which the chain length of the acyl donor was steadily increased. Dimethyl malonate (**239**) was synthesized to complement the dimethyl esters of adipic acid and sebacic acid (**Figure 89**). The enzyme-catalyzed polymerizations were stopped after 24 hours and analyzed by ^{1}H NMR to determine completeness. CRL suspensions in isooctane were not proficient at catalyzing the condensation polymerization of dimethyl malonate, dimethyl adipate or dimethyl sebacate with diol **213**. Total monomer conver-

sion failed to exceed 50% in any of the three cases. In fact when charged with diester **239** CRL showed the highest capacity to carry out the esterification. But even in these cases total conversion only reached 35% leaving much of the monomers unreacted; increasing the temperature to 55°C only improved monomer conversion to 41%. Increasing the chain length of the diester also failed to improve upon the degree of conversion to any extent, and in fact total conversion decreased as the chain length of the diester was increased. The polyesterification of dimethyl adipate **222** and dimethyl sebacate **225** with diol **213** only gave 30% and 25% conversion respectively. Despite the anticipation that CRL would be suitable for producing hybrid polyesters in a reasonably short time frame, such results were not attainable.

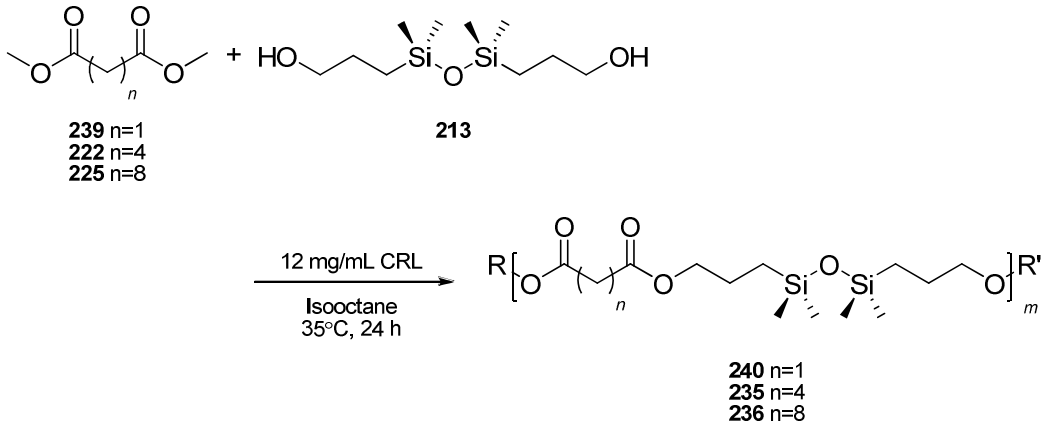

Figure 89 The CRL-catalyzed synthesis of semi-inorganic hybrid polyesters.

4.2.11 Branched Disiloxane Polyesters

The model studies employing N435 as a catalyst for synthesizing linear siloxane-containing polyesters were conducted to determine the feasibility of employing a lipase-

mediated approach for the production of cross-linked, branched, or hyper-branched siloxane polymeric materials. Keeping in line with a desire to develop bio-inspired materials it was decided to approach the synthesis of branched silicones employing two different branching agents of biological relevance: the trimethyl ester of citric acid and glycerol.

Trimethyl citrate was synthesized from citric acid as outlined in **Figure 90**. The synthesis of citrate-siloxane composites was carried out using 5wt% N435 as shown in **Figure 91**. It was postulated that the presence of an internal ester may prove to be sterically limiting for enzymatic catalysis by this lipase. With previous reports attempting to synthesize branched polyesters used diacids/diesters with branched polyols branched acyl donors seem to have been avoided. The increased steric bulk of trimethyl citrate did not appear to have a drastic effect on catalysis. After 24 hours more that 50% esterification was observed by ^{1}H NMR and after 48 hours this could be improved to 74%. In the absence of N435 esterification could not be detected by ^{1}H NMR spectroscopy.

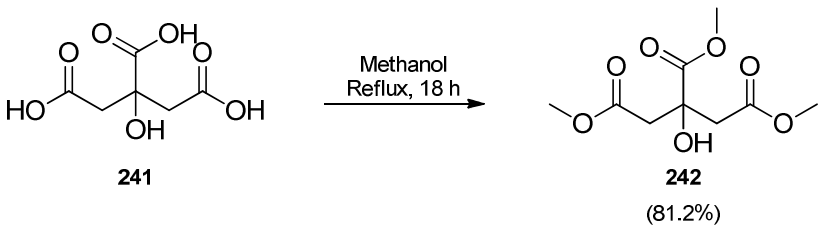

241 **242** (81.2%)

Figure 90 The synthesis of trimethyl citrate.

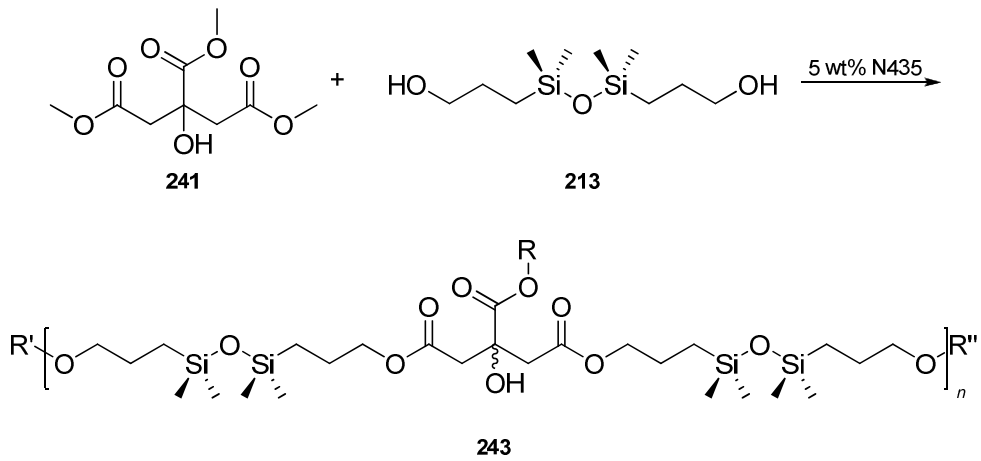

Figure 91 The attempted synthesis of branched siloxane polyesters based on citric acid.

Even though the advanced degree of esterification suggested that the internal ester was in fact incorporated as a branching point, the ^{1}H NMR data was somewhat ambiguous. To alleviate this ambiguity the microenvironments of the citrate siloxane copolymers were characterized using multiple 1D and 2D NMR techniques. The ^{1}H NMR spectrum provided clear evidence that transesterification between trimethylcitrate and diol **213** was successful. The *O*-methylene protons located at 3.59 ppm in the unreacted monomers and end groups became shifted down field to 4.03 ppm in the newly formed ester linkage. A third resonance at 4.16 ppm was present which potentially represented the ester formed between the ester at the 3-position of trimethylcitrate and the diol **213**; this is the source of the ambiguity. After 24 hours these resonances are in a 2.2:0.7:1 ratio for the terminal and internal esters and free hydroxyl groups respectively. There was a small difference in the chemical shifts for the -OCH_3 proton environments which change as esterification proceeds; a similar observation was noted for the diastereotopic methylene groups of trimethyl citrate.

Inverse gated ^{13}C NMR corroborated the esterification of the citrate siloxane co-polymers. There were three sets of carbonyl resonances located at 169.9, 170.2, and 173.9 ppm. The two down field resonances were assigned to unreacted ester groups of trimethyl citrate. The new resonance at 169.9 ppm was the transesterified product; the ratio of the resonances at 169.9 ppm and 170.2 ppm was 1.67:1 giving 62.5% esterification at the terminal carbonyl groups. Unfortunately, the carbonyl resonances did not unambiguously confirm the transesterification of the internal ester. A comparison of the resonances representing the *O*-methylene proton environment of the diol and ester located at 65.49 ppm and 67.54 ppm should confirm the extent of transesterification between the monomers. Integration of these resonances gave a ratio of 1.48:4 or 60% esterification. This is somewhat lower than that determined by ^{1}H NMR employing the same methylene groups which came in at 74% transesterified, but very close to that determined using the carbonyl resonances.

Correlation Spectroscopy (COSY), ^{1}H-^{13}C Heteronuclear Single Quantum Correlation (HSQC) and ^{1}H-^{13}C Heteronuclear Multiple Bond Correlation (HMBC) NMR techniques were employed to provide structural information on the copolymers, and unequivocally confirm or deny the presence of transesterification events involving the internal ester of trimethyl citrate. The COSY spectrum showed that the resonance located at 4.16 ppm in the ^{1}H NMR spectrum was coupled to the β-methylene, with respect to silicon, in the diol **213**. This would be interesting due to the increased steric bulk surrounding this chemical environment.[215,216] The inverse gated ^{13}C spectrum suggested that the internal ester was not transesterified as only a single resonance representing that particular carbonyl group could be identified but this may be due to the low concentration of this

chemical environment. The ^{1}H-^{13}C HSQC spectrum also did not show a correlation between this proton environment and a down field carbon resonance. Furthermore the available ^{1}H-^{13}C HMBC data did not show the expected ^{3}J coupling to the internal carbonyl, nor to the methylene carbons of the siloxane diol. It was reasoned that if the concentration of this particular ester was very low that spectroscopic evidence could be obtained by repeating the HMBC experiment at a higher field and increasing the number of acquired transients.

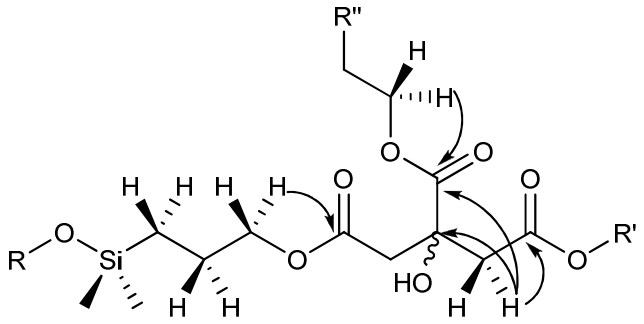

244

Figure 92 The arrows show the correlations that were used to establish the connectivity of possible branched structures in HMBC experiments (bottom).

Increasing the field strength, from 300 MHz to 600 MHz, and the number of transients that were acquired in the HMBC experiment produced a spectrum that unambiguously confirmed that the internal ester of trimethyl citrate had been esterified by N435. There is a distinct coupling seen between the protons at 4.16 ppm and the carbonyl group at -173.9 ppm. These methylene protons are also coupled to the nearest neighbor and next to nearest neighbor carbons at -13.9 ppm and -22.5 ppm. Therefore it can be stated that the multiplet seen at 4.16 ppm in the ^{1}H NMR spectrum corresponded to a second methylene environment that had been esterified. It is difficult to quantify how much of

the internal ester has been transesterified due to the complex splitting pattern which may be overlapped by the hydroxyl proton of the trimethyl citrate fragment. A revised proposed structure for the citrate siloxane polymer is presented in **Figure 94**.

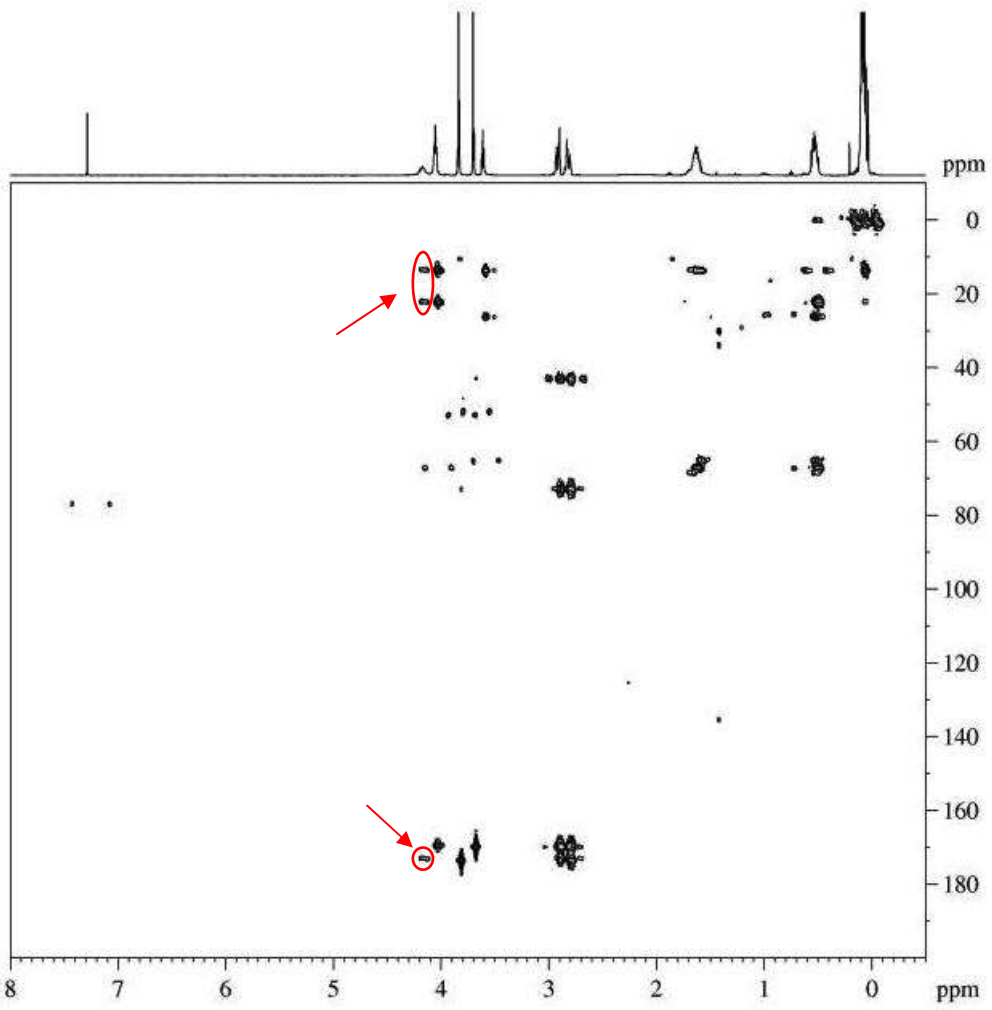

Figure 93 The ^{1}H-^{13}C HMBC NMR spectrum of a citrate-siloxane copolymer showing the correlation between the internal ester carbonyl and the disiloxane diol that formed a new ester linkage.

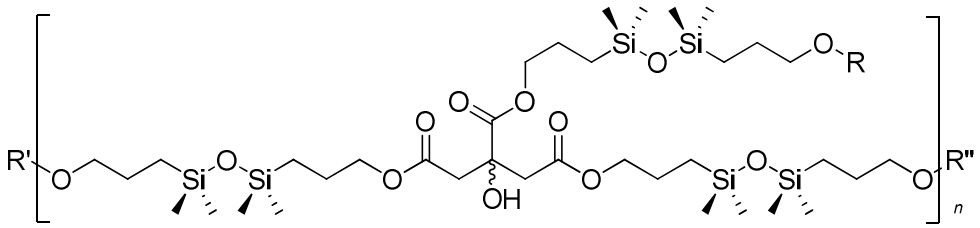

245

Figure 94 The structure of the lipase-catalyzed citrate siloxane copolymers.

The second approach taken to prepare branched polyesters involved using glycerol as the branching agent. Branched glycerol-siloxane copolymers were prepared by combining glycerol (**246**) and diester **212** in the presence of N435 at 100°C for 24 hours. The expected transformation is outlined in **Figure 95**. Enzyme-free reactions did not produce any polymeric materials with any degree of branching.

Glycerol-siloxane copolymers were isolated as uncoloured, moderately viscous liquids. At no time after the onset of polymerization or isolation did phase separation occur. The initial results from the lipase-mediated polymerization appeared promising as the ^{1}H NMR spectrum showed that the reaction had progressed to near 67% completion; exactly what would be expected by N435 catalysis if the primary hydroxyl groups of glycerol were esterified.

These results were both exciting and surprising. While the known selectivity of the CalB protein had led to the assumption that only linear polymers would be produced, it was hoped that some of the internal functional groups would also be esterified. The available evidence suggested that, at least to some small extent, that CalB, which normally performs hydrolysis/esterification at the first and third positions of triacylglycer-

ide/glycerol (*sn*-1/*sn*-3 selectivity), can change its selectivity to *sn*-2 performing hydrolysis/esterification at the second position of a triacylglyceride/glycerol.

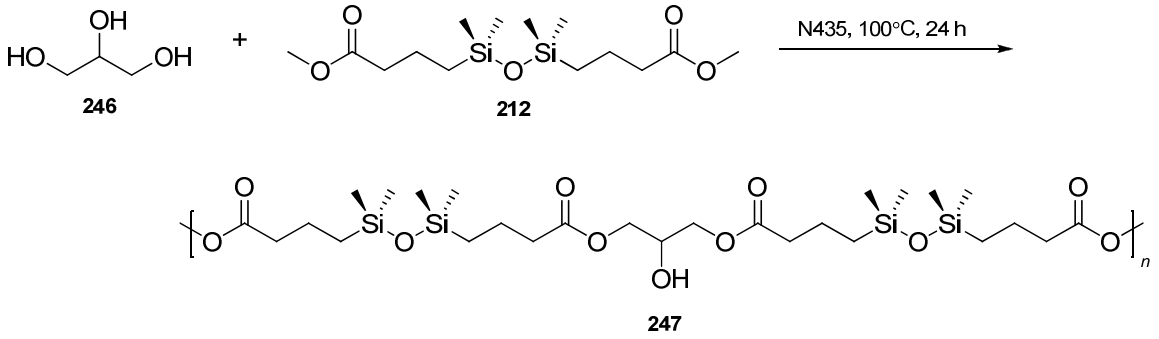

Figure 95 The enzymatic synthesis of linear polyesters from glycerol and siloxane diester **212**.

Candida antarctica lipase A (CalA) on the other hand is known to be a *sn*-2 specific lipase.[216] This prompted the exploration of an immobilized CalA to carry out the synthesis of glycerol siloxane copolymers. CalA has been previously shown to accept large tertiary alcohols as substrates and we felt that this approach would lead to a new method for preparing copolymeric materials with the selective esterification of the secondary alcohol of glycerol. CalA-mediated reactions were carried out at 80°C in the absence of solvent. We chose this temperature because it had been reported that CalA maintained good activity at temperatures as high as 90°C,[217] and in the absence of our own thermal tolerance experiments with CalA, 80°C was determined to be an ideal temperature for the reaction. Despite all hopes, there was no evidence that the immobilized CalA could perform the desired esterification.

4.2.12 Siloxane-Containing Polyamides

Polyamides are produced via the condensation polymerization of carboxylic acid derivatives and diamines and are typically carried out at temperatures in excess of 250°C. Polyamides synthesized from bis(acylchlorides) and diamines can be problematic when sensitive functional groups are present such as siloxanes due to the generation of stoichiometric quantities of HCl; this has the potential to cause redistribution of siloxane architectures or cleavage of the siloxane backbone. To avoid this, the incorporation of a stoichiometric amount of a nitrogenous base would be advantageous, but this results in the production of a stoichiometric amount of by-products. Additionally carboxylic acids can be activated using compounds such as dicyclohexyl carbodiimide, but again this leads to the production of large quantities of undesired by-products which may be difficult to remove from polymeric systems. An enzymatic approach afforded poly(aminoamides) of the same molecular weight distribution as a chemical synthesis, however, the benefit to using the enzyme was that less branching was observed.[218]

Following up on enzymatically synthesized siloxane polyesters, the investigation of N435 as a catalyst for siloxane-polyamide synthesis was undertaken. A series of enzyme-free control reactions were performed to determine the background rate of polyamide formation. At temperatures below 100°C there was no detectable rate of polyamidation within the first 1-2 hours. However, over the course of 24 hours, even at 35°C about 30% polyamidation was seen when using the disiloxane diamine (**216**) but only 5-7% polyamidation was detectable when the polysiloxane-diamine **217** was used. To allow for a meaningful comparison to be made with the enzymatically synthesized polyesters, the reported rates for polyamide synthesis have been corrected to account for the

background rate of polyamidation. The amount of enzyme catalyst that was used was maintained at 12.5 wt% relative to diester **212**.

4.2.13 Kinetics - Disiloxane and Polysiloxane Diamines

The addition of N435 to a 1:1 mixture of diester **212** and diamine **216** promoted the condensation of siloxane-polyamides. In the presence of the enzyme catalyst, the reaction mixture increased in viscosity over the course of a few hours, and even at the lowest temperature the reaction mixtures became so viscous that the magnetic stirring bar ceased to stir. Polyamides derived from the disiloxane diamine were recovered as viscous, straw coloured liquids. The polyamides produced from polysiloxane diamine **217** changed colours from colourless to varying shades of yellow-orange-red.

The lipase-mediated synthesis of disiloxane-polyamides progressed slowly at first but the rate constants increased with each increase in temperature (**Figure 96**). There was no detectable rate of polyamidation during the first hour or two at 35°C using N435 catalysis. Increasing the temperature changed this, as there was a steady increase in the rate constant for polyamidations conducted between 50°C (1.99×10^{-1} h^{-1}) and 130°C (2.14 h^{-1}). These reaction mixtures became so viscous within 4-6 hours after commencing the reaction that the magnetic stirring bar ceased to stir. This result is only marginally different from the lipase-mediated polyesterification in which 130°C was the temperature at which the enzyme exhibited the highest rates of ester formation. Reactions at 140°C were conducted; however, the data cannot be included as the relative concentration of amine compared to ester decreased as the reactions progressed. This was coupled with the observation that within 10 minutes of incubation at these temperatures the reaction mixture

began to show signs of decomposition; the contents of the reaction mixture began evolving smoke.

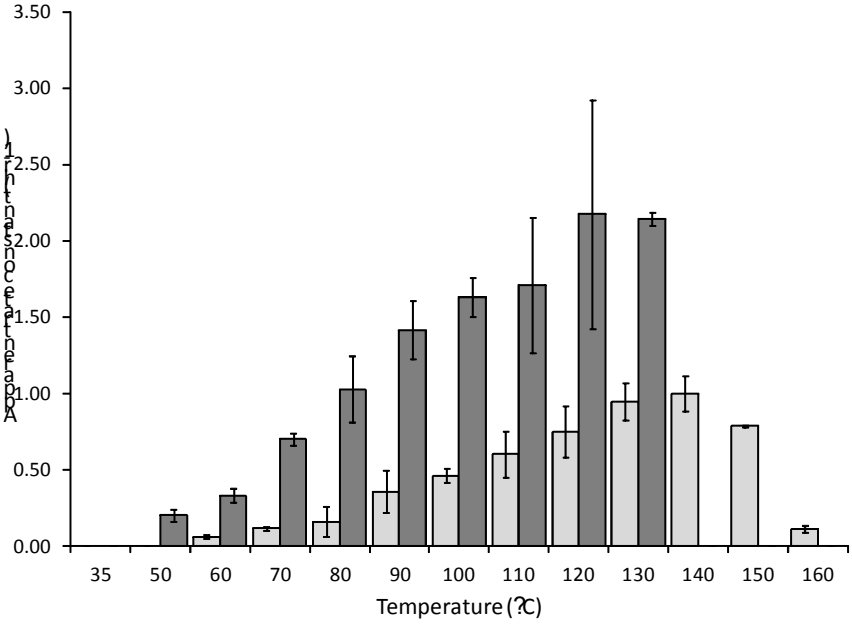

Figure 96 The change in the apparent rate constant due to changes in temperature for the enzymatic synthesis of siloxane-polyamides; disiloxane-polyamides (dark grey bars) and polysiloxane-polyamides (light grey bars)

Increasing the siloxane chain length had a profound effect on the initial rate of polyamidation. At all temperatures, the rate constants were lower than those polyamidation reactions between diester **212** and diamine **216**. At the lowest temperatures, 35°C and 50°C, there was no detectable polyamide formation by ^{1}H NMR (**Figure 96**). At temperatures between 60°C and 90°C the rate constant for polyamide elongation increased from 0.06 h^{-1} to 0.113 h^{-1}, to 0.158 h^{-1}, and finally 0.235 h^{-1}. At 90°C, an inflection point was reached where each successive increase in temperature led to a larger increase in the rate of polyamide formation than was observed between 50°C and 90°C. This was at-

tributed to the ease with which methanol was removed from the reaction matrix. At 100°C the rate constant of polymer elongation was 0.459 h^{-1} and this steadily increased to 0.945 h^{-1} at 130°C. Even at 140°C the rate continued to increase to its maximum at 0.998 h^{-1}. At the highest temperatures, 150°C and 160°C, enzyme denaturation became increasingly obvious due to the decreased reaction rates. The decline in the rate of polyamide synthesis was even more pronounced than it was in the case of the siloxane-derived polyesters; the reason for this is currently unknown.

Total monomer conversion and the number average molecular weight after 24 hours were monitored by ^{1}H NMR. While in the absence of an enzyme catalyst monomer conversion was evident, corrected monomer conversion levels were not insignificant. At 35°C on average 33% of the monomers were converted giving DP_{avg}=1.49 and M_n=3,150 g/mol. Monomer conversion steadily increased as the temperature of the reaction was increased. Polyamidation cycles conducted at 90°C and above gave fairly consistent monomer conversion levels between 90-95%. These levels of conversion correspond to DP_{avg}=10-20 and M_n=21,000 g/mol to 42,700 g/mol by ^{1}H NMR.

Four different acyl acceptors were chosen to be paired with diester **212**, and of those, diamine **217** routinely gave the lowest reaction rates at every temperature regime that was tested. This is formally attributed to two factors. First, the longer siloxane chain length of the polysiloxane diamine, for all intents and purposes, acts as a solvent for the ester and amine end groups. A similar effect was observed in the comparison of disiloxane diol **213** and polysiloxane diol **165**.

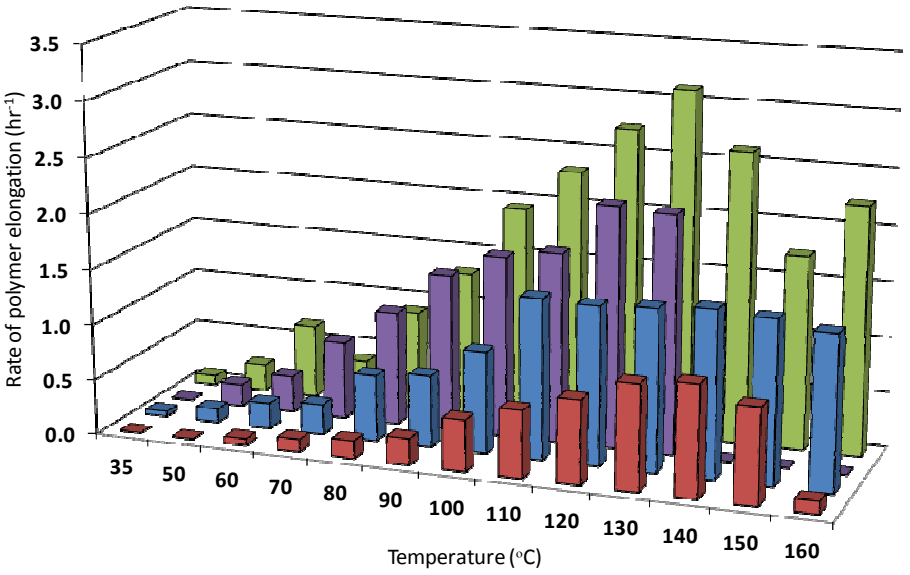

Figure 97 A comparison of all of the polymerization rates that were generated using N435 catalysis during the synthesis of polyesters and polyamides. *Legend*: Polysiloxane polyamide (red), polysiloxane polyester (blue), disiloxane polyamide (purple), and disiloxane polyester (green). Each bar is the result of triplicate trials; error bars are not shown only for the sake of clarity.

4.2.14 FTIR Analysis of Polyamide Formation

In addition to ^{1}H NMR, polyamide formation was probed using FTIR spectroscopy by following the decrease in the absorbance band associated with the methyl ester at from **212** and the growing band associated with the elongating polymer chain. **Figure 98** presents a representative FTIR spectrum for the N435-catalyzed polyamidation of diester **212** and diamine **216**. The peak at 1742 cm^{-1} represents the C=O group of the methyl ester and the peak at 1650 cm^{-1} represents the C=O of the newly forming amide functional group. With the exception of the spectrum for the time point T=0 min (red line), the other spectra show both the presence of the ester carbonyl and the amide carbonyl.

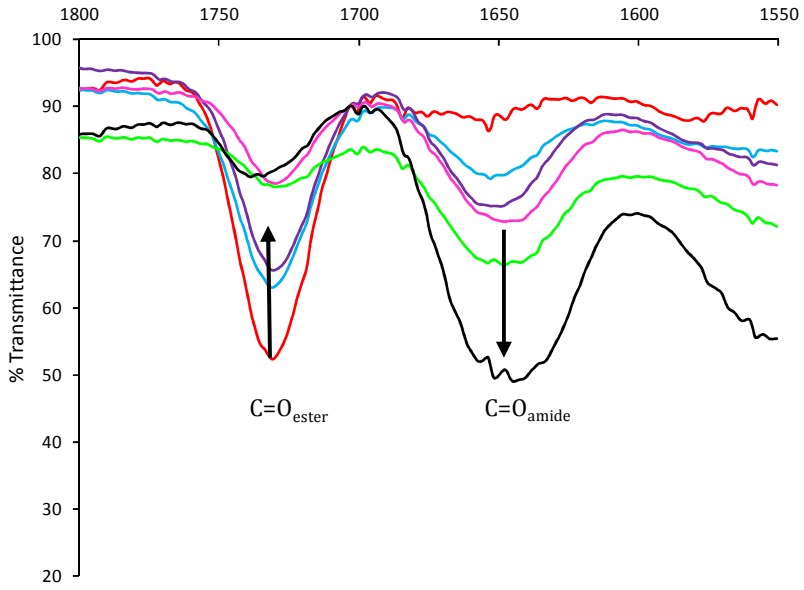

Figure 98 N435-catalyzed synthesis of siloxane-containing polyamides. Samples were removed from the reaction mixture at predetermined intervals. *Legend*: 0 minutes (red), 10 min (light blue), 20 min (purple), 30 min (green), 60 min (magenta), and 360 min (black).

4.2.15 Siloxane Polyesteramides

Polyester-amides are a promising class of polymeric material for use as coatings, tissue regeneration scaffolds and other medical applications.[219] The incorporation of amide linkages into a polymer chain improves the mechanical properties through such physical interactions such as hydrogen bonding between the amide N-H and C=O groups. A collaborative effort between the groups of Gross and Scandola showed that the kinetics of polyamide formation reversed when the diamine and diester blocks were combined in the presence of the diol block.[155] Co-polymerizations involving the diamine were slower than terpolymerizations which also included the diol block.

N435 was employed to produce siloxane polyester-amides because of the success that had been realized in the synthesis of siloxane polyesters and polyamides. Siloxane-containing polyester-amides were prepared using a 1:0.5:0.5 ratio of diester **212**, diol **162**, and diamine **217**. The amount of N435 included in the reaction was fixed at 5 wt% based on the total mass of the monomers. The general reaction scheme for these ter-polymerizations is outlined in **Figure 99**.

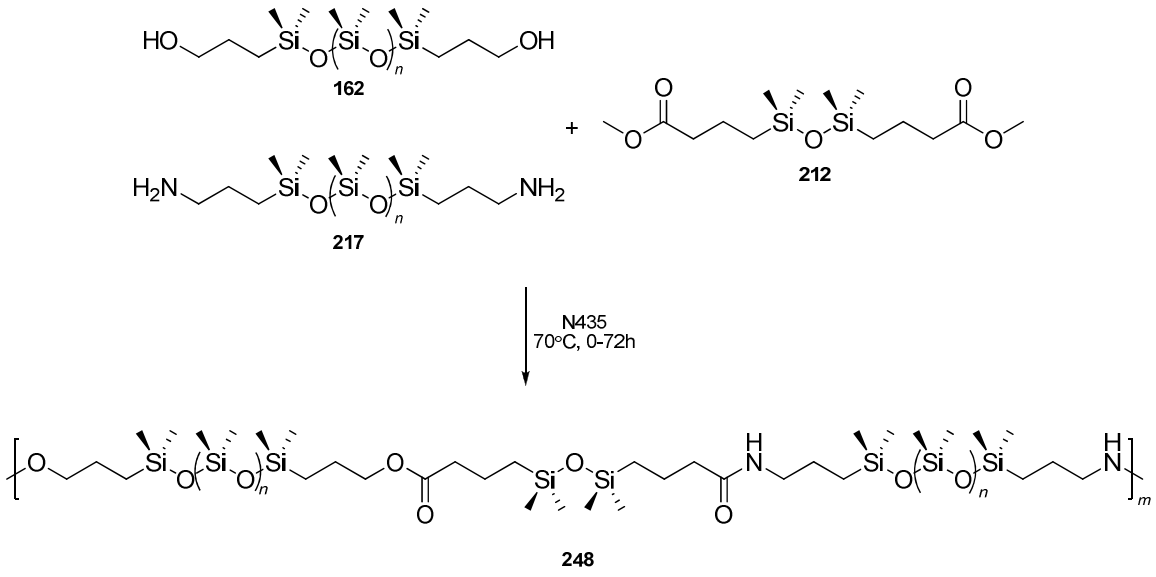

Figure 99 The lipase-catalyzed synthesis of siloxane polyester-amides. Each reaction was carried out at 70°C with 5 wt% of N435 over 72 hours.

Polyester-amides were successfully produced using 5 wt% N435 under solvent-free conditions at 70°C over 72 hours. As the growing polymer chains increased in length, the reaction mixture became more viscous. The consumption of each of the functional groups was monitored through ^{1}H NMR spectroscopy using the previously stated resonances. The value of each of the chosen integrals was compared to distinguish be-

tween free alcohol or amine moieties and the newly formed ester or amide linkages. This approach allowed for the determination of the relative rates of consumption of each of the monomers, but not the distribution of the monomers throughout the growing polymer chain.

An analysis of the relative rate of formation of presented in **Figure 100**. The early stages of the reaction, within the first hour, are dominated by amide formation. Within the first hour nearly 41% of the free amino groups had been consumed whereas only 30% of the hydroxyl groups were consumed. After approximately 2 hours this difference became even more pronounced with at about 68% of amines and 42% of hydroxyls groups being consumed. After 7 hours nearly all of the amines had been converted to amides but only 58% of the alcohol groups have been transesterified. By 24 hours of incubation, the conversion of amines to amides was quantitative, whereas the ester formation reached only 70%.

When N435 was charged with producing only polyesters or polyamides, the data showed that the formation of esters was the preferred process. We were not surprised by this result considering that lipases have evolved to function as ester hydrolases. However, during terpolymerizations in which two competing nucleophiles were included in the same reaction mixture, this trend was reversed and amide formation was the favoured process. The formation of esters showed a 38% decrease in the rate of formation in the terpolymerization whereas the rate of amide formation was 19% higher. Even when the background rate of amide formation is taken into consideration over the first hour of the reaction, the rate of amide formation is still higher than the rate of ester formation. While the reason for this selectivity switch is unclear, it has been proposed that upon transesteri-

fication, the presence of alcohol may participate in alcoholysis of the growing polyester chain fragments. However, owing to the stability of the amide linkage, alcoholysis of amides was not thought to occur, or occurred at a much lower rate.[155]

These observations from the terpolymerizations are in agreement with those provided by Gross and Scandola.[155] In the Gross and Scandola work amine consumption was the preferred process in terpolymerizations involving a polysiloxane diamine, 1,8-octanediol and adipic acid. Nearly 88% conversion within the first hour was observed compared to only 55% conversion of the free alcohol was seen. Furthermore, Gross and Scandola also showed that in the individual copolymerization reactions that ester formation was preferred. It should be noted that the amount of enzyme in their study was adjusted to reflect the total mass of the monomers. Explicit consideration was not given to controlling the stoichiometry of the catalyst between the two reacting systems. Additionally an aliphatic diol was used in lieu of a siloxane-containing diol which we have shown to be an important substitution.

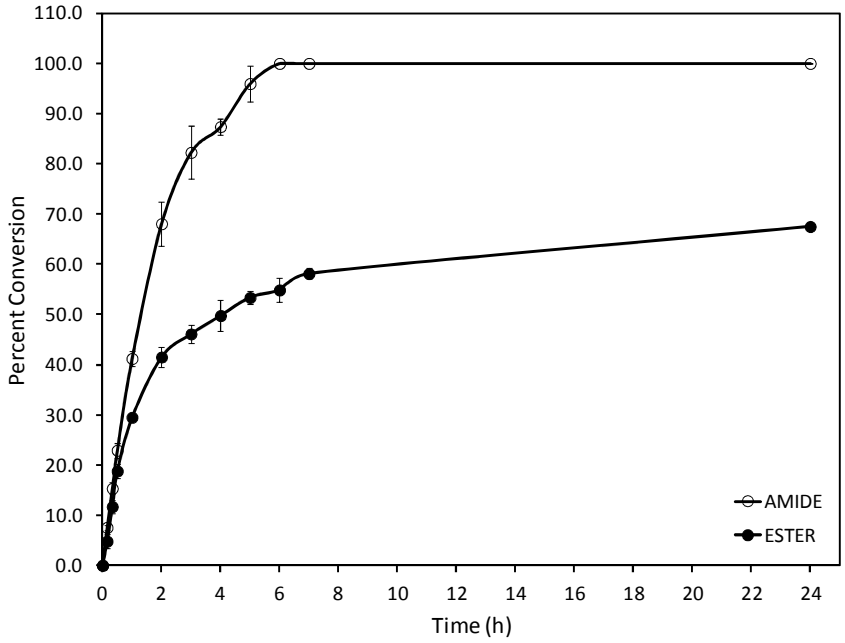

Figure 100 The consumption of alcohol and amine groups as a function of time during the terpolymerization of diester **212** with diol **212** and diamine **217**. The ratio of the reactants was 1:0.5:0.5 ester:alcohol:amine. *Legend*: Hollow circles (polyester formation) and black circles (polyamide formation), error bars are shown.

4.2.16 Residual Activity of N435

The residual enzymatic activity of the immobilized CalB was determined by recovering the enzyme containing beads and subsequently performing an assay designed to standardize for residual activity. The assay monitored the production of octyl palmitate from 1-octanol and palmitic acid in one hour at 37°C (**Figure 101**). Control assays consisting of N435 that had never been used as well as an enzyme-free control reaction were included. The results of each assay were monitored using ^{1}H NMR. The change in the intensity of the resonances for the *O*-methylene protons in 1-octanol and octyl palmitate was compared. In the absence of any enzyme, octyl palmitate was not detected. On the

contrary, virgin enzyme, that is enzyme beads that had not been used in a polymerization cycle, esterified 93% of the 1-octanol within the allotted time period. Every batch that was assayed retained in excess of 88% of their relative activity. Previous reports have mentioned between 5-85% residual activities for recovered enzymes.[220,222]

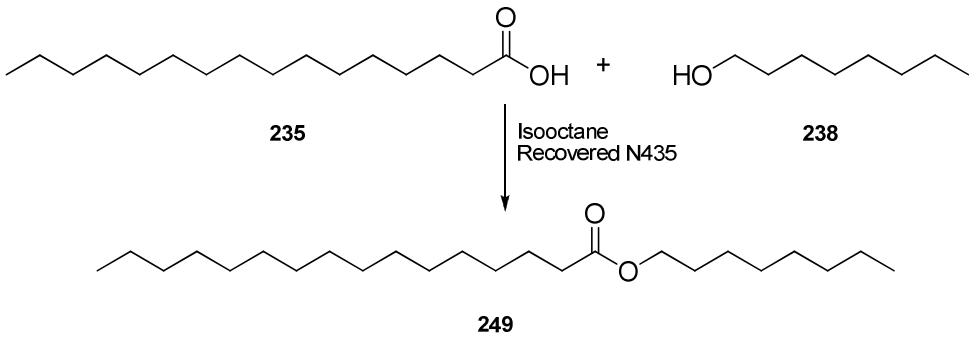

Figure 101 Residual enzyme activity was quantified using the production of octyl palmitate (**249**).

While it is difficult to account for the different processing parameters that have been employed, it generally appears that hydrophobic substrates tend to favour not only higher polymerization rates, but also the retention of higher amounts of residual activity. This is perhaps not surprising given the native environment in which lipases have evolved to function. Siloxanes are known to be some of the most hydrophobic materials synthesized and as such siloxane-containing polyesters should offer a suitable environment in which a lipase can function.

For example silicone-coated N435-beads were prepared by platinum-catalyzed hydrosilylation chemistry.[221] The cross-linked silicone polymer permeated into the pores of the beads as determined by Energy Dispersive X-ray spectroscopy. Not only did the silicone coating protect the acrylic resin from mechanical abrasion, but it did not adverse-

ly affect enzymatic catalysis. In fact, higher activity was found after the silicone coating was applied compared to uncoated enzyme beads. Furthermore, the silicone prevented the enzyme from leaching into an acetonitrile-water mixture over 30 minutes of incubation; the activity values for the enzyme after this treatment were significantly larger than for the uncoated beads. While the polymerization of a siloxane-containing diester and diol is not that similar to a cross-linked polymeric coating, similar effects are seen, particularly with the high residual activity that was observed.

4.2.17 Thermal Tolerance of N435

In order for biocatalysis to be viable on an industrial scale the catalyst must be cost efficient, reusable and reliably perform the desired reactions with high selectivity and turnover. In light of the high residual activity of N435 after prolonged exposure to elevated temperatures it was of interest to determine the long-term thermal tolerance of a single batch of the immobilized enzyme catalyst. A series of 24 hour reaction cycles at 100°C were performed using a single batch of N435. The changes in the initial rate constant and in total monomer conversion were used as metrics to quantify the effect of repeated long term reaction cycles. Between each consecutive use of the catalyst, the reaction mixture was cooled to room temperature and washed with cold diethyl ether for 10 minutes to cleanse the acrylic beads of any residual polymer. The acrylic beads were recovered by filtering through a medium porosity glass fritted filter and air dried prior to the next reaction cycle.

The change in the rate constant of polymer elongation and total monomer conversion for each of 10 successive uses of the same batch of N435 is presented in **Figure 102**.

With the exception of the first three trials in which the apparent rate remained fairly constant, each successive reaction cycle led to some loss in the catalytic activity of the enzyme. The rate decreased by approximately 50% after six reaction cycles and by the tenth reaction cycle more than 80% of the initial enzyme activity has been lost. Despite this loss, when the polymerizations continued for the full 24 hour reaction cycle, monomer conversion reached high levels, typically in the range of 80-93%.

The CalB molecule is adsorbed onto the surface of the acrylic beads only through electrostatic interactions thus allowing for the enzyme molecules to desorb from the surface under the appropriate conditions.[221] The reduction in the rate of polymerization may be a result of the enzyme desorbing from the beads during the polymerization cycle, or after polymerization when the reaction is being quenched with diethyl ether. However, this observed decrease may simply be due to small reductions in enzymatic activity due to thermal denaturation.

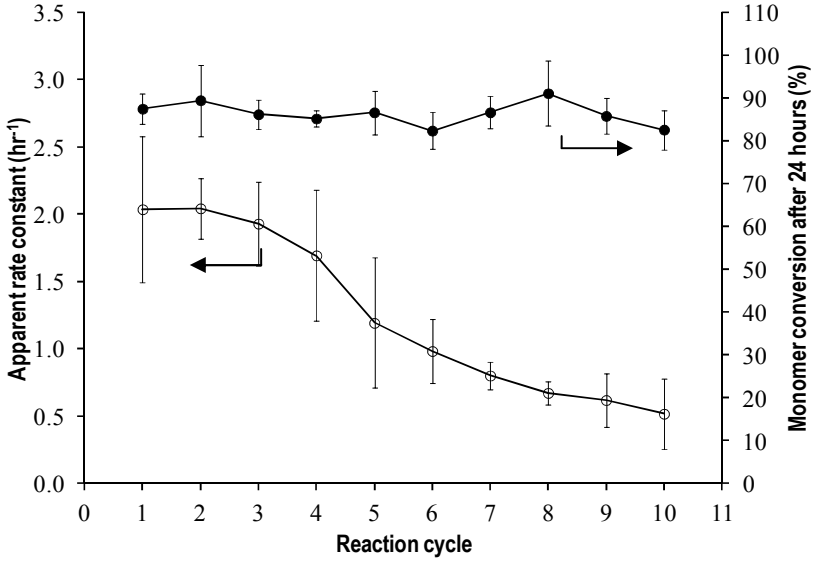

Figure 102 A single batch of N435 was used for ten 24 hour reaction cycles at 100°C. The DP_{avg} (open circles) and monomer conversion (black circles) are shown.

These results can be compared to a previous study where a single batch of N435 was used for the ring opening polymerization (ROP) of ε-caprolactone in toluene at 70°C over several 4 hour reaction cycles.[222] N435 exhibited lower activity in the first reaction cycle compared to all subsequent reaction cycles. It was postulated that swelling of the acrylic resin allowed for any lipase on the interior of the solid support to become available to the medium and participate in the ROP of PCL.

4.2.18 Thermal Tolerance of N435: Changing the Chain Length of the Acyl Donor

The residual activity of N435 is highly variable. The high level of residual enzymatic activity for N435 in our experiments was much greater than the results previously reported and consistently found to be >95%, even at temperatures above 130°C. However, when we compared the rate of polymerization between several acyl donors with 1,8-octanediol, the polymerization of siloxane-containing monomers was slower than the polymerization of aliphatic substrates. An examination of the polymerization of the same set of aliphatic diesters with 1,8-octanediol at elevated temperatures (100-140°C) was attempted to learn if the siloxane-derived monomers were preventing the enzyme from premature denaturation at higher temperatures.

Figure 103 graphically presents the rate constants that were obtained by the N435-catalyzed synthesis of aliphatic polyesters in the temperature range of 100-140°C. The data pertaining to the polymerization of the siloxane diester has already been discussed, and its inclusion in the figure is for comparative purposes only. Dimethyl sebacate (**225**), dimethyl succinate (**222**), dimethyl adipate (**224**), and disiloxane diester **212**

were polymerized with varying degrees of proficiency over the temperature range examined herein. The N435-catalyzed polymerization of **225** and 1,8-octanediol had the highest initial rate over 100-140°C. The rate constant increased from 3.84 to 4.83 h^{-1} between 100°C and 110°C, and then did not change significantly until it decreased to 3.42 h^{-1} at 140°C where it was slightly lower than the rate at 100°C. With **224** as the acyl donor, the rate constant at 100°C was nearly identical to that when **225** was the donor, at 3.88 h^{-1}. The rate constant continued to increase until 120°C was reached where the rate constant was 5.19 h^{-1}. At 130°C and 140°C the rate constant deceased to 3.97 h^{-1} and 0.36 h^{-1} respectively.

The use of diester **222** as the acyl donor proved to be somewhat detrimental to the functioning of the lipase at high temperature. The initial rate constant for polymer elongation was 3.09 h^{-1} at 100°C; this increased only marginally to 3.24 h^{-1} at 110°C. At 120°C the enzyme was still showing some signs of activity, but thermal denaturation was setting in as the rate constant decreased to 1.78 h^{-1}. At higher temperatures, the rate of elongation was no longer linear, and in fact did not increase after 20 minutes, which was taken to mean that the enzyme was denatured or at the very least denaturing at an excellerated rate, and as such, accurate rate constants could not be obtained.

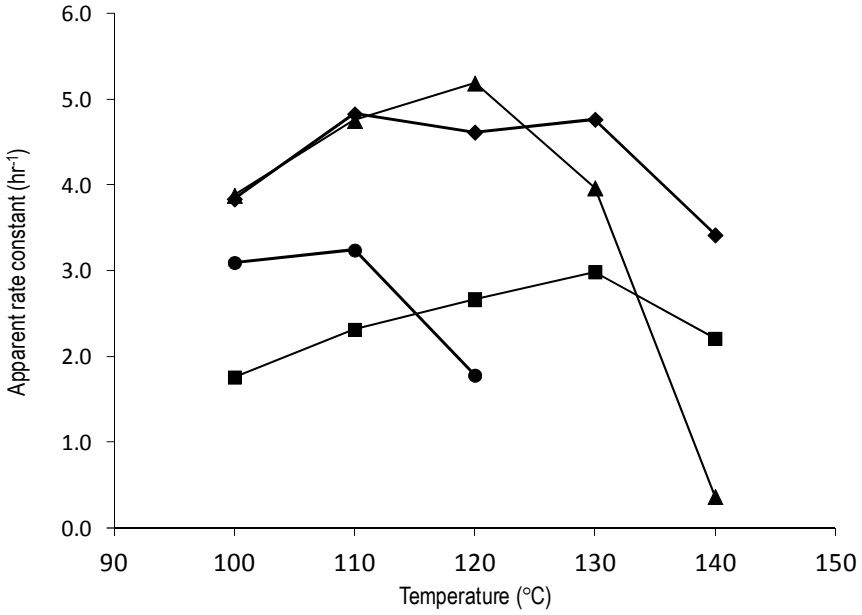

Figure 103 The lipase-mediated synthesis of aliphatic polyesters. *Legend*: Diethyl sebacate (triangles), dimethyl succinate (circles), dimethyl adipate (diamonds), and disiloxane diester (squares).

From the available data it appeared that dimethyl succinate did not afford any thermal protection to the enzyme as evident by the decrease in the reaction rate. Dimethyl adipate seemed to offer more thermal protection as the rate of polyester formation did not decrease until the reaction temperature was increased to 140°C. Dimethyl sebacate offered a similar degree of protection, but exceeded dimethyl adipate at 140°C. Similar to dimethyl sebacate, diester **212**, which may be received by the enzyme as a C11 diester, also did not elicit a large reduction in the rate of polymer elongation by N435. The number of methylene units, or disiloxane in the case of diester **212**, between the terminal ester groups, shows some correlation with the onset of the enzymes decreased performance. From these observations it was concluded that the more hydrophobic sub-

strates, at least in terms of the diester, offered some degree of thermal protection to the enzyme catalyst.

5 Conclusions

In this thesis the results are presented from work in two major areas of organosilicon biotechnology, namely the bio-inspired hydrolysis of alkoxysilanes, and the use of enzymes as practical catalysts for the condensation polymerization of siloxane-containing polyesters, polyamides, and polyester amides.

The amino acid-catalyzed hydrolysis of tetraethoxysilane was examined. The side chain of the amino acid played an important role in mediating hydrolysis. The basic amino acids, histidine, ornithine and arginine were the most proficient at mediating hydrolysis, while the neutral and non-polar amino acids were not well equipped for hydrolysis. This approach was extended to the use of enzymes which gave variable results depending on the pH of the reaction medium. Of the enzymes studied trypsin was responsible for the highest rates of hydrolysis of tetraethoxysilane.

The serine proteases trypsin and α-chymotrypsin and the carboxypeptidase pepsin were examined for their catalytic activity towards phenyltrimethoxysilane. The architecture of the binding pockets near the active site played a role in determining the activity of any enzyme towards that substrate. The enzymes were ranked from best to worst as pepsin, α-chymotrypsin and trypsin.

The N435-catalysed synthesis of siloxane-containing polyesters, polyamides and polyester-amides has been presented. There was a positive correlation between the temperature of the reactions and the rate at which the enzyme performed each of the desired transformations. When temperatures in excess of 130°C were employed, the enzyme still functioned, but denaturation was becoming apparent. The success with which the lipase-catalyzed esterifications and amidations were carried out should be tempered by the

knowledge that the use of organosilicon monomers were not as readily incorporated into polymer chains as were purely aliphatic substrates. The lower reaction rates are tentatively being attributed to both electronic and steric factors which will be the focus of a future project involving both synthetic and computational methods.

N435 has been shown to remain functional at temperatures well above those which typically denature proteins. The lipase molecule retains a large fraction of its inherent activity after being used for polymerizing organosilicon compounds. In fact the same batch of catalyst was shown to retain activity over ten reaction cycles. While the rate of reaction slowly decreased with each successive use, the total monomer conversion was not affected. The organosilicon compounds that were employed throughout the bulk of this thesis appeared to offer thermal protection to the enzyme when compared to purely organic substrates.

The synthesis of branched siloxane-containing polymers using N435 was probed. The available evidence suggested that the CalB molecule could perform the esterification of both the primary and secondary esters of trimethyl citrate with a siloxane diol, and between glycerol and a siloxane diester. This avenue will be further explored using a two-enzyme approach.

The interaction between organosilicon compounds and some lipases is not necessarily a detrimental relationship. This thesis has shown that biocatalysis is a viable alternative to the more traditional methods employed in organosilicon chemistry.

6 Experimental

6.1 Materials

Novozym-435 (EC.3.1.1.3), *Candida antarctica* lipase A immobilized on Immobead 150, lipase from *Candida antarctica* (EC.3.1.1.3, 10,000 U/g), lipase Type VII from *Candida rugosa* (1,180 U/mg solid), lipase Type I from wheat germ (EC.3.1.1.3, 7.9 U/mg solid, 8.2 U/mg protein), porcine pancreatic lipase, tetravinylsilane, trypsin from bovine pancreas (EC 3.4.21.4), pepsin from porcine stomach mucosa 1:10,000 (EC 3.4.23.1), α-chymotrypsin type II from bovine pancreas (EC.3.4.2.1, 83.9 U/mg solid), human serum albumin (96-99% purity), hydride terminated polydimethylsiloxane (M_n 580 g/mol), platinum(0)-1,3-divinyl-1,1,3,3-tetramethyldisiloxane complex in xylenes, L-histidine methyl ester dihydrochloride, L-proline, L-serine, L-aspartic acid, L-valine, N-benzoyl-L-arginine ethyl ester, L-tyrosine methyl ester, glycine, L-tryptophan, L-phenylalanine, acetonitrile and tetramethylsilane (TMS) were acquired from Sigma-Aldrich (Oakville, Ontario, Canada).

Ornithine, sodium sulphite, L-isoleucine, L-leucine and sodium phosphate monobasic (>98% purity) were obtained from British Drug House (Poole, England).

Papain from *Carica papaya* (EC. 3.4.22.2, 3.36 U/mg) was obtained from Fluka Analytical (Oakville, Ontario, Canada).

Allyl alcohol, allyl acetate, *p*-toluene sulphonic acid, ammonium molybdate tetrahydrate, and triethoxysilane were obtained from Alfa Aesar (Ward Hill, Massachusetts, USA).

Phenyltrimethoxysilane (95% purity), methyltrimethoxysilane (97% purity), ethyltrimethoxysilane (97% purity), tetraethoxysilane (98% purity), trimethoxysilane, allyltrimethoxysilane (95% purity), allyltriethoxysilane (>95% purity), α,ω-bis(10-carboxydecyl)-polydimethylsiloxane (M_w 1000 g/mol), α,ω-bis(3-aminopropyl)-polydimethylsiloxane, 1,3-bis(3-carboxypropyl)-1,1,3,3-tetramethyldisiloxane and 1,1,3,3-tetramethyldisiloxane were obtained from Gelest, Inc. (Morristown, Pennsylvania, USA).

Isooctane, pentane, hydrochloric acid (35-28%), sodium hydroxide, isopropanol, methanol, ethanol, and sodium phosphate dibasic (minimum 99% purity) were obtained from Caledon Chemicals (Georgetown, Ontario, Canada).

Soybean inhibitor was acquired from Worthington Biochemical Corporation (Lakewood, New Jersey).

Chloroform and tetrahydrofuran were obtained from Fisher Scientific (Fair Lawn, New Jersey, USA).

Chloroform-*d* (99.8% deuterated), deuterium oxide, DMSO-d_6, and acetone-d_6 were obtained from Cambridge Isotope Laboratories, Inc. (Landover, Maryland, USA).

Toluene and diethyl ether were obtained from EMD (Gibbstown, NJ, USA).

Diethyl ether was acquired from Anachemia (Montreal, Quebec, Canada).

Distilled water was used for all preparations. All reagents were used as received without further modification or purification unless stated in the text of this thesis.

6.2 General Experimental Procedures

Nuclear Magnetic Resonance Spectroscopy (NMR). NMR spectra were acquired using a Bruker Avance 300 MHz equipped with a broadband probe. Samples were typically dissolved into $CDCl_3$, unless otherwise stated. ^{1}H NMR spectra were recorded at 300 MHz and the residual protons of $CHCl_3$ were used as the internal standard at 7.26 ppm. ^{13}C NMR spectra were recorded at 75 MHz and the $CDCl_3$ was used as the internal standard, and set to 77.0 ppm, except when tetramethylsilane was included in which case the peak for TMS was set to 0.0 ppm. ^{29}Si NMR spectra were recorded at 59.6 MHz and TMS was used as the internal standard and was set at 0.00 ppm. NMR spectra recorded on a Bruker Avance Ultra-Shield 600 MHz spectrometer were acquired using a PABBO probe. The resonance frequency for each nucleus was ^{1}H - 600 MHz, ^{13}C - 150 MHz, and ^{29}Si - 119 MHz. Spectra were analyzed using the Bruker TopSpin v2.0 software platform.

Fourier-Transform Infrared Spectroscopy (FTIR). FTIR spectra were acquired using a Mattison Research Series scanning infrared spectrometer. Samples were prepared as neat

films on KBr windows. Each spectrum that was acquired was the average of 32 or 64 scans at 2 cm^{-1} resolution. Spectra were analyzed using the WinFirst software platform.

Matrix Assisted Laser Desportion Ionization Time of Flight Mass Spectrometry (MALDI-ToF). MALDI-TOF MS spectra were acquired using a Bruker Autoflex spectrometer operated in the positive reflectance mode. Samples were prepared as solutions in THF containing dithranol as the matrix.

Ultra Violet/Visible Spectroscopy (UV/Vis). UV-Vis spectra were recorded using a Red Tide USB650 UV-Vis spectrophotometer.

Differential Scanning Calorimetry (DSC). DSC spectra were acquired using a TA-60 differential scanning calorimeter.

6.3 Detailed Experimental Methods

Amino acid-catalyzed hydrolysis of tetraethoxysilane for silicomolybdate analysis. *N*-benzoyl-L-arginine ethyl ester, L-histidine methyl ester hydrochloride, L-aspartic acid, proline, L-ornithine, L-tyrosine ethyl ester, L-isoleucine, L-leucine, L-valine, L-tryptophan, glycine, L-phenylalanine, and L-serine were prepared to 20 mM in 0.2 M phosphate buffer at pH 7.03±0.02. The pH of the buffer was adjusted with NaOH or HCl as needed. Tetraethoxysilane (250 μL, 112 mM) was added to a 2.0 mL Eppendorf tube. To this was added 1.0 mL of the amino acid preparation. Each Eppendorf tube was mixed vigorously by hand for 30 seconds then incubated for 24 hours at room tempera-

ture. Silica was isolated by centrifuging the Eppendorf tubes at 15,000 rpm for 10 minutes at 4°C. The supernatant was removed and the silica pellet was washed twice with 1.0 mL of distilled water, to remove any residual amino acid and phosphate buffer, and centrifuged for 5 minutes at 15,000 rpm at 4°C. The silica pellet was washed a final time with 1.0 mL of isopropanol to remove any residual tetraethoxysilane and then centrifuged for 10 minutes at 15,000 rpm at 4°C. The supernatant was discarded and the pellet was allowed to air dry. Total silica was quantified using a modification of the silicomolybdate method as described by Iler.[1] Sodium silicate standards were prepared by dissolving sodium silicate pentahydrate into distilled water. Standards were prepared to contain 0.1075 μg, 1.075 μg, and 10.75 μg of silicic acid. In a plastic, 1 cm cuvette, 1.0 mL of each standard was diluted to 1.2 mL with distilled water and combined with 180 μL of 12 g/L ammonium molybdate containing 60 g/mL hydrochloric acid. This solution was allowed to stand at room temperature for 10 minutes to allow the oxidized form of silicomolybdic acid to develop. After this period of time 900 μL of the reducing solution (4.5 N sulfuric acid) and 720 μL of distilled water were added to begin the formation of the blue silicomolybdic acid complex. After 2 hours the absorbance at 810 nm was recorded and a calibration curve was constructed. The equation of the best fit line was subsequently used to determine the total dissolved silicic acid in each of the experimental preparations. The experimental preparations were performed in the same way with the exception of using between 1.0-10.0 μL of the prepared silicic acid solution.

Enzyme-catalyzed hydrolysis and condensation of tetraethoxysilane. Trypsin, α-chymotrypsin, pepsin, papain, bromelain, and lipase from *Candida rugosa* were prepared

to 100 mM in 0.04 mM phosphate buffer at pH 7.0 or in distilled water. Tetraethoxysilane (250 μL, 112 mM) was added to a 1.8 or 2.0 mL Eppendorf tube. To this was added 1.0 mL of the enzyme solution. Each Eppendorf tube was mixed vigorously for 30 seconds then incubated for 48 hours at room temperature. Silica was isolated by centrifuging the Eppendorf tubes at 15,000 rpm for 10 minutes at 4°C. The supernatant was removed and the silica pellet was washed twice with 1.0 mL of distilled water, to remove any residual amino acid and phosphate buffer, and centrifuged for 5 minutes at 15,000 rpm at 4°C. The silica pellet was washed a final time with 1.0 mL of isopropanol to remove any residual tetraethoxysilane and then centrifuged for 10 minutes at 15,000 rpm at 4°C. The supernatant was discarded and the pellet was allowed to air dry overnight. Total silicic acid was quantified using a modification of the silicomolybdate method as described by Iler.[1] Sodium silicate standards were prepared by dissolving sodium silicate pentahydrate into distilled water. Standards were prepared to contain 0.1075 μg, 1.075 μg, and 10.75 μg of silicic acid. In a plastic 1 cm cuvette, 1.0 mL of each standard was diluted to 1.2 mL with distilled water and combined with 180 μL of 12 g/L ammonium molybdate containing 60 g/mL hydrochloric acid. This solution was allowed to stand at room temperature for 10 minutes to allow the oxidized form of silicomolybdic acid to develop. After this period of time 900 μL of the reducing solution and 720 μL of distilled water were added to begin the formation of the blue silicomolybdic acid complex. After 2 hours the absorbance at 810 nm was recorded and a calibration curve was plotted. The equation of the best fit line was subsequently used to determine the total dissolved silica in each of the experimental preparations. The experimental preparations were performed in the same way with the exception of using 10 μL of the prepared silica solution.

Enzyme-catalyzed hydrolysis of phenyltrimethoxysilane. Trypsin, α-chymotrypsin, and pepsin were prepared to 5 mg/mL in distilled water. Phenyltrimethoxysilane was combined with the enzyme preparations and mixed vigorously by inversion. The ^{29}Si NMR scale experiments were initiated by charging a glass NMR tube with 600 μL of the silane-enzyme mixture and acquiring spectra. ^{29}Si NMR spectra were recorded on a Bruker Avance AV-300 NMR spectrometer using a 5mm broadband probe. Each spectrum was the average of 60 transients of 60 seconds duration and experiments were run for between 12-80 hours. Spectra were analyzed using the Bruker Topspin v2.0 software platform.

Trypsin-mediated hydrolysis of α,ω-bis(3-trimethoxysilylpropyl)-polydimethylsiloxane.

A 4-dram glass vial was charged with 500 μL of TMSPr-PDMS and 500 μL of water or a 10 mg/mL trypsin solution and mixed by end-over-end inversion for 5 minutes. The reaction mixture was transferred to a fresh vial and exposed to air for 30 minutes after which point the screw cap was fastened and the mixture incubated at room temperature for 24 hours. The supernatant was analyzed by ^{29}Si NMR spectroscopy. The reaction mixture was visualized by phase contrast microscopy.

Residual enzyme activity of recovered N435.

The recovered N435 was assayed for residual activity by measuring the production of octyl palmitate from 1-octanol and palmitic acid. A stock solution of 200 mM 1-octanol and 200 mM palmitic acid in isooctane was freshly prepared before each assay. For each

reaction 5 mg of lipase was combined with 1 mL of the assay mixture and incubated at 35°C for 1 h with magnetic stirring. A 20μL aliquot of the reaction mixture was analyzed by ^{1}H NMR. The ratio of the resonances associated with the *O*-methylene protons in 1-octanol and octyl palmitate was used to determine the degree of esterification. The methylene resonance in the ester is located at 4.02 ppm while the corresponding methylene resonance in the 1-octanol is located at 3.66 ppm. A fresh enzyme preparation, that is enzyme that had not been used to synthesize disiloxane polyester systems, was prepared for use as a control. The amount of esterification achieved from the fresh enzyme was set to a default value of 100% and all other assays were calibrated to this value. An enzyme-free control reaction was also performed to determine the background rate, if any, for the esterification of octyl palmitate.

Thermal tolerance and reuse of N435.

A single batch of N435 was subjected to multiple 24 h reaction cycles at 100°C to determine the number of times that the enzyme could be reused before it was determined to be unsuitable for catalysis. The apparent second-order rate constant, which was derived from the slope of the line from a plot of the average degree of polymerization versus time, as well as the extent of monomer conversion were compared. Between each 24 h reaction cycle, the N435 beads were recovered by the addition of 5 mL of diethyl ether at room temperature for 10 minutes. After stirring, the beads were filtered through a glass filter of medium porosity and washed with three 10 mL aliquots of diethyl ether. The mass of the beads recovered was determined and the volumes of each reagent for subsequent reaction mixtures were adjusted accordingly.

6.3.1 Synthetic Experimental Procedures

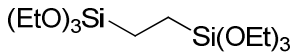

197

1,2-Bis(triethoxysilyl)ethane (197)

A round bottomed flask was charged with 3.0 mL (14.4 mmol) of vinyltriethoxysilane and 1 drop (~10 uL) of Karstedt's platinum catalyst complex in xylenes under an air atmosphere and stirred at room temperature for 10 minutes. Triethoxysilane (2.63 mL, 14.3 mmol) was added drop-wise over 10 minutes at room temperature, and fitted with a rubber septum. The reaction mixture stirred at room temperature for 48 hours after which point the mixture was diluted with pentane and two scoops of activated carbon and stirred for an additional 2 hours. The contents of the reaction mixture were filtered through Celite 545 and excess solvent was removed under reduced pressure to yield 5.16 g (13.11 mmol, 91 %) of a colourless oil. ^{1}H NMR (300 MHz, $CDCl_3$): δ 0.67 (*m*, 4H), 1.23 (*t*, 18 H, J_{ab}=6.9 Hz), 3.82 (*q*, 12 H, J_{ab}=6.9 Hz); ^{13}C NMR (75 MHz, $CDCl_3$): δ 1.5, 18.3, 58.4; ^{29}Si NMR (59.6 MHz): δ -45.2.

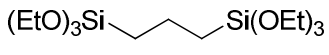

198

1,3-Bis(triethoxysilyl)propane (198)

A round bottomed flask was charged with 0.5 mL (2.2 mmol) of allyltrimethoxysilane and combined with 10 μL of Karstedt's platinum catalyst complex in xylenes. This mixture was stirred at room temperature for 10 minutes after which 0.4 mL (2.2 mmol) tri-

ethoxysilane was added. The reaction was allowed to continue for 24 hours at room temperature. The complete consumption of starting material was confirmed by monitoring the disappearance of the resonance at 4.3 ppm representing the Si-H functional group. The crude reaction mixture was decolourized by the addition of activated carbon and 2.0 mL of pentane over 3 hours. The reaction mixture was filtered through Celite, rinsed with 2 x 10 mL of pentane, followed by solvent removal *in vacuo* to yield 0.66 g (1.8 mmol, 81%) of a clear and colourless liquid. ^{1}H NMR (300 MHz, $CDCl_3$): δ 0.72 (*m*, 4H), 1.22 (*t*, 18 H, J_{ab}=6.9 Hz), 1.58 (*m*, 2H), 3.810 (*q*, 12 H, J_{ab}=6.9 Hz); ^{13}C NMR (75 MHz, $CDCl_3$): δ 14.3, 16.5, 18.3, 58.3; ^{29}Si NMR (59.6 MHz, $CDCl_3$): δ -45.4; FTIR (KBr, cm^{-1}): 773, 819, 1082, 1105, 1167, 1390, 2885, 2927, 2974.

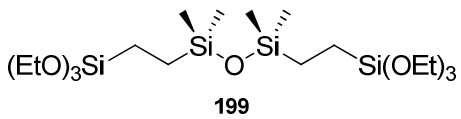

199

1,3-Bis(2-triethoxysilylethyl)-1,1,3,3-tetramethyldisiloxane (199)

A round bottomed flask was charged with 0.25 mL (1.42 mmol) of 1,1,3,3-tetramethyldisiloxane and 10 μL of Karstedt's platinum catalyst complex in xylenes to form a bright yellow solution. This mixture was stirred for 5 minutes at room temperature after which time 0.61 mL (2.9 mmol) of vinyltriethoxysilane was added. The reaction mixture was stirred at room temperature for 16 hours. The reaction mixture was decolourized by the addition of activated carbon in 3.0 mL of pentane for 3 hours at room temperature. The reaction mixture was filtered through Celite and the solvent was removed *in vacuo* to give 0.448 g (0.872 mmol, 79%) of clear, colourless oil. The reaction mixture was not purified and was known to contain a mixture of compounds resulting

from anti-Markovnokov and Markovnikov hydrosilylation. ^{1}H NMR (300 MHz, $CDCl_3$): δ 0.04 (*s*, 12 H), 0.10 (*m*), 0.54 (*d*), 1.21 (*t*,), 1.21 (*t*), 3.82 (*q*), 3.81 (*q*). ^{13}C NMR (75 MHz, $CDCl_3$): δ -0.5, -0.4, 0.1, 1.1, 1.8, 6.1, 7.7, 9.2, 18.3, 58.3, 58.4. ^{29}Si NMR (59.6 MHz, $CDCl_3$): δ 7.9, 8.2, -44.9, -45.6. FTIR (KBr, cm^{-1}):786, 840, 957, 1053, 1080, 1105, 1139, 1167, 1252, 2885, 2926, 2976.

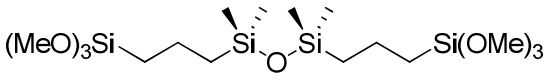

200

1,3-Bis(3-trimethoxysilylpropyl)-1,1,3,3-tetramethyldisiloxane (200)

A flame-dried flask was charged with a magnetic stirring bar, 1.0 mL of PhMe, and 0.81 mL (4.8 mmol) of allyltriethoxysilane. Karstedt's platinum catalyst (2 drops) was added to this mixture and stirred at room temperature for 5 minutes. Tetramethyldisiloxane (0.6 mL, 2.4 mmol) was added drop wise over 5 minutes. The reaction mixture was heated to reflux for 3 hours after which point an aliquot was removed and analyzed by FTIR to show that all of the disiloxane was consumed in the reaction. The mixture was diluted with 4 mL of pentane and activated carbon was added to decolourize over 3 hours. Activated carbon was removed by filtering the reaction mixture through Celite and volatiles were removed *in vacuo* to yield 1.10 g (2.4 mmol, 98%) of clear colourless oil. ^{1}H NMR (300 MHz, $CDCl_3$): δ 0.04 (*s*, 12 H), 0.60 (*m*, 4H), 0.72 (*m*, 4H), 1.46 (*m*, 4H), 3.57 ppm (*s*, 18H). ^{13}C NMR (75 MHz, $CDCl_3$): δ 0.4, 13.5, 16.7, 22.6, 50.4. ^{29}Si NMR (59.6 MHz, $CDCl_3$): δ -41.9, 6.8. FTIR (KBr, cm^{-1}):843, 906, 1089, 1147, 1192, 1253, 2840, 2925, 2943, 2953.

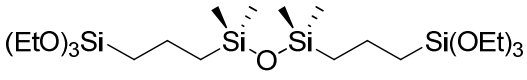

201

1,3-Bis(3-triethoxysilylpropyl)-1,1,3,3-tetramethyldisiloxane (201)

A flame-dried flask was charged with a magnetic stirring bar, 1.0 mL of PhMe, and 0.2 mL (0.88 mmol) of allyltriethoxysilane. Karstedt's platinum catalyst (2 drops) was added to this mixture and stirred at room temperature for 5 minutes. Tetramethyldisiloxane (0.6 mL, 2.4 mmol) was added drop wise over 5 minutes. The reaction mixture was heated to reflux for 3 hours after which point an aliquot was removed and analyzed by FTIR to show that all of the disiloxane was consumed in the reaction. The mixture was diluted with 4 mL of pentane and activated carbon was added to decolourize over 2 hours. Activated carbon was removed by filtering the reaction mixture through Celite and volatiles were removed *in vacuo*. ^{1}H NMR (300 MHz, $CDCl_3$): δ 0.03 (*s*, 12 H), 0.60 (*m*, 4H), 0.69 (*m*, 4H^{+}), 1.22 (*t*, 18H), 1.44 (*m*, 4H), 3.81 (*q*, 12H).^{13}C NMR (75 MHz, $CDCl_3$): 0.38 ppm (**C**$\mathbf{H_3}$Si), δ 14.7 7, 16.5, 18.3, 22.6, 58.2.^{29}Si NMR (59.6 MHz, $CDCl_3$): δ -45.2 and 6.79. FTIR (KBr, cm^{-1}):842, 957, 1082, 1104, 1146, 1167, 1256, 1390, 2883, 2925, 2973.

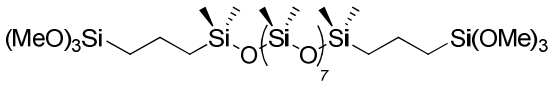

202

α,ω-Bis(3-trimethoxysilylpropyl)-polydimethylsiloxane (202)

A round bottomed flask was charged with 2.7 mL (16.0 mmol) of allyltrimethoxysilane and 10 μL of Karstedt's platinum catalyst complex in xylenes. After stirring at room

temperature for 10 minutes 5.0 mL (8.0 mmol) of hydride terminated polydimethylsiloxane (M_n= 580 g/mol) was added drop wise over 60 minutes and the reaction was stirred at room temperature for 48 hours. The reaction mixture was decolourized with activated carbon in 20 mL of pentane at room temperature for 2 hours. The reaction mixture was separated from the solid impurities by filtering through Celite and solvents were removed *in vacuo* to give 6.95 g (95.9%) of colourless oil. ^{1}H NMR (300 MHz, $CDCl_3$): δ 0.03 (*s*), 0.05 (s), 0.62 (*m*, 4 H), 0.70 (*m*, 4 H), 1.46 (*m*, 4H), 3.55 (*s*, 18 H); ^{13}C NMR (75 MHz, $CDCl_3$): δ 0.2, 1.1, 1.1, 13.4, 16.6, 22.3, 50.4; ^{29}Si NMR (59.6 MHz, $CDCl_3$): δ 6.8, -21.7, -22.0, and -22.2, -42.1; FTIR (KBr, cm^{-1}): 2959, 2838, 1463, 1409, 1266, 1189, 1113, 1023, 812.

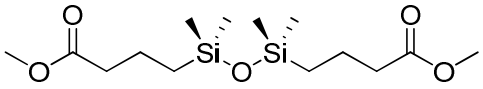

212

1,3-Bis(3-carboxypropyl)-1,1,3,3-tetramethyldisiloxane dimethyl ester (**212**)

A round bottomed flask was charged with 5.02 g (16.38 mmol) of 1,3-bis(3-carboxypropyl)-1,1,3,3-tetramethyldisiloxane, 303.9 mg (1.58 mmol) of pTsOH and dissolved in to 15.0 mL of methanol and refluxed for 6 hours. The progress of the reaction was monitored by FTIR by following the decrease in the carbonyl resonance associated with the carboxylic acid. When this resonance was no longer visible the reaction was refluxed for an additional hour. The solvent was removed *in vacuo* and the remaining crude residue was extracted into 3x20 mL of diethyl ether and washed with 10 mL of saturated NaCl and 10 mL of saturated $NaHCO_3$. The combined organic fractions were

dried over $MgSO_4$, filtered through a medium porosity glass filter. Removal of the solvent *in vacuo* gave 5.15 g (15.42 mmol, 94%) of a clear and colourless liquid. ^{1}HNMR (300 MHz, $CDCl_3$): δ 0.05 (*s*, 12H), 0.53 (*m*, 4H, *J*=18, 3 Hz), 1.64 (*m*, 4H), 2.33 ppm (*t*, 4H, *J*=6 Hz), 3.66 (*s*, 6H); ^{13}C NMR (75 MHz, $CDCl_3$): δ 0.3 ppm, 18.0, 19.1, 37.5, 51.4, 174.1; ^{29}Si NMR (59.6 MHz, $CDCl_3$): δ 7.3; EI MS: M^+-CH_3 = 319 m/z; FTIR (KBr, cm^{-1}): 796, 840, 1020, 1058, 1123, 1165, 1205, 1254, 1436, 1742, 2954. Analytical calculated for $C_{14}H_{40}O_5Si_2$ C 50.26%; H 9.04%. Found C50.05%; H 8.94%.

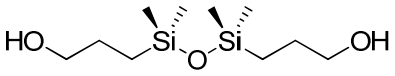

213

1,3-Bis(3-hydroxypropyl)-1,1,3,3-tetramethyldisiloxane (213)

An oven dried round bottom flask was charged with allyl acetate (600 µL, 5.6 mmol) and dissolved into 6.0 mL of toluene. To this mixture Karstedt's platinum complex (2% in xylenes, 5 µL) was added and the reaction mixture stirred at room temperature for 10 minutes. 1,1,3,3-tetramethyldisiloxane (400 µL, 2.2 mmol) was added drop wise at room temperature. The reaction mixture was refluxed for 3.5 hours. Upon completion of the reaction activated carbon was added to remove colloidal platinum by stirring overnight. The carbon was separated by filtering through Celite 545 and the solvent was removed *in vacuo* to yield 443.8 mg (1.3 mmol, 58%) of a clear and colourless liquid. ^{1}H NMR (300 MHz, $CDCl_3$): δ 0.06, 0.11 (*m*, 12H), 2.05 (*s*, 6H), 0.53 (*m*, 4H), 1.64 (*m*, 4H), 4.01 (*t*, 4H, *J*=7.2 Hz). 1,3-bis(3-acetoxypropyl)-1,1,3,3-tetramethyldisiloxane (443.8 mg, 1.288 mmol) was dissolved into 5.0 mL of methanol and 200 µL of 1M NaOH and stirred for 24 hours at room temperature. Methanol was removed *in vacuo* and the residue was ex-

tracted into 5.0 mL of ether and washed with 5.0 mL of water and brine. The ethereal layer was dried over $MgSO_4$ and the volatiles were removed *in vacuo* to yield a clear and colourless liquid in 92% (2.85 g, 11.4 mmol) yield. ^{1}H NMR (300 MHz, $CDCl_3$): δ 0.11 (*m*, 12H), 2.05 (*s*, 6H), 0.54 (*m*, 4H), 1.62 (*m*, 4H), 3.60 (*t*, 4H, *J*=6 Hz); ^{13}C NMR (75 MHz, $CDCl_3$): δ -0.1, 0.04, 0.91, 13.8, 26.3, 65.2; ^{29}Si NMR (59.6 MHz, $CDCl_3$): δ -20.6, 7.7, 8.26. MS (EI): M^+=429 m/z. FTIR (KBr, cm^{-1}): 797, 840, 1056, 1179, 1257, 1412, 2874, 2932, 2957, 3355.

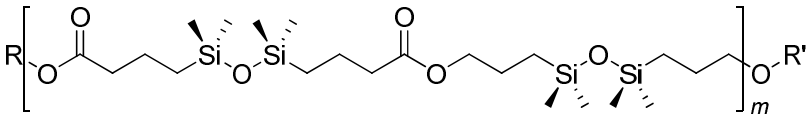

214

Disiloxane polyester (214)

Disiloxane polyesters were prepared under solvent-free conditions using 12.5 wt% N435 (with respect to the mass of diester **212**). Diol **213** was combined in a 1:1 mole ratio with diester **212**, using approximately 0.50-0.75 grams of combined the monomers. Individual reactions were incubated at temperatures between 35°C-150°C with stirring for 24 hours. See **Appendix Table 6** for a complete list of reagent amounts and temperatures utilised for these experiments. The reactions were terminated with the addition of 5.0 mL of diethyl ether after cooling to room temperature. The enzyme beads were removed by filtration through a glass fritted Buchner filter of medium porosity and washed with two 10 mL volumes of diethyl ether. Solvents were removed *in vacuo* to yield siloxane-polyesters as clear and colourless, viscous liquids. ^{1}HNMR (300 MHz, $CDCl_3$): δ 0.06 (*s*), 0.54 (*m*), 1.64 (*m*), 2.32 (*t, J*=5.1 Hz), 3.67 (s), 4.02 (*t, J*=6.6 Hz); ^{13}C NMR (75 MHz, $CDCl_3$): δ 0.02, 0.19, 14.0, 18.0, 19.1, 22.6, 37.6, 66.6, 173.6; ^{29}Si NMR (59.6

MHz, $CDCl_3$): δ 7.3, 7.72. FTIR (KBr, cm^{-1}): 705, 797, 839, 1054, 1200, 1256, 1737, 2879, 2899, 2956.

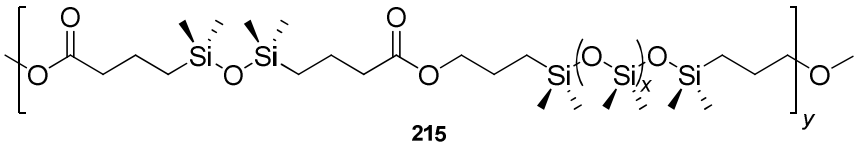

215

Polysiloxane polyester (215)

Disiloxane polyesters were prepared under solvent-free conditions using 12.5 wt% N435 (with respect to the mass of diester **212**). Diol **162** was combined in a 1:1 mole ratio with diester **212**, using approximately 1.25-1.75 grams of combined the monomers. Individual reactions were incubated at temperatures between 35°C-150°C with stirring for 24 hours. See **Appendix** Table 6 for a complete list of reagent amounts and temperatures utilised for these experiments. The reactions were terminated with the addition of 5.0 mL of chloroform after cooling to room temperature. The enzyme beads were removed by filtration through a glass fritted Buchner filter of medium porosity and washed with two 10.0 mL volumes of chloroform. Solvents were removed *in vacuo* to yield polysiloxane-polyesters as clear and colourless to slightly straw coloured, viscous liquids. ^{1}HNMR (300 MHz, $CDCl_3$): δ 0.06 (*s*), 0.53 (*m*), 1.64 (*m*), 2.32 (*t*, *J*=5.1 Hz), 3.67 (s), 4.02 (*t*, *J*=6.6 Hz); ^{13}C NMR (77 MHz, $CDCl_3$,): δ 0.0, 0.2, 14.0, 18.0, 19.1, 22.6, 37.6, 66.6, 173.6; ^{29}Si NMR (59.6 MHz, $CDCl_3$): δ 7.3, 7.7; FTIR (KBr, cm^{-1}): 703, 761, 806, 1034, 1056, 1260, 1412, 1739, 2905, 2933, 2962.

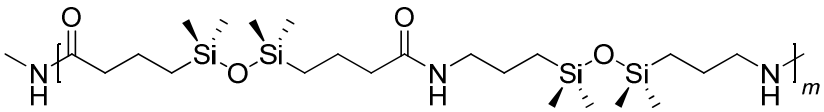

218

Disiloxane polyamide (218)

Disiloxane polyesters were prepared under solvent-free conditions using 12.5 wt% N435 (with respect to the mass of diester **212**). Diamine **216** was combined in a 1:1 mole ratio with diester **212**, using approximately 0.5-0.75 grams of combined the monomers. Individual reactions were incubated at temperatures between 35°C-150°C with stirring for 24 hours. See **Appendix Table 8** for a complete list of reagent amounts and temperatures utilised for these experiments. The reactions were terminated with the addition of 5.0 mL of chloroform after cooling to room temperature. The enzyme beads were removed by filtration through a glass fritted Buchner filter of medium porosity and washed with two 10.0 mL volumes of chloroform. Solvents were removed *in vacuo* to yield polysiloxane-polyamidess as clear, colourless to slightly straw coloured, viscous liquids. ^{1}HNMR (300 MHz, $CDCl_3$): δ -0.01 (*s*), 0.45 (*m*), 1.46 (*m*), 1.64 (*m*), 2.17 (*t*, *J*=7.5 Hz), 3.15 (*m*), 3.61 (*s*), 5.71 (*br*), 6.81 (*br*); ^{13}C NMR (75 MHz, $CDCl_3$): δ -0.15, -0.05, 0.34, 0.73, 15.6, 18.2, 20.1, 23.6, 40.2, 42.4, 42.5, 173.3; ^{29}Si NMR ($CDCl_3$, 59.6 MHz):δ 7.21, 7.25; FTIR (KBr, cm^{-1}): 703, 796,803, 816, 833, 862, 1027, 1032, 1053, 1060, 1069, 1091, 1099, 1102, 1122, 1260, 1412, 1443, 1556, 1644, 1650, 2877, 2904, 2962, 3082, 3289, 3304.

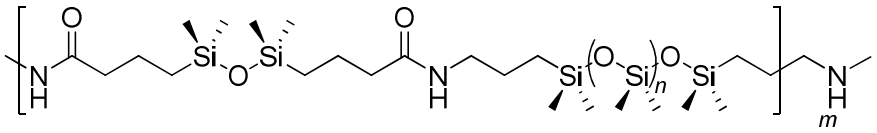

219

Polysiloxane polyamide (219)

Disiloxane polyesters were prepared under solvent-free conditions using 12.5 wt% N435 (with respect to the mass of diester **212**). Diamine **217** was combined in a 1:1 mole ratio with diester **212**, using approximately 1.3-1.6 grams of combined the monomers. See **Appendix Table 9** for a complete list of reagent amounts and temperatures utilised for these experiments. Individual reactions were incubated at temperatures between 35°C-150°C with stirring for 24 hours. The reactions were terminated with the addition of 5.0 mL of chloroform after cooling to room temperature. The enzyme beads were removed by filtration through a glass fritted Buchner filter of medium porosity and washed with two 10.0 mL volumes of chloroform. Solvents were removed *in vacuo* to yield polysiloxane polyamides as coloured, viscous liquids. ^{1}HNMR (300 MHz, $CDCl_3$): δ 0.00 (*s*), 0.05 (*br*), 0.57 (*m*), 1.52 (*m*), 1.67 (*m*), 2.18 (*t*, *J*=7.5 Hz), 2.33 (*t*, *J*=7.5 Hz), 3.22 (*m*), 3.67 (*s*) ; ^{13}C NMR (75 MHz, $CDCl_3$): δ -0.2, -0.14, 0.09, 0.8, 1.0, 15.3, 18.0, 19.9, 23.4, 40.2, 42.2, 76.4, 172.8; ^{29}Si NMR (59.6 MHz, $CDCl_3$): δ 7.5, 7.3, -21.2, -21.9; FTIR (KBr, cm^{-1}): 796, 836, 1047, 1060, 1256, 1411, 1435, 1532, 1538, 1548, 1557, 1563, 1567, 1574, 1635, 1644, 1651, 1567, 2876, 2898, 2926, 2955, 3082, 3090, 3283.

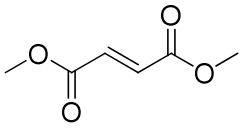

220

2-Butenedioic acid (2*E*)-1,4-dimethyl ester (220)[223]

A round bottomed flask was charged with 10.02 g (86.3 mmol) of fumaric acid, 0.97 g (5.1 mmol, 3 mol%) of pTsOH, an inert boiling chip, and dissolved into 50.0 mL of anhydrous methanol. The reaction mixture was refluxed for 3 hours after which time the solvent was removed *in vacuo*. The remaining crude residue was extracted into 80 mL of $CHCl_3$ and washed with two 10.0 mL portions of 1M $NaHCO_3$. The organic fraction was dried over $MgSO_4$ and the solvent was removed *in vacuo* to yield 10.19 g (70.7 mmol, 82%) of a white solid (m.p. 102-105°C): ^{1}H NMR (300 MHz, $CDCl_3$): δ 3.81 (*s*, 6H), 6.86 (*s*, 2 H); ^{13}CNMR (76 MHz, $CDCl_3$): δ 52.3, 133.4, 165.4; EI-MS: M^+ = 144 m/z; FTIR (KBr, cm^{-1}): 1215, 1439, 1644, 1723, 3019.

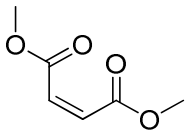

221

2-Butenedioic acid (2*Z*)-1,4-dimethyl ester (221)[223]

Maleic anhydride (15.77 g, 160.9 mmol) and p-toluene sulfonic acid (0.47 g, 2.47 mmol) were combined in a 100 mL round bottomed flask and dissolved into 50.0 mL of methanol. The reaction mixture was refluxed for 21 hours after which time the remaining methanol was removed *in vacuo*. The remaining crude residue was extracted into 2 x 30

mL of diethyl ether and washed with 10 mL of water, 3 x 10.0 mL of 1 M $KHCO_3$, and 3 x 10.0 mL of brine. The combined aqueous fractions were extracted with 10.0 mL of diethyl ether. The combined ethereal fractions were dried over Na_2SO_4, and the solvents were removed in vacuo to give a clear and colourless liquid in 94% yield (19.11 g, 132.71 mmol): ^{1}H NMR (300 MHz, $CDCl_3$): δ 3.79 (*s*, 6H), 6.26 (*s*, 2H); ^{13}CNMR(76 MHz, $CDCl_3$): δ 52.2, 129.7, 165.6; EI-MS: M^+ = 144 m/z; FTIR (KBr, cm^{-1}): 3057, 1727, 1648.

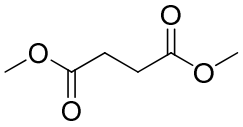

222

Dimethyl succinate (222)[224]

Succinic anhydride (5.00 g, 49.97 mmol) and p-toluene sulfonic acid (0.43 g, 2.26 mmol) were combined in a 100 mL round bottomed flask and dissolved into 45.0 mL of methanol. The reaction mixture was refluxed for 4.5 hours after which time the remaining methanol was removed *in vacuo*. The remaining crude residue was extracted into 40.0 mL of diethyl ether and washed with 10.0 mL of water, 3 x 10.0 mL of 1 M $KHCO_3$, and 3 x 10.0 mL of brine. The combined aqueous fractions were extracted with 20.0 mL of diethyl ether. The combined ethereal fractions were dried over Na_2SO_4, and the solvents were removed *in vacuo* to give a clear and colourless liquid 84% yield (6.14 g, 42.1 mmol): ^{1}H NMR (300 MHz, $CDCl_3$): δ 2.63 (*s*, 2H), 3.69 (*s*, 3H); ^{13}CNMR (75 MHz, $CDCl_3$): δ 28.9, 51.8, 172.8; FTIR (KBr, cm^{-1}): 1735, 1741, 2874, 2954, 2995.

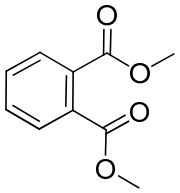

223

Dimethyl phthalate (223)[225]

Phthalic acid (4.00 g, 24.08 mmol) and p-toluene sulfonic acid (0.48 g, 2.53 mmol) were combined in a 100 mL round bottomed flask and dissolved into 40 mL of methanol. The reaction mixture was refluxed for 3.5 hours after which time the remaining methanol was removed *in vacuo*. The remaining crude residue was extracted into 20.0 mL of diethyl ether and washed with 10.0 mL of water, 3 x 10.0 mL of 1 M $KHCO_3$, and 3 x 10.0 mL of brine. The combined aqueous fractions were extracted with 20.0 mL of diethyl ether. The combined ethereal fractions were washed with 2 x 10.0 mL of brine and dried over Na_2SO_4, and the solvents were removed *in vacuo* to give a clear and colourless liquid 15% yield (0.7 g, 3.6 mmol): ^{1}H NMR (300 MHz, $CDCl_3$): δ 3.91 (*s*, 6H), 7.64 (*m*, 4H); ^{13}C NMR (75 MHz, $CDCl_3$): δ 52.6, 128.9, 131.1. 131.9, 168.0; EI MS: M^+ = 194 m/z; FTIR (KBr, cm^{-1}): 1434, 1579, 1599, 1727, 2843, 2953, 3003, 3026, 3072.

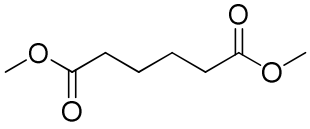

224

Hexanedioic acid-1,6-dimethyl ester (224)[226]

Adipic acid (8.09g, 55.32 mmol) and p-toluene sulfonic acid (0.1934 g, 1.01 mmol) were combined in a 100 mL round bottomed flask and dissolved into 20.0 mL of methanol. The reaction mixture was refluxed for 19 hours after which time the remaining methanol

was removed *in vacuo*. The remaining crude residue was extracted into 3 x 20.0 mL of chloroform and washed with 10.0 mL of water, 10.0 mL of saturated $NaHCO_3$, and 10.0 mL of brine. The combined ethereal fractions were dried over $MgSO_4$, and the solvents were removed *in vacuo* to give a clear and colourless liquid 97% yield (9.4 g, 54.0 mmol): ^{1}H NMR (300 MHz, $CDCl_3$): δ 1.66 (*m*, 2H), 2.33 (*m*, 2H), 3.66 (*s*, 3H); ^{13}C NMR (75 MHz, $CDCl_3$): δ 24.4, 33.7, 51.6, 173.8; FTIR (KBr, cm^{-1}): 1735, 1741, 2874, 2954, 2995.

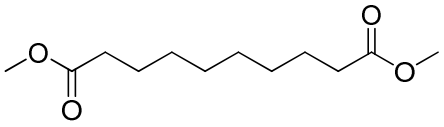

225

Decanedioic acid-1,10-dimethyl ester (225)[227]

Sebacic acid (11.49 g, 56.9 mmol) and p-toluene sulfonic acid (0.53 g, 2.8 mmol) were combined in a 250 mL round bottomed flask and dissolved into 75.0 mL of methanol. The reaction mixture was refluxed for 24 hours after which time the remaining methanol was removed *in vacuo*. The remaining crude residue was extracted into 50 mL of diethyl ether and washed with 20.0 mL of water, 10.0 mL of saturated $KHCO_3$, and 3 x 5.0 mL of brine. The combined aqueous fraction was extracted with 20.0 mL of diethyl ether. The combined ethereal fractions were washed with 10.0 mL of brine and subsequently dried over $MgSO_4$, and the solvents were removed *in vacuo* to give a clear and colourless liquid 92% yield (2.24 g, 9.74 mmol): ^{1}HNMR (300 MHz, $CDCl_3$): δ 1.28 (*s,* 8H), 1.60 (*m,* 4H), 2.29 (*t,* 4H), 3.65 (*s,* 6H); ^{13}C NMR (75 MHz, $CDCl_3$): δ 24.9, 29.0, 34.1, 51.4, 174.3; FTIR (KBr, cm^{-1}): 2931, 2856, 1741; EI-MS: (M^+-OCH_3) = 199 m/z. Analytical Calculated for $C_{12}H_{22}O_4$: C, 62.58%; H, 9.63%. Found C, 62.88%; H, 9.72%.

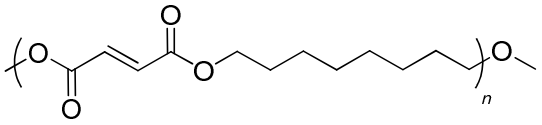

226

Poly(octylene fumarate) (226)

Polyoctylene fumarate was prepared under solvent-free conditions using 5 wt% N435 compared to the mass of the total monomers. Dimethyl fumarate (0.319g, 2.22 mmol) and 0.324g (2.22 mmol) 1,8-octanediol were combined in a 5 mL round bottomed flask with a magnetic stirring bar under an air atmosphere. The reaction flask was incubated at 110C to melt the the monomers into a single liquid phase. After transferring the reaction mizxture to an oil bath at 100C, 31.8 mg of N435 (corresponding to 3.18 mg ($9.5x10^{-7}$ mol) of CalB) was added. Aliquots (10 μL) were removed at fixed time points. The re-actions were terminated after 24 hours by the addition of 5.0 mL of diethyl ether and cooling to room temperature. The enzyme beads were removed by filtration through a glass fritted Buchner filter of medium porosity and washed with two 10.0 mL volumes of diethyl ether. Solvents were removed *in vacuo* to yield polyoctylene succinate as a white solid. ^{1}H NMR (300 MHz, $CDCl_3$): δ 1.36 (*br*); 1.56 (*m*), 1.67 (*m*), 3.63 (*t*, *J*= 7.5Hz), 3.803 (*s*), 4.18 (*t*, *J*= Hz), 6.84 (*s*); ^{13}C NMR (75 MHz, CDCl3): δ 25.6, 25.7, 28.5, 29.1, 29.1, 29.2, 32.7, 62.9, 65.4, 133.6, 165.0; FTIR (KBr, cm^{-1}): 669, 757, 1161, 1215, 1261, 1301, 1723, 2933, 3019, 3425.

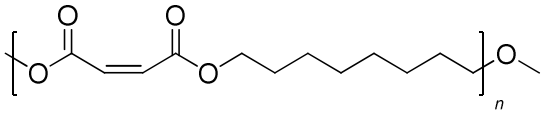

227

Poly(octylene maleate) (227)

A round bottomed flask was charged with a 1:1 mixture of 1,8-octanediol (0.304 g, 2.08 mmol) and 0.261 mL (2.08 mmol) dimethyl maleate. The monomers were melted together at 110°C to form a homogenous solution. The mixture was transferred to an oil bath at 100°C. N435 (5 wt %, 29.9 mg) was added and 10.0 μL aliquots were removed at predetermined time intervals and analyzed by ^{1}H NMR spectroscopy. The reaction was stopped by the addition of 5.0 mL of $CHCl_3$ at room temperature. The enzyme beads were removed by filtration through a glass fritted Buchner filter of medium porosity and washed with two 10.0 mL volumes of $CHCl_3$. Solvents were removed *in vacuo* to yield a clear, colourless liquid. This material was not characterized spectroscopically as less than 5% esterification could be detected by ^{1}H NMR.

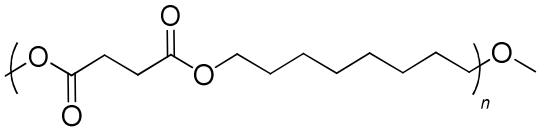

228

Poly(octylene succinate) (228)

For a typical reaction, dimethyl succinate (0.29 mL, 2.2 mmol) and 0.325 mL (2.2 mmol) of 1,8-octanediol were combined in a round bottomed flask, containing a magnetic stirring bar, under an air atmosphere. N435 beads (31.3 mg) were added to the reaction mixture and incubated at 100°C with stirring for 24 hours. For a complete listing of reagents and temperatures see **Appendix 1 Table 10**. The reaction was terminated by the addition

of 5.0 mL of diethyl ether after cooling to room temperature. The enzyme beads were removed by filtration through a glass fritted Buchner filter of medium porosity and washed with two 10.0 mL volumes of diethyl ether. Solvents were removed *in vacuo* to yield polyoctylene succinate as a white solid. ^{1}H NMR (300 MHz, $CDCl_3$): δ 1.31 (*m*), 1.31 (*m*), 1.62 (*t*), 2.61 (*s*), 3.64 (*t*), 3.63 (*s*), 4.07 (*t*); ^{13}C NMR (75 MHz, $CDCl_3$): δ 25.8, 28.5, 29.1, 29.1, 64.7, 172.4; FTIR (KBr, cm^{-1}): 757, 1164,1215, 1261, 1271, 1728, 2858, 2934, 3021, 3440, 3445.

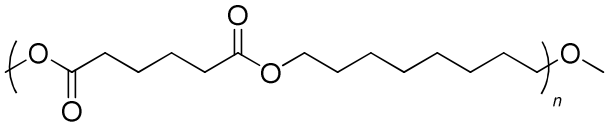

229

Poly(octylene adipate) (229)

For a typical reaction, dimethyl adipate (0.27 mL, 1.6 mmol) was combined with 234.6 mg (1.6 mmol) of 1,8-octanediol in a round bottomed flask, containing a magnetic stirring bar, under an air atmosphere. The reaction flask was incubated at 100°C and 26.2 mg of N435 was added and the reaction was stirred for 24 hours. For a complete listing of reagents and temperatures see **Appendix 1 Table 11**. The reactions were terminated with the addition of 5.0 mL of $CHCl_3$ after cooling to room temperature. The enzyme beads were removed by filtration through a glass fritted Buchner filter of medium porosity and washed with two 10 mL volumes of $CHCl_3$. Solvents were removed *in vacuo* to yield polyoctylene succinate as a white solid. ^{1}H NMR (300 MHz, $CDCl_3$): δ 1.30, 1.63 (*m*), 2.31 (*t, J*= 6.9 Hz), 3.63 (*t, J*= 6.6 Hz), 4.05 (*t*, *J*= 6.6 Hz); ^{13}C NMR (75 MHz,

$CDCl_3$): δ 24.4, 25.8, 28.5, 29.1, 33.9, 64.7, 173.4; FTIR (KBr, cm^{-1}): 1183,1265, 1375, 1400, 1416, 1466, 1724, 2854, 2918, 2937, 3446 .

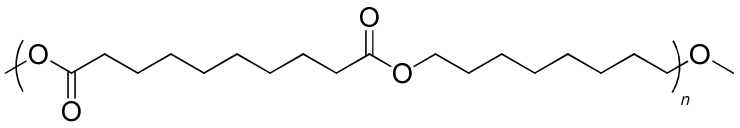

230

Synthesis of polyoctylene sebacate (230)

Dimethyl sebacate (374 μL, 1.56 mmol) was with 228.9 mg (1.56 mmol) of 1,8-octanediol in a round bottomed flask, containing a magnetic stirring bar, under an air atmosphere. The reaction mixture was incubated at 100°C and N435 (29.1 mg) was added. A complete list of reagent amounts and temperatures can be found in **Appendix 1 Table 12**. The reaction was terminated with the addition of 5.0 mL of $CHCl_3$ after cooling to room temperature. The enzyme beads were removed by filtration through a glass fritted Buchner filter of medium porosity and washed with two 10.0 mL volumes of $CHCl_3$. Solvents were removed *in vacuo* to yield unfractionated polyoctylene succinate as a white solid. ^{1}H NMR (300 MHz, $CDCl_3$): δ 1.31 (*br*), 1.59 (*m*), 2.26 (*t*, *J*=6.6 Hz), 3.65 (*s*), 4.03 (*t*, *J*=6.6 Hz); ^{13}C NMR (75 MHz, $CDCl_3$): δ 24.9, 25.8, 28.6, 29.1, 29.1, 35.3, 64.3, 173.9; FTIR (KBr, cm^{-1}): 757, 1215, 1725, 2858, 2933, 3021, 3417, 3427, 3434, 3440, 3445.

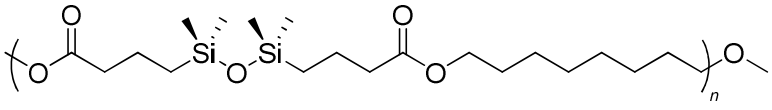

231

Synthesis of poly(octylene-*co*-(1,1,3,3-tetramethyldisiloxy-1,3-bis(*n*-butanoate)) (231)

Diester **212** (530 μL, 1.5 mmol) was combined with 221.2 mg (1.5 mmol) of 1,8-octanediol in a round bottomed flask, containing a magnetic stirring bar, under and air atmosphere. The monomers were melted together at 100°C and then N435 (36.0 mg) was added to the reaction mixture. After 24 hours the reaction was cooled to room temperature and terminated by the addition of 5.0 mL of diethyl ether. The enzyme beads were removed by filtration through a glass fritted Buchner filter of medium porosity and washed with two 10.0 mL volumes of diethyl ether. Solvents were removed *in vacuo* to yield poly(octylene-*co*-(1,1,3,3-tetramethyldisiloxy-1,3-bis(*n*-butanoate)) as a clear, colourless liquid. ^{1}H NMR (300 MHz, $CDCl_3$): δ 0.05 (*s*), 0.53 (*m*), 1.32 (*br*), 1.63 (*m*), 2.31 (*t*), 3.56 (*t*, *J*=7.5 Hz), 3.67 (*s*), 4.05 (*t*, *J*=7.5 Hz); ^{13}C NMR (75 MHz, $CDCl_3$): δ 0.13, 17.8, 19.0, 25.7, 28.4, 29.0, 37.5, 64.1, 173.5; ^{29}Si NMR (59.6 MHz, $CDCl_3$): δ 7.3; FTIR (KBr, cm^{-1}): 758, 795, 839, 1059, 1121, 1164, 1196,1253, 1288, 1736, 2859, 2932, 2952, 3446; MALDI-ToF MS: M^{+}=7666 m/z.

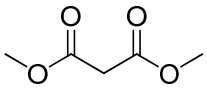

239

Dimethyl malonate (239)[228]

Malonic acid (3.09 g, 29.7 mmol) and p-toluene sulfonic acid (0.90 g, 0.47 mmol) were combined in a 100 mL round bottomed flask and dissolved into 30.0 mL of methanol. The reaction mixture was refluxed for 4 hours after which time the remaining methanol was removed *in vacuo*. The remaining crude residue was extracted into 10.0 mL of chloroform and washed with 10.0 mL of water, 5.0 mL of saturated $NaHCO_3$. The combined organic fractions were dried over $MgSO_4$, and the solvent was removed *in vacuo* to give a

clear and colourless liquid 72% yield (2.84 g, 21.5 mmol): ^{1}H NMR (300 MHz, $CDCl_3$): δ 3.40 (*s*), 3.75 (*s*); ^{13}C NMR (75 MHz, $CDCl_3$): δ 41.1, 52.6, 166.9; FTIR (KBr, cm^{-1}): 1742, 1754; EI MS: M^+ = 132 m/z.

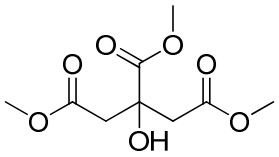

242

Trimethyl citrate (242)[229]

Citric acid (3.0851 g, 16.057 mmol) was dissolved into 100.0 mL methanol and refluxed overnight. Excess methanol was removed *in vacuo*. The crude residue was extracted into 20.0 mL of chloroform and washed with 10.0 mL of distilled water and 10 mL of $KHCO_3$. The organic fraction was dried over Na_2SO_4, filtered and the solvent removed in vacuo. Trimethylcitrate was obtained as a white solid in 81% yield (3.08 g, 13.0 mmol, m.p. 76-79°C). ^{1}H NMR (300 MHz, $CDCl_3$): δ 2.86 (*dd*, 4H), 3.69 (*s,*6H), 3.84 (*s*, 3H); ^{13}C NMR (75 MHz, $CDCl_3$): δ 43.1, 52.0, 53.2, 73.3, 170.2, 173.8; FTIR (KBr, cm^{-1}): 699, 758, 1215, 1439, 1741, 2955, 3020, 3464.

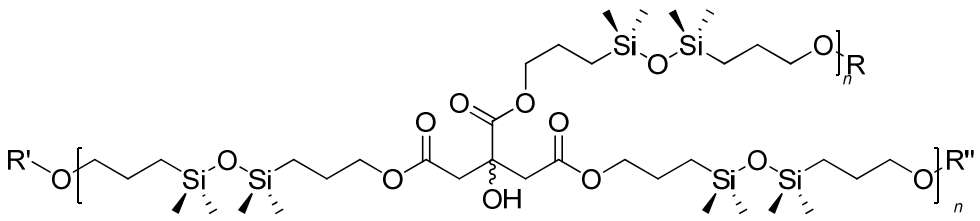

245

Branched siloxane polyesters based on citric acid (245)

A 10.0 mL round bottomed flask was charged with 190.6 mg (8.145×10^{-4} mol) of **242** and 0.42 mL (1.22×10^{-3} mol) of 1,3-bis(3-hydroxypropyl)-1,1,3,3-tetramethyldisiloxane and placed in an oil bath at 100°C intil a homogeneous solution formed. N435 (23.9 mg, 5 wt%) was added and the reaction mixture was allowed to stir for 48 hours. The reaction mixture was diluted with 2.0 mL of $CHCl_3$ and filtered through a medium porosity glass filter to remove the N435. The solvent was removed *in vacuo* to give a clear, colourless, viscous liquid. ^{1}H NMR (300 MHz, $CDCl_3$): δ 0.07 (*s*), 0.51 (*m*), 1.32 (*m*), 1.60 (*m*), 2.85 (*dd*), 3.59 (*t*, *J*=7.5 Hz), 3.67 (*s*), 3.68 (*s*), 3.81 (*s*), 3.82 (*s*), 4.05 (*t*, *J*=7.5 Hz), 4.17 (*m*); ^{13}C NMR (75 MHz, $CDCl_3$): δ 0.3, 1.1, 1.2, 1.2, 13.96. 14.03, 22.5, 26.5, 43.2, 43.2, 52.0, 53.2, 65.5, 67.5, 73.3, 169.9, 170.2, 173.9; ^{29}Si NMR (59.6 MHz, $CDCl_3$): δ 7.3; FTIR (KBr, cm^{-1}): 798, 840, 1053, 1180, 1204, 1257, 1742, 2899, 2956, 3446.

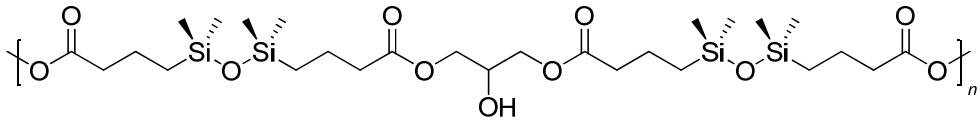

247

Branched siloxane polyesters based on glycerol (247)

A 10 mL round bottomed flask was charged with 121.8 mg (1.32×10^{-3} mol) of glycerol and 694 μL (1.98×10^{-3} mol) of 1,3-bis(3-carboxypropyl)-1,1,3,3-tetramethyldisiloxane

dimethyl ester and stirred at room temperature for 2 minutes. To this was added 41.5 mg (5.3 wt%) of N435. The reaction mixture was stirred at 100°C for 24 hours. The reaction mixture was diluted with 2.0 mL of $CHCl_3$ and filtered through a medium porosity glass filter to remove the N435. The solvent was removed *in vacuo* to give a clear, colourless, viscous liquid. An enzyme-free control reaction was prepared from 111.4 mg ($1.21x10^{-3}$ mol) of glycerol and 673 μL ($1.92x10^{-3}$ mol) of 1,3-bis(3-carboxypropyl)-1,1,3,3-tetramethyldisiloxane dimethyl ester and stirred at room temperature for 2 minutes. This reaction mixture remained biphasic for the duration of the attempted polymerization cycle. ^{1}H NMR(300 MHz, $CDCl_3$): δ 0.05 (*s*), 0.52 (*m*), 1.64 (*m*), 2.34 (*m*), 3.66 (*s*), 4.07-4.32 (*br*), 5.06 (*m*), 5.25 (*m*) ; ^{13}C NMR (75 MHz, $CDCl_3$): δ 0.3, 14.95, 19.98, 19.03, 19.08, 37.3, 37.4, 37.4, 51.35, 51.39, 62.03, 64.99, 68.1, 77.3, 173.0, 173.6, 174.1, 174.2; FTIR (KBr, cm^{-1}): 796, 839, 1057, 1121, 1164, 1200, 1254, 1287, 1741, 2880, 2898, 2954, 3446, 3450 cm^{-1}.

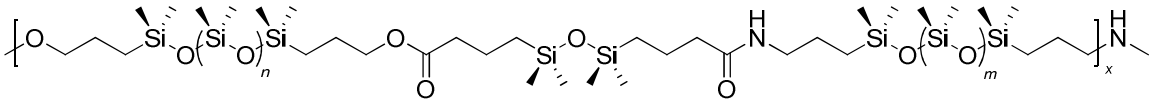

248

Siloxane polyester amides (248)

Siloxane-containing polyester amides were synthesized from a 2:1:1 mixture of **212**:**162**:**217** under solvent free conditions at 100°C. A round bottomed flask was charged with 206 μL of **179**, 693 μL of **165**, and 510 μL of **212**. The contents of the flask were placed in an oil bath at 100°C and stirred for one minute to ensure the homogeneity of the solution. N435 (25.2 mg) was added to start the polymerization. Aliquots of 15 μL were removed at predetermined time points and analyzed by ^{1}H NMR spectroscopy. The re-

actions were stopped by the addition of 5.0 mL of $CHCl_3$ at room temperature. The enzyme beads were removed by filtration through a glass fritted Buchner filter of medium porosity and washed with two 10.0 mL volumes of $CHCl_3$. Solvents were removed *in vacuo* to yield polysiloxane-polyester amides as viscous liquids. Control reactions were conducted in the same manner without the addition of an enzyme catalyst. ^{1}H NMR (300 MHz, $CDCl_3$): δ 0.035-0.063 (*s*), 0.525 (*m*), 1.36 (*s*), 1.44-1.70 (*br*), 2.18 (*t*, *J*=7.2 Hz), 2.32 (*t*, *J*=7.2 Hz), 3.21 (*br*), 3.63 (*m*), 4.04 (*t*, *J*=6.6 Hz); ^{13}C NMR (75 MHz, $CDCl_3$):δ ; ^{29}Si NMR (59.6 MHz, $CDCl_3$): δ -22.2, -22.0, 7.2, 7.4; FTIR (KBr, cm^{-1}): 760, 802, 862, 1033, 1059, 1087, 1260, 1412, 1647, 1736, 2879, 2904, 2932, 2962, 3290.

7 Appendices

Appendix 1 -Tables of reagent amounts and temperatures for polymerization reactions.

Table 6 Experimental amounts for the polymerization of disiloxane polyester.

Experiment	**Diester 212** (μL)	**Diol 213** (μL)	**N435** (mg)	**Temp.** (°C)
MF7-041	200	196	15.7	35
MF7-059	240	245	19.6	35
MF6-114-2	279	227	37.5	35
MF7-039	200	196	15.7	50
MF7-050	245	240	18.8	50
MF7-115	195	146	22.9	50
MF10-113-1	260	357	31.0	60
MF10-113-2	264	363	31.5	60
MF10-113-3	216	297	25.8	60
MF7-088	245	250	20.0	70
MF6-112	300	244	39.5	70
MF7-012	200	196	16.3	70
MF8-085	400	443	31.4	80
MF8-094	457	505	35.9	80
MF8-096	452	500	35.8	80
MF8-060	313	347	24.6	90
MF8-069	328	364	25.8	90
MF8-075	400	443	31.4	90
MF8-140-1	200	332	27.6	100
MF8-140-2	234	323	28.1	100
MF8-140-3	218	300	28.0	100
MF9-101-4	125	171	14.9	110
MF9-101-11	155	213	18.5	110
MF9-101-1	115	158	13.7	120
MF9-101-5	129	177	15.4	120
MF9-101-8	131	179	15.6	120
MF9-101-2	95	130	11.3	130
MF9-101-6	173	236	20.6	130
MF9-101-9	157	215	18.7	130
MF9-101-3	98	133	11.6	140
MF9-101-7	175	240	20.9	140
MF9-101-10	146	200	17.4	140
MF10-113-4	257	354	30.7	150
MF10-113-5	212	292	25.3	150
MF10-113-6	213	293	25.4	150

Table 7 Experimental amounts for the polymerization of polysiloxane polyester.

Experiment	**Diester 212** (μL)	**Diol 162** (mL)	**N435** (mg)	**Temp.** (°C)
MF10-026-1	200	1.348	24.5	35
MF10-026-2	198	1.337	24.3	35
MF10-026-3	188	1.265	23.0	35
MF10-026-4	172	1.161	21.1	50
MF10-026-5	182	1.227	22.3	50
MF10-026-6	200	1.348	24.5	50
MF10-026-7	184	1.243	22.6	60
MF10-026-8	195	1.315	23.9	60
MF10-026-9	186	1.254	22.8	60
MF10-026-10	212	1.431	26.0	70
MF10-026-11	193	1.298	23.6	70
MF10-026-12	172	1.161	21.1	70
MF10-026-13	179	1.205	21.9	80
MF10-026-14	182	1.227	22.3	80
MF10-026-15	189	1.271	23.1	80
MF10-026-16	178	1.199	21.8	90
MF10-026-17	180	1.210	22.0	90
MF10-026-18	200	1.348	24.5	90
MF10-026-19	219	1.475	26.8	100
MF10-026-20	190	1.282	23.3	100
MF10-026-21	176	1.188	21.6	100
MF10-026-22	170	1.144	20.8	110
MF10-026-23	206	1.387	25.2	110
MF10-026-24	161	1.084	19.7	110
MF10-026-25	147	990	18.0	120
MF10-026-26	189	1.271	23.1	120
MF10-026-27	207	1.392	25.3	120
MF10-026-28	191	1.287	23.4	130
MF10-026-29	180	1.210	22.0	130
MF10-026-30	215	1.453	26.4	130
MF10-026-31	175	1.183	21.5	140
MF10-026-32	214	1.442	26.2	140
MF10-026-33	189	1.270	23.2	140
MF10-026-34	205	1.381	25.1	150
MF10-026-35	204	1.376	25.0	150
MF10-026-36	202	1.365	24.8	150

Table 8 Experimental amounts for the polymerization of disiloxane polyamide.

Experiment	**Diester 212** (μL)	**Diamine 216** (μL)	**N435** (mg)	**Temp.** (°C)
MF10-126-1	289	228	35.4	35
MF10-126-2	304	240	37.3	35
MF10-126-3	239	189	29.3	35
MF10-126-4	251	198	30.8	50
MF10-126-5	248	196	30.4	50
MF10-126-6	238	188	29.2	50
MF10-126-7	262	207	32.1	60
MF10-126-8	279	220	34.2	60
MF10-126-9	265	209	32.5	60
MF10-126-10	347	274	42.6	70
MF10-126-11	309	242	37.6	70
MF10-126-12	275	218	32.9	70
MF10-126-13	244	193	29.9	80
MF10-126-14	273	216	33.5	80
MF10-126-15	293	232	36.0	80
MF10-126-16	329	260	40.3	90
MF10-126-17	214	169	26.3	90
MF10-126-18	232	184	28.5	90
MF10-126-19	214	169	26.3	100
MF10-126-20	234	185	28.7	100
MF10-126-21	229	181	28.1	100
MF10-126-22	224	177	27.5	110
MF10-126-23	216	171	26.5	110
MF10-126-24	271	214	33.3	110
MF10-126-25	271	214	33.3	120
MF10-126-26	260	206	31.9	120
MF10-126-27	256	202	31.4	120

Table 9 Experimental amounts for the polymerization of polysiloxane polyamide.

Experiment	**Diester 212** (μL)	**Diamine 217** (μL)	**N435** (mg)	**Temp.** (°C)
MF10-077-1	200	990	24.5	35
MF10-077-2	217	1075	26.6	35
MF10-077-3	189	937	23.2	35
MF10-077-4	212	1050	26.0	50
MF10-077-5	230	1140	28.2	50
MF10-077-6	228	1127	27.9	50
MF10-077-7	182	901	22.3	60
MF10-077-8	192	950	23.5	60
MF10-077-9	198	978	24.2	60
MF10-077-10	202	1002	24.8	70
MF10-077-11	203	1006	24.9	70
MF10-077-12	231	1144	28.3	70
MF10-077-13	211	1224	25.9	80
MF10-077-14	191	1108	23.4	80
MF10-077-15	228	1127	27.9	80
MF10-077-16	202	1002	24.8	90
MF10-077-17	200	990	24.5	90
MF10-077-18	257	1273	31.5	90
MF10-077-19	214	1059	26.2	100
MF10-077-20	221	1095	27.1	100
MF10-077-21	246	1216	30.1	100
MF10-077-22	231	1144	28.3	110
MF10-077-23	243	1204	29.8	110
MF10-077-24	210	1038	25.7	110
MF10-077-25	210	1038	25.7	120
MF10-077-26	242	1196	29.6	120
MF10-077-27	227	1123	27.8	120
MF10-077-28	192	954	23.6	130
MF10-077-29	219	1087	26.9	130
MF10-077-30	160	788	19.5	130
MF10-077-31	208	1034	25.6	140
MF10-077-32	194	962	23.8	140
MF10-077-33	220	1091	27.0	140
MF10-077-34	226	1123	27.8	150
MF10-077-35	213	1055	26.1	150
MF10-077-36	197	978	24.2	150

Table 10 Experimental amounts for the polymerization of poly(octylene succinate).

Experiment	**Dimethyl succinate** (μL)	**1,8-octanediol** (mg)	**N435** (mg)	**Temp. (°C)**
MF9-153-1	290	324.6	31.3	100
MF9-153-2	306	311.9	32.7	100
MF9-153-3	346	352.5	36.7	100
MF9-153-4	343	349.7	37.3	110
MF9-153-5	263	268.4	29.0	110
MF9-153-6	357	364.3	38.0	110
MF9-153-7	396	403.3	43.1	120
MF9-153-8	364	370.9	39.7	120
MF9-153-9	319	324.8	34.6	120
MF9-153-10	306	342.1	33.1	130
MF9-153-11	246	250.3	27.1	130
MF9-153-12	348	355.1	37.7	130
MF9-153-13	307	312.6	34.4	140
MF9-153-14	313	318.9	33.8	140
MF9-153-15	166	169.0	18.2	140

Table 11 Experimental amounts for the polymerization of poly(octylene adipate).

Experiment	**Dimethyl adipate** (μL)	**1,8-octanediol** (mg)	**N435** (mg)	**Temp. (°C)**
MF9-017	553	479.4	54.3	100
MF9-053	571	495.6	56.1	100
MF9-120-1	270	234.6	26.2	110
MF9-120-5	332	288.2	31.5	110
MF9-120-9	212	183.9	19.3	110
MF9-120-2	252	218.2	24.7	120
MF9-120-6	261	226.4	23.8	120
MF9-120-10	254	220.4	23.0	120
MF9-120-3	298	258.0	27.5	130
MF9-120-7	383	332.6	35.8	130
MF9-120-11	290	252.0	25.8	130
MF9-120-4	276	238.9	26.1	140
MF9-120-8	288	250.3	27.3	140
MF9-120-12	315	272.4	28.2	140

Table 12 Experimental amounts for the polymerization of poly(octylene sebacate).

Experiment	**Dimethyl sebacate** (μL)	**1,8-octanediol** (mg)	**N435** (mg)	**Temp.** (°C)
MF9-145-1	374	228.9	29.1	100
MF9-145-2	403	246.8	31.0	100
MF9-145-3	283	218.4	22.2	100
MF9-145-4	406	248.4	30.5	110
MF9-145-5	467	285.9	36..4	110
MF9-145-6	424	259.6	32.5	110
MF9-145-7	314	12.2	23.9	120
MF9-145-8	465	284.5	35.9	120
MF9-145-9	416	254.7	31.0	120
MF9-145-10	395	242.0	30.0	130
MF9-145-11	479	293.2	36.4	130
MF9-145-12	330	201.9	25.3	130
MF9-145-13	409	250.8	30.4	140
MF9-145-14	474	290.4	36.9	140
MF9-145-15	386	236.7	30.4	140

Appendix 2 - Selected Spectra

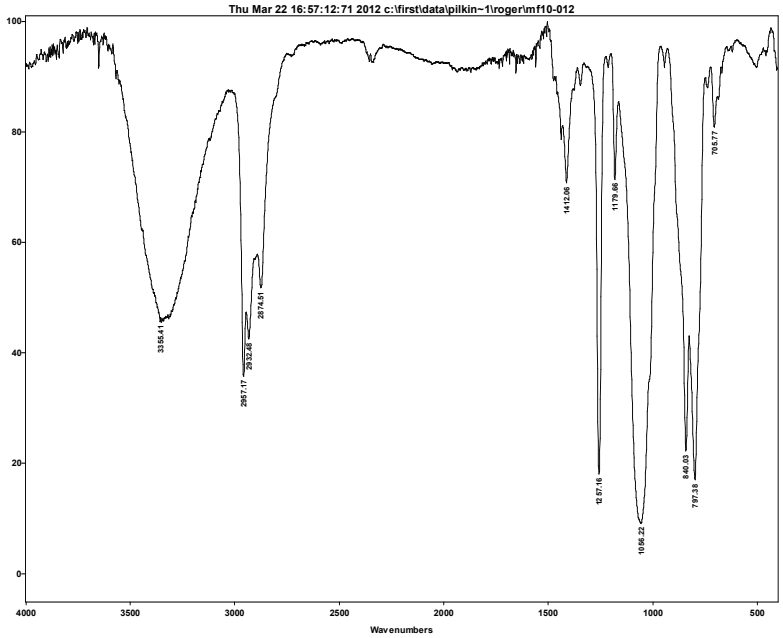

Appendix Figure 1 FTIR spectrum of 1,3-bis(3-hydroxypropyl)-1,1,3,3-tetramethyldisiloxane (**212**).

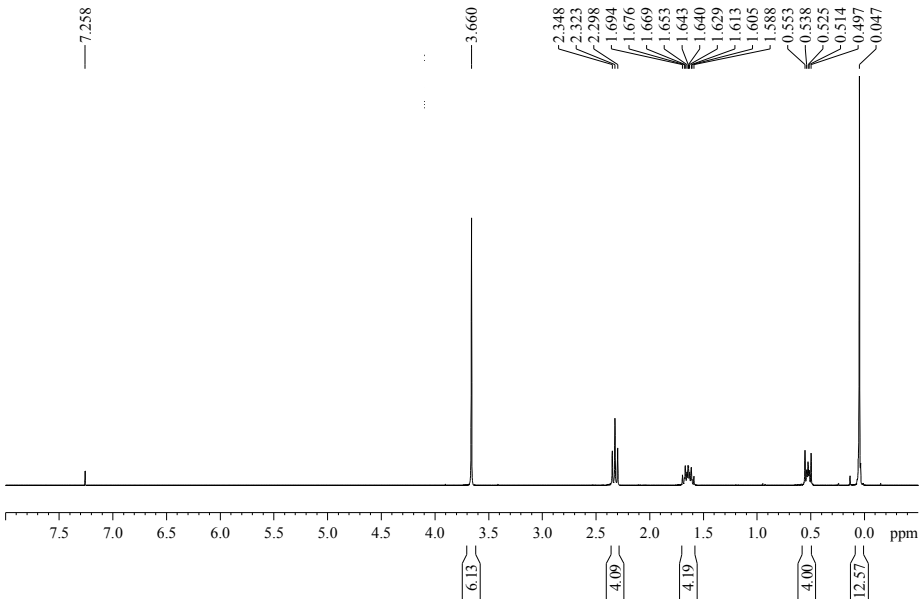

Appendix Figure 2 ^{1}H NMR spectrum of 1,3-bis(3-carboxypropyl)-1,1,3,3-tetramethyldisiloxane dimethyl ester (**212**) in $CDCl_3$.

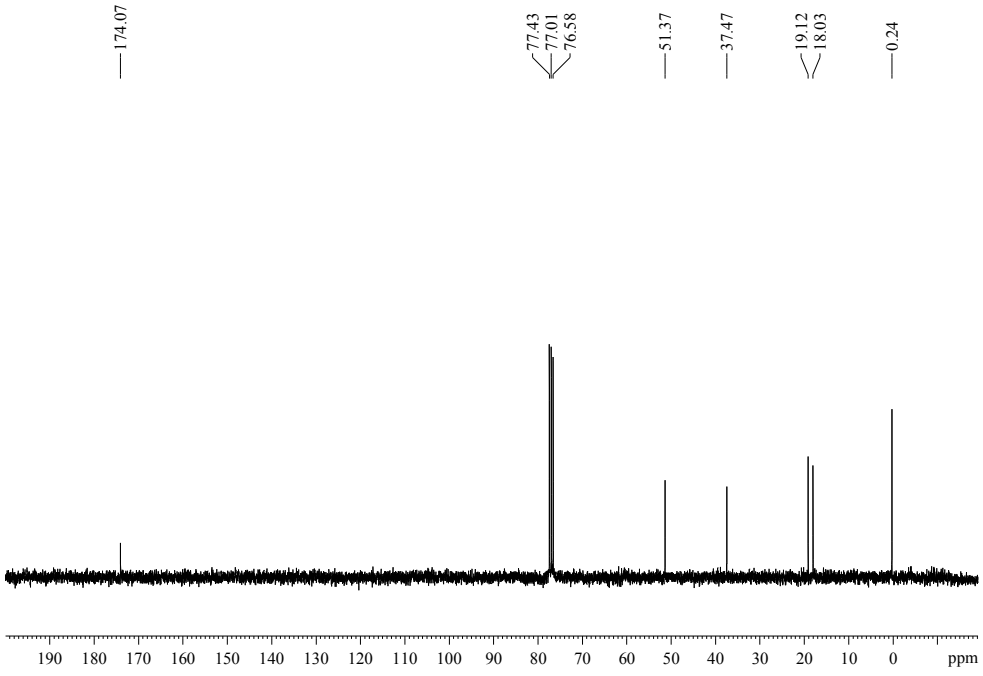

Appendix Figure 3 ^{13}C NMR spectrum of 1,3-bis(3-carboxypropyl)-1,1,3,3-tetramethyldisiloxane dimethyl ester (**212**) in $CDCl_3$.

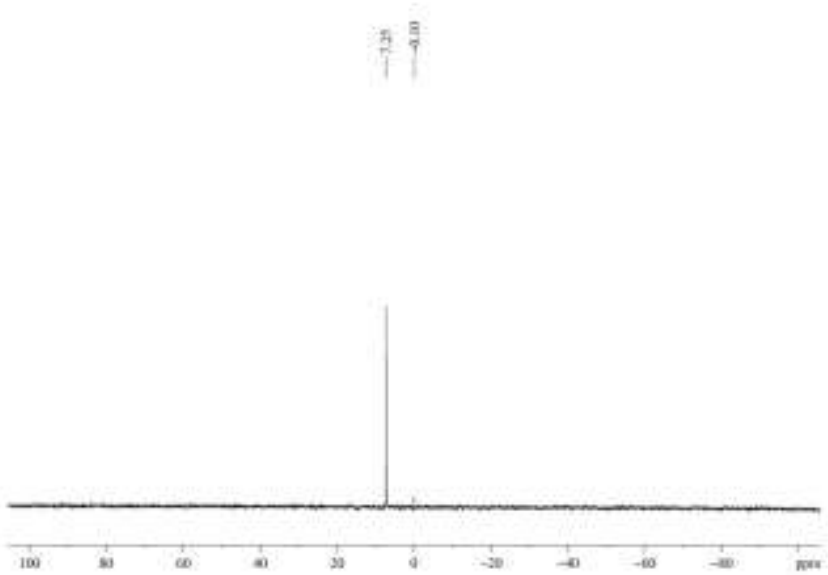

Appendix Figure 4 ^{29}Si NMR spectrum of 1,3-bis(3-carboxypropyl)-1,1,3,3-tetramethyldisiloxane dimethyl ester (**212**) in $CDCl_3$.

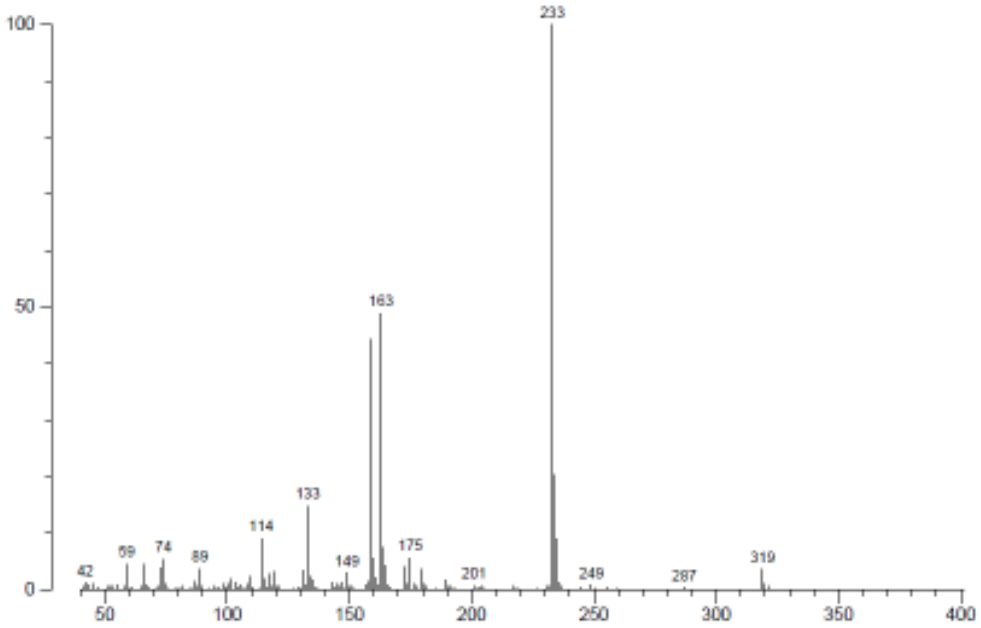

Appendix Figure 5 EI-MS spectrum of 1,3-bis(3-carboxypropyl)-1,1,3,3-tetramethyldisiloxane dimethyl ester (**212**).

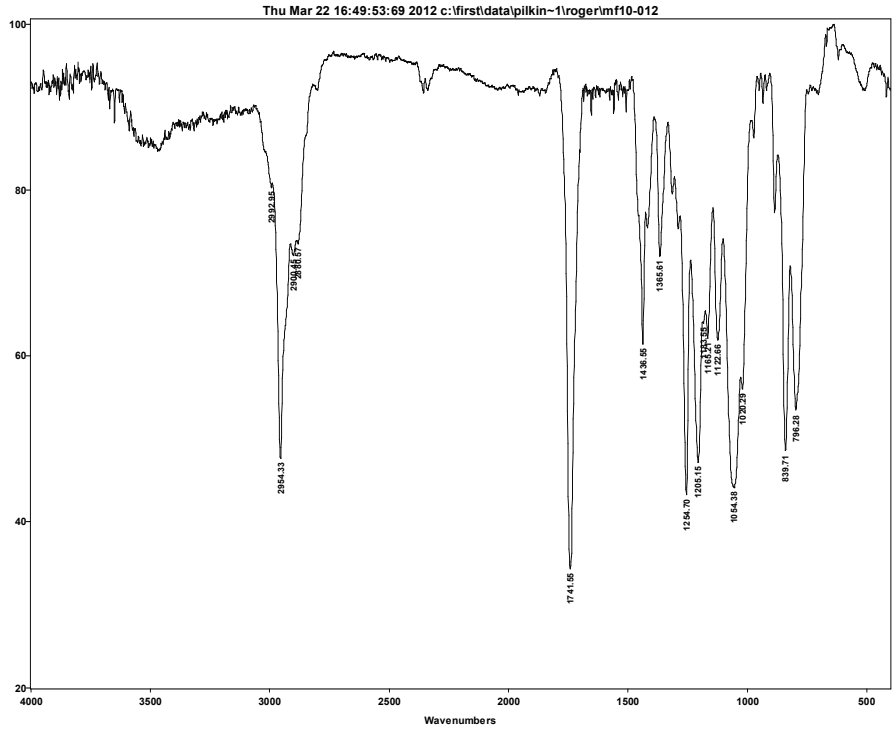

Appendix Figure 6 FTIR spectrum of 1,3-bis(3-carboxypropyl)-1,1,3,3-tetramthyldisiloxane dimethyl ester (**212**).

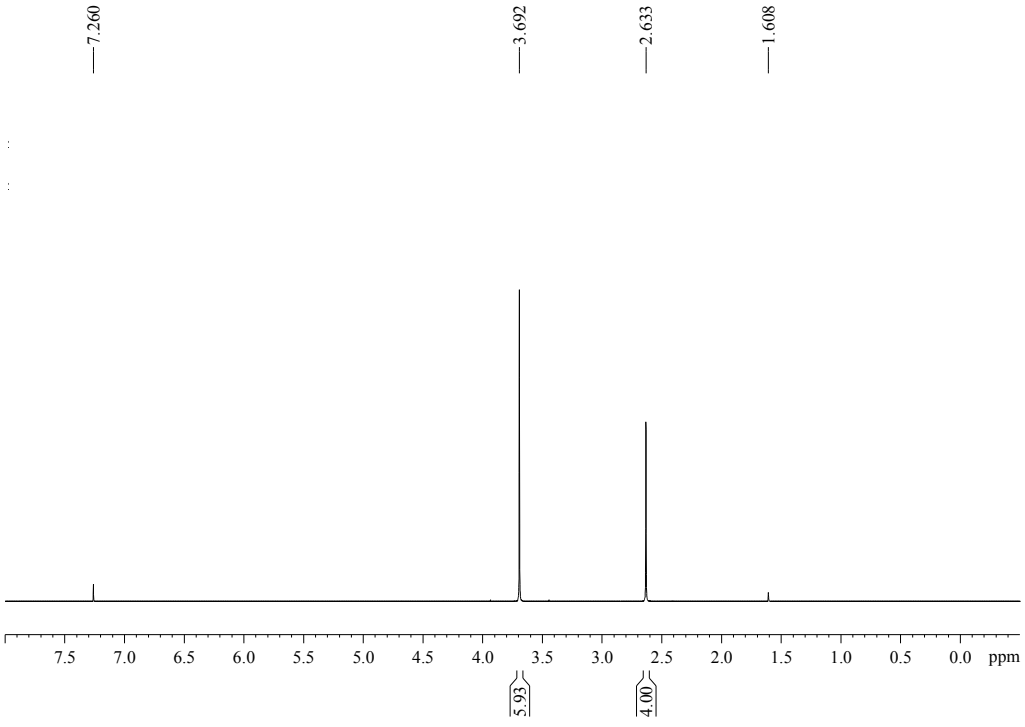

Appendix Figure 7 ^{1}H NMR spectrum of dimethyl succinate (**222**) in $CDCl_3$.

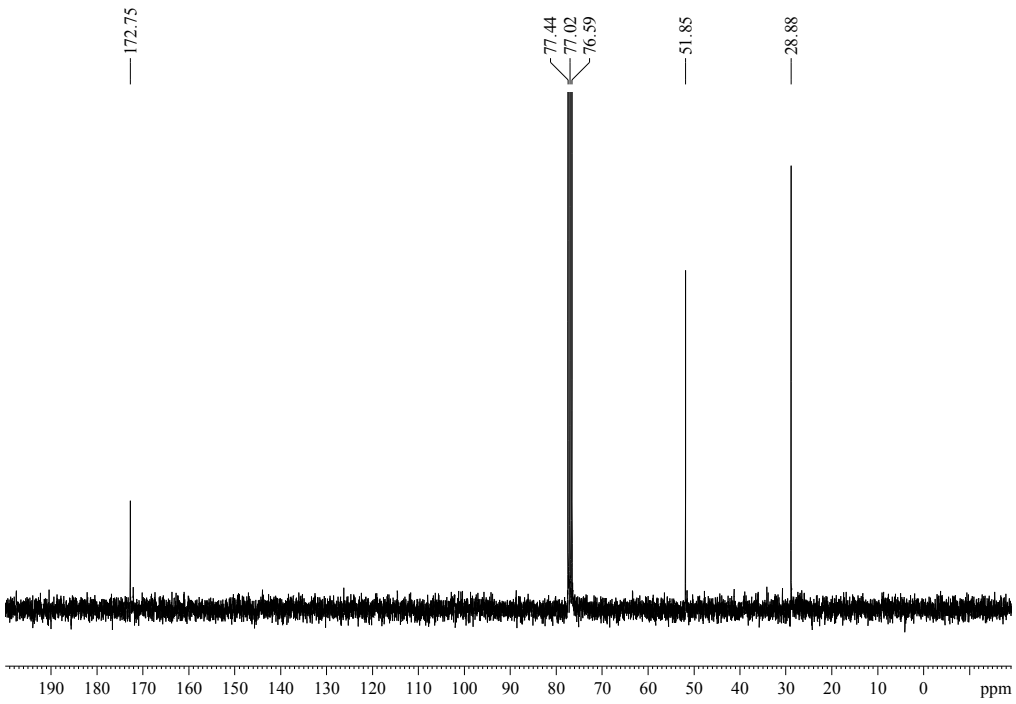

Appendix Figure 8 ^{13}C NMR spectrum of dimethyl succinate (**222**) in $CDCl_3$.

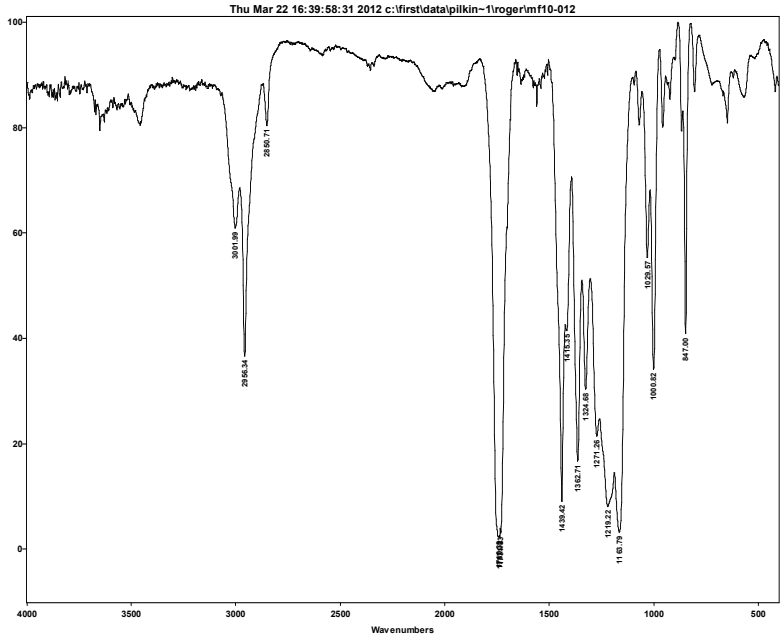

Appendix Figure 9 FTIR spectrum of dimethyl succinate (**222**).

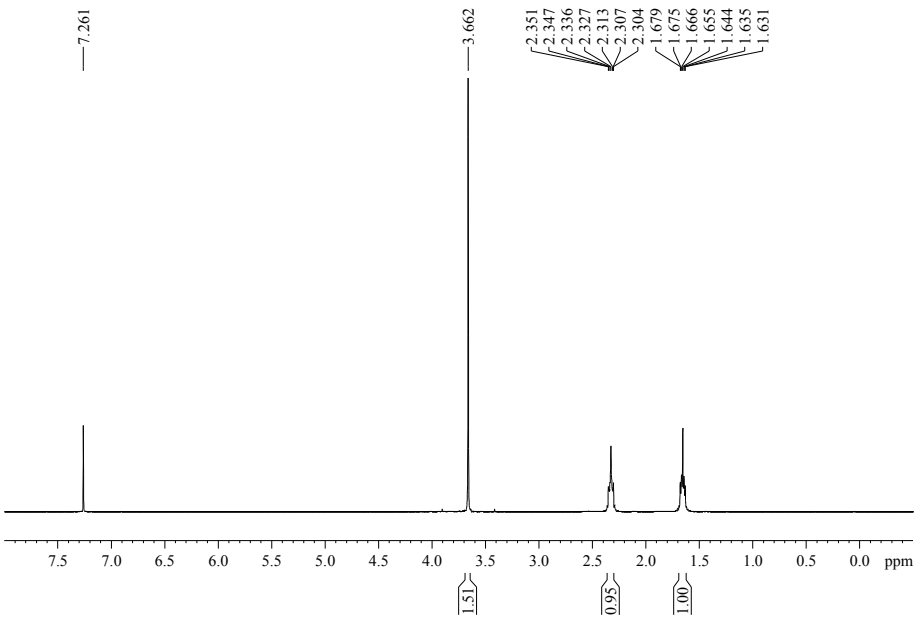

Appendix Figure 10 ^{1}H NMR spectrum of dimethyl adipate (**224**) in $CDCl_3$.

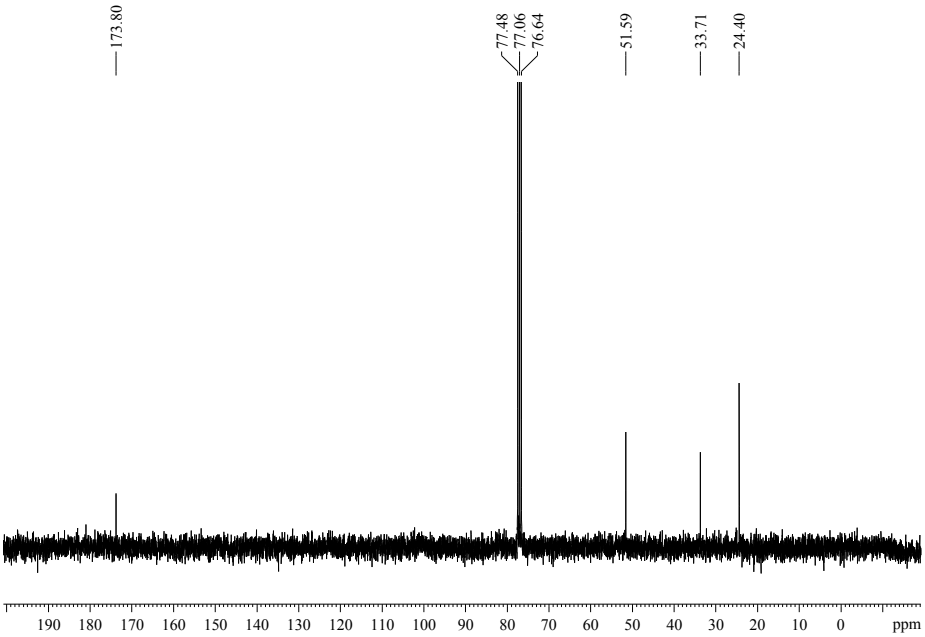

Appendix Figure 11 ^{13}C NMR spectrum of dimethyl adipate (**224**) in $CDCl_3$.

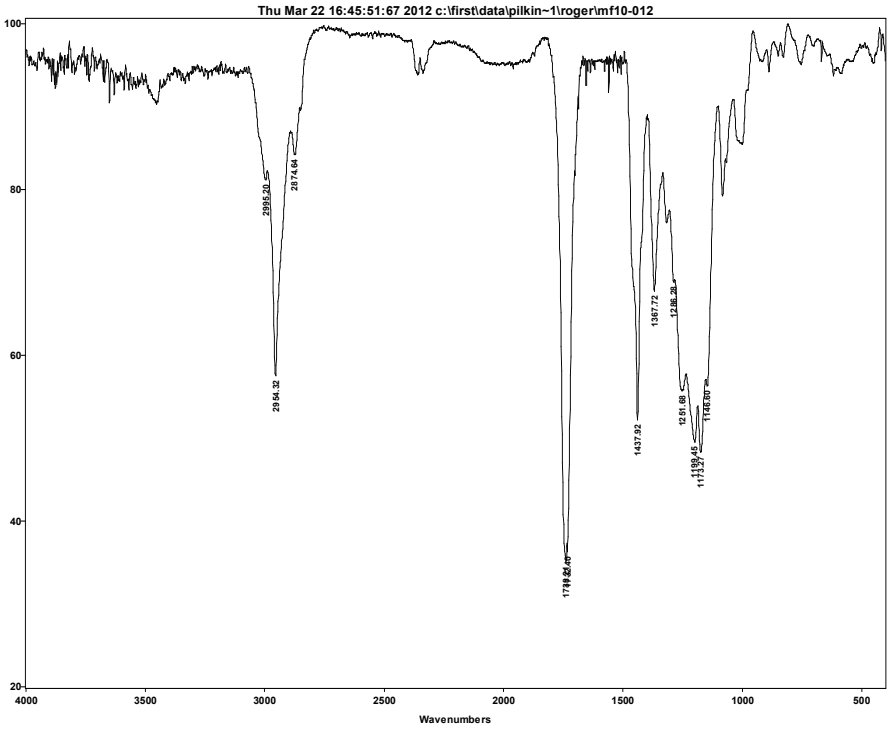

Appendix Figure 12 FTIR spectrum of dimethyl adipate (**224**).

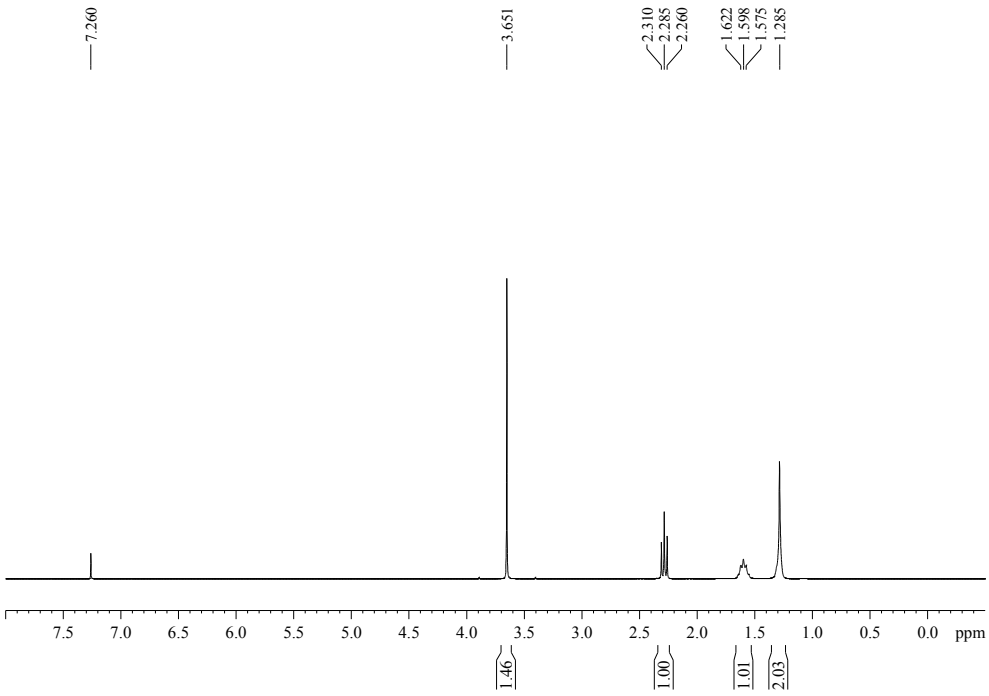

Appendix Figure 13 ^{1}H NMR spectrum of dimethyl sebacate (**225**) in $CDCl_3$.

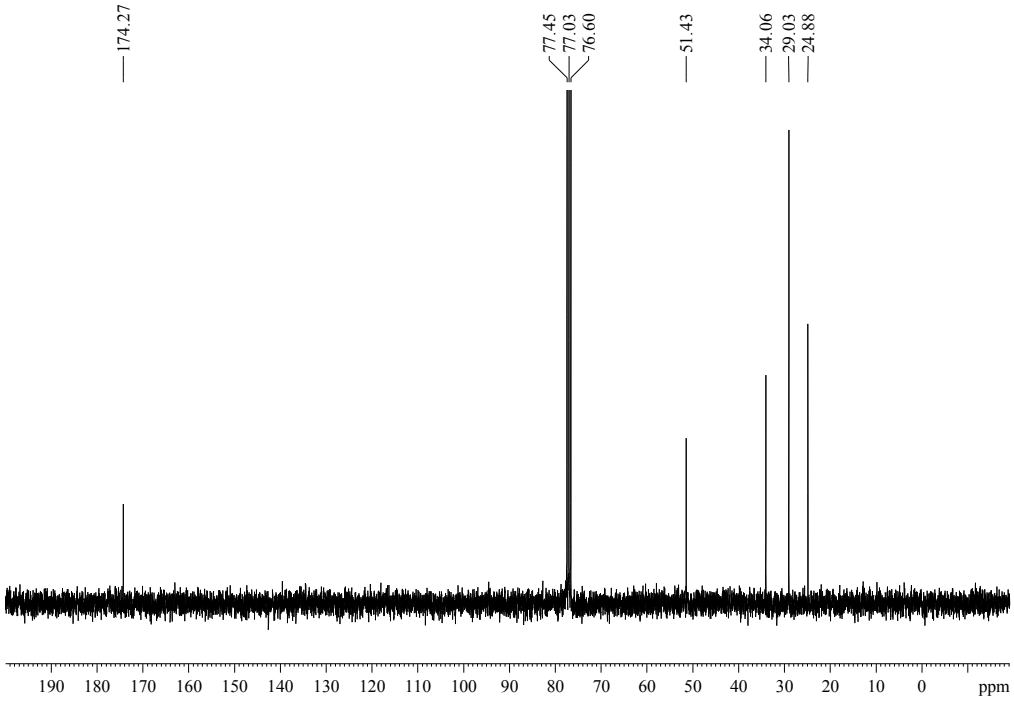

Appendix Figure 14 The ^{13}C NMR spectrum of dimethyl sebacate (**225**) in $CDCl_3$.

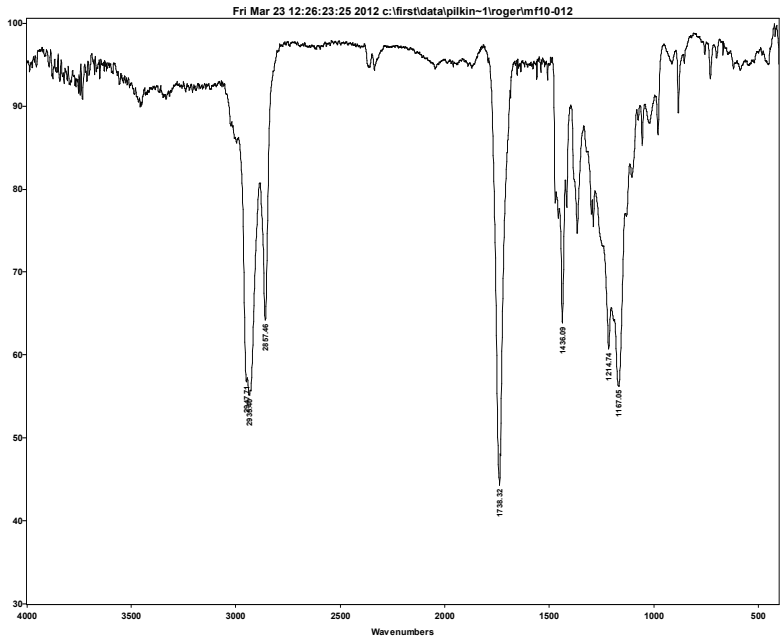

Appendix Figure 15 The FTIR spectrum of dimethyl sebacate (**225**).

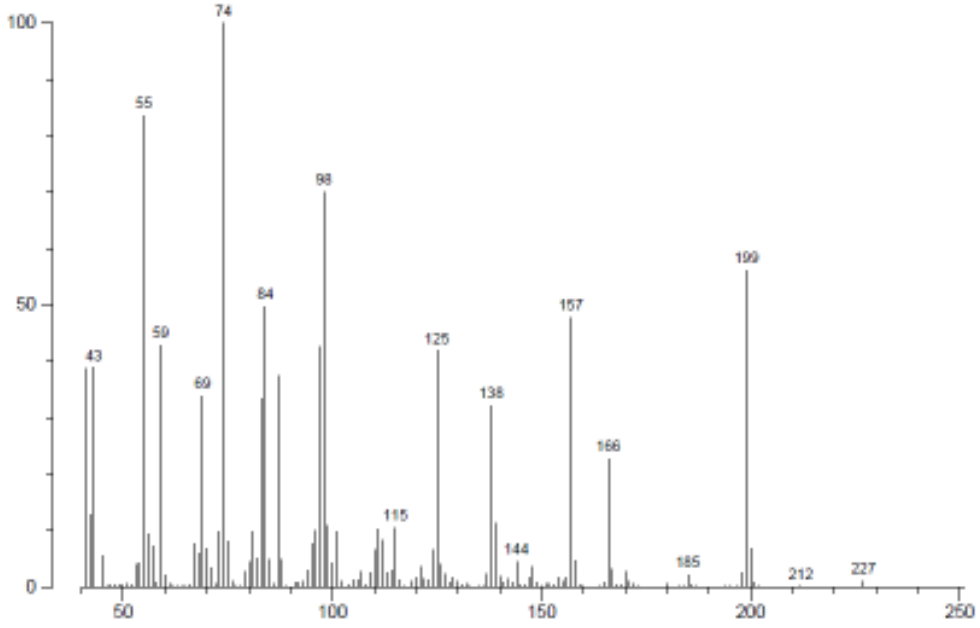

Appendix Figure 16 EI-MS spectrum of dimethyl sebacate (**225**).

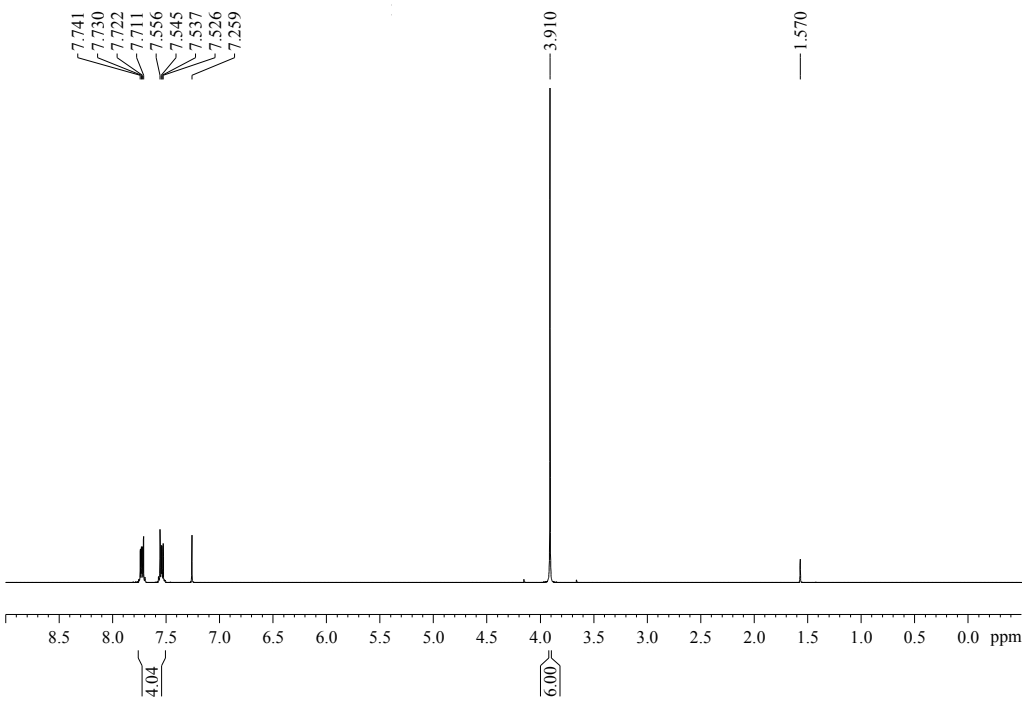

Appendix Figure 17 ^{1}H NMR spectrum of dimethyl phthalate (**223**) in $CDCl_3$.

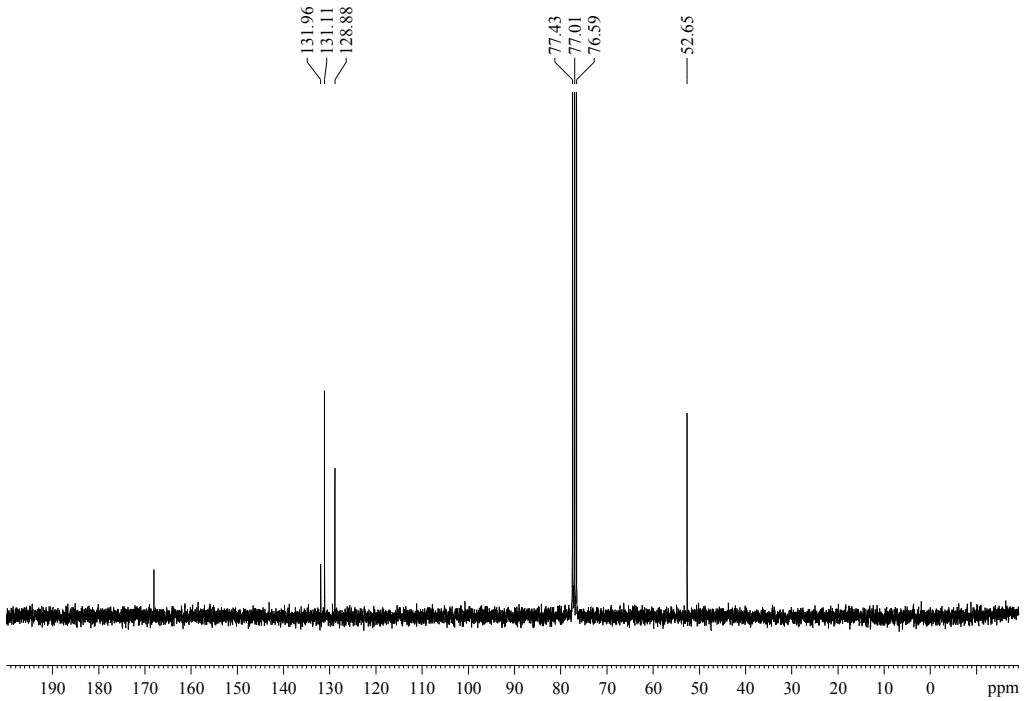

Appendix Figure 18 ^{13}C NMR spectrum of dimethyl phthalate (**223**) in $CDCl_3$.

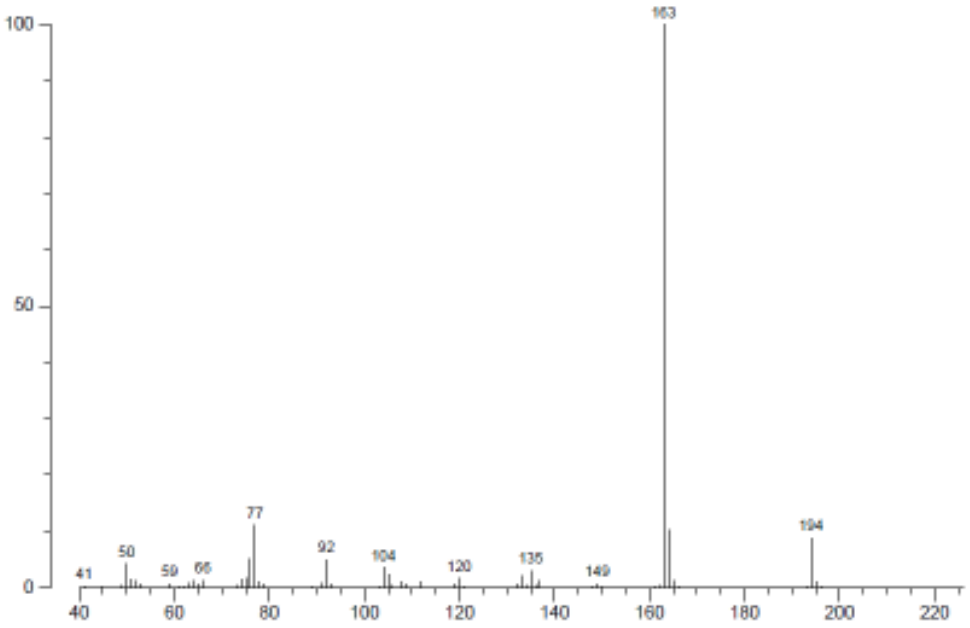

Appendix Figure 19 EI-MS spectrum of dimethyl phthalate (**223**).

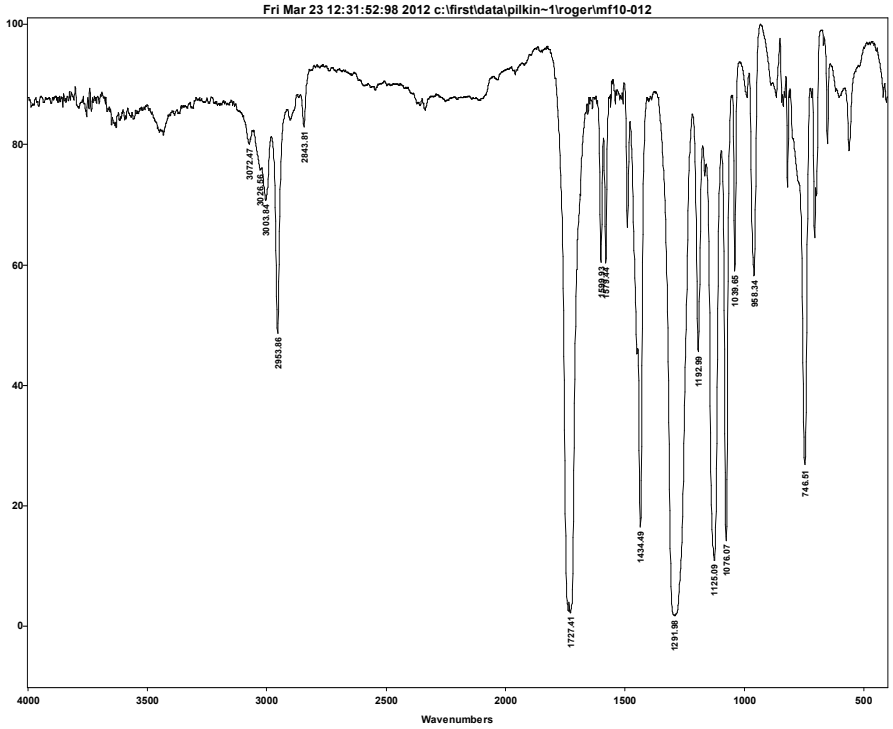

Appendix Figure 20 The FTIR spectrum of dimethyl phthalate (**223**).

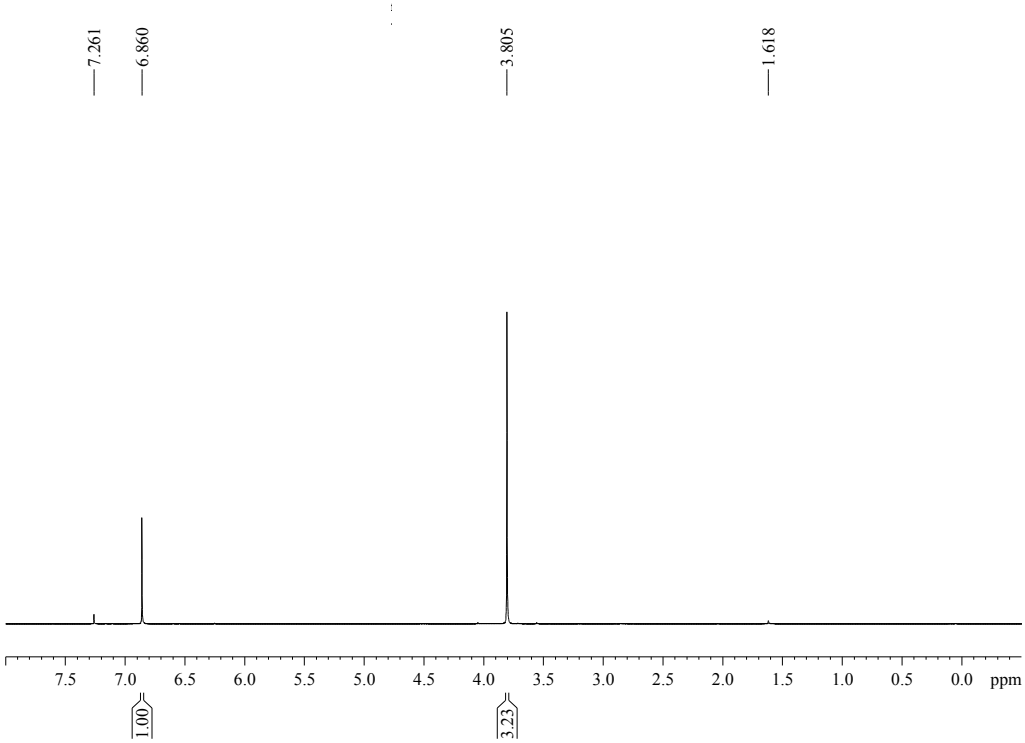

Appendix Figure 21 ^{1}H NMR spectrum of dimethyl fumarate (**220**) in $CDCl_3$.

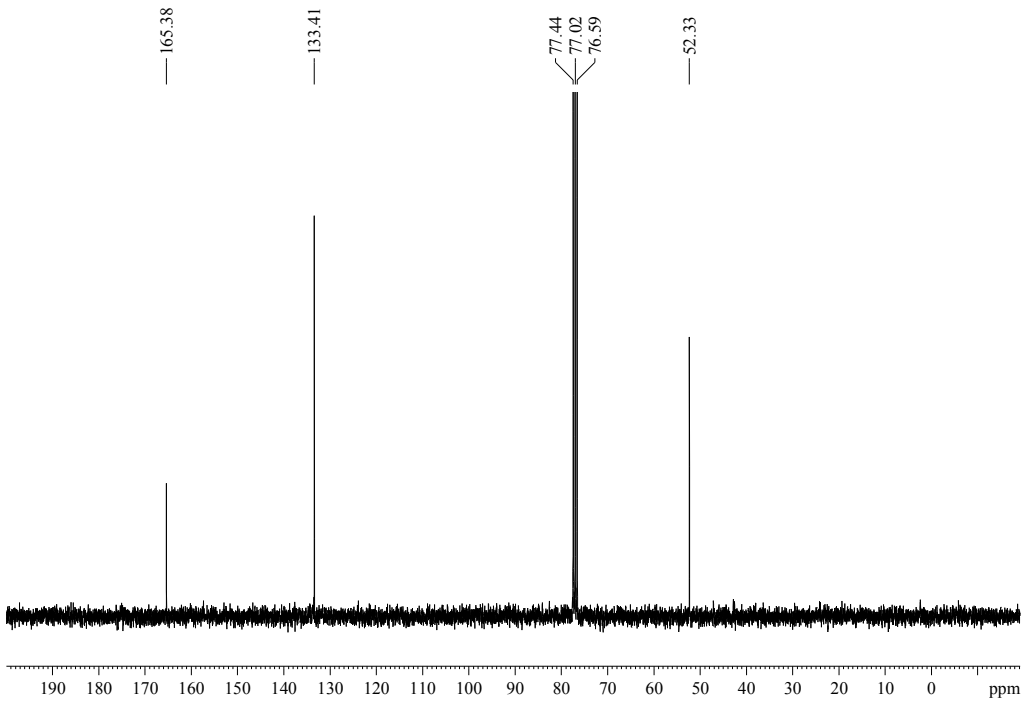

Appendix Figure 22 ^{13}C NMR spectrum of dimethyl fumarate (**220**) in $CDCl_3$.

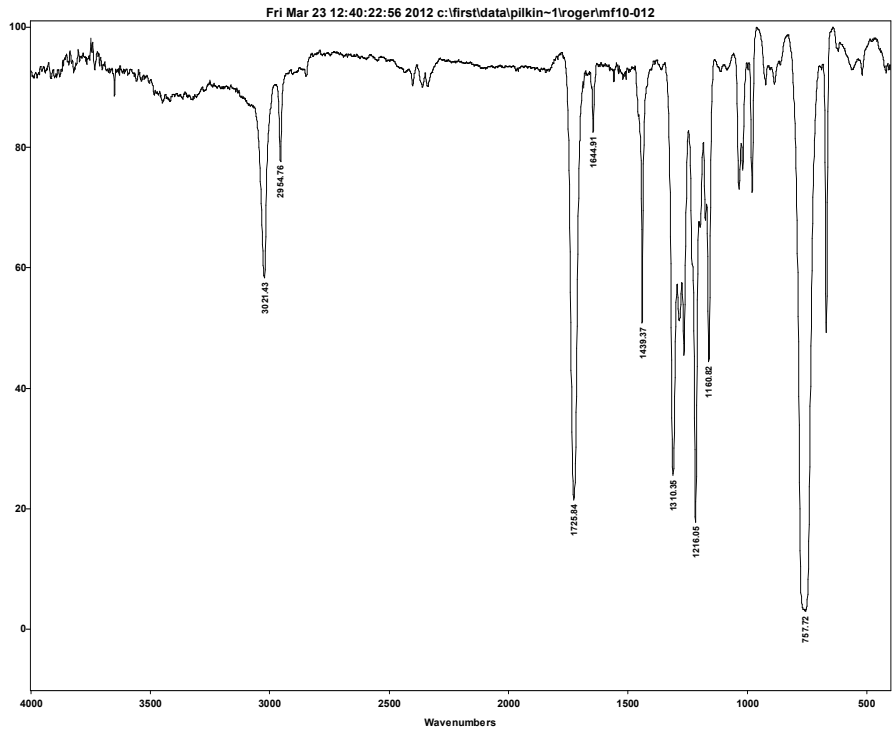

Appendix Figure 23 FTIR spectrum of dimethyl fumarate (**220**).

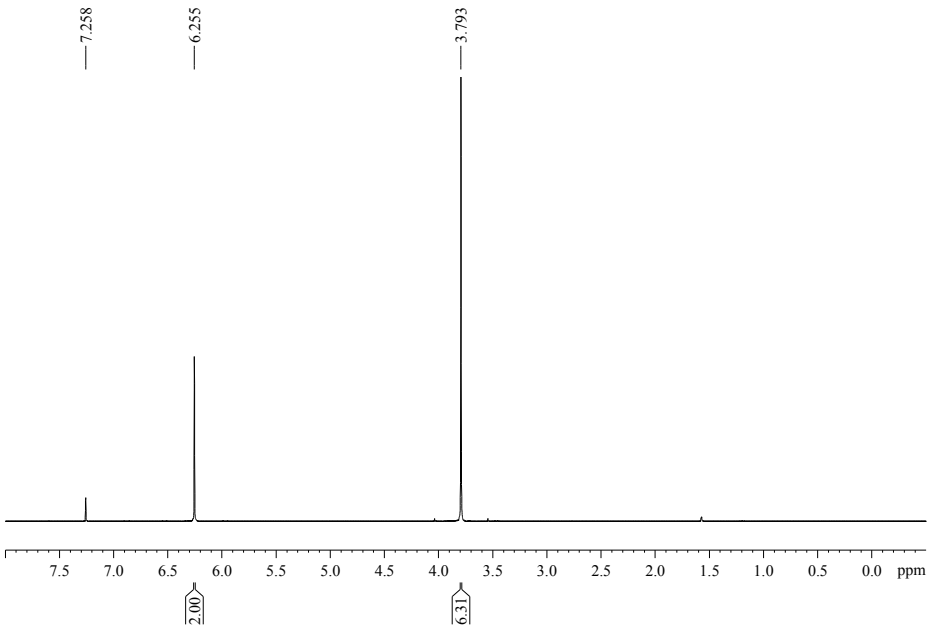

Appendix Figure 24 ^{1}H NMR spectrum of dimethyl maleate (**221**) in $CDCl_3$.

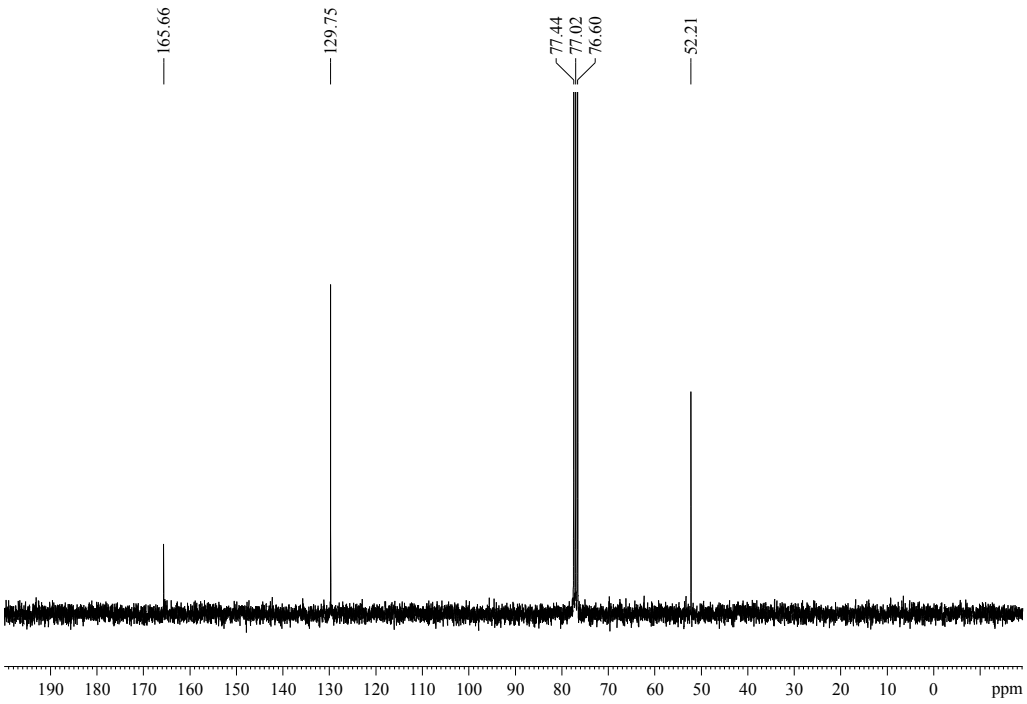

Appendix Figure 25 ^{13}C NMR spectrum of dimethyl maleate (**221**) in $CDCl_3$.

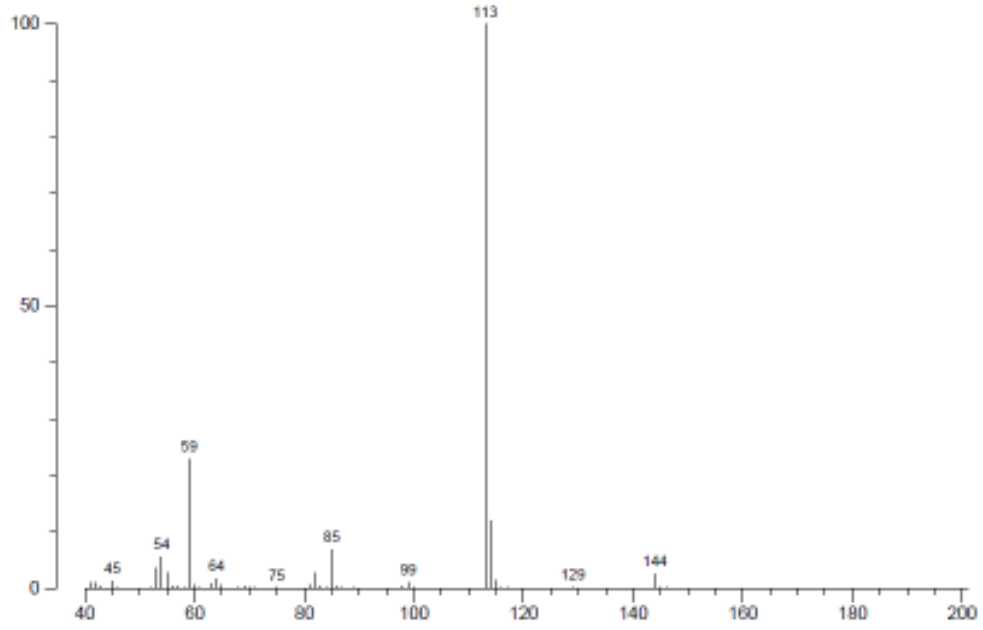

Appendix Figure 26 EI-MS spectrum of dimethyl maleate (**221**).

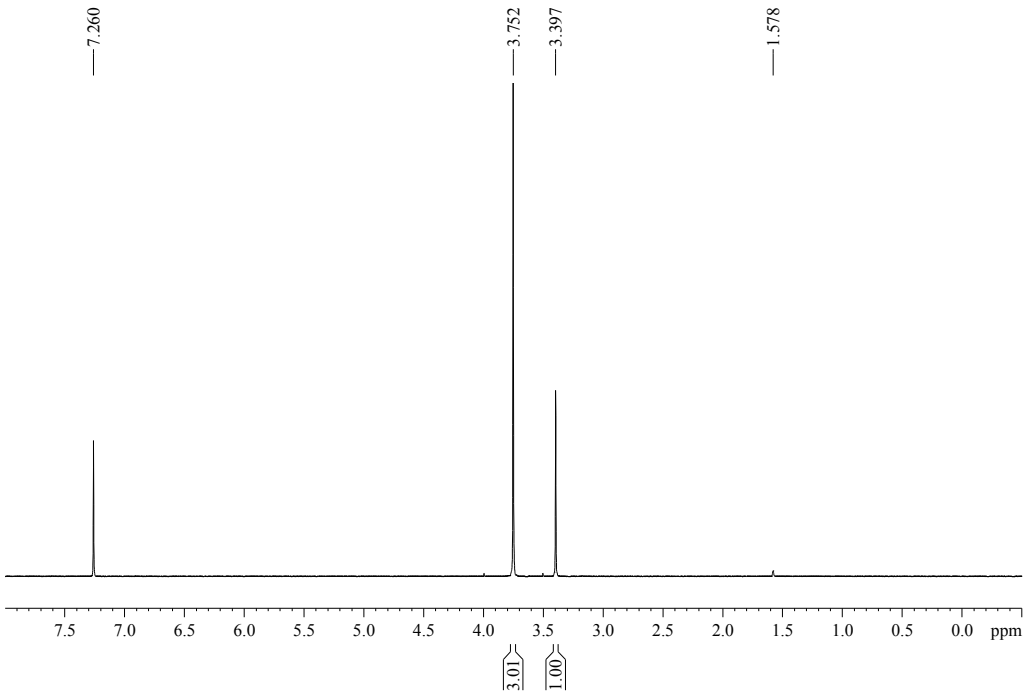

Appendix Figure 27 ^{1}H NMR spectrum of dimethyl malonate (**239**) in $CDCl_3$.

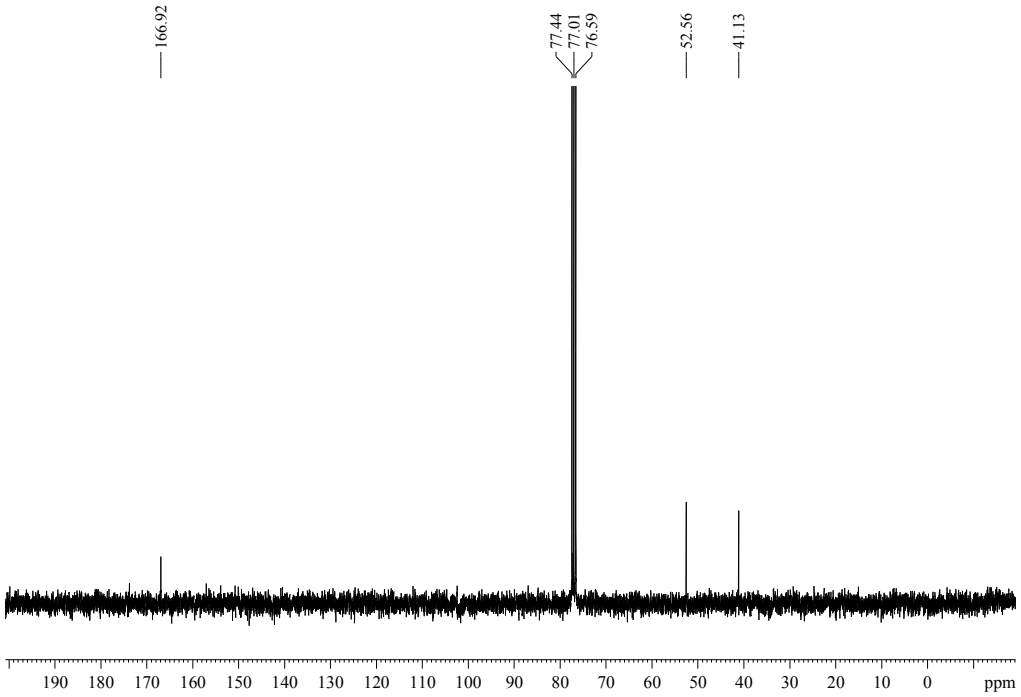

Appendix Figure 28 ^{13}C NMR spectrum of dimethyl malonate (**239**) in $CDCl_3$.

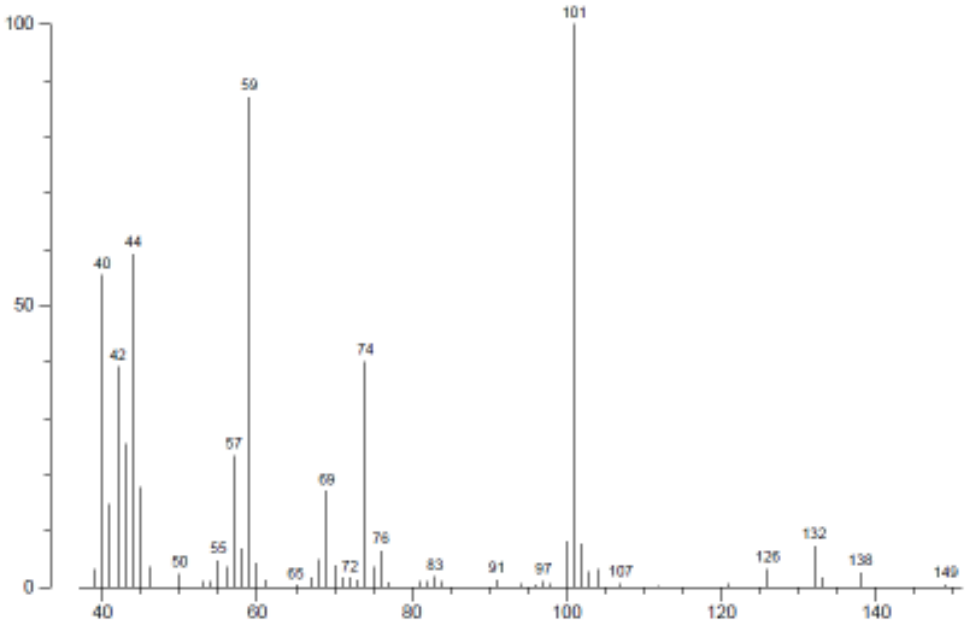

Appendix Figure 29 EI-MS of dimethyl malonate (**239**).

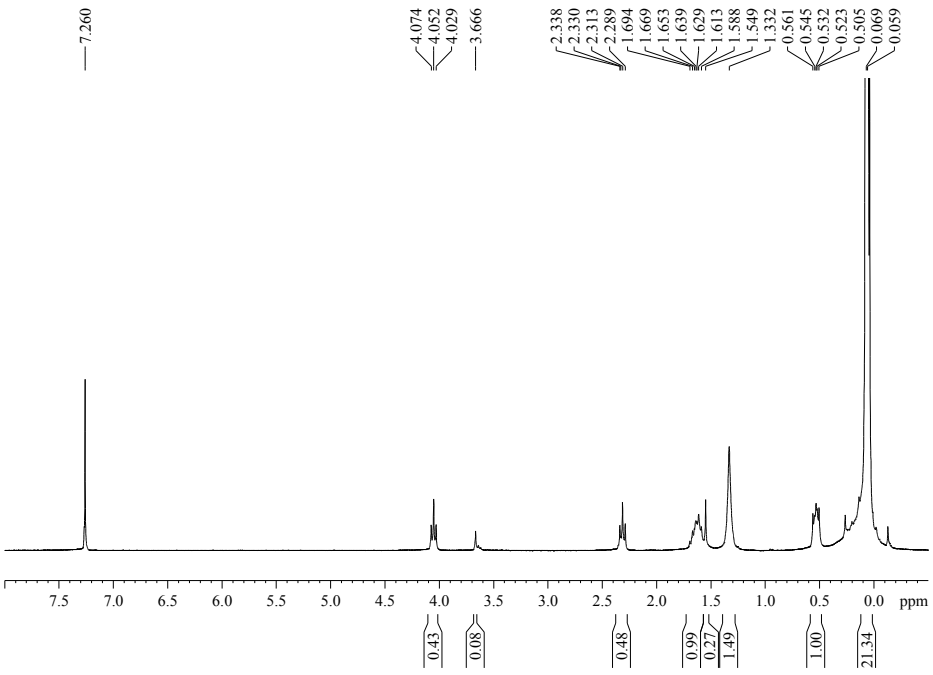

Appendix Figure 30 ^{1}H NMR spectrum of a polysiloxane polyester (**215**) in $CDCl_3$.

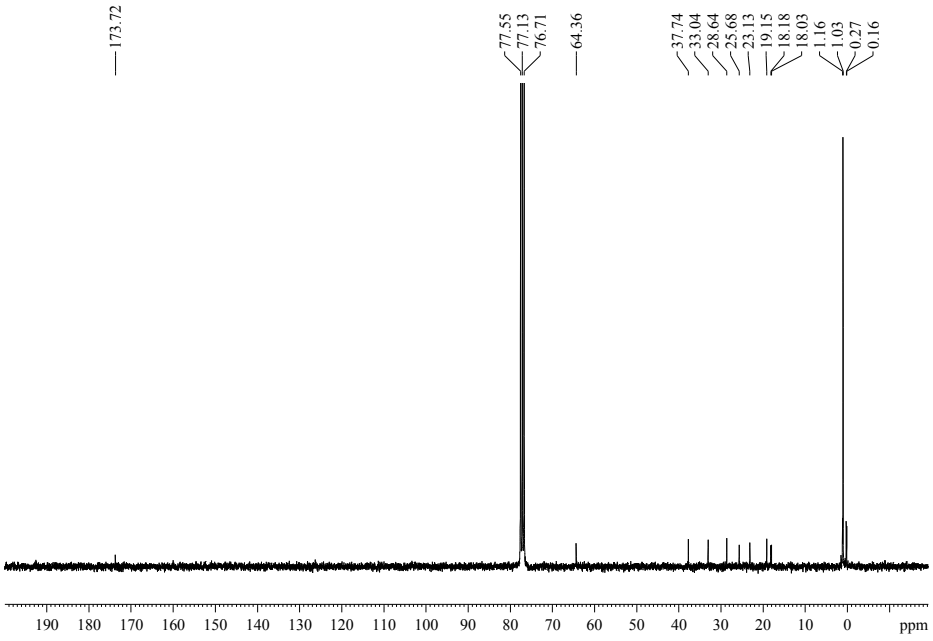

Appendix Figure 31 ^{13}C NMR spectrum of a polysiloxane polyester(**215**) in $CDCl_3$.

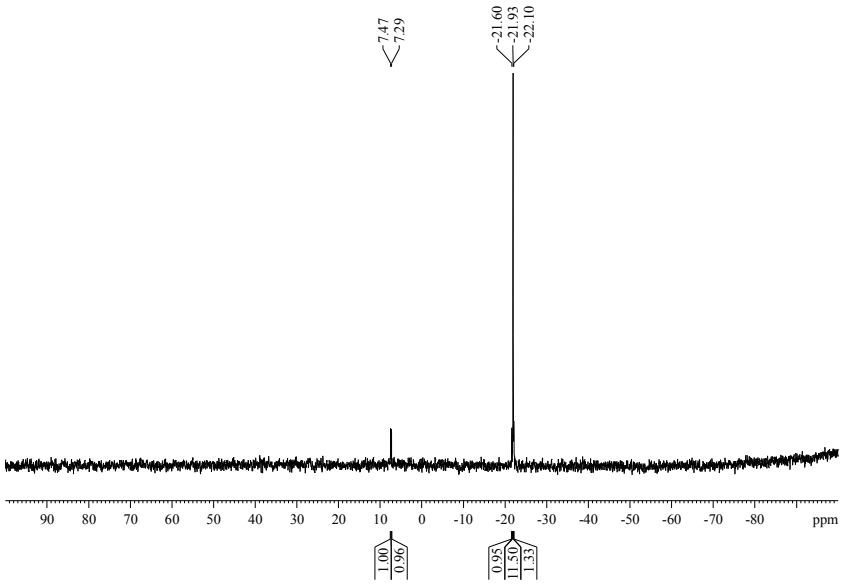

Appendix Figure 32 ^{29}Si NMR spectrum of a polysiloxane polyester (**215**) in $CDCl_3$.

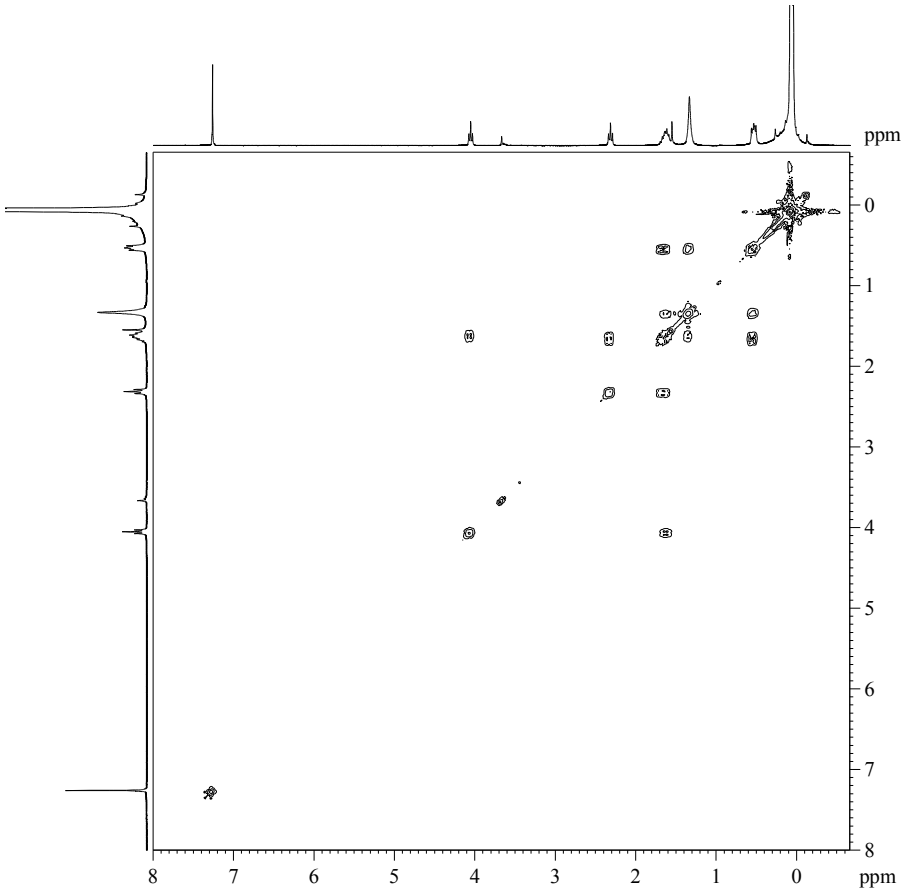

Appendix Figure 33 ^{1}H-^{1}H COSY NMR spectrum of a polysiloxane polyester (**215**) in $CDCl_3$.

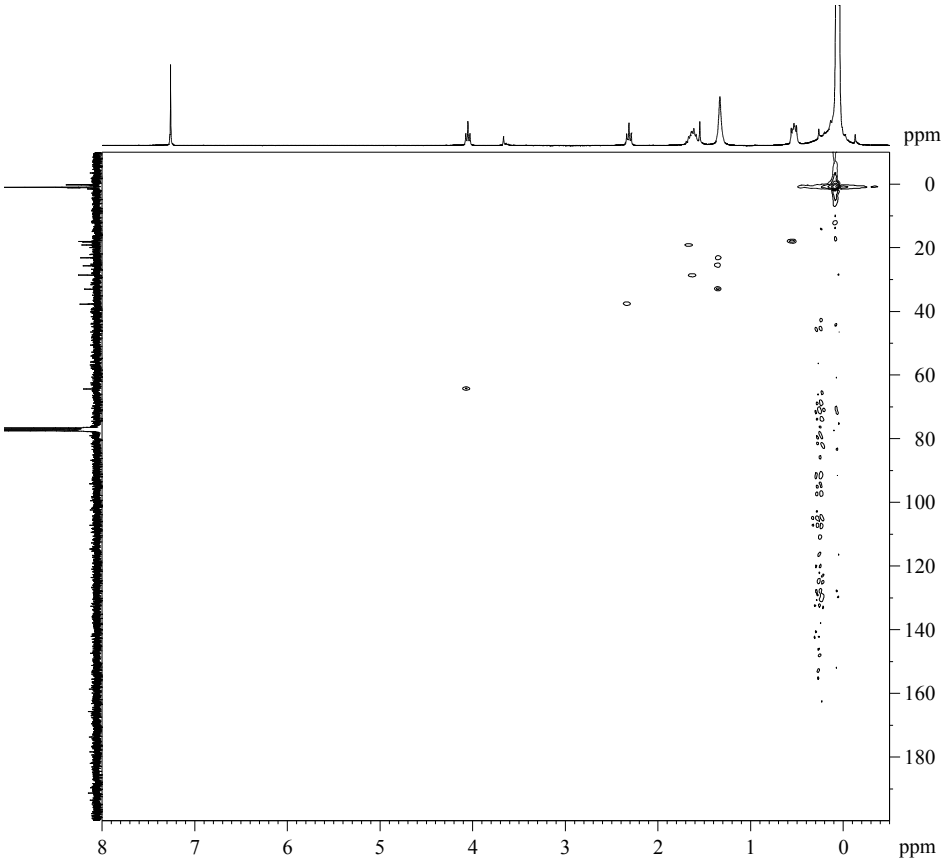

Appendix Figure 34 ^{1}H-^{13}C HSQC NMR spectrum of a polysiloxane polyester (**215**) in $CDCl_3$.

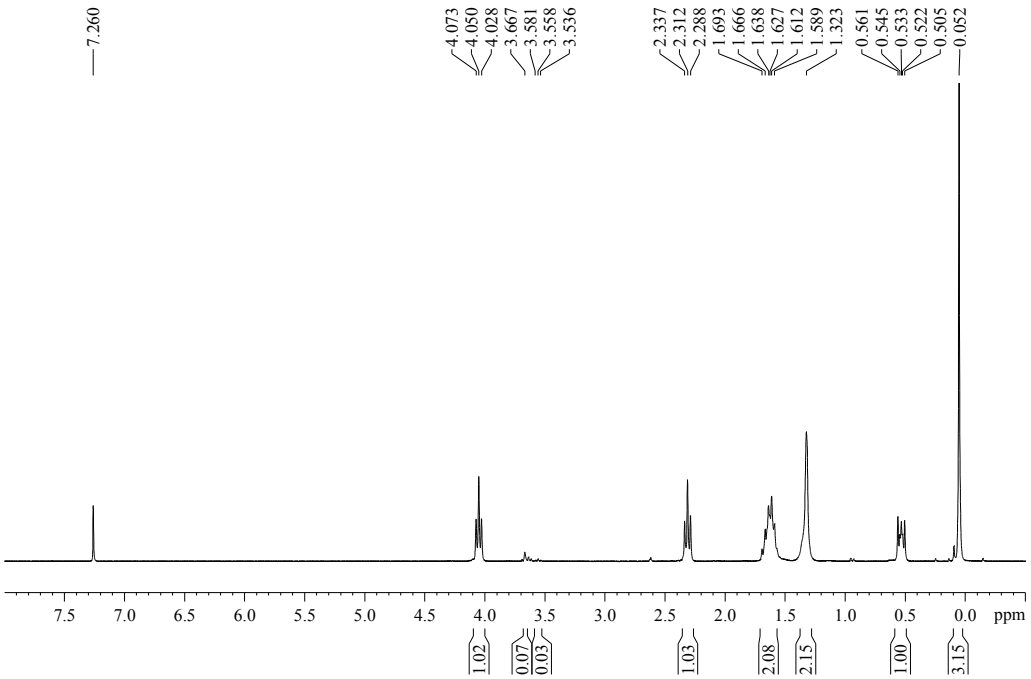

Appendix Figure 35 ^{1}H NMR spectrum of poly(octylene-*co*-(1,1,3,3-tetramethyldisiloxy-1,3-bis(*n*-butanoate)) (**231**) in $CDCl_3$.

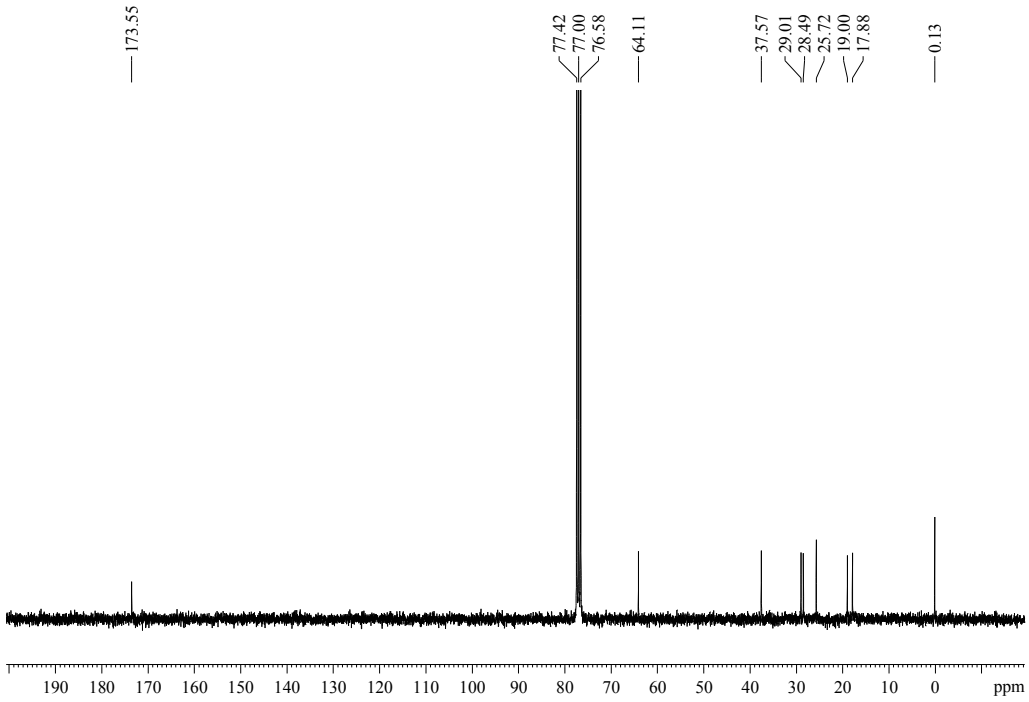

Appendix Figure 36 ^{13}C NMR spectrum of a poly(octylene-*co*-(1,1,3,3-tetramethyldisiloxy-1,3-bis(*n*-butanoate)) (**231**) in $CDCl_3$.

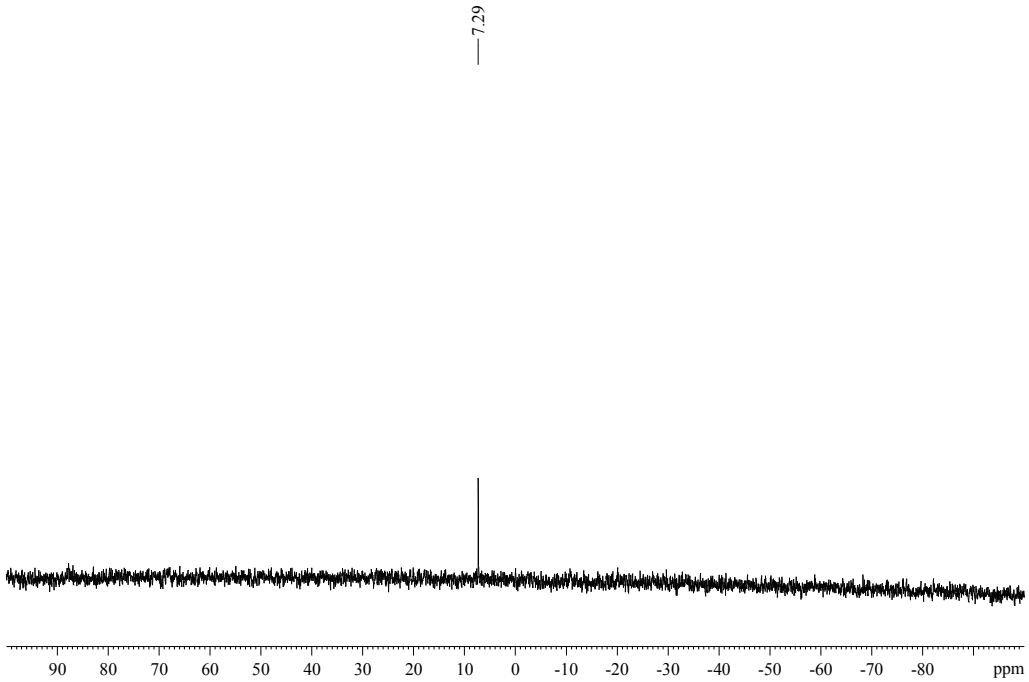

Appendix Figure 37 ^{29}Si NMR spectrum of poly(octylene-*co*-(1,1,3,3-tetramethyldisiloxy-1,3-bis(*n*-butanoate)) (**231**) in $CDCl_3$**.**

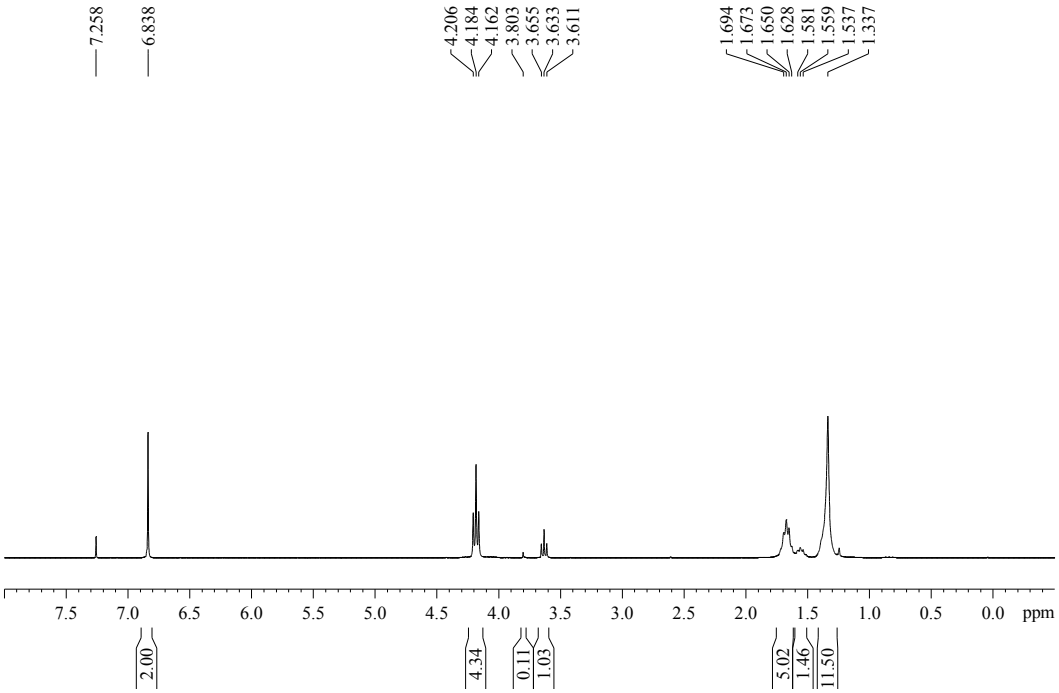

Appendix Figure 38 ^{1}H NMR spectrum of poly(octylene fumarate) (**226**) in $CDCl_3$.

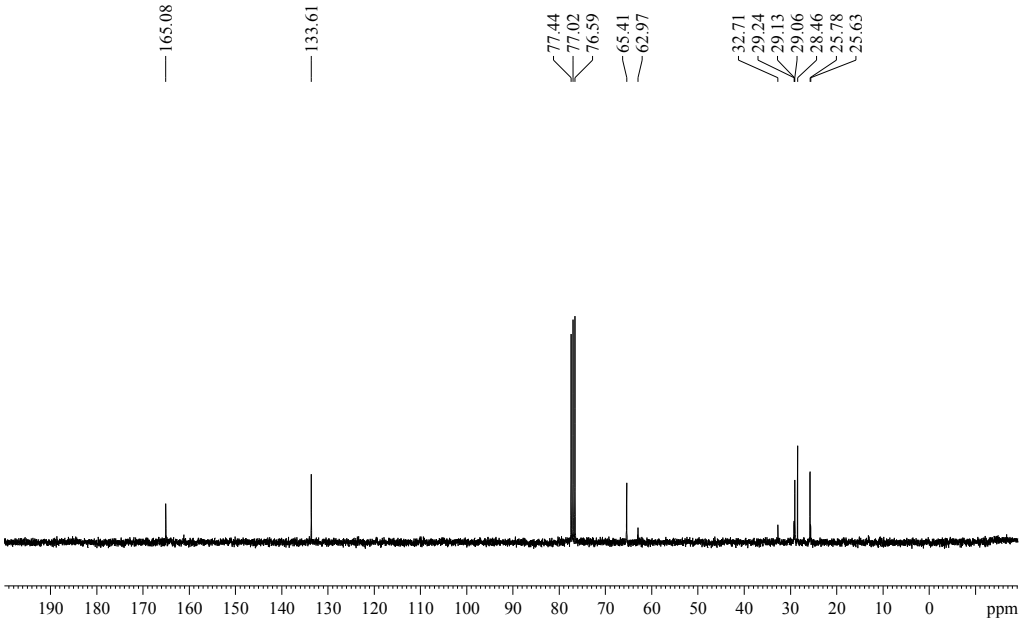

Appendix Figure 39 ^{13}C NMR spectrum of poly(octylene fumarate) (**226**) in $CDCl_3$.

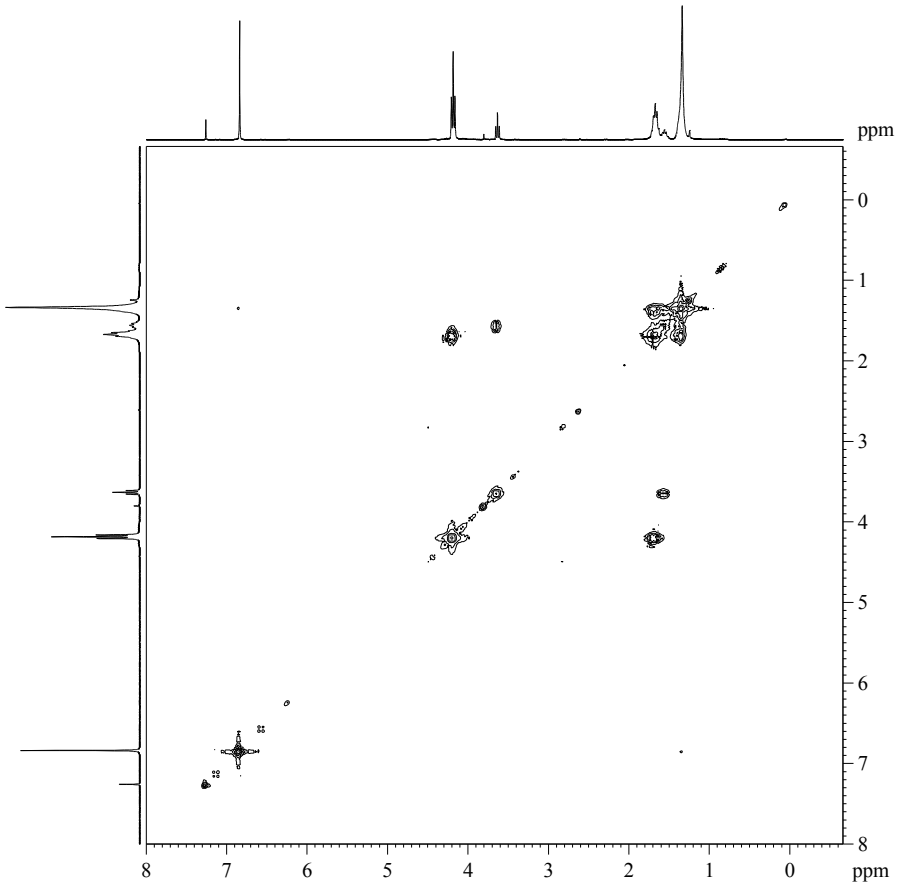

Appendix Figure 40 ^{1}H-^{1}H COSY NMR spectrum of poly(octylene fumarate) (**226**) in $CDCl_3$.

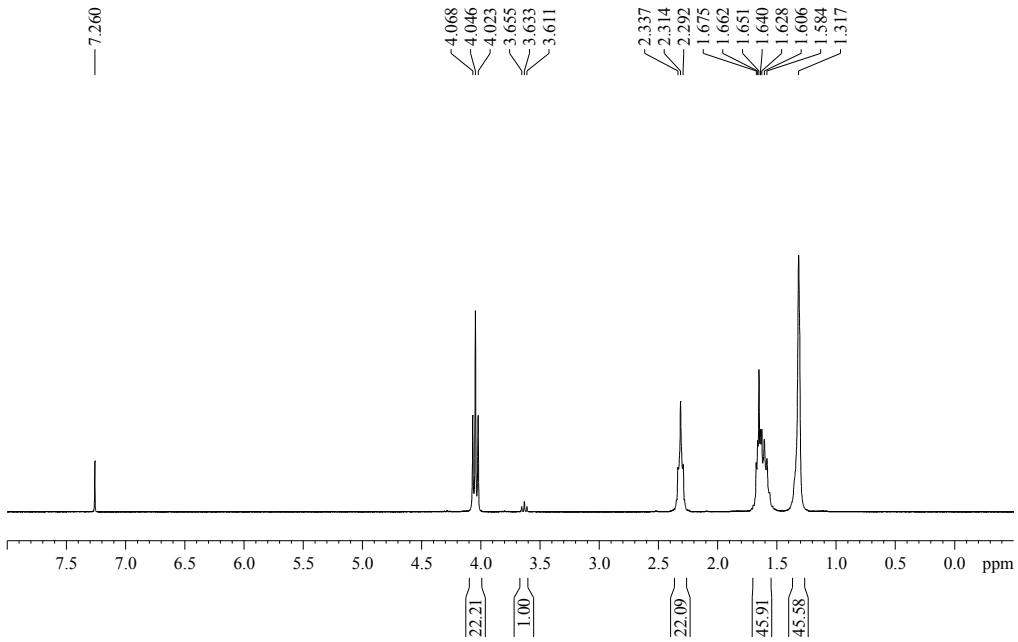

Appendix Figure 41 ^{1}H NMR spectrum of pol(octylene adipate) (**229**) in $CDCl_3$.

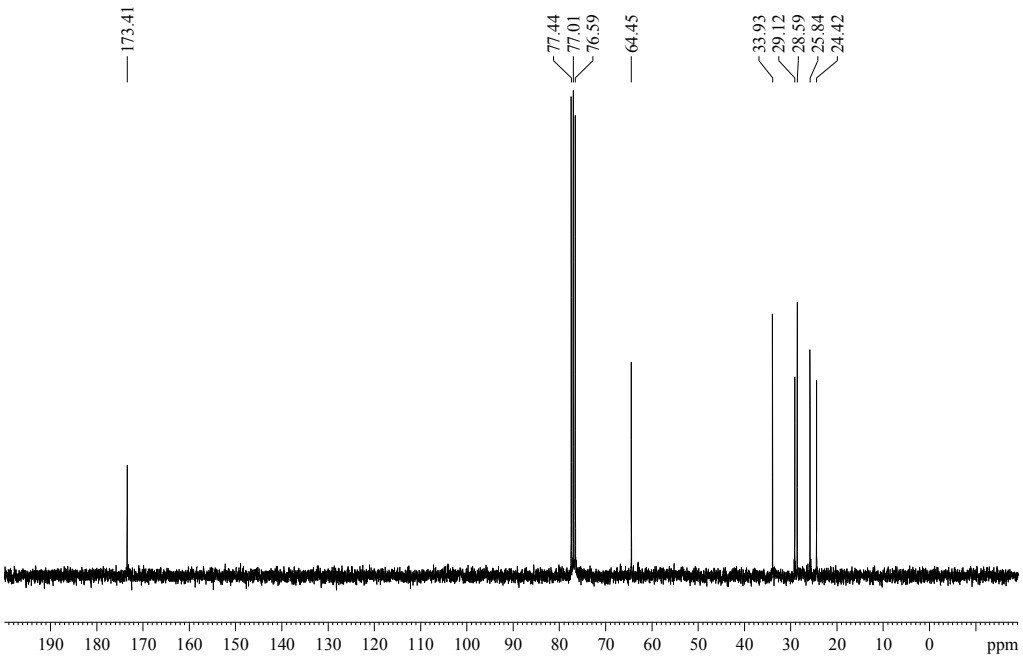

Appendix Figure 42 ^{13}C NMR spectrum of pol(octylene adipate) (**229**) in $CDCl_3$.

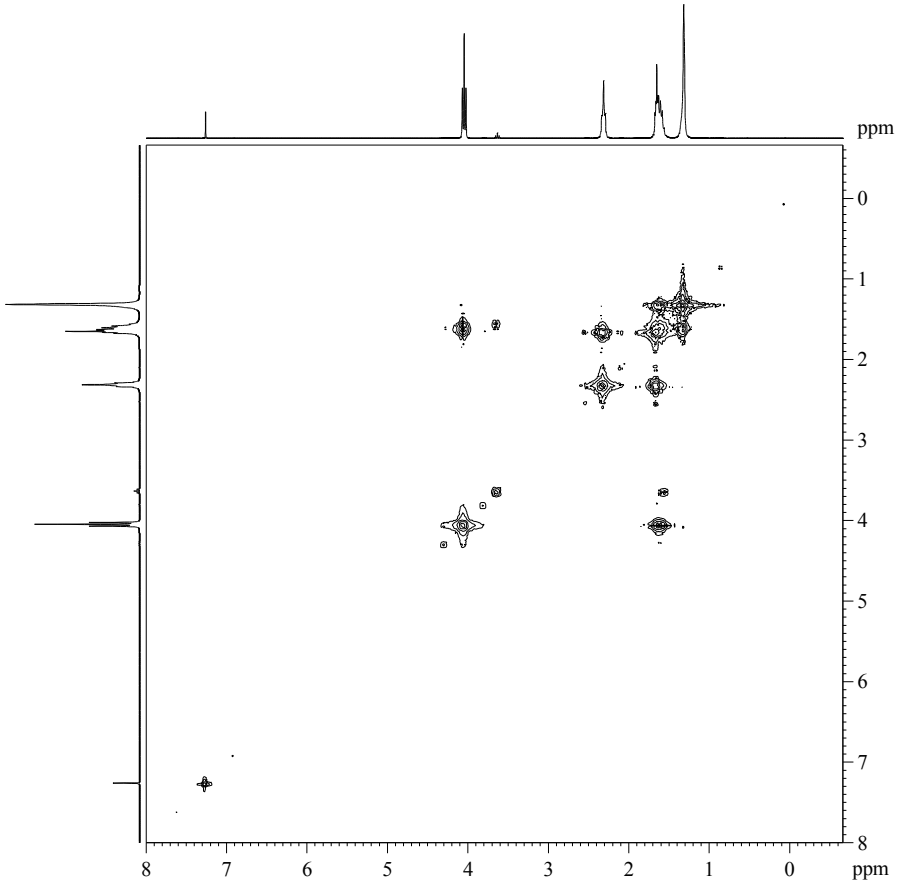

Appendix Figure 43 ^{1}H-^{1}H COSY NMR spectrum of pol(octylene adipate) (**229**) in $CDCl_3$.

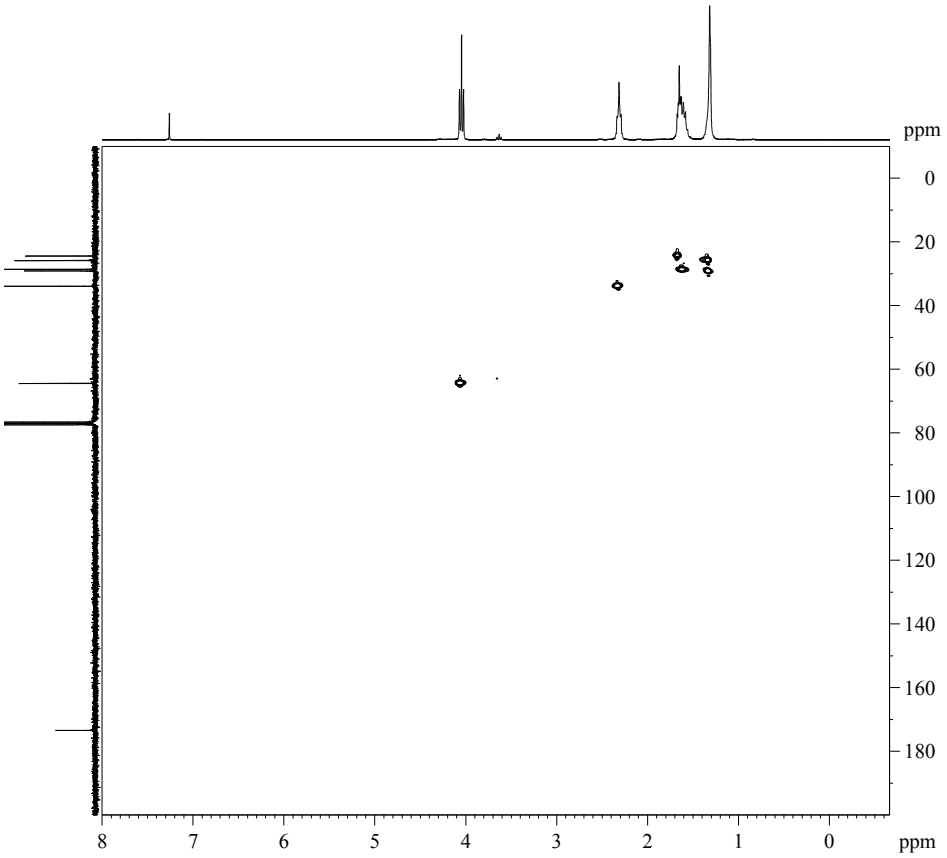

Appendix Figure 44 ^{1}H-^{13}C HSQC NMR spectrum of pol(octylene adipate) (**229**) in $CDCl_3$.

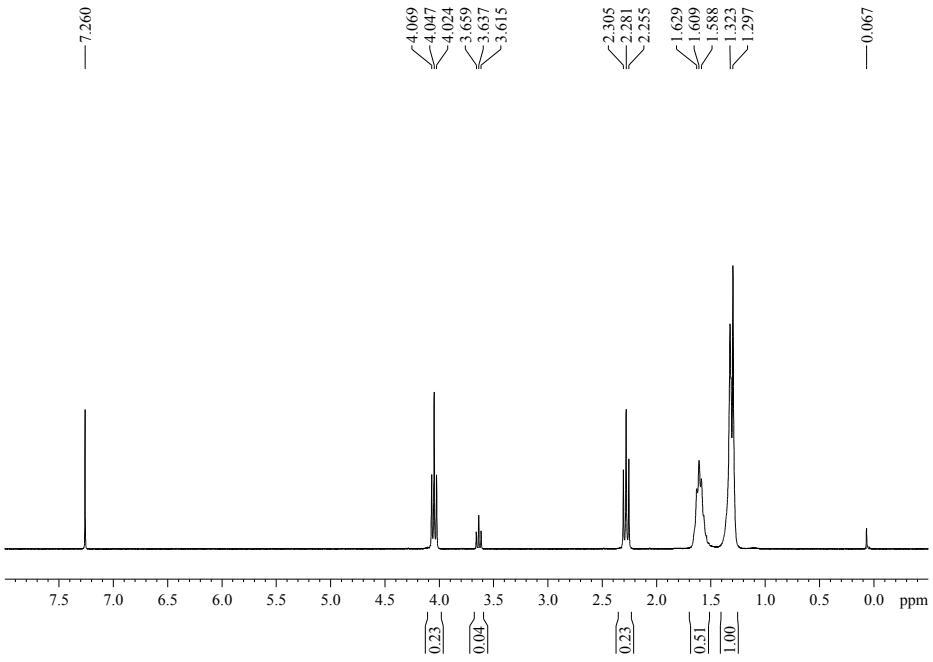

Appendix Figure 45 ^{1}H NMR spectrum of a poly(octylene sebacate) (**230**) in $CDCl_3$.

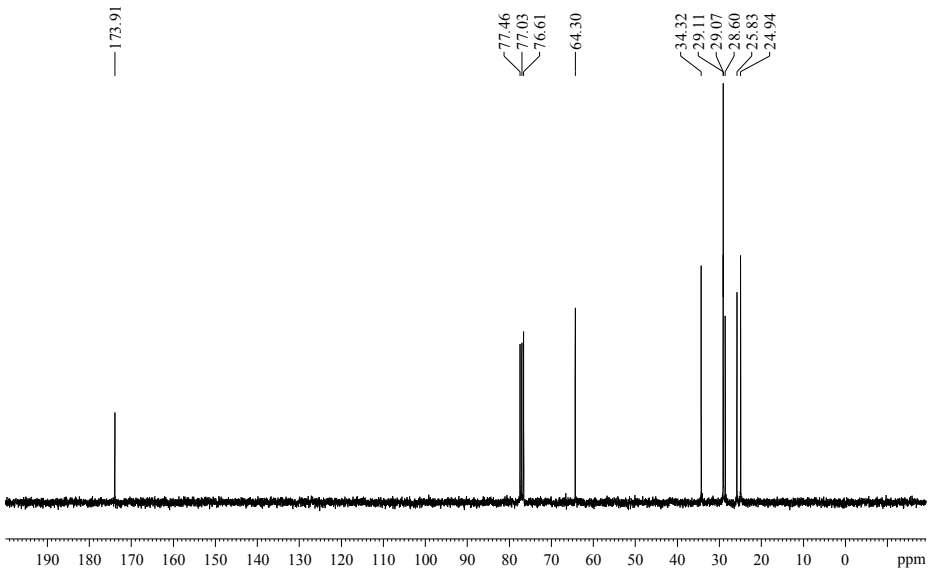

Appendix Figure 46 ^{13}C NMR spectrum of poly(octylene sebacate) (**230**) in $CDCl_3$.

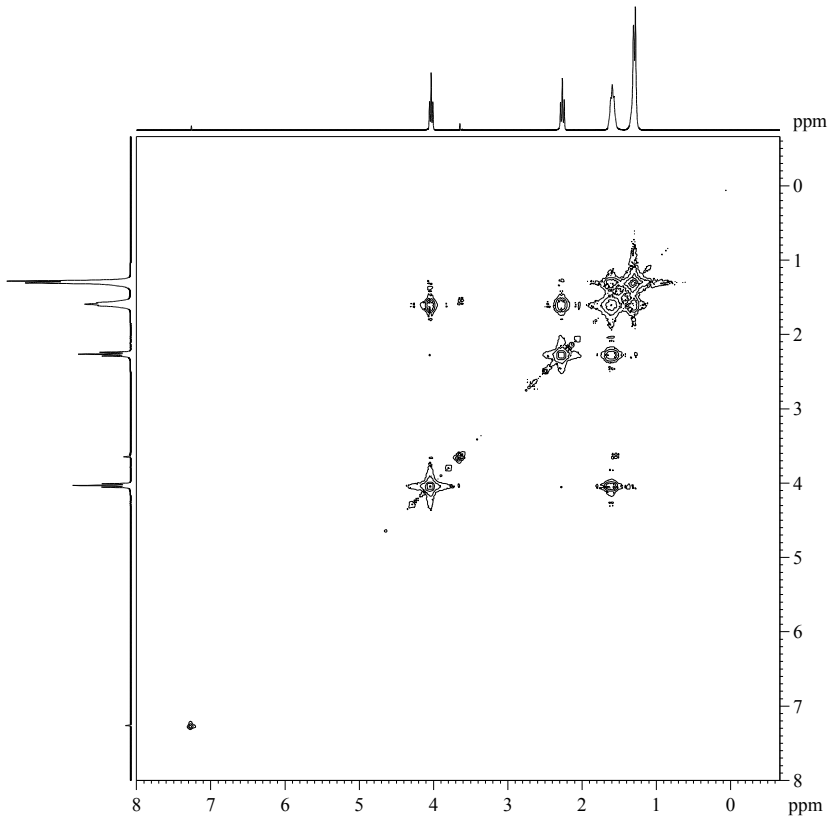

Appendix Figure 47 ^{1}H-^{1}H COSY NMR spectrum of poly(octylene sebacate) (**230**) in $CDCl_3$.

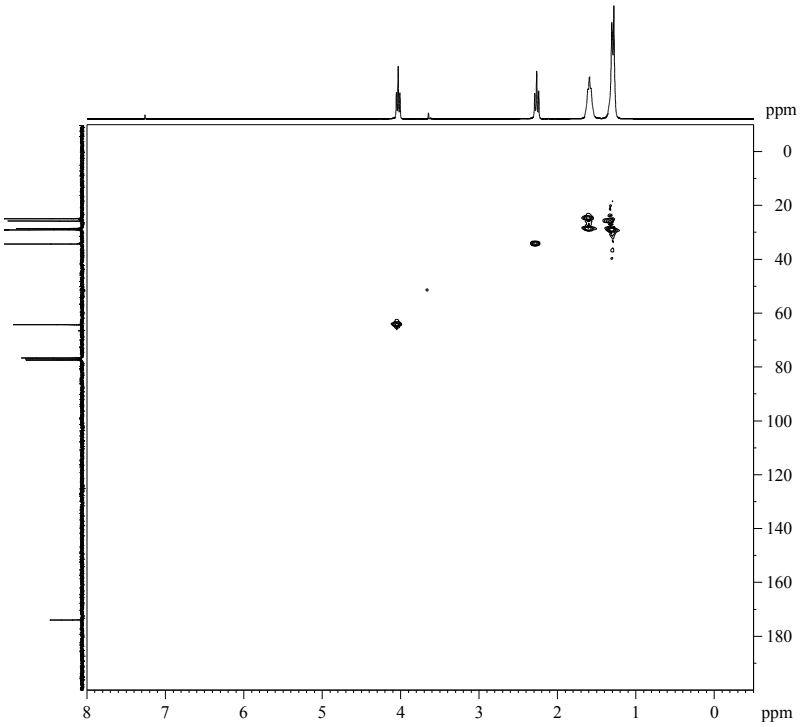

Appendix Figure 48 ^{1}H-^{13}C HSQC NMR spectrum of poly(octylene sebacate) (**230**) in $CDCl_3$.

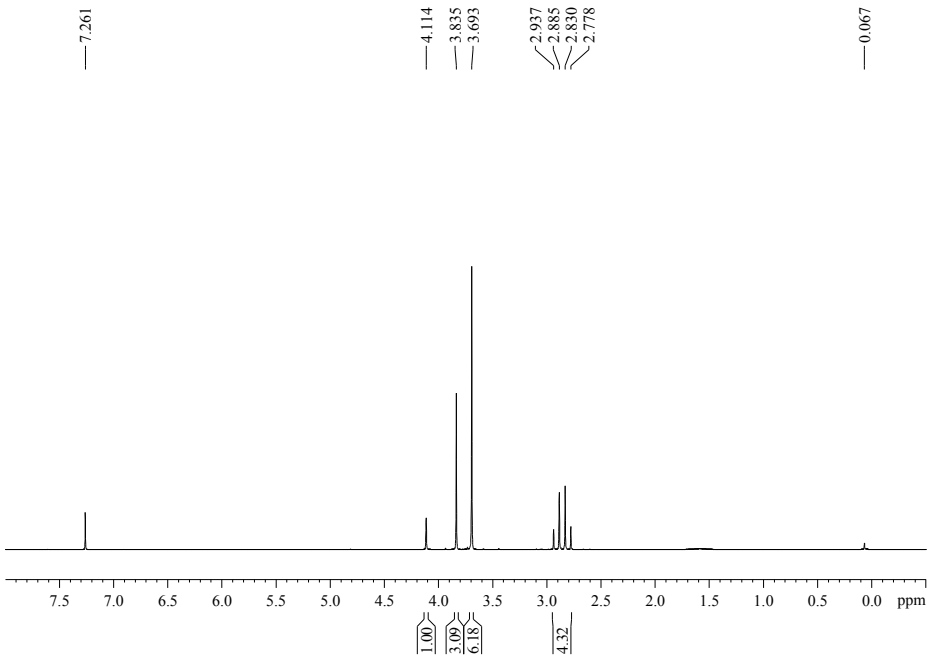

Appendix Figure 49 ^{1}H NMR spectrum of trimethyl citrate (**242**) in $CDCl_3$.

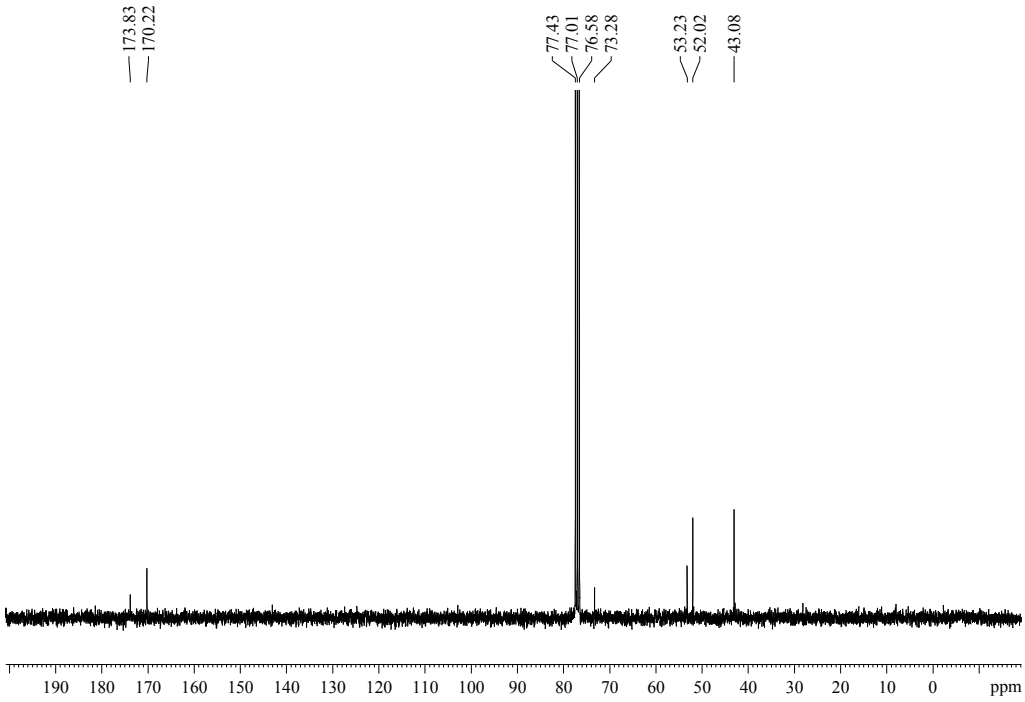

Appendix Figure 50 ^{13}C NMR spectrum of trimethyl citrate (**242**) in $CDCl_3$.

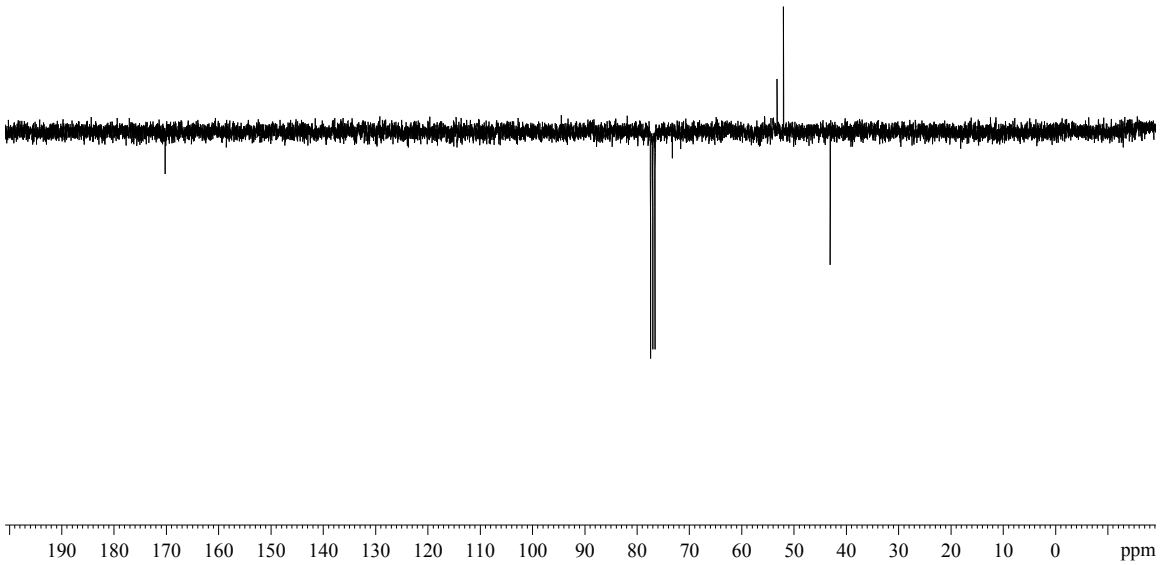

Appendix Figure 51 ^{13}C DEPT Q spectrum of trimethyl citrate (**242**) in $CDCl_3$.

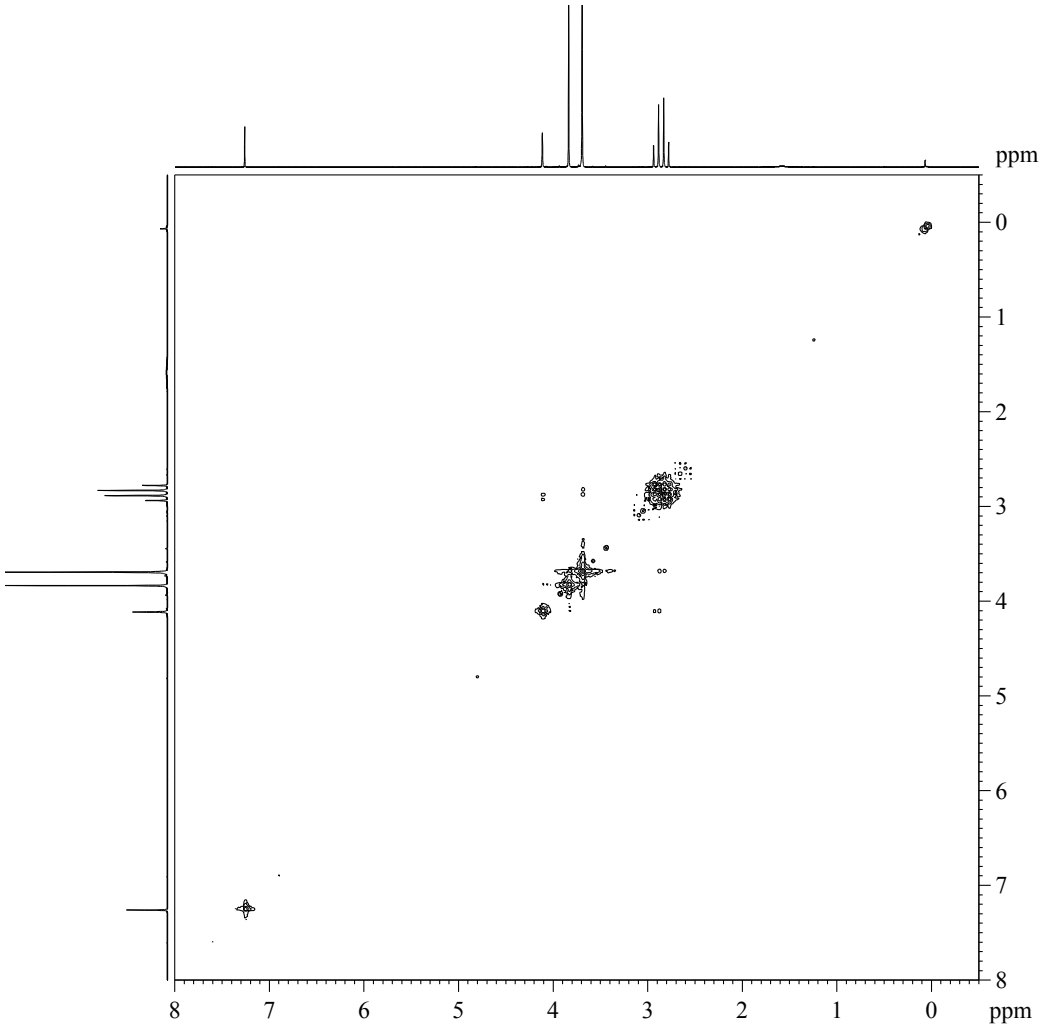

Appendix Figure 52 ^{1}H-^{1}H COSY NMR spectrum of trimethyl citrate (**242**) in $CDCl_3$.

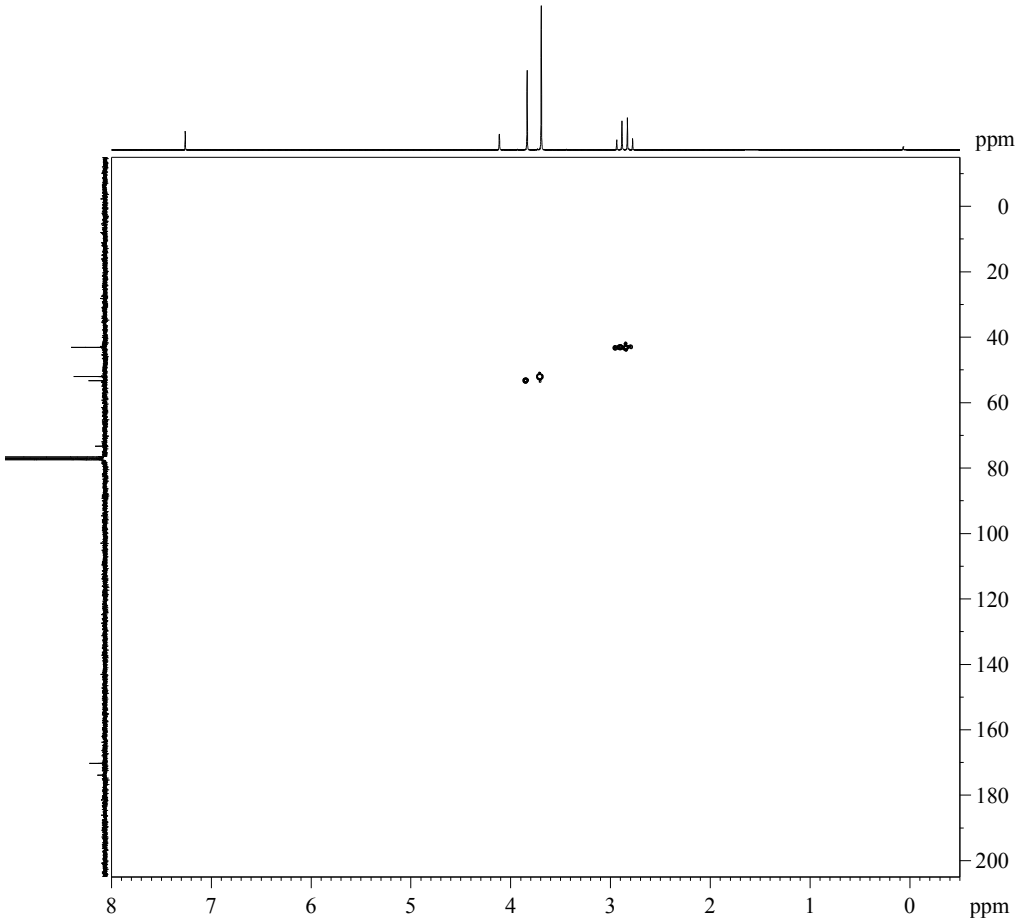

Appendix Figure 53 ^{1}H-^{13}C HSQC NMR spectrum of trimethyl citrate (**242**) in $CDCl_3$.

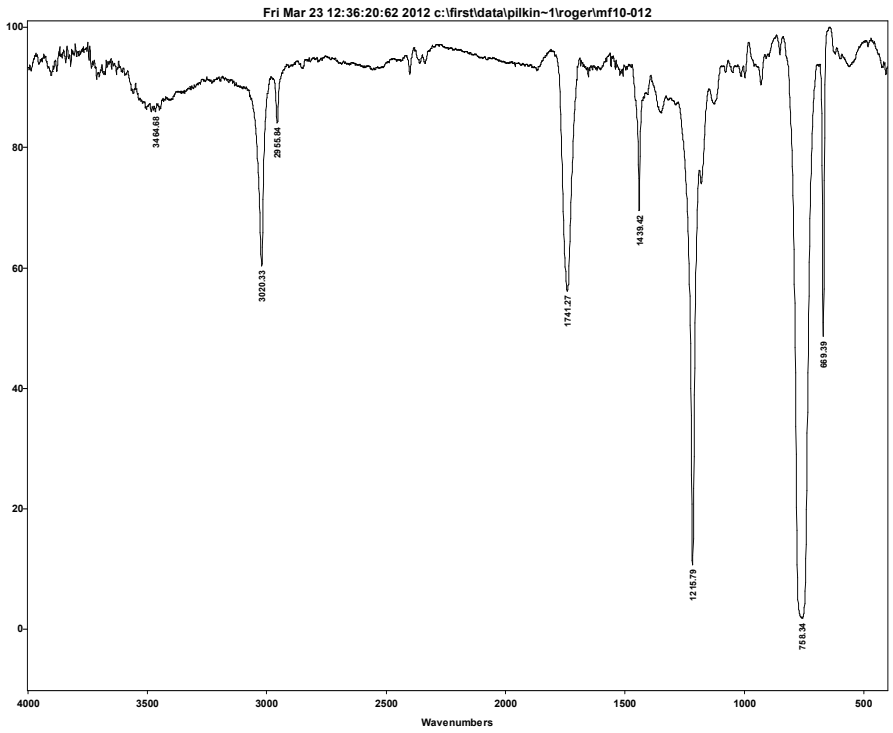

Appendix Figure 54 FTIR spectrum of trimethyl citrate (**242**).

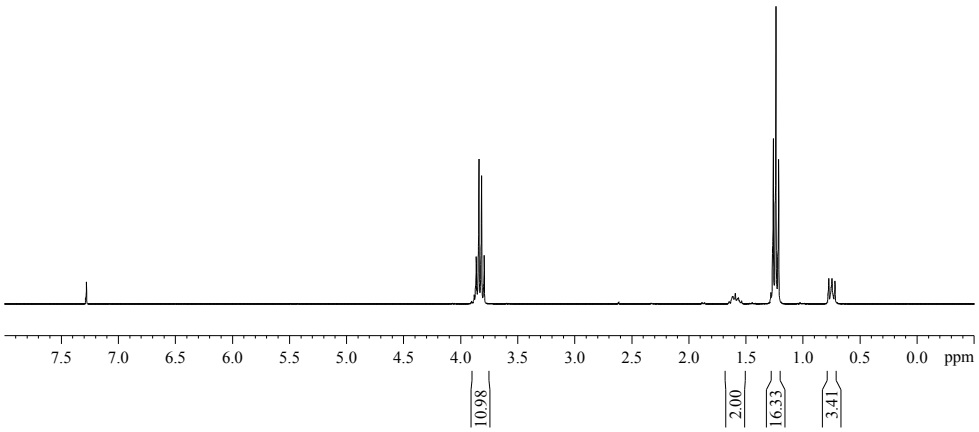

Appendix Figure 55 ^{1}H NMR spectrum of 1,3-bis(triethoxysilyl)propane (**198**) in $CDCl_3$.

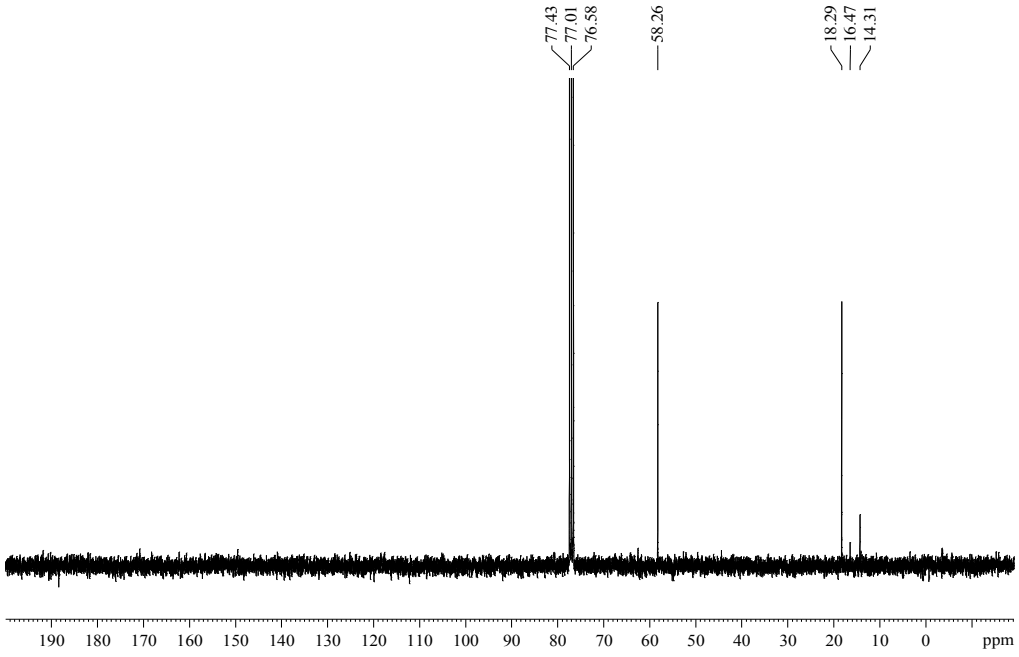

Appendix Figure 56 ^{13}C NMR spectrum of 1,3-bis(triethoxysilyl)propane (**198**) in $CDCl_3$.

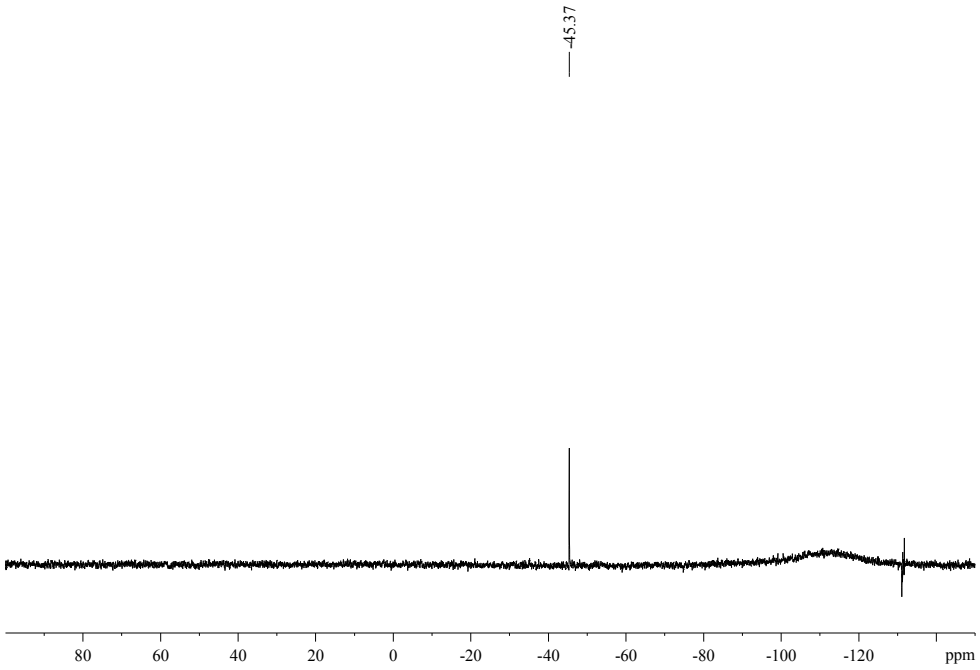

Appendix Figure 57 ^{29}Si NMR spectrum of 1,3-bis(triethoxysilyl)propane (**198**) in $CDCl_3$.

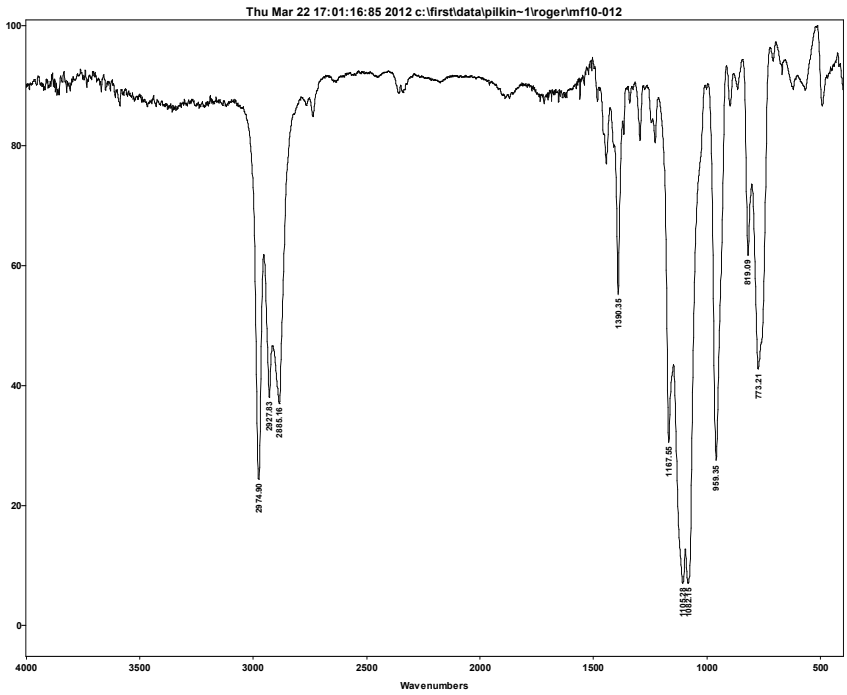

Appendix Figure 58 FTIR spectrum of 1,3-bis(triethoxysilyl)propane (**198**).

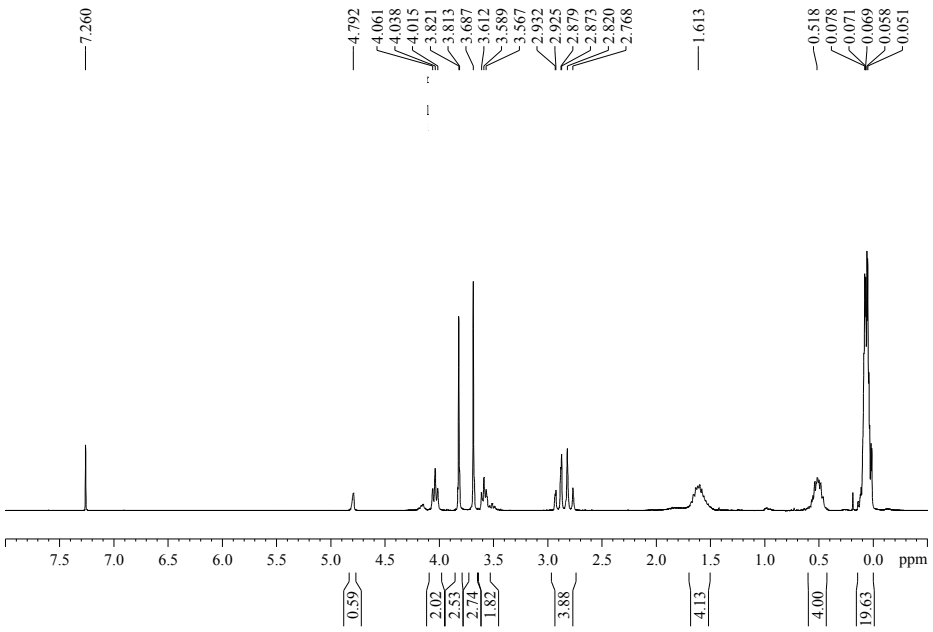

Appendix Figure 59 ^{1}H NMR spectrum of a citrate-siloxane copolymer (**245**) in $CDCl_3$

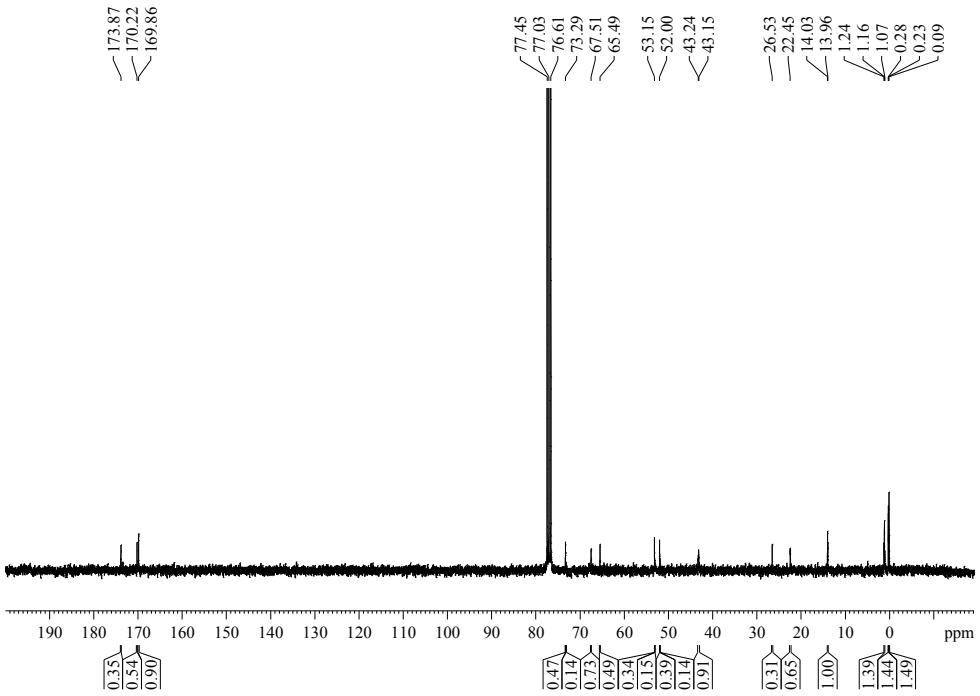

Appendix Figure 60 Inverse gated ^{13}C NMR spectrum of a citrate-siloxane copolymer (**245**) in $CDCl_3$.

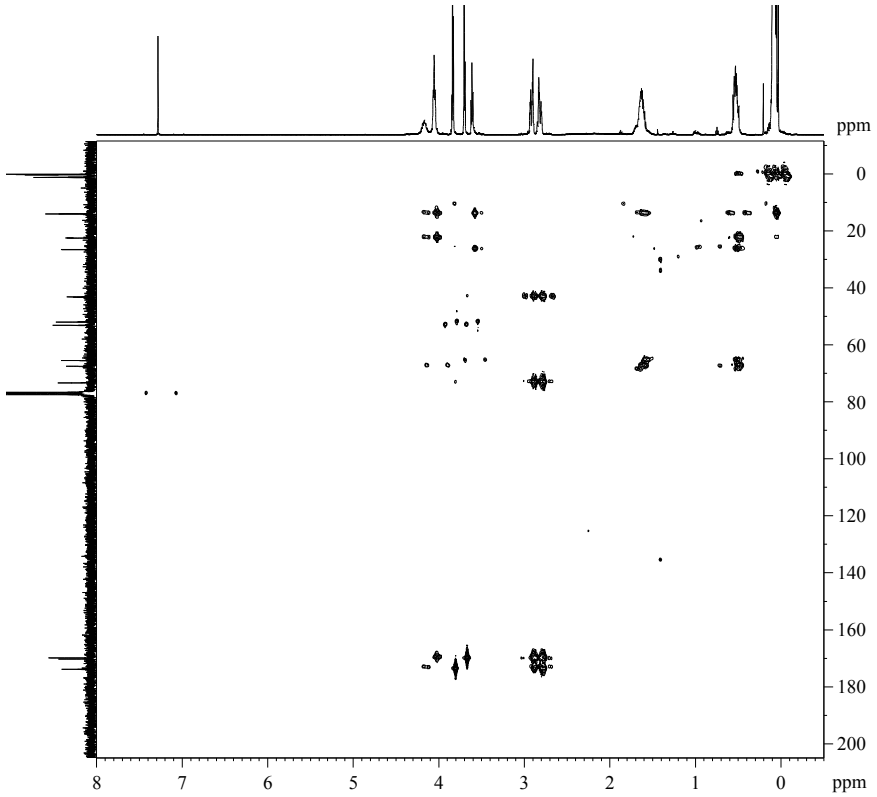

Appendix Figure 61 ^{1}H-^{13}C HBMC NMR spectrum of a citrate-siloxane copolymers (**245**) in $CDCl_3$.

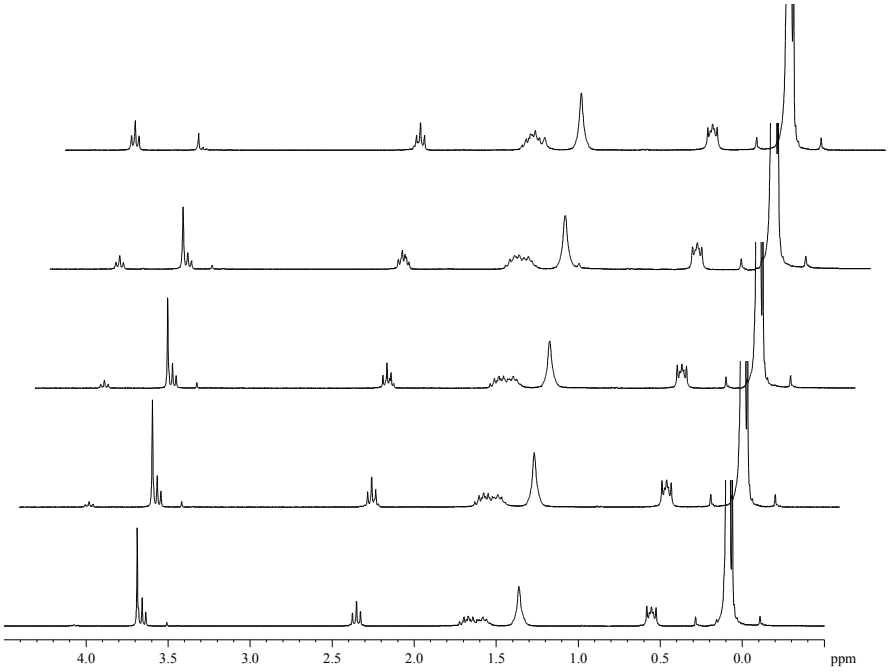

Appendix Figure 62 A stack plot of ^{1}H NMR spectra for the lipase-mediated polyesterification of diester **212** and diol **162**.

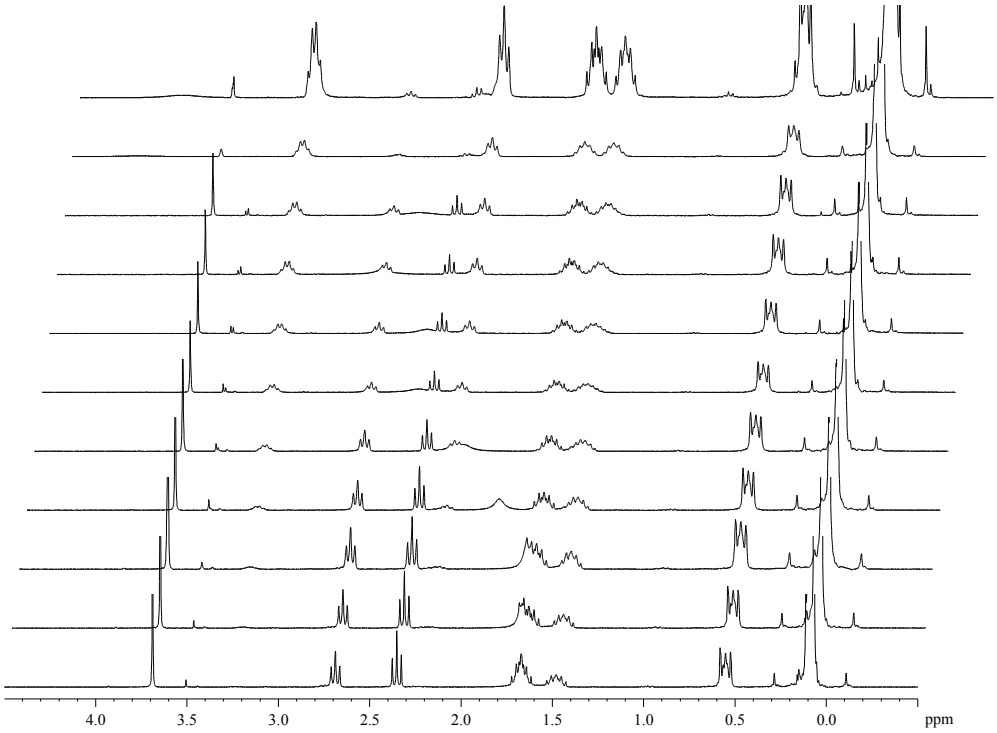

Appendix Figure 63 A stack plot of the ^{1}H NMR spectra for the lipase-mediated polyamidation of diester **212** and diamine **216**. The spectra represent the time intervals 0, 10, 20, and 30 min, 1, 2, 3, 4 and 24 h from bottom to top.

8 Vita

Mark B. Frampton was born in Sydney, Nova Scotia, Canada on December 8, 1972. He and his sister were raised by their parents Maisie and Warrant Officer (ret.) Chesley Frampton. He attended several elementary schools, junior high schools and high schools as a result of his father's career in the Canadian Air Force. His high school education was completed at Trenton High School in 1991 at which point he attended McMaster University. In 2002 he enrolled at Loyalist College of Applied Arts and Technology in Belleville, Ontario, Canada to complete a Technicians Diploma in Chemical Engineering which was completed in 2004. He attended Brock University in St. Catharines, Ontario, Canada where he attained his B.Sc. in biological sciences with a minor in chemistry under the supervision of Dr. Miriam H. Richards. In 2007 he began his doctoral studies at Brock University under the supervision of Dr. Paul M. Zelisko. He is presently completing his Ph.D. in chemical biotechnology.

9 References

[1] R.K. Iler. *The Chemistry of Silica, Solubility, Polymerization, Colloid and Surface properties, and Biochemistry*. Wiley, New York, NY, USA. **1979**.

[2] M.A. Brook. *Silicon in Organic, Organometallic, and Polymer Chemistry*. Wiley, New York, NY, USA. **2000**.

[3] R. Tacke. *Angew. Chem. Int. Ed*., **1999**, *38*, 3015-3018.

[4] S. Wenzl, R. Hett, P. Richthammer, and M. Sumper. *Angew. Chem. Int. Ed*., **2008**, *47*, 1729-1732.

[5] N. Kröger, R. Deutzman, and M. Sumper. *Science*, **1999**, *286*, 1129-1133.

[6] N. Kröger, R. Deutzman, C. Bergsdorf, and M. Sumper. *Proc. Natl. Acad. Sci. USA.*, **2000**, *97*, 14133-14138.

[7] N. Kröger, R. Deutzman, and M. Sumper. *J. Biol. Chem*., **2001**, *276*, 26066-26070.

[8] K. Shimizu, J.N. Cha, G.D. Stucky, and D.E. Morse. *Proc. Natl. Acad. Sci. USA*., **1998**, *95*, 6234-6238.

[9] J.N. Cha, K. Shimizu, Y. Zhou, S.C. Christensen, B.F. Chmelka, G.D. Stucky, and D.E. Morse. *Proc. Natl. Acad. Sci. USA*., **1999**, *96*, 361-365.

[10] Y. Zhou, Y. Shimizu, J.N. Cha, G.E. Stucky, and D.E. Morse. *Angew. Chem. Int. Ed*., **1999**, *38*, 779-782.

[11] A. Krasko, B. Lorenz, R. Batel, H.C. Schröder, I.M. Müller, and W.E.G. Müller. *Eur. J. Biochem*., **2000**, *267*, 4878-4887.

[12] M.N. Tahir, P. Theato, W.E.G. Müller, H.C. Schröder, A. Janshoff, J. Zhang, J. Huth, and W. Tremel. *Chem. Commun*., **2004**, 2848-2849.

[13] C.C. Perry and T. Keeling-Tucker. *Chem. Commun*., **1998**, 2587-2588.

[14] C.C. Perry and T. Keeling-Tucker. *Colloid Polym. Sci*., **2003**, *281*, 652-664.

[15] L. Sapei , R. Nöske, P. Strauch, and O. Paris. *Chem. Mater*., **2008**, *20*, 2020-2025.

[16] C.C. Perry, R.J.P. Williams, and S.C. Fry. *J. Plant Physiol*., **1987**, *126*, 437-448.

[17] V. Martin-Jézéquel, M. Hildebrand, and M.A. Brzezinski. *J. Phycol*., **2000**, *36*, 821-840.

[18] E. Brunner, C. Gröger, K. Lutz, P. Richthammer, K. Spinde, and M. Sumper. *Appl. Microbiol. Biotechnol*., **2009**, *84*, 607-616.

[19] R.A. Gross, A. Kumar, and B. Kalra. *Chem. Rev*., **2001**, *101*, 2097-2124.

[20] M.P Stevens. *Polymer Chemistry, An Introduction Third Edition*. Oxford University Press, New York, NY, USA. **1999**.

[21] J.E. Mark, H.R. Allcock, and R. West. *Polysiloxanes and Related Polymers*, in *Inorganic Polymers*, Oxford University Press, New York, NY, USA. **2005**.

[22] W.M. Darley and B.E. Volcani. *Exp. Cell Res*., **1969**, *58*, 334-342.

[23] C.D. Reeves and B.E. Volcani. *J. Gen. Microbiol*., **1985**, *131*, 1735-1744.

[24] M. Hildebrand, D.R. Higgins, K. Busser, and B.E. Volcani. *Gene*, **1993**, *132*, 213-218.

[25] K. Thamatrakoln and M. Hildebrand. *Eukaryotic Cell*, **2006**, *6*, 271-279.

[26] C.C. Perry and T. Keeling-Tucker. *J. Biol. Inorg. Chem*., **2000**, *5*, 537-550.

[27] N. Kröger, C. Bergsdorf, and M. Sumper. *The EBMO Journal*, **1994**, *13*, 4676-4683.

[28] M. Hildebrand, B.E. Volcani, W. Gassmann, and J.I. Schroeder. *Nature*, **1997**, *385*, 688-689.

[29] P. Bhattacharyya and B. E. Volcani. *Proc. Natl. Acad. Sci. USA*., **1997**, *77*, 6386-6390.

[30] C.W. Sullivan. *J. Phycol*., **1976**, *12*, 390-396.

[31] J.B. Lambert, S.A. Gurusamy-Thangavalu, and K. Ma. *Science*, **2010**, *327*, 984-986.

[32] S.D. Kinrade, J.W. Del Nin, A.S. Schach, T.A. Sloan, K.L. Wilson, and C.T.G. Knight. *Science*, **1999**, *285*, 1542-1545.

[33] S.D. Kinrade, R.J. Balec, A.S. Schach, J. Wang, and C.T.G. Knight. *Dalton Trans*., **2004**, 3241-3243.

[34] N. Poulson and N. Kröger. *J. Biol. Chem*., **2004**, *279*, 42993-.

[35] M. Sumper, R. Hett, G. Lehmann and S. Wenzl. *Angew. Chem. Int. Ed*., **2007**, *46*, 8405-8408.

[36] N. Kröger, S. Lorenz, E. Brunner, and M. Sumper. *Science*, **2002**, *298*, 584-586.

[37] K.D. Lobel, J.K. West, and L.L. Hench. *Mar. Biol*., **1996**, *126*, 353-360.

[38] K.D. Lobel, J.K. West, and L.L. Hench. *J. Mater, Sci. Lett*., **1996**, *15*, 648-650.

[39] N. Kröger, R. Deutzmann, C. Bergsdorf, and M. Sumper. *Proc. Natl. Acad. Sci. USA*., **2000**, *97*, 14133-14138.

[40] M. Sumper and G. Lehmann. *ChemBioChem*., **2006**, *7*, 1419-1427.

[41] S. Matsunaga, R. Sakai, M. jimbo, and H. Kamiya. *ChemBioChem*, **2007**, *8*, 1729-1735.

[42] M. Sumper. *Science*, **2002**, *285*, 2430-2433.

[43] W.E.G. Müller, A. Boreiko, U. Schloβmacher, X. Wang, C. Eckert, K. Kropf, J. Li, and H.C. Schröder. *J. Exp. Biol*., **2007**, *211*, 300-309.

[44] T. Eliseeva, M.J. Panzer, W.J. Youngs, and C.A. Tessier. *J. Organomet. Chem*., **2010**, *695*, 1507-1512.

[45] H.C. Schröder, M. Weins, U. Schloβmacher, D. Brandt, and W.E.G. Müller. *Silicon*, **2012**, *4*, 33-38.

[46] G. Holzhüter, K. Narayanan, and T. Gerber. *Anal. Bioanal. Chem*., **2003**, *376*, 512-517.

[47] L. Sapei, N. Gierlinger, J. Hartmann, R. Nöske, P. Strauch, and O. Paris. *Anal. Bio-anal. Chem*., **2007**, *389*, 1249-1257.

[48] C.J. Brinker and G.W. Scherer. *Sol-Gel Science, The Physics and Chemistry of Sol-Gel Processing*. Academic Press Inc., San Diego, CA, USA. **1990**.

[49] P.C. Carmen. *Trans. Faraday Soc*., **1940**, *36*, 964-973.

[50] C.J. Brinker. *J. Non-Cryst. Solids*, 1988, *100*, 31-50.

[51] J.C. Pouxviel, J.P. Boilot, J.C. Beloeil, and J.Y. Lallemand. *J. Non-Cryst. Solids*, **1987**, *89*, 345-360.

[52] I. Artaki, M. Bradley, T.W. Zerda, and J. Jonas. *J. Phys. Chem*., **1985**, *89*, 4399-4404.

[53] B.D. Kay and R.A. Assink. *J. Non-Cryst. Solids*, **1988**, *104*, 112-122.

[54] B.D. Kay and R.A. Assink. *J. Non-Cryst. Solids*, **1988**, *99*, 359-370.

[55] M.T. Harris, R.R. Brunson, and C.H. Byers. *J. Non-Cryst. Solids*, **1990**, *121*, 397-403.

[56] C.T.G. Knight, R.J. Balec, and S.D. Kinrade. *Angew. Chem. Int. Ed*., **2007**, *46*, 8148-8152.

[57] R. Liu, Y. Xu, D. Wu, Y. Sun, H. Gao, H. Yuan, and F. Deng. *J. Non-Cryst. Solids*, **2004**, *343*, 61–70.

[58] H. Dong, M. Lee, R.D. Thomas, Z. Zhang, R.F. Reidy, and D.W. Meuller. *J. Sol-Gel Sci. Technol*., **2003**, *28*, 5-14.

[59] R.B. Taylor, B. Parbhoo, and D.M. Fillmore, *Chapter 12 Nuclear Magnetic Resonance Spectroscopy*, in A.L. Smith (Ed.) *The Analytical Chemistry of Silicones*. John Wiley & Sons, Inc., New York, USA. **1991**.

[60] T. Coradin and J. Livages. *Colloids and Surfaces B: Biointerfaces*, **2001**, *21*, 329-336.

[61] D. Belton, G. Paine, S.V. Patwardhan, and C.C. Perry. *J. Mater. Chem*., **2004**, *14*, 2231-2241.

[62] L. Sudheendra and A.R. Raju. *Mater. Res. Bull*., **2002**, *37*, 151-159.

[63] K.D. Hartlen, A.P.T. Athanasopolous, V. Kitaev. *Langmuir*, **2008**, *24*, 1714-1720.

[64] T.M. Davis, M.A. Snyder, J.E. Krohn, and M. Tsapatsis. *Chem. Mater*., **2006**, *18*, 5814-5816.

[65] M.A. Snyder, J.A. Lee, T.M. Davis, L.E. Scriven, and M. Tsapatsis. *Langmuir*, **2007**, *23*, 9924-9928.

[66] T. Yokoi, J. Wakabayashi, Y. Otsuka, W. Fan, M. Iwana, R. Watanabe, K. Aramaki, A. Shimojima, T. Tatsumi, and T. Okubo. *Chem. Mater.*, **2009**, *21*, 3719-3729.

[67] S.V. Patwardhan and S.J. Clarson. *J. Inorg. Organomet. Polym*., **2002**, *12*, 109-116.

[68] S.V. Patwardhan and S.J. Clarson. *Mater. Sci. and Eng. C*, **2003**, *23*, 495-499.

[69] S.V. Patwardhan and S.J. Clarson. *Silicon Chem*., **2002**, *1*, 207-214.

[70] S.V. Patwardhan, N. Mukherjee, and S.J. Clarson. *J. Inorg. Organomet. Polym*., **2002**, *11*, 193-198.

[71] T. Coradin, O. Durupthy, and J. Livages. *Langmuir*, **2002**, *18*, 2331-2336.

[72] C. Gautier, P.J Lopez, J. Livages, and T. Coradin. *J. Colloid and Interface Sci*., **2007**, *309*, 44-48.

[73] P.A. Mirau, J.L. Serres, and M. Lyons. *Chem. Mater*., **2008**, *20*, 2218-2223.

[74] S.V. Patwardhan, R. Maheshwari, N. Mukherjee, K.L. Kiick, and S.J. Clarson. *Biomacromolecules*, **2006**, *7*, 491-497.

[75] M.M. Tomczak, D.D. Glawe, L.F. Drummy, C.G. Lawrence, M.O. Stone, C.C. Perry, D.J. Pochan, T.J. Deming, and R.R.Naik. *J. Am. Chem. Soc*., **2005**, *127*, 12577-12582.

[76] M.K. Liang, S.V. Patwardhan, E.N. Danilovtseva, V.V. Annenkov, and C.C. Perry. *J. Mater. Res*., **2009**, *24*, 1077-1708.

[77] S.V. Patwardhan and S.J. Clarson. *J. Inorg. Organomet. Polym*., **2003**, *13*, 49-53.

[78] S.V. Patwardhan and S.J. Clarson. *J. Inorg. Organomet. Polym*., **2003**, *13*,193-203.

[79] J.N. Cha, G.D. Stucky, D.E. Morse, and T.J. Deming. *Nature*, **2000**, *403*, 289-292.

[80] M.N. Tahir, P. Théato, W.E.G. Müller, H.C. Schröder, A. Janshoff, J. Ziang, J. Huth, and W. Tremel. *Chem. Commun*., **2004**, 2848-2849.

[81] P.M. Zelisko, T. Dudding, K.R. Arnelien, and H. Stanisic. *Trypsin-Catalyzed Cross-Linking of α,ω-Triethoxysilyl-terminated polydimethylsiloxane: An experimental and computational approach*, in S.J. Clarson, M.J. Owen, S.D. Smith, M.E. Van Dyke (Eds.) *Advance of Silicones and Silicone-Modified Materials*. p. 47-57. **2010**.

[82] P.M. Zelisko, K.Arnelian, and M. Frampton. . *Enzyme-mediated Cross-Linking of Silicone Polymers*. PCT/CA2008/001150, **2008**. Patent pending.

[83] T. Coradin, A. Coupé, and J. Livage. *Coll. Surf. B: Biointerfaces*, **2003**, *29*, 189-196.

[84] R. Tacke, H. Linoh, B. Stumpf, W. Abraham, K. Kieslich, and L. Ernst. *Z. fur Naturforsch*., **1983**, *38b*, 616-620.

[85] S. Sydlatk, H. Andree, A. Stoffregen, F. Wagner, B. Stumpf, L. Ernst, H. Zilch H, and R. Tacke. *Appl. Microbiol. Biotechnol*,. **1987**, *27*, 152-158.

[86] There is even less evidence for bioconversions of organogermanium and organotin compounds. Notable exceptions to this also come from R. Tacke and coworkers. For further reading on the subject of enzymatic transformations of organogermanes see Tacke *et al*., *Organometallics*, **1998**, *17*, 1687-1699; Tacke *et al*., *Chem. Ber*., **1994**, *127*, 639-642; and Wagner *et al*., in *Organosilicon Chemistry II-From Molecules to Materials*, **1996**, 37-242. And for organostannes see M. Therisod. *J. Organomet. Chem*., **1989**, *361*, C8-C10.

[87] R. Csuk and B.I. Glanzer. *Chem. Rev*., **1991**, *91*, 49-97.

[88] B. Zhou, A.S. Goaolan, V. Van Middlesworth, W. Shieh, and C.J. Sih. *J. Am. Chem. Soc*., **1983**, *105*, 5925-5926.

[89] P. Zani. *J. Mol. Catal. B: Enz*., **2001**, *11*, 279-285.

[90] R. Tacke, H. Hengelsberg, H. Zilch, and B. Stumpf. *J. Organomet. Chem*., **1989**, *379*, 211-216.

[91] R. Tacke in: H. Sakuri (Ed.) *Organosilicon and Bioorganosilicon Chemistry: Structure, Bonding, Reactivity and Synthetic Application.* Ellis Horwood Limited, Chichester, West Sussex, England. **1985**.

[92] R. Tacke, S. Brakmann, F. Wuttke, J. Fooladi, C. Sydlatk, and D. Schomburg. *J. Organomet. Chem*., **1991**, *403*, 29-41.

[93] R. Tacke, F. Wuttke, and H. Henke. *J. Organomet. Chem*., **1992**, *424*, 273-280.

[94] P. Huber, S. Bratovanov, S. Beinz, C. Syldatk, and M. Pietzsch. *Tetrahedron: Assym*., **1996**, *7*, 69-78.

[95] D.T. Gibson, J.R. Koch, and R.E. Kallio. *Biochemistry*, **1968**, *7*, 2653-2662.

[96] W.C. Smith, G.M. Whited, T.H. Lane, K. Sanford, J.C. McAuliffe. *Enzymatic Dihydroxylation of Aryl Silanes*, in N.H. Cheng and R.A. Gross (Eds.) *ACS Symposium Series*: *Polymer Biocatalysis and Biomaterials II*: 434-459. **2008**.

[97] S.M. Resnick, D.S. Torok, and D.T. Gibson. *J. Org. Chem*., **1995**, *60*, 3546-3549.

[98] A.D. Ryabov. *Angew. Chem. Int. Ed. Engl*., **1991**, *30*, 931-941.

[99] K. Fritsche, C. Sydlatk, F. Wagner, H. Hengelsberg, and R. Tacke. *Appl. Microbiol. Biotechnol*., **1989**, *31*, 107-111.

[100] A. Tanaka, T. Kawamoto, and K. Sonomoto. *Ann. NY Acad. Sci*., **1990**, *613*, 702-706.

[101] C. Eaborn. *Organosilicon Compounds*. Butterworths Scientific Publications, London, England. **1960**.

[102] B. De Jeso, N. Belair, H. Deleuze, M. Rascale, and B. Maillard. *Tetrahedron Lett*., **1990**, *31*, 653-654.

[103] E. Santaniello, P. Ferraboschi, and P. Grisenti. *Tetrahedron Lett*., **1990**, *31*, 5657-5660.

[104] A. Djerourou and L. Blanco.*Tetrahedron Lett*., **1991**, *32*, 6325-6336.

[105] M.A. McDonough, H.E. Klei, and J.A. Kelly. *Protein Sci*., **1999**, *8*, 1971-1981.

[106] H. Hengelsberg, R. Tacke, K. Fritsche, C. Syldatk, and F. Wagner. *J. Organomet. Chem*., **1991**, *415*, 39-45.

[107] H.R. Horton, L.A. Moran, K.G. Scrimgeour, M.D. Perry, and J.D. Rawn. *Principles of Biochemistry Fourth Edition*. Pearson Prentice Hall, Upper Saddle River New Jersey. **1993**.

[108] M. Zong, T. Fukui, T. Kawamoto, and A.Tanaka. *Appl. Microbiol. Biotechnol*., **1991**, *36*,40-43.

[109] H. Eklund. *Pharm. Biochem. and Behaviour*, **1983**, *18(Suppl. 1*), 73-81.

[110] T. Fukui, M. Zong, T. Kawamoto, and A. Tanaka. *Appl. Microbiol. Biotechnol*., **1992**, *38*, 208-213.

[111] A. Uejima, T. Fukui, E. Fukusaki, T. Omata, T. Kawamoto, K. Sonomoto, and A. Tanaka. *Appl. Microbiol. Biotechnol*., **1993**, *38*, 482-486.

[112] Y. Tsuji, T. Fukui, T. Kawamoto, and A. Tanaka. *Appl. Microbiol. Biotechnol*., **1994**, *41*, 219-224.

[113] H. Yamanaka, T. Fukui, T. Kawamoto, and A. Tanaka. *Appl. Microbiol. Biotechnol*., **1996**, *45*, 51-55.

[114] Y. Tsuji, H. Yamanaka, T. Fukui, T. Kawamoto, and A. Tanaka. *Appl. Microbiol. Biotechnol*., **1997**, *47*, 114-119.

[115] H. Yamanaka, T. Kawamoto, and A. Tanaka. *J. Ferment. Bioeng*., **1997**, *84*, 181-184.

[116] M. Pietzsch, T. Waniek, R.J. Smith, S. Bratovanov, A. Bienz, and C. Syldatk. *Monatshefte für Chemie*, **2000**, *131*, 645-653.

[117] R.J. Smith, M. Pietzsch, T. Waniek, C. Syldatk, and S. Bienz. *Tetrahedron: Asymm*., **2001**, *12*, 157-165.

[118] O. May, M. Siemann, M. Pietzsch, M. Kiess, R. Mattes, and C. Syldatk. *J. Biotechnol*., **1988**, *61*, 1-13.

[119] H. Ishikawa, H. Yamanaka, T. Kawamoto, and A. Tanaka. *Appl. Microbiol. Biotechnol*., **1999**, *51*, 470-473.

[120] S. Falgner, C. Burschka, S. Wagner, A. Böhm, J.O. Daiss, and R. Tacke. *Organometallics*, **2009**, *28*, 6059-6066.

[121] N. Li, M. Zong, C. Liu, H. Peng, and H. Wu. *Biotechnol. Lett*., **2003**, *25*, 219-222.

[122] N. Li, M. Zong, H. Peng, H. Wu, and C. Liu. *J. Mol. Catal. B: Enz*., **2003**, *22*, 7-12.

[123] S. Huang, S. Liu, M. Zong, and R. Xu. *Biotechnol. Lett*., **2005**, *27*, 79-82.

[124] R. Tacke , S.A.Wagner, S. Brakmann, F. Wuttke, U. Eilert, L. Fisher, and C. Syldatk. *J. Organomet. Chem*., **1993**, *458*, 13-17.

[125] J.J. Berzelius. *Isomierie, Unterscheidung von damit analogen Verhältnissen*, in *Jahresberichte über die Fortschritte der physichen der Wissenschaften*, **1833**, *12*, 63-67.

[126] L. H. Sperling. *Chapter 1: Introduction to Polymer Science*, in *Introduction to Physical Polymer Science, 3rd Edition*. John Wiley & Sons, Inc. New York, USA. **2001**.

[127] L.H. Bakeland. *Ind. Eng. Chem*., **1909**, *1*, 149-161.

[128] W. Carothers. *Linear Polyamides and Their Production*. United States Patent 2,130,523. **1937**.

[129] C. Bonduelle, B. Martin-Vaca, and D. Bourissou. *Biomacromolecules*, **2009**, *10*, 3069-3073.

[130] S. Kobayashi and A. Makino. *Chem. Rev*., **2009**, *109*, 5288-5353.

[131] S. Kobayashi, H. Uyama, and S. Kimura. *Chem. Rev*., **2001**, *101*, 3793-3818.

[132] N.R. Thomas. *Silicon*, **2010**, *2*, 187-193.

[133] M.J. Owen, *Siloxane Surface Activity*, in J.M. Zeigler and F.W.G. Feardon (Eds.) *Silicon-Based Polymer Science, A Comprehensive Resource*, American Chemical Society, Washington, D.C. **1990**.

[134] J.W. White and R.C. Treadgold, *Organofunctional siloxanes*, in S.J. Clarson and J.A. Semlyen (Eds.), *Siloxane Polymers*, Prentice Hall, Engelwood Cliffs, New Jersey, USA. **1993**.

[135] S.J. Clarson. *Depolymerization, Degradation and Thermal Properties of Siloxane polymers*, in S.J. Clarson and J.A. Semlyen (Eds.), *Siloxane Polymers*, Prentice Hall, Engelwood Cliffs, New Jersey, USA. Pp216-244. **1993**.

[136] G. Budden. *Some Like It Hot* (Technical paper). Dow Corning. Bath, UK.

[137] C. Eaborn, *Organosilicon Compounds*, Butterworths Scientific Publications, London, England, **1969**.

[138] D.R. Thomas. *Cross-Linking of Polydimethylsiloxanes*, in S.J. Clarson and J.A. Semlyen (Eds.), *Siloxane Polymers*, Prentice Hall, Engelwood Cliffs, New Jersey, USA. **1993.**

[139] M. Jang and J.V. Crivello. *J. Polym. Sci. Part A: Polym. Chem*., **2003**, *41*, 3056-3073.

[140] A. Saxena, S. Rajaraman, and M. Leatherman. *Macromolecules*, **2007**, *40*, 752-755.

[141] J.B. Grande, D.B. Thompson, F. Gonzaga, and M.A. Brook. *Chem. Commun*., **2010**, *46*, 4988-4990.

[142] J.B. Grande, F. Gonzaga, and M.A. Brook. *Dalton Trans*., **2010**, *39*, 9369-9378.

[143] M.A. Brook, J.B. Grande, and F. Ganachaud. *Adv. Polym. Sci*., **2011**, *235*, 161-183.

[144] H. Nishino, T. Mori, and Y. Okahata. *Chem. Commun*., **2002**, 2684-2685.

[145] W.E.G. Müller, Ute Schloßmacher, X. Wang, A. Boreiko, D. Brandt, S.E. Wolf, W. Tremel, and H.C. Schröder. *FEBS Journal*, **2008**, *275*, 362-370.

[146] S.E. Wolf, U. Schlößmacher, A. Pietuch, B. Mathiasch, H.C. Schröder,W.E.G. Müller, and W. Tremel. *Dalton Trans*., **2010**, *39*, 9245-9249.

[147] A.R. Bassindale, K.F. Brandstadt, T.H. Lane, and P.G. Taylor. *J. Inorg. Biochem*., **2003**, *96*, 401-406.

[148] V. Abbate, A.R. Bassindale, K.F. Brandstadt, R.Lawson, and P.G. Taylor. *Dalton Trans*., **2010**, *39*, 9361-9368.

[149] V. Abbate, A.R. Bassindale, K.F. Brandstadt, and P.G. Taylor. *J. Inorg. Biochem*., **2011**, *105*, 268-275.

[150] A.R. Bassindale, K.F. Brandstadt, T.H. Lane and P.G. Taylor. *Polym. Preprints*, **2003**, *44*, 570-571.

[151] A. Maraite, M.B. Ansorge-Schumacher, B. Ganchequi, W. Leitner, and G. Grogan. *J. Mol. Cat. B: Enz*., **2009**, *56*, 24-28.

[152] V. van Braunmühl, G. Jonas, and R. Stadler. *Macromolecules*, **1995**, *28*, 17-24.

[153] B. Sahoo, K.F. Brandstadt, T.H. Lane, and R.A. Gross. *Org. Lett*., **2005**, *7*, 3857-3860.

[154] R. Mosurkal, L.A. Samuelson, V.S. Parmar, J. Kumar, and A.C. Watterson. *Macromolecules*, **2007**, *40*, 7742-7744.

[155] B. Sharma, A. Azim, H. Azim, and R.A. Gross, E. Zini, M.L. Focarete, and M. Scandola, *Macromolecules*, **2007**, *40*, 7919-7927.

[156] Y. Poojari, A. Palsule, M. Cai, S.J. Clarson, and R.A. Gross. *Eur. Polym. J*., **2008**, *44*, 4139-4145.

[157] Y. Poojari and S.J. Clarson, *J. Inorg. Organomet. Polym*., **2010**, *20*, 46-52.

[158] Y. Poojari and S.J. Clarson, *Silicon*, **2009**, *1*, 165-172.

[159] Y. Poojari and S.J. Clarson, *Chem. Commun*., **2009**, 6834-6835.

[160] Y. Poojari and S.J. Clarson, *Macromolecules*, **2010**, *43*, 4616-4622.

[161] L. Guo, Z. Zhang, Y. Zhu, J. Li, and Z. Xie. *J. Appl. Polym. Sci.* **2008**, *108*, 1901–1907.

[162] P. Reis, K. Holmberg, H. Watzke, M.E. Leser, and R. Miller. *Adv. Colloid and Interface. Sci*., **2009**, *147-148*, 237-250.

[163] J. Uppenberg, N. Öhrner, M. Norin, K. Hult, G.J. Kleywegt, S. Patkar, V. Waagen, T. Anthonsen, and T.A. Jones. *Biochemistry*, **1995**, *34*, 16838-16851.

[164] P. Grochulski, Y. Li, J.D. Schrag, and M. Cygler. *Prot. Sci*., **1994**, *3*, 82-91.

[165] J. Uppenberg, M.T. Hansen, S. Patkar, and T.A. Jones. *Structure*, **1994**, *2*, 293-308.

[166] N. Guex and M.C. Peitsch. *Electrophoresis*, **1997**, *18*, 2714-2723.

[167] K.E. Jaeger and T. Eggert. *Curr. Op. Biotechnol*., **2002**, *13*, 390-397.

[168] A. Mahapatro, A. Kumar, B. Kalra, and R.A. Gross. *Macromolecules*, **2004**, *37*, 35-40.

[169] Z. Jiang, C. Liu, W. Xie, and R.A. Gross. *Macromolecules*, **2007**, *40*, 7934-7943.

[170] Z. Jiang, C. Liu, and R.A. Gross. *Macromolecules*, **2008**, *41*, 4671-4680.

[171] Y. Mei, L. Miller, W. Gao, and R.A. Gross. *Biomacromolecules*, **2003**, *4*, 70-74.

[172] K.D. Keefer. *Mat. Res. Soc. Symp. Proc*., **1984**, *32*, 15-24.

[173] Y. Tang, E.C. Tehan, Z. Tao, and F.V. Bright. *Anal. Chem*., **2003**, *75*, 2407-2413.

[174] T.R. Besanger, Y. Chen, A.K. Deisingh, R. Hodgson, W Jin, S. Mayer, M.A. Brook, and J.D. Brennan. *Anal. Chem*., **2003**, *75*, 2382-2391.

[175] In the nomenclature of GE Silicones to note different environments, M, T, D and Q refer to a silicon atom that is bonded to one, two, three or four different oxygen atoms. The subscript notation comes from Brinker and Scherer to denote that the silicon environment in question has *n* number of siloxane bonds.

[176] F.K. Winkler, A. D'Arcy, and W. Hunziker, *Nature*, **1990**, *343*, 771-774.

[177] A.R. Bassindale, K.F. Brandstadt, V. Abbate, and P.G. Taylor. *J. Mater. Chem*., **2009**, *19*, 7606-7609.

[178] P. Buisson, E. El Rassy, S. Maury and A. C. Pierre, *J. Sol–Gel Sci. Technol*., **2003**, *27*, 373-379.

[179] R.H. Baney, M. Itoh, A. Sakakibara, and T. Suzuki. *Chem. Rev*., **1995**, *95*, 1409-1430.

[180]D.M. Blow, J. Janin, and R.M. Sweet. *Nature*, **1974**, *249*: 54-56.

[181] R.A. Assink and B.D. Kay. *Ann. Rev. Mater. Sci*., **1991**, *21*, 491–513.

[182] H. Dong, Z. Zhang, M. Lee, D.W. Mueller, and R.F. Reidy. *J. Sol-Gel. Sci. Technol*., **2007**, *41*, 11-17.

[183] S.H. Hung and L. Hedstrom. *Prot. Eng*., **1998**, *11*, 669-673.

[184] D. Voet and J.G. Voet. *Biochemistry, 3rd Edition*, **1990**, Wiley, New York, NY.

[185] J.M. Berg, J. Tymoczko, and J.Stryer. *Biochemistry, 5th Edition*, **2002**, W.H. Freeman and Company, New York, NY.

[186] J.S. Fruton. *Acc. Chem. Res*., **1974**, *7*, 241-246.

[187] H.C. Schröder, M. Wiens, U. Schlößmacher, D. Brandt, and W.E.G. Mueller. *Silicon*, **2012**, *4*, 33-38.

[188] D.J. Tantillo, J. Chen, and K.N. Houk. *Curr. Opin. Chem. Biol*., **1998**, *2*, 743–750.

[189] G. Ujaque, D.J. Tantillo, Y. Hu, K.N. Houk, K. Hotta, and D. Hilvert. *J. Comput. Chem*., **2003**, *24*, 98–110.

[190] A.D. Becke. *J. Chem. Phys*., **1993**, *98*, 1372-1377.

[191] A.D. Becke. *J. Chem. Phys*., **1993**, *98*, 5648-5652.

[192] C. Lee, W. Yang, and R.G. Parr. *Phys. Rev. B*., **1998**, *37*, 785-789.

[193] R. Ditchfield, W.J. Hehre, and J.A. Pople. *J. Chem. Phys*., **1971**, *54*, 724-728.

[194] W.J. Here, R. Ditchfield, and J.A. Pople. *J. Chem. Phys*., **1972**, *56*, 2257-2261.

[195] P.C. Hariharan and J.A. Pople. *Theor. Chim. Acta*, **1973**, *28*, 213-222.

[196] M.B. Frampton, R. Simionescu, T. Dudding, and P.M. Zelisko. *J. Mol. Cat. B: Enz*., **2010**, *66*, 105-112.

[197] J.B. Lambert, Y. Zhao, and S.M. Zhang. *J. Phys. Org. Chem*., **2001**, *14*, 370-379.

[198] H.R. Allcock, F.W. Lampe, and J.E. Mark, in *Contemporary Polymer Chemistry 3rd Edition*, Pearson-Prentice Hall, Upper Saddle River, New Jersey, USA, pp.310-324. **1981**.

[199] K.S. Bisht, L.A. Henderson, R.A. Gross, D.L. Kaplan, and D.L. Swift. *Macromolecules*, **1997**, *30*, 2705.

[200] S. Naik, A. Basu, R. Saikia, B. Madan, P. Paul, R. Chaterjee, J. Brask, and A. Svendsen. *J. Mol. Cat. B: Enz*., **2010**, *65*, 18-23.

[201] C.R. Thomas and P. Dunnill, *Biotechnol. Bioeng*., **1979**, *21*, 2279-2302.

[202] Y-K. Lee and C-L. Choo. *Biotechnol. Bioeng*., **1989**, *33*, 183-190.

[203] C.R. Thomas, A.W Nienow, and P. Dunnill, *Biotechnol. Bioeng*., **1979**, *21*, 2263-2278.

[204] R.W. Lencki, A. Tecante, and L. Choplin. *Biotechnol. Bioeng*., **1993**, *42*, 1061-1067.

[205] S.E. Charm and B.L. Wong. *Biotechnol. Bioeng*., **1970**, *12*, 1103-1109.

[206] R.A. Gross, M. Ganesh, and W. Lu. *Trends in Biotechnology*, **2010**, *28*, 435-443.

[207] Y.Yang, W. Lu, J. Cai, Y. Hou, S. Ouyang, W. Xie, and R.A. Gross. *Macromolcules*, **2011**, *44*, 1977-1985.

[208] D.H. Guimarãesa, M. de Meireles Brioudea, R. da Paz Fiúzaa,.L.A. Sanches de Almeida Pradob, J. S. Boaventuraa, and N.M. Joséa. *Mater. Res*., **2007**, *10*, 257-260.

[209] J. Yang, S. Zhang, X. Liu, and A. Cao. *Polym. Degrad. Stabil*., **2003**, *81*, 1-7.

[210] D.J. Brunelle. Macrocyclic polyester oligomer preparation with Lewis acid as catalyst, US Patent 5,321,117. June 14, **1994**.

[211] E.D. Lipp and A.L. Smith. *Chapter 11*: *Infrared, Raman, Near-infrared, and Ultraviolet Spectroscopy*, in Smith, A.L. (Ed.) *The Analytical Chemistry of Silicones*, John Wiley & Sons, Inc. New York, USA. **1991**.

[212] J.W. White and R.C. Treadgold, in S.J. Clarson and J.A. Semlyen (Eds.), *Siloxane Polymers*, Prentice Hall, Engelwood Cliffs, New Jersey, **1993**, pp. 193-215.

[213] D. O'Hagan and A.H. Parker. *Polym. Bull*., **1998**, *41*, 519-524.

[214] Y. Linko, Z. Wang, and J. Seppälä. *Enzyme and Microbial Technol*., **1995**, *17*, 506-511.

[215] J. Pleiss, H. Scheib, and R.D. Schmid. *Biochemie*, **2000**, *82*, 1043-1052.

[216] E. Rogalska, C. Cudrey, F. Ferrato, and R.Verger. *Chirality*, **1993**, *5*, 24-30.

[217] P.D. Maria, C. Carboni-Oerlemans, B. Tuin, G. Bargeman, A. van der Meer, and R. van Gemert. *J. Mol. Cat. B: Enz*., **2005**, *37*, 36-46.

[218] Q.M. Gu, W.W. Maslanka, and H.N. Cheng. *Chapter 21: Enzyme-catalyzed polyamides and their derivatives*, in N.H. Cheng and R.A. Gross (Eds.) *ACS Symposium Series Polymer Biocatalysis and Biomaterials II*, **2008**, 309-319.

[219] H. Cheng, P.S. Hill, D.J. Siegwart, N. Vacanti, A.K.R. Lytton-Jean, S-W. Cho, A. Ye, R. Langer, and D.G. Anderson. *Adv. Mater*., **2011**, *23*, H95-H100.

[220] F. Binns, P. Harffey, S.M. Roberts, and A. Taylor. *J. Chem. Soc. Perk. Trans.,* **1999**, *1*, 2671-2676.

[221] L.O. Wiemann, P. Weisshaupt, R. Nieguth, O. Thum, and M.B. Ansorge-Schumacher. *Org. Proc. Red Dev*., **2009**, *13*, 617-620.

[222] Y. Poojari. *Enzyme immobilization and biocatalysis of polysiloxanes*, Ph.D. Dissertation, University of Cincinnati, Cincinnati, Ohio, USA. **2009**.

[223] C. Belger, M.N. Neisius, and B. Pleitker. *Chemistry: A European Journal*, **2010**, *16*, 12214-12220.

[224] G.K. Rao, N.B. Gowda, and R.A. Ramakrishna. *Synthetic Communicaions*, **2012**, *42*, 893-904.

[225] P. Dawar, M.B. Raju, and R.A. Ramakrishna. *Tetrahedron Letters*, **2011**, *52*, 4262-4265.

[226] K. Miyamoto, Y. Sei, K. Yamaguchi, and M. Ochiai. *J. Am. Chem. Soc*., **2009**, *131*, 1382-1383.

[227] M. Pramanik, M. Nandi, H. Uyama, and A. Bhaumik . *Green Chemistry*, **2012**, *14*, 2273-2281.

[228] J.G. Avila-Zárraga and R. Martínez. *Synth Commun*., **2001**, *31*, 2177-2183.

[229] H.-B. Sun, R. Hua, and Y. Yin. *Molecules*, **2006**, *11*, 263-271.